Evaluation of Structure-Activity Relationship of Microtubule (MT)-Targeting 1,2,4-Triazolo[1,5-*a*]pyrimidines Identifies New Candidates for Neurodegenerative Tauopathies.

Killian Oukoloff,[a] Goodwell Nzou,[b] Carmine Varricchio,[c] Bobby Lucero,[d] Thibault Alle,[a] Jane Kovalevich,[b] Ludovica Monti,[a] Anne-Sophie Cornec,[e] Yuemang Yao,[b] Michael J. James,[b] John Q. Trojanowski,[b] Virginia M.-Y. Lee,[b] Amos B. Smith III,[e] Andrea Brancale,[c] Kurt R. Brunden[b,*] and Carlo Ballatore[a,*]

[a]Skaggs School of Pharmacy and Pharmaceutical Sciences, University of California, San Diego, 9500 Gilman Drive, La Jolla, CA 92093; [b]Center for Neurodegenerative Disease Research, Perelman School of Medicine, University of Pennsylvania, 3600 Spruce St., Philadelphia, PA 19104; [c]Cardiff School of Pharmacy and Pharmaceutical Sciences, Cardiff, King Edward VII Avenue, Cardiff CF103NB, UK; [d]Department of Chemistry & Biochemistry, University of California San Diego, 9500 Gilman Drive, La Jolla, CA, 92093, USA; [e]Department of Chemistry, School of Arts and Sciences, University of Pennsylvania, 231 South 34th St., Philadelphia, PA 19104-6323;

*Corresponding Author.

ABSTRACT: Studies in tau and Aβ plaque transgenic mouse models demonstrated that brain-penetrant microtubule (MT)-stabilizing compounds, including the 1,2,4-triazolo[1,5-*a*]pyrimidines, hold promise as candidate treatments for Alzheimer's disease (AD) and related neurodegenerative tauopathies. Triazolopyrimidines have already been investigated as anti-cancer agents; however, the anti-mitotic activity of these compounds does not always correlate with stabilization of MTs in cells. Indeed, previous studies from our laboratories identified a critical role for the fragment linked at C6 in determining whether triazolopyrimidines promote MT stabilization or, conversely, disrupt MT integrity in cells. To further elucidate the structure-activity relationship (SAR) and to identify potentially improved MT-stabilizing candidates for neurodegenerative disease, a comprehensive set of 68 triazolopyrimidine congeners bearing structural modifications at C6 and/or C7 was designed, synthesized and evaluated. These studies expand upon prior understanding of triazolopyrimidine SAR and enabled the identification of novel analogues that, relative to the existing lead, exhibit improved physicochemical properties, MT-stabilizing activity and pharmacokinetics.

KEYWORDS: Triazolopyrimidine; tau; microtubule; microtubule-stabilizing agents; Alzheimer's disease; neurodegenerative tauopathies.

Introduction. In Alzheimer's disease (AD) and related neurodegenerative tauopathies,[1] the hyperphosphorylation of the microtubule (MT)-associated protein tau promotes its dissociation from MTs and eventual deposition into insoluble aggregates, which are commonly referred to as neurofibrillary tangles (NFTs) and neuropil threads (NTs). Reduced tau binding to MTs is believed to trigger alterations in the normal structure and dynamics of MTs in the axons of neurons that ultimately cause or contribute to impaired axonal transport and resulting axonal dystrophy.[2] Given the evidence of neuronal MT abnormalities in AD patients and in tau and Aβ plaque transgenic (Tg) mouse models,[3] CNS-active MT-

stabilizing agents have been proposed as molecules that may provide therapeutic benefits in AD and related tauopathies.[4] Multiple preclinical studies[5-8] in tau Tg animals have shown that relatively low and infrequent doses of CNS-active MT-stabilizing natural products, such as epothilone D (**1**, Figure 1) and dictyostatin (**2**, Figure 1), can lead to significant improvements in several endpoints including an increase in MT density, a reduction in axonal dystrophy, and a significant lowering of both tau pathology and neuron loss.[5-7] More recently, brain-penetrant MT-stabilizing 1,2,4-triazolo[1,5-*a*]pyrimidines that are structurally simpler and are endowed with generally more favorable drug-like ADME-PK properties than MT-stabilizing natural products[9] have also shown promising results both *in vitro* and *in vivo*.[10-12] Although the MT binding site of the triazolopyrimidines is known to be different than that of taxol, epothilone D and other taxane site binders,[13] evaluation of a selected prototype (**3**, Figure 1) in a mouse model of tauopathy revealed that this compound could exert similar beneficial effects to those previously observed with **1,** indicating that triazolopyrimidines hold promise as candidate treatments for neurodegenerative tauopathies.[12] More recently, **3** has also been shown to decrease axonal dystrophy, with a resulting reduction of Aβ peptide and Aβ plaque deposition, in a Tg mouse model of senile plaque formation.[14]

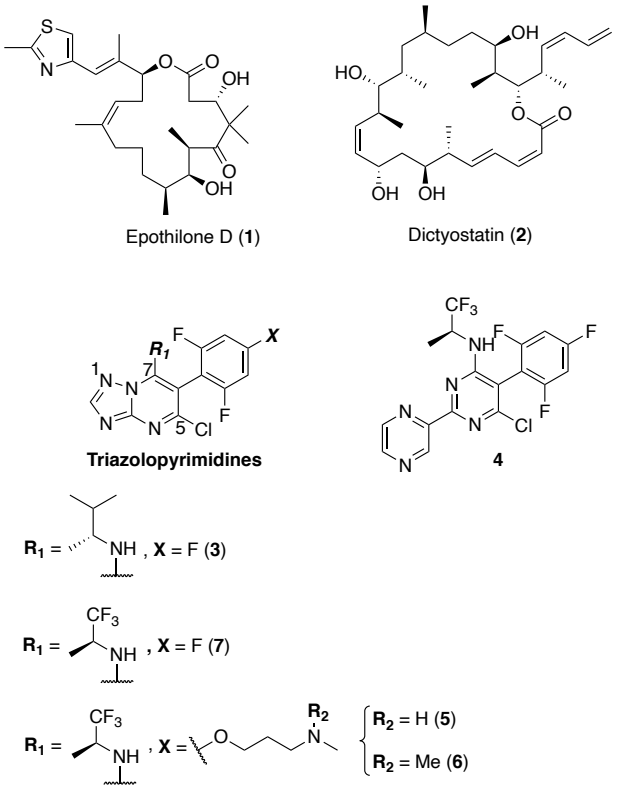

Figure 1. The structure of MT-stabilizing natural products, epothilone D and dictyostatin, and selected examples of MT-binding triazolopyrimidines and phenylpyrimidines.

MT-active triazolopyrimidines and structurally related phenylpyrimidines (*e.g.*, **4**) have already been evaluated as candidate treatments for cancer chemotherapy.[15, 16] This effort, which culminated in the identification of cevipabulin (**5**) as a clinical candidate,[17, 18] included a comprehensive assessment of the SAR in cytotoxicity assays that used rapidly dividing cancer cell-lines.[15] More recent studies from our laboratories suggested that the anti-mitotic activity of these compounds may not always correlate with stabilization of MTs in cells. Indeed, evaluation of representative examples of triazolopyrimidines and related phenylpyrimidines in cell-based assays of MT stabilization revealed that varying the scaffold (*i.e.*, triazolopyrimidine or phenylpyrimidine) or substitution pattern results in molecules that can either promote MT stabilization or, conversely, disrupt MT integrity.[11] For example, an evaluation of a selected set of triazolopyrimidines and phenylpyrimidines for their ability to produce elevations in known cellular markers of stable MTs,[19] such as acetylated and de-tyrosinated α-tubulin (AcTub and GluTub,

respectively), revealed that typically the phenylpyrimidines, such as **4**, produce an unusual bell-shaped concentration-response curve in these assays. In addition, these compounds cause a concentration-dependent decrease in total cellular α- and β-tubulin resulting from proteasome-mediated degradation, with a visible reduction of MT networks. Interestingly, although similar observations were made for some triazolopyrimidines, including **5** and its brain-penetrant[10] congener **6** (Figure 1), replacement of the alkoxide side-chain of these molecules with a fluorine atom, as in **7** (Figure 1) or **3**, had a dramatic impact on the MT-stabilizing properties of the compounds as demonstrated by the fact that the latter molecules caused the desired linear concentration-dependent increase in MT stabilization and MT mass in cells, without decreased cellular tubulin levels or changing MT morphology.[11] These findings, combined with the observation that the amine fragment linked at C7 of lead compound, **3**, is likely to be the primary site of metabolism,[12] led to a more systematic exploration of the SAR of triazolopyrimidines modified at C6 and C7. The results from these studies led to the identification of selected congeners that, relative to the existing lead, **3**, exhibit improved physicochemical properties, MT-stabilizing activity and pharmacokinetics.

Chemistry. As part of these studies a total of 68 compounds (**7**–**75**, Scheme 1–5) have been synthesized and tested, including 8 previously described triazolopyrimidines (*i.e.*, **7**,[15] **11**,[15] **25**,[15] **31**–**33**,[20] **34**,[12] and **54**[13]); 23 compounds exemplified in the patent literature (*i.e.*, **10**, **12**, **14**, **16**, **18**, **24**, **28**–**30**, **35**, **41**, **45**–**48**, **50**, **51**, **52**, **57**, **60**, **61**, **64**, **65**); and 37 structurally novel congeners. In all cases, the triazolopyrimidine ring was accessed via cyclocondensation reaction between the appropriate diethylmalonate (**76**–**92**, Scheme 1) and 1*H*-1,2,4-triazol-5-amine. Next, treatment with phosphorous oxychloride provided the corresponding 5,7-dichloro triazolopyrimidines (**93**–**109**, Scheme 1). Chemoselective amination at C7 with (*S*)-1,1,1-trifluoropropan-2-amine furnished triazolopyrimidines **7**–**22** (Scheme 1). Reduction of the *para* nitro derivative **22** provided the corresponding aniline derivative **23** (Scheme 1).

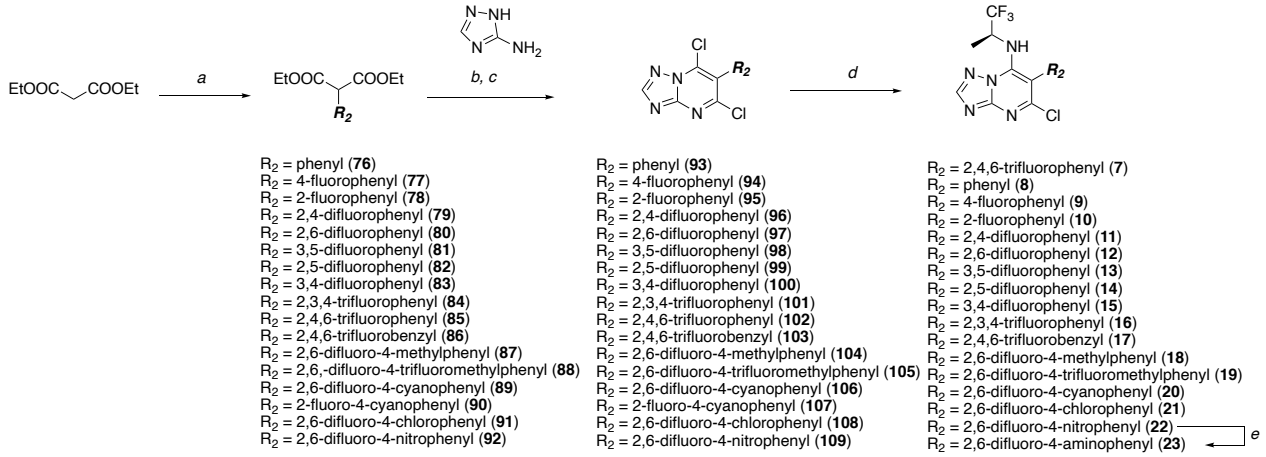

Scheme 1. *Reagents and Reaction conditions:* ***a***) For **76**–**85**, **87**–**89**, **91**: Ar-X, CuBr, NaH, 1,4-dioxane, 60–100 ˚C, 12 h, 19–74%; For **86**: Ar-CH_2Br, NaH, *N*,*N*-dimethylformamide, 0 ˚C, 1 h, 90%; For **90** and **92**: Ar-F, K_2CO_3, *N*,*N*-dimethylformamide, 60 ˚C, 4 h, 84–86%; ***b***) *N*-tributylamine, 170–180 ˚C, 2–6 h; ***c***) phosphorus oxychloride, 110–130 ˚C, 6–16 h, 46–58% over two steps; ***d***) appropriate amine, *N*,*N*-dimethylformamide, rt–90 ˚C, 1–18 h, 12–50%; ***e***) Fe, NH_4Cl, H_2O/MeOH (40/50), 80 ˚C, 2 h, 69%.

Triazolopyrimidine **7** was then used to access additional derivatives bearing different substitutions at the *para* position of the fluorinated phenyl ring (**24**–**33**, Scheme 2). In these cases, the installation of the appropriate alcohol or thiol side-chain was conducted via S_NAr followed by HPLC purification of the final product. Sulfoxide (**26**, **29**) and sulfone (**27**, **30**) derivatives were obtained from the corresponding thioethers (*i.e.*, **25**, and **28,** respectively) upon treatment with *m*-CPBA (Scheme 2).

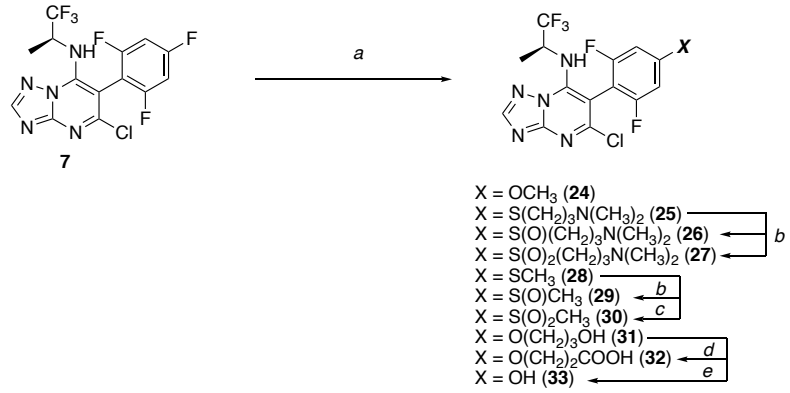

Scheme 2. *Reagents and Reaction conditions:* ***a***) For **24**: NaOMe, THF, 0 ˚C to 60 ˚C, 14 h, 71%; For **25**, **31**: ROH *or* RSH, NaH, DMSO, 60 ˚C, 3 h, 81–95%; For **28**: CH_3SNa, DMSO, 60 ˚C, 3 h, quant.; ***b***)

m-CPBA (1 equiv), CH_2Cl_2, 20 ˚C, 2 h, 32% of **26**, 52% of **27**, 70% of **29**; ***c***) *m*-CPBA (3 equiv), CH_2Cl_2, 20 ˚C, 3 h, 71%; ***d***) TEMPO, BAIB, CH_2Cl_2/H_2O (90/70), 20 ˚C, 2 h, 59%; ***e***) LiOH, MeOH/H_2O (1/1), 20 ˚C, 16 h, 39%.

Triazolopyrimidine dichloride **102** was used to access a series of congeners modified at position C7 (*i.e.*, **34**–**61**, Scheme 3). In these cases, chemoselective displacement of the chloro substituent at C7 was accomplished in moderate to good yields by treating **102** with the appropriate amine. The synthesis of C7 alkyl derivative **62** (Scheme 4) was initially attempted adopting a known procedure[21] by reacting dichloride **102** with the methyl ester of 4,4,4-trifluoro-3-methylbutanoic acid in the presence of LiHMDS to obtain **110**, followed by a Krapcho decarboxylation.[22] The main product isolated from this synthesis was the tetracyclic compound **111** (Scheme 4) whose structure was confirmed by X-ray crystallography. Desired compound **62** was ultimately obtained employing a similar approach in which alkylation reaction at C7 was conducted using the *tert*-butyl ester of 4,4,4-trifluoro-3-methylbutanoic acid to obtain intermediate **112**, which was then subjected to TFA-mediated cleavage of the ester moiety and *in situ* decarboxylation (Scheme 4).

Finally, the synthesis of compounds **63–75** (Scheme 5) was conducted by reacting the appropriate triazolopyrimidine dichlorides (*i.e.*, **95**, **97**, **106**, or **107**) with amine fragments (Scheme 5). In selected cases (*i.e.*, **67** and **68**) purification via silica gel column chromatography afforded individual atropoisomers, the structures of which could be determined via single crystal X-ray structure determination of **68** (Scheme 5).

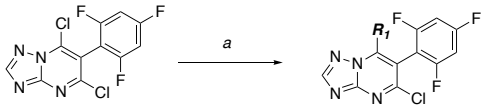

102

$R_1 = NH_2$ (**34**)	$R_1 =$  (**49**)
$R_1 = NHiPr$ (**35**)	$R_1 =$  (**50**)
$R_1 = NH(CH_2)_2CH_3$ (**36**)	$R_1 =$  (**51**)
$R_1 = NHtBu$ (**37**)	$R_1 =$  (**52**)
$R_1 = OH$ (**38**)	$R_1 =$  (**53**)
$R_1 =$  (**39**)	$R_1 =$ 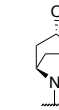 (**54**)
$R_1 =$ 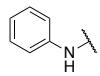 (**40**)	$R_1 =$  (**55**)
$R_1 =$ 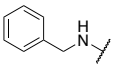 (**41**)	$R_1 =$  (**56**)
$R_1 =$  (**42**)	$R_1 =$  (**57**)
$R_1 =$  (**43**)	$R_1 =$  (**58**)
$R_1 =$  (**44**)	$R_1 =$  (**59**)
$R_1 =$  (**45**)	$R_1 =$  (**60**)
$R_1 =$  (**46**)	$R_1 =$  (**61**)
$R_1 =$  (**47**)	
$R_1 =$  (**48**)	

Scheme 3. *Reagents and Reaction conditions:* ***a***) appropriate amine, base, *N*,*N*-dimethylformamide, 20–90 °C, 1–18 h, 12–50%.

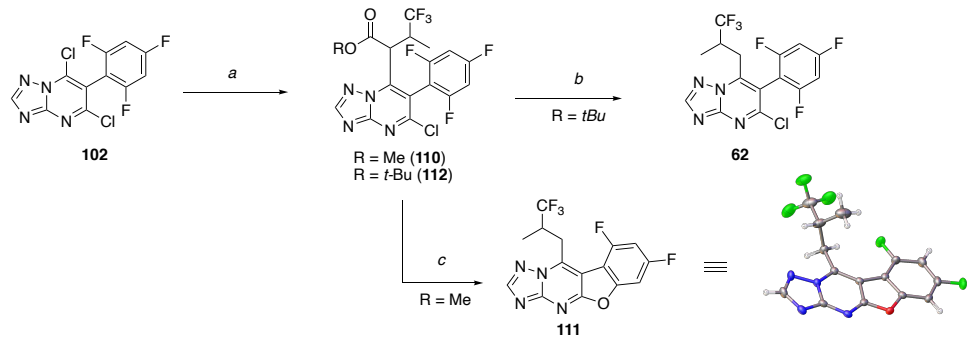

Scheme 4. *Reagents and Reaction conditions:* ***a***) appropriate ester of 4,4,4-trifluoro-3-methylbutanoic acid, HMDS, *n*-BuLi, THF, -78 ˚C, 2.5 h, 70% for **110**, 25% for **112**; ***b)*** TFA, CH_2Cl_2, 20 ˚C, 16 h, 68%; ***c)*** LiCl, DMSO, 130 ˚C (microwave irradiation), 3 h, 76%.

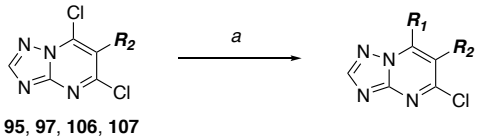

Cpd #	R_1	R_2
63		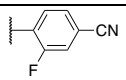
64		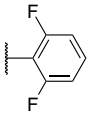
65		
66		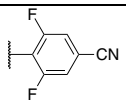
67		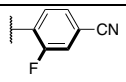
68		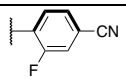
	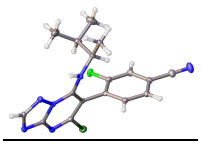	

69	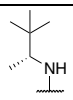	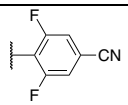
70		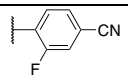
71	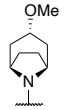	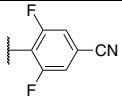
72		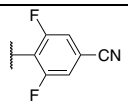
73		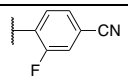
74	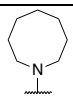	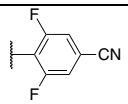
75		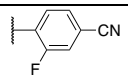

Scheme 5. *Reagents and Reaction conditions:* ***a***) appropriate amine, *N*,*N*-dimethylformamide, r.t., 1 h, 56–86%.

Results. All test compounds were evaluated in a previously described[11] cell-based assay of MT-stabilization, in which compound-dependent changes in tubulin polymerization and total tubulin levels were determined after 4 h of incubation of QBI293 cells with 1 and 10 μM compound via quantification of acetylated α-tubulin (AcTub) and total α-tubulin (α-Tub) in cell lysates by ELISA. Although the changes in AcTub levels of compound-treated cells relative to DMSO-treated cells provide a valid assessment of the MT-stabilizing activity of test compounds, day-to-day differences in the responsiveness of cells to MT-stabilizing treatment can result in occasional variability in the fold-change in AcTub levels. Thus, to account for this variability and ultimately enable a ranking of different triazolopyrimidines based on MT-stabilizing activity, compound-dependent changes in AcTub levels relative to DMSO-treated cells

(*i.e.*, negative control) were also normalized to the corresponding changes caused by 100 nM of cevipabulin (**5**), which was routinely used as positive control.[10]

Previous evaluations of the MT-stabilizing activity of selected examples of triazolopyrimidines in this assay suggested that the nature of the substituent in the *para* position of the fluorinated phenyl can elicit one of two distinct cellular responses: one characterized by a linear concentration-dependent increase of markers of stable MTs (*i.e.*, acetylated- and detyrosinated-α-tubulin) with no effect on total tubulin levels, which is typically observed with triazolopyrimidines such as **3** and **7**; and a second response caused by compounds bearing the alkoxy side-chain (*e.g.*, **5** and **6)** that is characterized by a proteasome-dependent degradation of tubulin that is often associated with the appearance of a bell-shaped concentration-response relationship in the AcTub assay.[11] To facilitate the presentation and discussion of the SAR results, we will refer here to these two distinct cellular responses as "Class I" and "Class II", respectively, and triazolopyrimidines **7** and **6** are used as defining examples of these classes.

Table 1. MT-stabilizing activity of triazolopyrimidines modified at C6. Fold-changes in acetylated α-tubulin (AcTub) and total α-tubulin (α-Tub) levels in QBI293 cells after 4 h incubation with test compounds at either 1 or 10 μM. Reported values for AcTub and α-Tub represent the fold-change over control (DMSO)–treated cells (*p<0.05 and**p<0.01 by one-way ANOVA); numbers in parentheses represent the fold-change of AcTub over positive control-treated cells (*i.e.*, 100 nM of **5**).

Cpd #	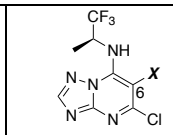	***AcTub***		***α-Tub***		***Class[a]***
		1 μM	***10 μM***	***1 μM***	***10 μM***	
6	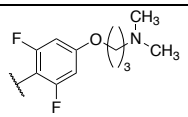	13.2 ± 1.8** (1.28)	1.92 ± 0.14 (0.19)	0.74 ± 0.05**	0.40 ± 0.01**	II
7	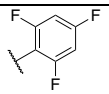	2.78 ± 0.17** (0.45)	5.04 ± 0.45** (0.82)	1.18 ± 0.09	1.22 ± 0.18	I
8		1.11 ± 0.04 (0.12)	2.07 ± 0.10** (0.30)	1.09 ± 0.03	1.03 ± 0.02	I

9	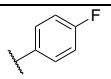	1.05 ± 0.05 (0.07)	2.41 ± 0.13** (0.16)	1.04 ± 0.06	1.13 ± 0.06	I
10		1.73 ± 0.02* (0.13)	3.56 ± 0.08** (0.26)	1.09 ± 0.01	1.05 ± 0.06	I
11	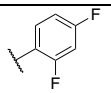	1.54 ± 0.05 (0.13)	3.19 ± 0.18** (0.27)	0.99 ± 0.02	0.86 ± 0.01	I
12		2.20 ± 0.13 (0.16)	5.28 ± 0.54** (0.39)	1.06 ± 0.14	1.02 ± 0.04	I
13	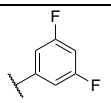	1.52 ± 0.074 (0.12)	3.97 ± 0.82* (0.30)	1.12 ± 0.13	1.12 ± 0.02	I
14	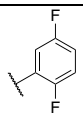	1.40 ± 0.38 (0.07)	4.10 ± 0.44* (0.22)	1.05 ± 0.11	0.90 ± 0.06	I
15	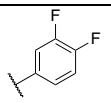	1.85 ± 0.09 (0.05)	4.76 ± 0.62** (0.12)	1.01 ± 0.08	1.13 ± 0.06	I
16	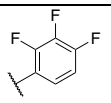	1.50 ± 0.03 (0.12)	4.28 ± 0.33** (0.34)	1.11 ± 0.05	0.88 ± 0.04	I
17	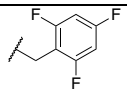	1.26 ± 0.06 (0.09)	1.43 ± 0.02 (0.10)	1.01 ± 0.07	1.05 ± 0.04	NA
18	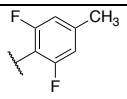	1.62 ± 0.18** (0.28)	2.73 ± 0.18** (0.48)	0.99 ± 0.09	0.78 ± 0.07*	II
19	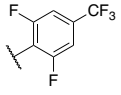	1.09 ± 0.04 (0.13)	1.39 ± 0.11* (0.16)	1.06 ± 0.02	1.02 ± 0.03	I
20	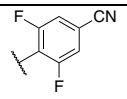	1.90 ± 0.06* (0.27)	3.56 ± 0.31** (0.51)	0.94 ± 0.02	0.95 ± 0.05	I
21	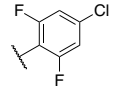	1.88 ± 0.03** (0.31)	4.28 ± 0.17** (0.70)	0.93 ± 0.02	0.81 ± 0.06**	II
22	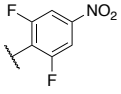	3.24 ± 0.36** (0.60)	6.65 ± 0.45** (1.23)	0.96 ± 0.01	0.94 ± 0.05	I

23	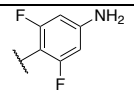	0.94 ± 0.27 (0.17)	0.69 ± 0.37 (0.13)	0.97 ± 0.03	0.96 ± 0.02	NA
24	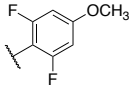	3.16 ± 0.29** (0.64)	2.07 ± 0.07** (0.42)	0.72 ± 0.09**	0.51 ± 0.05**	II
25	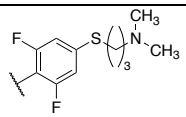	3.90 ± 0.66** (0.90)	1.49 ± 0.48 (0.34)	0.83 ± 0.05*	1.07 ± 0.02	II
26	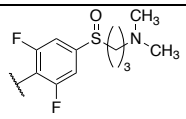	1.49 ± 0.48 (0.34)	1.39 ± 0.11 (0.32)	1.22 ± 0.06	0.98 ± 0.24	NA
27	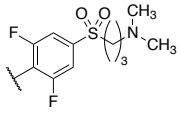	1.13 ± 0.10 (0.24)	1.08 ± 0.11 (0.23)	0.70 ± 0.58	1.07 ± 0.07	NA
28	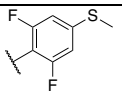	1.75 ± 0.37* (0.27)	2.23 ± 0.15** (0.35)	0.88 ± 0.05*	0.56 ± 0.06**	II
29	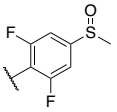	0.84 ± 0.21 (0.21)	0.87 ± 0.21 (0.21)	0.96 ± 0.02	0.93 ± 0.03	NA
30	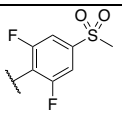	1.21 ± 0.38 (0.19)	1.23 ± 0.37 (0.19)	1.03 ± 0.02	1.02 ± 0.04	NA
31	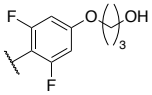	7.25 ± 0.23** (1.34)	1.33 ± 0.15 (0.25)	0.73 ± 0.06**	0.37 ± 0.02**	II
33	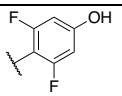	1.22 ± 0.73 (0.23)	4.11 ± 0.76** (0.77)	0.84 ± 0.07	0.57 ± 0.02**	II

[a] Class I compounds are those producing a concentration-dependent increase in AcTub levels and that do not cause >15% reduction in α-tubulin at either concentration; Class II compounds are those that cause >15% decrease in α-tubulin at either 1 or 10 μM compound concentration. NA = not applicable as the test compound does not cause significant changes in AcTub or total α-tubulin when tested at 1 or 10 μM concentration.

Table 2. MT-stabilizing activity of triazolopyrimidines modified at C7. Fold-changes in acetylated α-tubulin (AcTub) and α-tubulin (α-Tub) levels in QBI293 cells after 4 h incubation with test compounds at either 1 or 10 μM. Reported values for AcTub and α-Tub represent the fold-change over control (DMSO)–treated cells (*p<0.05 and**p<0.01 by one-way ANOVA); numbers in parentheses represent the fold-change of AcTub over positive control-treated cells (*i.e.*, 100 nM of **5**).

Cpd #	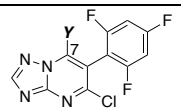	***AcTub***		***α-Tub***		***Class[a]***
		1 μM	***10 μM***	***1 μM***	***10 μM***	
3		2.14 ± 0.15* (0.59)	2.57 ± 0.15* (0.71)	1.10 ± 0.17	0.90 ± 0.16	I
34		1.18 ± 0.01 (0.09)	1.12 ± 0.08 (0.08)	1.08 ± 0.07	1.05 ± 0.02	NA
35		1.15 ± 0.15 (0.15)	2.01 ± 0.17** (0.27)	0.92 ± 0.10	0.98 ± 0.03	I
36		1.15 ± 0.07 (0.27)	1.14 ± 0.14 (0.26)	1.14 ± 0.23	0.86 ± 0.24	NA
37		1.63 ± 0.14** (0.38)	2.28 ± 0.17** (0.53)	1.30 ± 0.04	0.99 ± 0.25	I
38		1.04 ± 0.04 (0.17)	1.03 ± 0.08 (0.17)	1.06 ± 0.03	1.02 ± 0.05	NA
39		1.09 ± 0.01 (0.07)	1.31 ± 0.47 (0.09)	1.00 ± 0.03	0.97 ± 0.07	NA
40	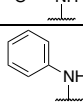	1.14 ± 0.26 (0.09)	1.05 ± 0.06 (0.08)	1.10 ± 0.17	0.96 ± 0.01	NA
41	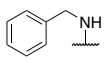	1.05 ± 0.16 (0.16)	1.49 ± 0.04* (0.22)	1.00 ± 0.12	1.06 ± 0.06	I
42		0.91 ± 0.04 (0.19)	1.01 ± 0.07 (0.21)	1.03 ± 0.04	1.04 ± 0.05	NA
43		1.28 ± 0.09 (0.30)	1.82 ± 0.10** (0.35)	1.19 ± 0.13	1.17 ± 0.01	I
44		1.32 ± 0.26 (0.30)	1.50 ± 0.09* (0.35)	0.92 ± 0.12	1.09 ± 0.03	I
45		1.32 ± 0.14 (0.06)	3.49 ± 0.07** (0.15)	0.95 ± 0.01	0.89 ± 0.01*	I
46		3.12 ± 0.25** (0.17)	6.78 ± 0.18** (0.38)	1.04 ± 0.01	1.06 ± 0.01	I
47		2.79 ± 0.04** (0.16)	13.0 ± 0.54** (0.73)	1.10 ± 0.09	0.61 ± 0.02**	II
48		1.39 ± 0.11 (0.24)	2.47 ± 0.10* (0.43)	1.23 ± 0.21	1.47 ± 0.06*	I
49		0.98 ± 0.07 (0.26)	1.22 ± 0.02* (0.32)	0.96 ± 0.07	1.17 ± 0.05	I

50		1.14 ± 0.37 (0.07)	2.74 ± 0.23* (0.16)	1.12 ± 0.31	1.18 ± 0.10	I
51		2.21 ± 0.36 (0.13)	5.84 ± 1.38** (0.33)	1.23 ± 0.05	1.20 ± 0.22	I
52		4.16 ± 0.97** (0.45)	6.87 ± 0.04** (0.74)	0.99 ± 0.03	0.99 ± 0.04	I
53		3.70 ± 0.32** (0.36)	7.16 ± 0.11** (0.70)	1.01 ± 0.14	1.28 ± 0.03**	I
54	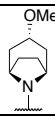	3.65 ± 0.15** (0.54)	7.43 ± 0.93** (1.11)	1.12 ± 0.08	1.38 ± 0.19**	I
55		1.17 ± 0.15 (0.07)	1.27 ± 0.06 (0.07)	1.20 ± 0.03	1.26 ± 0.03	NA
56		0.97 ± 0.15 (0.13)	1.75 ± 0.03** (0.23)	0.94 ± 0.01	0.95 ± 0.02	I
57		2.03 ± 0.04* (0.27)	4.83 ± 0.04** (0.45)	1.03 ± 0.02	0.98 ± 0.02	I
58		1.13 ± 0.11 (0.07)	3.51 ± 0.19** (0.23)	1.07 ± 0.05	0.99 ± 0.05	I
59	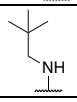	2.04 ± 0.11* (0.30)	4.79 ± 0.74** (0.71)	1.03 ± 0.07	1.06 ± 0.08	I
60		5.70 ± 0.27** (0.56)	8.42 ± 0.20** (0.83)	0.97 ± 0.02	1.08 ± 0.03	I
61[§]		3.36 ± 0.13** (10 μM) (0.43)	4.29 ± 0.04** (30 μM) (0.55)	1.08 ± 0.05 (10 μM)	1.22 ± 0.03 (30 μM)	I
62		2.30 ± 0.59* (0.53)	2.29 ± 0.38* (0.53)	1.03 ± 0.07	0.78 ± 0.05	II

[a] Class I compounds are those producing a concentration-dependent increase in AcTub levels and that do not cause >15% reduction in α-tubulin at either concentration; Class II compounds are those that cause >15% decrease in α-tubulin at either 1 or 10 μM compound concentration. NA = not applicable as the test compound does not cause significant changes in AcTub or total α-Tub when tested at 1 or 10 μM concentration. [§] Test compound was tested at 10 and 30 μM.

Since the replacement of the alkoxy side-chain of **5** or **6** (Class II) with a fluorine atom (as in **7**, Class I) was found to produce a profound impact in the MT-stabilizing activity of the triazolopyrimidine compounds,[11] our investigations of SARs began by synthesizing and testing selected analogues (**18**–**33**,

Table 1) that could help identify specific stereoelectronic characteristics of the substituent in the *para* position of the fluorinated phenyl ring that may be necessary/sufficient to impart Class I activity. Evaluation of these compounds in the QBI293 assay of MT-stabilization revealed a possible general trend indicating that active congeners bearing electron-donating groups at the *para* position generally elicit a significant (*i.e.*, >15%) loss of α-tubulin levels when tested at either 1 and/or 10 μM concentration, which is characteristic of Class II compounds. For example, both *para* hydroxyl- (**33**) and methoxy- (**24**) derivatives, as well as thioalkyl compounds, **25** and **28**, were all found to produce >20% reduction in cellular α-tubulin. In contrast, active analogues bearing electron-withdrawing groups, such as cyano (**20**) and nitro (**22**) were found to increase AcTub levels without producing a significant reduction in α-tubulin levels (*i.e.*, Class I phenotype). However, in cases such as **21**, where the chloro substituent produces opposite mesomeric (+M) and inductive (–I) effects, a comparatively more moderate but still significant loss of α-tubulin (19%) was observed when the compound was tested at 10 μM concentration. These results indicate that the electronic properties of the substituent in *para* may play an important role in determining the phenotypic response. However, differences in the shape/volume and/or the geometry of hydrogen bonding of the substituent can modulate significantly the MT-stabilizing activity, independent of the phenotype. This is best represented by comparing selected pairs of compounds, such as nitrile (**20**) and sulfone (**30**), or alkyl-sulfone (**27**) and the corresponding alkoxy compound (**6**). Docking studies (*vide infra*) indicate that the larger volume of the sulfone moiety is likely to affect negatively the interaction of the triazolopyrimidine with the binding site.

To investigate the effect of the degree and pattern of fluorination of the phenyl ring at C6, compounds **8**–**16** were evaluated in comparison with Class I control compound, **7**. The results of these studies, summarized in Table 1 and Figure 2, show that all compounds within this series maintain MT-stabilizing activity that is qualitatively similar to **7** (*i.e.,* all compounds elicit Class I phenotype); however, depending on the number and position of the fluorine atoms, these triazolopyrimidine congeners can differ significantly in terms of potency. In general, the Class I MT-stabilizing activity appears to increase with the number of fluorine atoms in the ring, with a preferred arrangement within the series being the 2,4,6-

trifluorophenyl (Figure 2). Among derivatives bearing a mono-fluorinated phenyl fragment at C6, the *ortho* fluoro derivative (**10**) appeared to be more active than the corresponding *para* substituted compound (**9**) at both 1 and 10 μM concentrations. Likewise, among triazolopyrimidines bearing a di-fluorinated phenyl at C6 (**11**–**15**), the 2,6-difluoro compound (**12**) was found to be the most active. Finally, homologation of the 2,4,6-trifluorophenyl of **7** to the corresponding 2,4,6-trifluorobenzyl congener (**17**) led to a drastic reduction of MT-stabilizing activity.

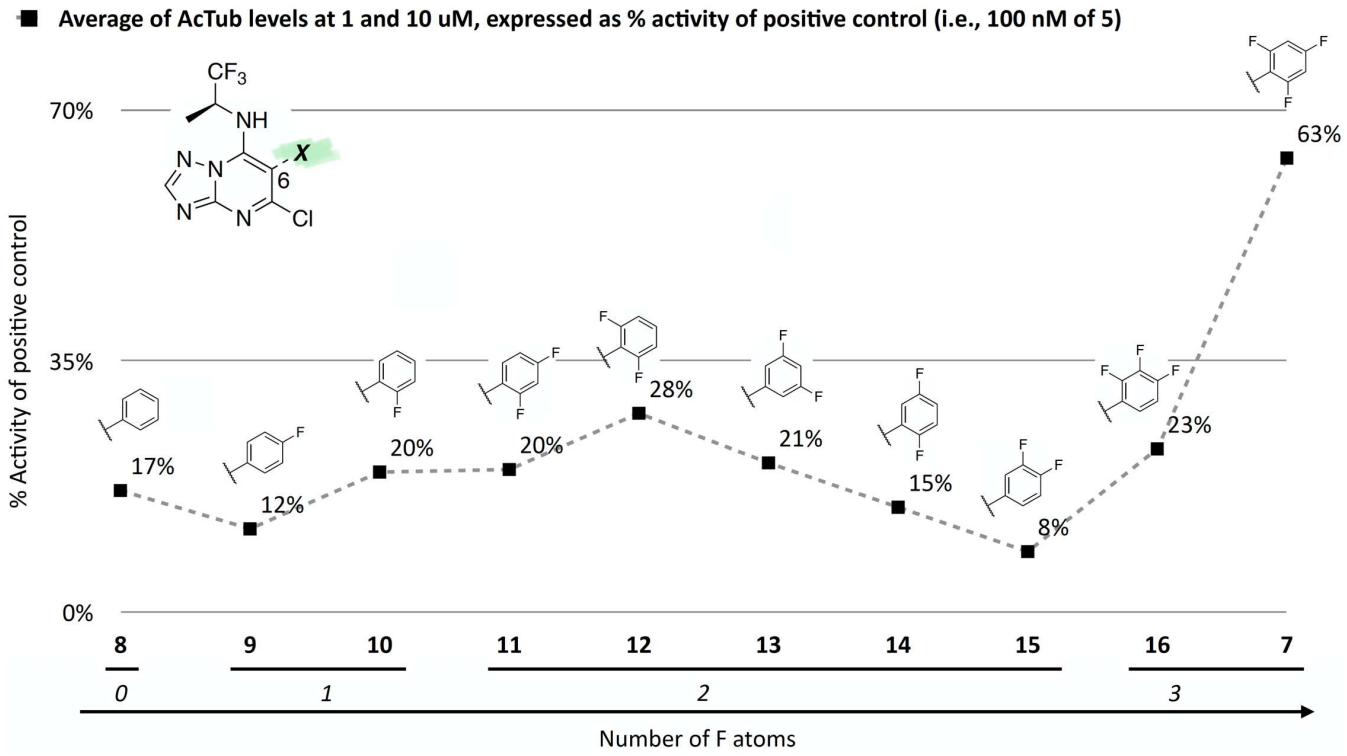

Figure 2. Effect of fluorination of the aryl group at C6 on MT-stabilizing activity of Class I triazolopyrimidines. Black squares indicate the average activity of test compounds at 1 and 10 μM, normalized to the activity of 100 nM of **5** (positive control).

Comparative evaluation of Table 2 compounds (**3**, **34**–**62**) and **7** in the cell-based MT-stabilization assay helped define several SAR elements of the fragment linked at the C7 position of the triazolopyrimidine ring. Truncation of this fragment as in **34** and **38** led to a dramatic loss of MT-stabilizing activity. Replacement of the nitrogen atom at C7 of control compound, **7**, with an oxygen atom (**42**) revealed that the ether linkage is not permitted as it resulted in a drastic reduction of activity in the cellular assay.

Conversely, replacement of the nitrogen atom at C7 with a methylene, as in **62**, showed that the alkyl linkage allows for retention of significant activity in the AcTub assay at both 1 and 10 μM. However, this compound was found to cause a significant reduction of α-tubulin (*i.e.*, ~22%) when tested at 10 μM. These observations demonstrate that the nature of the fragment linked at C7 can play an important role in determining both potency as well as cellular phenotype elicited by MT-active triazolopyrimidines, and that the presence of a substituted nitrogen at this position may be a necessary condition for Class I activity.

Further investigation of the SAR of triazolopyrimidines featuring a substituted nitrogen at C7 included a comparison between selected aliphatic and aromatic amines, as well as amides. Comparison of lead compound **3** with amide derivative, **39**, indicates that aliphatic amines may be preferred over amides. Likewise, comparison of aniline derivative, **40**, with the corresponding cyclohexyl amine congener, **58**, shows that whereas the former is essentially devoid of activity at both 1 and 10 μM, the aliphatic derivative, **58**, is significantly active at 10 μM without decreasing α-tubulin levels. These results suggest that aliphatic amines at C7 may be generally preferred and, as a result, further exploration of the SAR focused on identifying the key requisites of the aliphatic amine fragment, which included an evaluation of linear, branched, and cyclic amines of different sizes. Comparison of the *in vitro* MT-stabilizing activity of lead compound, **3**, with congeners featuring amine substituents at C7 that are either substructures (*i.e.*, **35**–**37**) or that are incrementally larger fragments than the C7 substituent of **3** (*e.g.*, **60**) clearly suggest that the MT-stabilizing activity of triazolopyrimidines may increase with the size and branching of the aliphatic fragment. As highlighted in Figure 3, the extreme examples within this series are the linear amine derivative, **36**, which is devoid of MT-stabilizing activity in the QBI293 assay, and the *t*-butyl derivative, **60**, which exhibits relatively potent activity as revealed by the marked increases in AcTub levels at both 1 and 10 μM concentrations. A similar trend also emerges from the comparison of series of *homologs* featuring different endo- (*i.e.,* **49**–**54**) or exo-cyclic (*i.e.*, **55**–**58**) amines. Within each of these series, relatively bulky fragments led to marked elevations of AcTub levels. However, comparison of the average MT-stabilizing activity at 1 and 10 μM, relative to positive control, suggested that the optimal ring size in the endo- and exo-cyclic amine series may be different. Whereas in the exocyclic amine series, the 5-

membered ring (**57**) seemed optimal, in the case of endocyclic amines, the presence of a 7-membered ring system (**52**) or a fused bicyclic system (**54**) produced the highest activity (Figure 3). Finally, an evaluation of the effect of fluorination and chiral configuration of the branched amine fragment at C7 was also conducted. Comparison of **7**, which features a fluorinated isopropyl amine at C7, with corresponding analogues **43**, **44**, and **35** that exhibit either 2, 1 or no fluorine substituents in the amine fragment indicates the general trend linking the degree of fluorination of the amine fragment with potency. Similarly, fluorination of **45** resulted in a comparatively more potent congener (**46**). With respect to the chiral configuration, in the majority of cases examined the chirality of the amine was found to influence the potency of the compound with one enantiomer being typically more active than the other (*cf.*, **3** and **45**; **7** and **48**; **60** and **61**). In one case, however, the chiral configuration of the amine substituent of **46** (*R*) and **47** (*S*) was also found to impact significantly the cellular phenotype. Whereas the *R*-enantiomer was found to be relatively potent in the AcTub QBI293 assay without evidence of a reduction in α-tubulin levels, the opposite enantiomer (*S*) produced a marked reduction in cellular α-tubulin of approximately ~39% when tested at 10 μM, suggesting that **47** is likely to negatively impact MT-integrity. Notwithstanding this notable exception, all other MT-active triazolopyrimidines shown in Table 2 that feature an amine fragment at C7 were found to be MT-stabilizing without producing losses in α-tubulin.

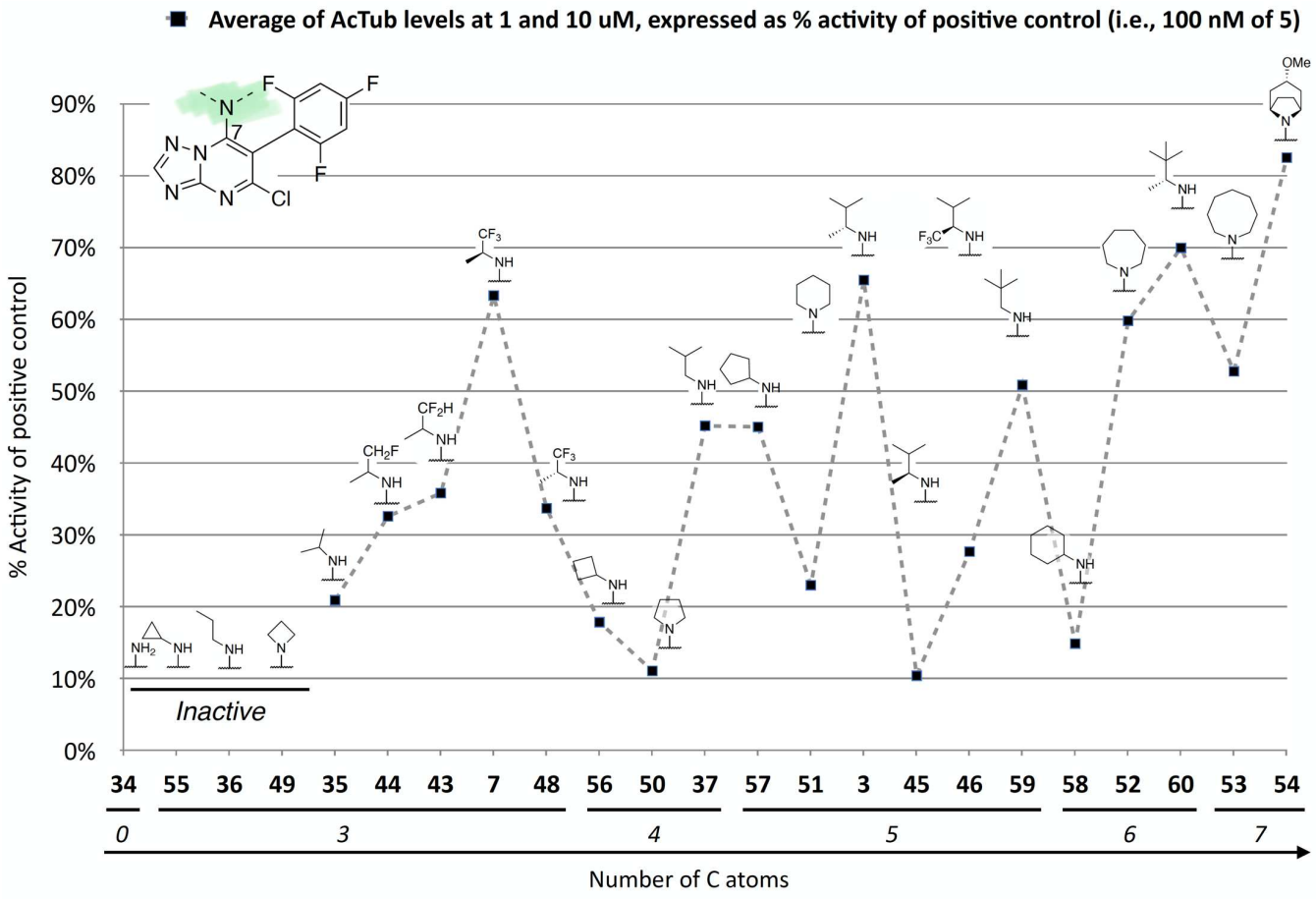

Figure 3. The effect of both branching of aliphatic acyclic amines and homologation of endo- and exo-cyclic amines on MT-stabilizing activity of Class I triazolopyrimidines. Test compounds are ordered along the X-axis based on the number of carbon atoms in the amine fragment. Black squares indicate the average activity of test compounds at 1 and 10 μM, normalized to the activity of 100 nM of **5** (positive control). Compounds that did not produced a statistically significant elevation in AcTub at either 1 or 10 μM are not plotted and marked as inactive.

Having identified the main characteristics of both the C6 and C7 fragments that may be required to obtain Class I MT-stabilizing triazolopyrimidines, a focused series of derivatives was designed by combining the most promising C6 and C7 fragments. In particular, since the C6 fragment SAR studies highlighted the importance of a fluorine atom in the *ortho* position of the phenyl ring, whereas the *para* position may be left unsubstituted or occupied by an electron-withdrawing group, such as a fluorine, a nitro or a nitrile, we chose, in addition to the 2,4,6-trifluorophenyl fragment, the corresponding 2-fluoro-,

2,6-difluoro-, 2-fluoro-4-cyano-, and 2,6-difluoro-4-cyano-phenyl C6 fragments. Likewise, among the amine fragments at C7, all instances that by matched molecular pair analysis were found to produce comparable or better activity than **3** (*i.e.*, **7**, **52**–**54** and **60**) were selected. By systematically combining the preferred set of C6 and C7 fragments, a panel of 25 compounds could be designed that based on SAR findings would be expected to exhibit relatively potent Class I MT-stabilizing activity. As summarized in Table 3, several examples (13) from this set were synthesized and tested. In all cases, these compounds were confirmed to be active Class I triazolopyrimidines. Nine analogues exhibited comparable (*i.e.*, **66**, **67**, **73**, and **74**) or improved (*i.e.*, **64**, **69** and **70**–**72**) *in vitro* potency compared to lead compound **3**, with **72** being particularly effective in the AcTub assay when tested at either 10 or 1 μM. Evaluation of individual atropoisomers, **67** and **68**, indicated that the former may be more potent than the latter. Among derivatives bearing fluorinated cyanobenzene fragments at C6, evaluation of a representative example (**69**) in primary neurons confirmed that compounds of this type increase AcTub levels and prevent the characteristic loss of neuronal MTs that is observed after incubation with the phosphatase inhibitor, okadaic acid (Figure 4). Although the cellular data do not allow for resolution of detailed MT structure, the AcTub staining clearly shows that incubation with **69** protects the MT network from okadaic acid-induced collapse (Figure 4).

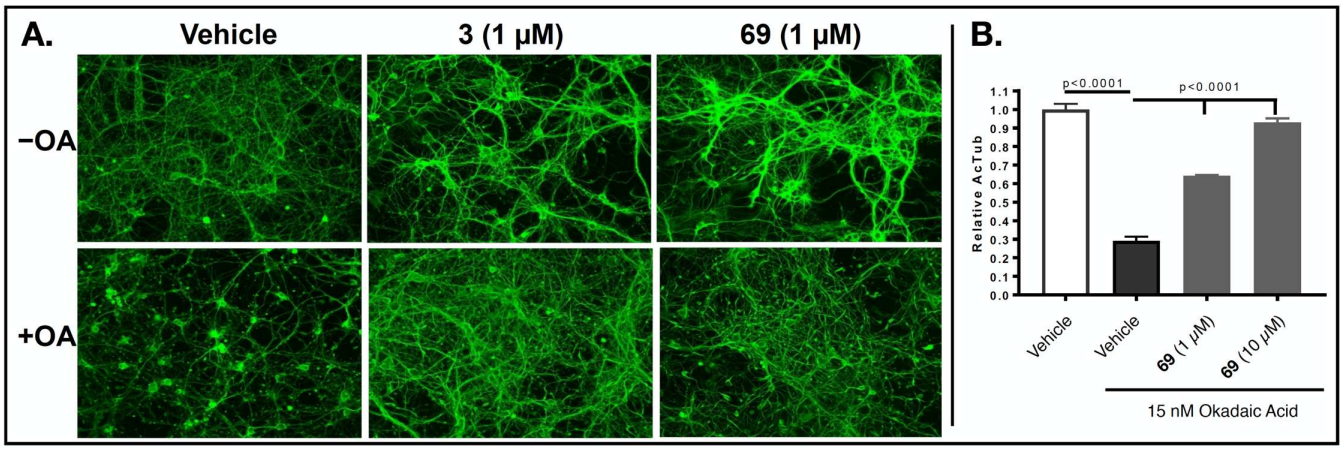

Figure 4. To confirm that the nitrile containing triazolopyrimidine derivatives identified in these studies can stabilize neuronal MTs under conditions of tau loss-of-function, we examined the ability of representative compound, **69**, to prevent the MT collapse that occurs from reduced binding of

hyperphosphorylated tau to axonal MTs after treatment of neuron cultures with the phosphatase inhibitor, okadaic acid (OA). **A.** Primary rat cortical neurons treated with 1 μM reference compound **3**, or **69** in the absence of OA (−OA) show increased axonal acetyl-tubulin staining relative to those receiving vehicle only. Upon treatment with OA (+OA) in the absence of compound (Vehicle), there is a dramatic reduction in axonal AcTub staining with fragmentation of MTs and neuronal processes (also see[11]). Co-addition of **3** or **69** (1 μM) with OA results in normalization of AcTub staining and axonal processes. **B.** ELISA determination of AcTub levels in homogenates from primary mouse cortical neurons treated with 1 or 10 μM of **69**, or vehicle, in the presence of OA. The higher concentration of **69** resulted in AcTub levels comparable to those in neurons without OA treatment.

Interestingly, an assessment of lipophilicity of several compounds (Figure 5), as determined by experimental determinations of the distribution coefficient between *n*-octanol and water at pH 7.4 (*i.e.*, $\log D_{7.4}$ values), revealed that the presence of a nitrile moiety in the *para* position of the phenyl ring at C6 produces a significant lowering of $\log D_{7.4}$ values that becomes more pronounced in 2,6-difluorophenyl congeners, such as **66**, **69** and **72**.

Table 3. MT-stabilizing activity of triazolopyrimidines modified at C7 and/or C6. Fold-changes in acetylated α-tubulin (AcTub) and α-tubulin (α-Tub) levels in QBI293 cells after 4 h incubation with test compounds at either 1 or 10 μM. Reported values for AcTub and α-Tub represent the fold-change over control (DMSO)–treated cells (*p<0.05 and**p<0.01 by one-way ANOVA); numbers in parentheses represent the fold-change of AcTub over positive control-treated cells (*i.e.*, 100 nM of **5**).

Cpd #	***Structure***	***AcTub***		***α-Tub***	
		1 μM	***10 μM***	***1 μM***	***10 μM***
63	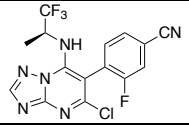	2.01 ± 0.38* (0.37)	3.64 ± 0.26** (0.67)	1.00 ± 0.01	1.00 ± 0.01

64	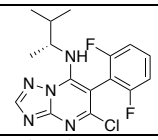	4.36 ± 0.72** (0.96)	4.88 ± 0.72** (1.07)	1.00 ± 0.02	0.96 ± 0.01
65	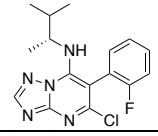	0.95 ± 0.26 (0.20)	2.10 ± 0.31** (0.43)	1.00 ± 0.04	1.04 ± 0.07
66	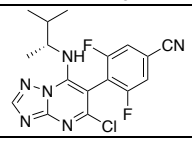	3.80 ± 0.15* (0.62)	4.28 ± 0.14** (0.69)	0.93 ± 0.02	0.94 ± 0.02
67	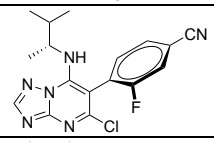	2.79 ± 1.11 (0.61)	3.42 ± 0.55* (0.75)	0.99 ± 0.02	0.93 ± 0.02
68	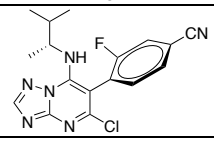	2.15 ± 0.36* (0.47)	2.29 ± 0.30* (0.50)	0.95 ± 0.02	0.92 ± 0.01
69	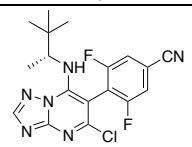	2.83 ± 0.33** (0.68)	4.60 ± 0.35** (1.10)	0.98 ± 0.03	1.03 ± 0.03
70	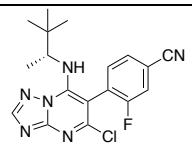	4.41 ± 0.27** (0.71)	7.67 ± 0.70** (1.24)	0.86 ± 0.03	0.93 ± 0.08
71	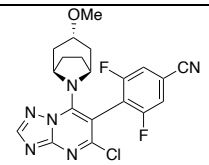	2.61 ± 0.26** (0.64)	4.32 ± 0.29** (1.06)	0.99 ± 0.01	1.00 ± 0.03
72	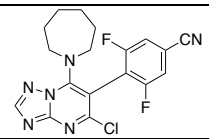	6.40 ± 0.61** (1.04)	11.2 ± 0.77** (1.82)	0.98 ± 0.03	0.99 ± 0.02
73	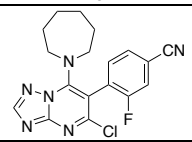	7.17 ± 1.09** (0.55)	12.6 ± 2.8** (0.97)	1.04 ± 0.05	0.99 ± 0.03
74	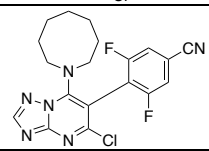	3.24 ± 0.80** (0.58)	4.40 ± 0.34** (0.79)	1.01 ± 0.02	0.99 ± 0.02
75	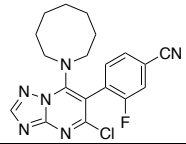	1.09 ± 0.22 (0.22)	2.89 ± 0.56** (0.59)	0.97 ± 0.02	0.95 ± 0.07

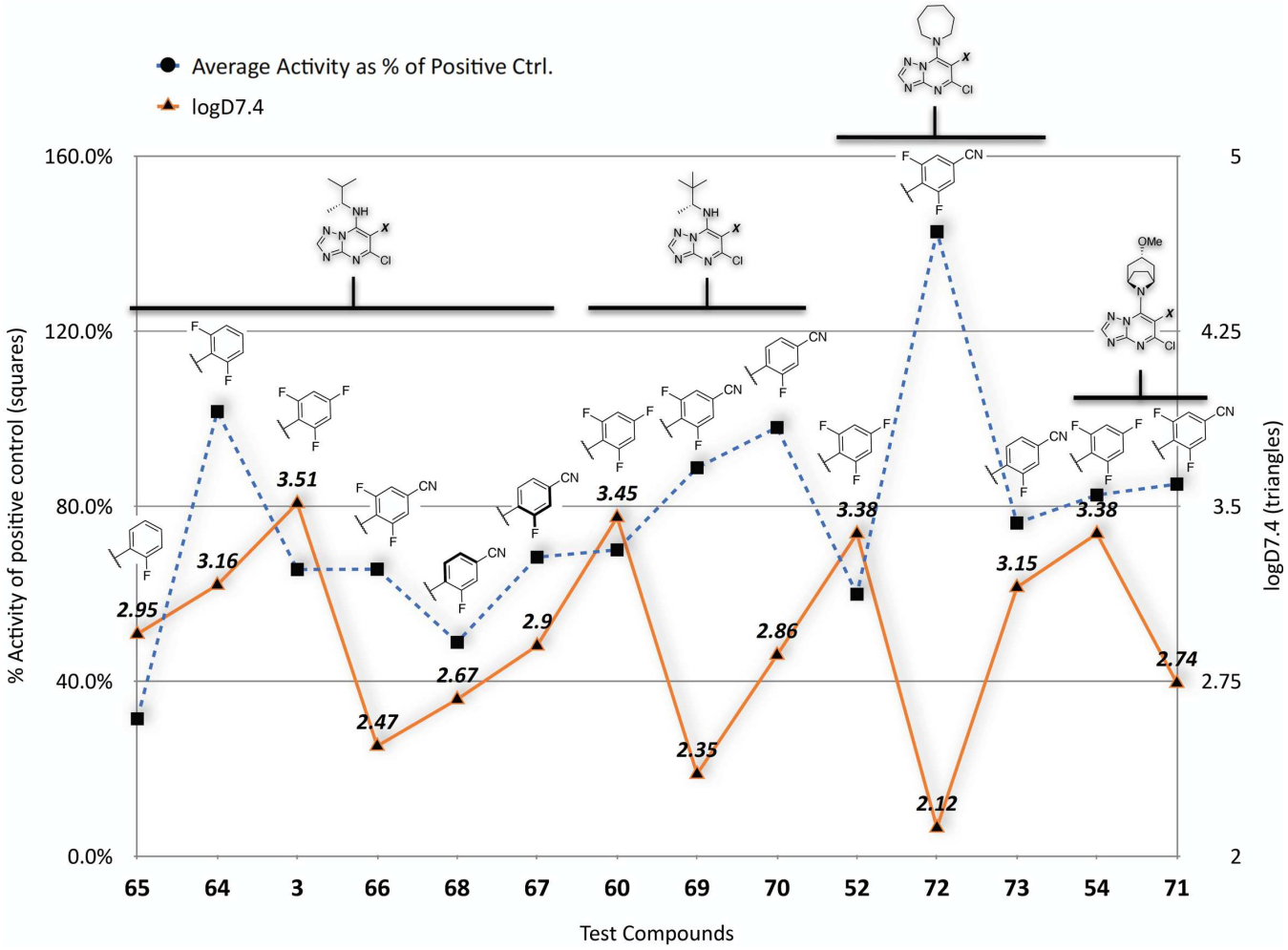

Figure 5. Comparison of selected compounds based on experimental $logD_{7.4}$ values (triangles) and MT-stabilizing activity (squares) expressed as the average activity in the AcTub assay at 1 and 10 μM normalized to positive control (*i.e.,* 100 nM **5**). $LogD_{7.4}$ values were determined via shake flask method (experiments run by Analiza, Inc.)

Importantly, an evaluation of brain-to-plasma (B/P) ratios of selected examples 1 h after administration to mice confirmed that the nitrile derivatives **66**, **69** and **72** are readily brain penetrant with B/P values > 0.6 (Table 4). This result was confirmed by a 16 h brain and plasma PK study with **69 (**Figure 6A). Moreover, a comparison of plasma PK of lead compound **3** and **69** indicates a greater metabolic stability of the nitrile-containing congener (Figure 6B).

Table 4. The ratio between brain and plasma compound concentration 1 h after administration (i.p. injection) of test compound.

Cpd #	*i.p. dose*	*B/P*
3	5 mg/kg	2.7
66[*]	2.5 mg/kg	0.7
60	5 mg/kg	2.1
69[*]	2.5 mg/kg	0.7
52	5 mg/kg	1.4
72[*]	2.5 mg/kg	0.7

∗Cassette dosing of three compounds (**66**, **69**, and **72**)

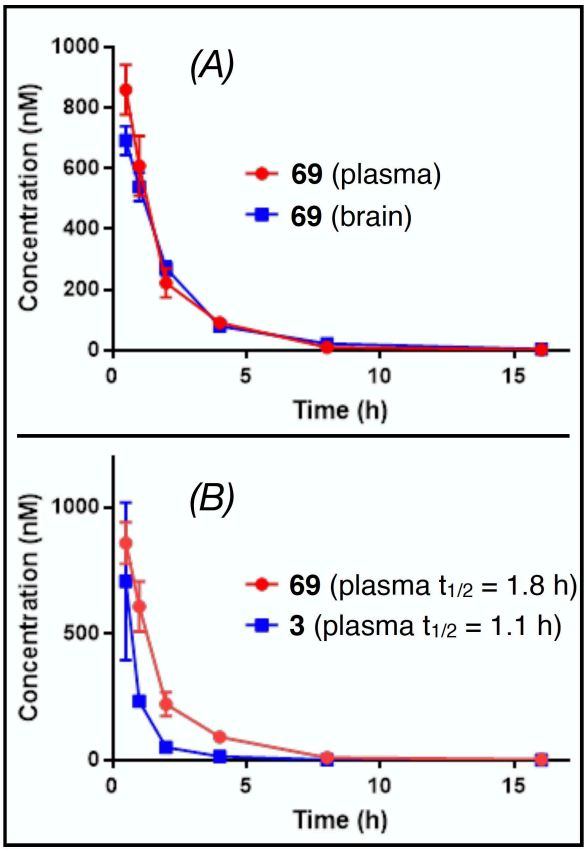

Figure 6. Brain and plasma pharmacokinetics of **69** after 5 mg/kg i.p. dosing to CD1 mice (A), and comparison of plasma pharmacokinetics of **69** and **3**.[12]

Computational Studies. To investigate the nature of the interaction of Class I triazolopyrimidines with tubulin and to develop an *in silico* model that may ultimately be predictive of MT-stabilizing activity, we conducted docking studies with both active and inactive triazolopyrimidine congeners using the X-ray co-crystal structure of a tubulin preparation in complex with Class I triazolopyrimidine **54**[13, 23] (PDB: 5NJH; Figure 7A). The X-ray studies highlighted two key π-π interactions between **54** and tubulin: one involving the pyrimidine core and Tyr224 of α-tubulin, and a second between the trifluorophenyl group and Tyr210 (α-tubulin).[13] Both of these interactions are likely essential for a correct orientation of the triazolopyrimidine derivative within the binding pocket and substituents that interfere with these critical interactions are likely to result in reduced binding and biological activity. Indeed, docking of inactive derivative, **30**, within the triazolopyrimidine binding site suggests that the relatively large volume of the sulfone moiety disrupts the critical π-π stacking interaction with the two tyrosine residues, leading to a different binding pose (Figure 7B) and, ultimately, a dramatic loss in MT-stabilizing activity. In the case of active Class I compounds, including lead compound **3** (Figure 7C), docking studies generally identify very similar binding poses and sets of interactions as seen in the co-crystal structure of **54**. However, for derivatives bearing a nitro or a nitrile at the *para* position of the fluorinated ring at C6, an additional H-bond interaction with the backbone of Glu207 (α-tubulin) is also observed, which in some cases (*e.g.*, **72**) may contribute to better ΔG of binding (Figure 7D) and MT-stabilizing activity (see Figure 5).

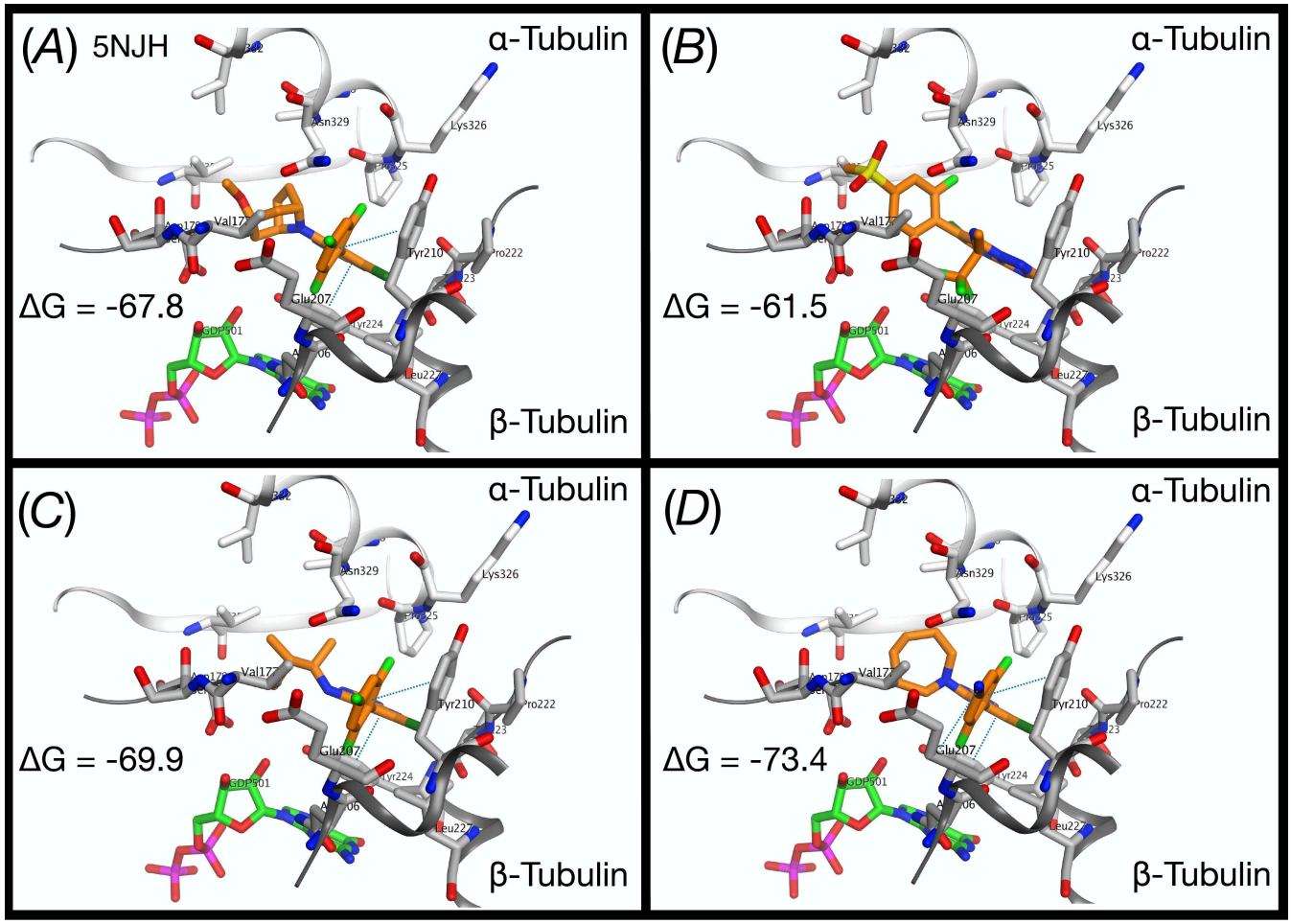

Figure 7. Different views of the co-crystal structure (PBD: 5NJH) of **54** bound within a tubulin preparation (A); and the docked structures of **30** (B), **3** (C) and **72** (D) within the triazolopyrimidine binding site.

The binding modes of the different compounds were further evaluated by calculating the free energy of binding via a "molecular mechanics generalized Born surface area" (MMGBSA) approach.[24] Interestingly, by plotting the computed MMGBSA free energetics of the Class I ligands in complex with tubulin against the MT-stabilizing activity (expressed as the average of the activity at 1 and 10 μM compound concentration in the QBI293 AcTub assay, relative to positive control), a moderately high Pearson correlation was found [$r = -0.70$, P-value (two-tailed) < 0.0001, Figure 8].

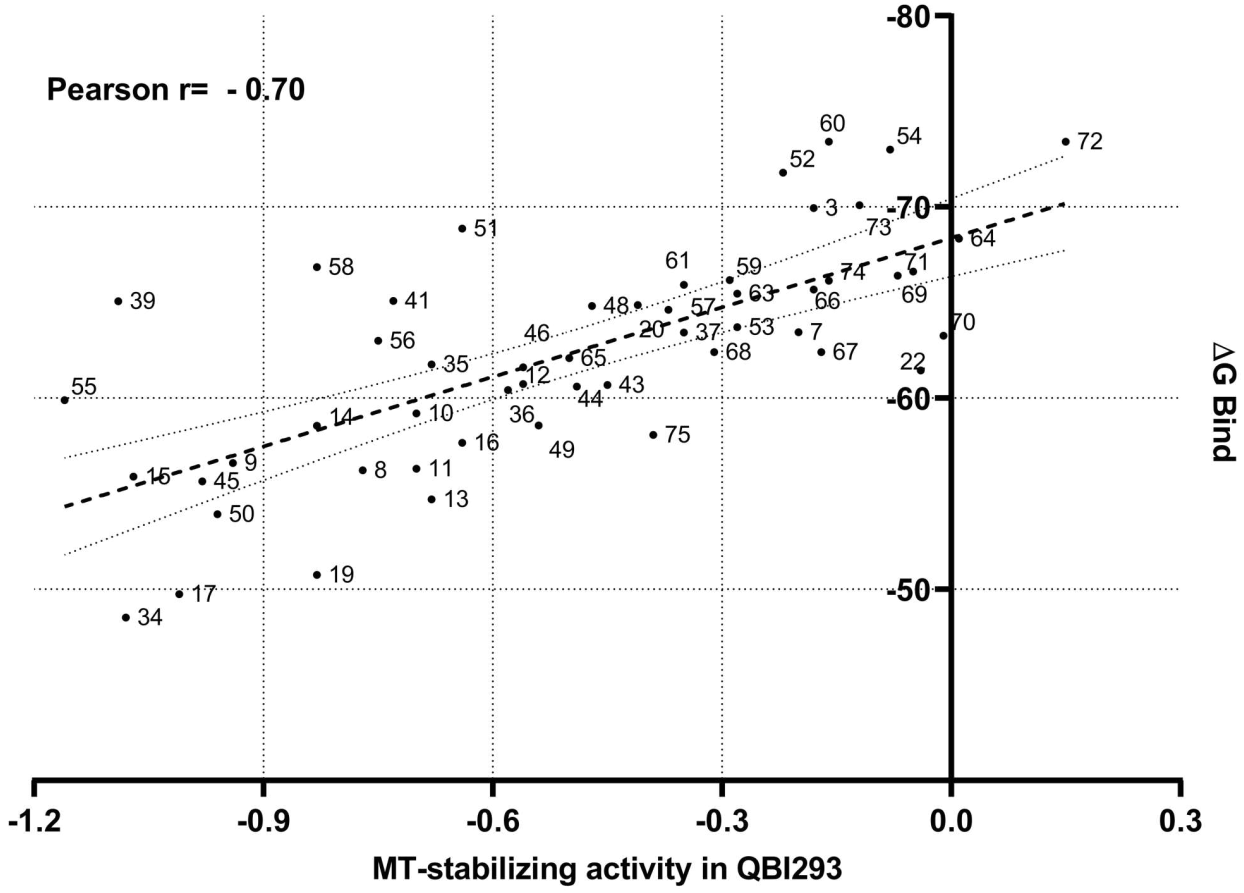

Figure 8. MMGBSA scores for the Class I compounds *vs* MT-stabilizing activity in QBI293 cells expressed as the log of the average of the activity at 1 and 10 μM in the AcTub assay, relative to positive control, $\log\left(\frac{Avg\ AcTub_{1\&10\mu M}}{AcTub_{0.1\mu M}\ \text{of}\ \mathbf{5}}\right)$.

A 3D-QSAR study was also performed through a "field points" template, obtained from the co-crystallized compound. These field points define the shape, electrostatic and hydrophobic property of the molecule and their spatial distribution.[25] For this study, 52 active and inactive Class I compounds were randomly partitioned to a training set (47) and a test set (5), while the experimental *in vitro* activity was computed using the normalized activity, expressed as the log of the average of the activity at 1 and 10 μM in the AcTub assay relative to positive control (**5**), and defined as a dependent variable. In this case, the model shows a comparatively better correlation with a Pearson r = 0.90 (Figure 9A), which was cross-validated by leave-one-out (LOO) technique, q^2= 0.62. Interestingly, the 3D-QSAR model highlighted the

following steric and electrostatic contributions to the predicted activity (Figure 9B): a favorable electrostatic contribution (green) near the *para* position of the phenyl ring at C6, and strong steric contributions of the amine fragment at C7, as indicated by the large size of the dark teal field point (Figure 9B). Importantly, the combination of the binding free energies and the QSAR models (Figure 10) appeared to accurately place all of the most active MT-stabilizing compounds identified in this study within a well-defined area of lower ΔG of binding and higher QSAR predicted activity. Thus, the combinations of these models may provide a valuable tool to guide future design of novel potent MT-stabilizing triazolopyrimidines.

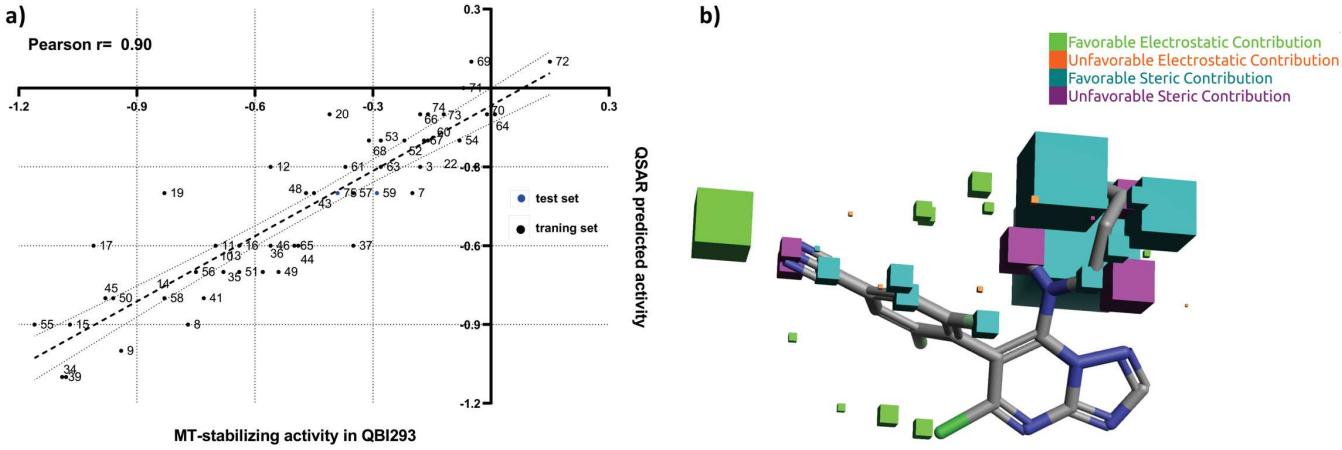

Figure 9. (A) QSAR predicted *vs* experimental MT-stabilizing activity in QBI293 cells for training and test sets. In both cases, MT-stabilizing activity is expressed as the log of the average of the activity at 1 and 10 μM in the AcTub assay, relative to positive control, $\log\left(\frac{Avg\ AcTub_{1\&10\mu M}}{AcTub_{0.1\mu M}\ \text{of}\ \mathbf{5}}\right)$. (B) The visual representation of the field and steric contributions to predicted activity for compound **72**.

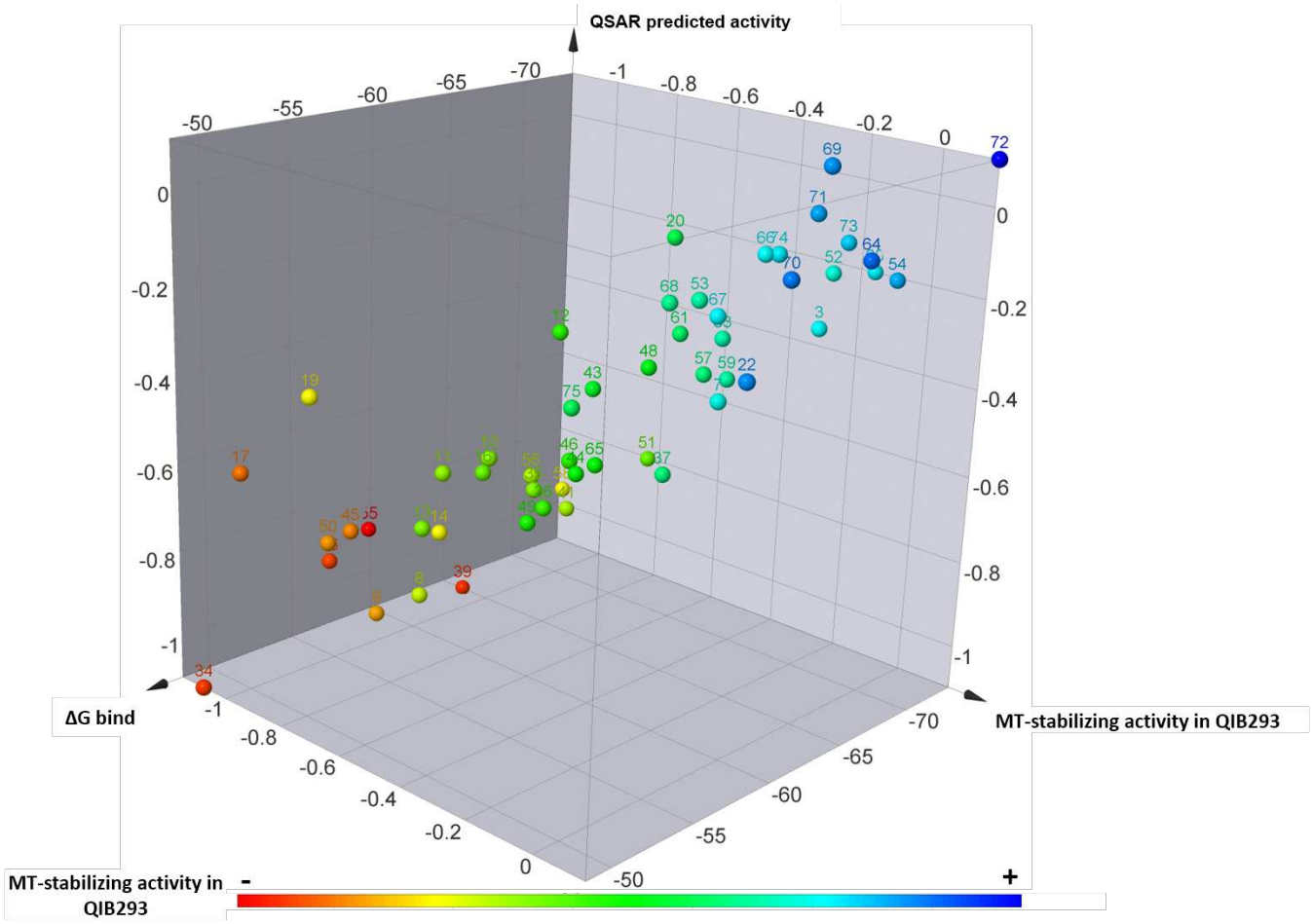

Figure 10. 3D summary plot of Class I triazolopyrimidines showing the experimental MT-stabilizing activity in the QBI293 assay, the MMGBSA score value (ΔG bind), and the QSAR predicted activity. The experimental MT-stabilizing activity of test compounds is plotted both via color coding and as the log of the average of the activity at 1 and 10 μM in the AcTub assay, relative to positive control, $\log\left(\frac{Avg\ AcTub_{1\&10\mu M}}{AcTub_{0.1\mu M}\ \text{of}\ \mathbf{5}}\right)$, see Experimental for further details.

Discussion.

CNS-active MT-stabilizing compounds have been proposed as promising therapeutic candidates to treat AD and related neurodegenerative tauopathies.[26] In this context, the essential prerequisites for compound selection and advancement are both the ability to cross the blood-brain barrier (BBB) and normalize the dynamics of MTs in the axons of neurons, such that an efficient axonal transport could be maintained or restored. MT-stabilizing triazolopyrimidines have a number of potentially attractive features as MT-

stabilizing compounds for CNS indications,[9] including synthetic tractability, a generally good brain penetration and oral bioavailability. Selected members from this class of compounds have already been the focus of mechanism-of-action[13] and SAR studies that were based largely on cell-free experiments and cytotoxicity studies in cancer cell-lines.[15, 16, 27] Although clearly informative, such studies did not provide particular insight into the effects that triazolopyrimidines can have on cellular MTs. Studies from our laboratories in which the activity of MT-active triazolopyrimidines was evaluated by monitoring compound-dependent changes in cellular levels of tubulin, as well as changes in levels of known markers of MT-stabilization, such as acetylated- and detyrosinated-α-tubulin, showed that different congeners can generally elicit one of two cellular responses discriminated by whether (Class II) or not (Class I) these compounds reduce tubulin levels.[11] Furthermore, although one selected prototype from Class I triazolopyrimidines, **3**, has proven useful in obtaining validation of this class in mouse models of AD, further characterization of the structural determinants that may be most important to impart the desired MT-stabilizing effect in cells is a necessary step that could facilitate the identification of candidates for clinical development.

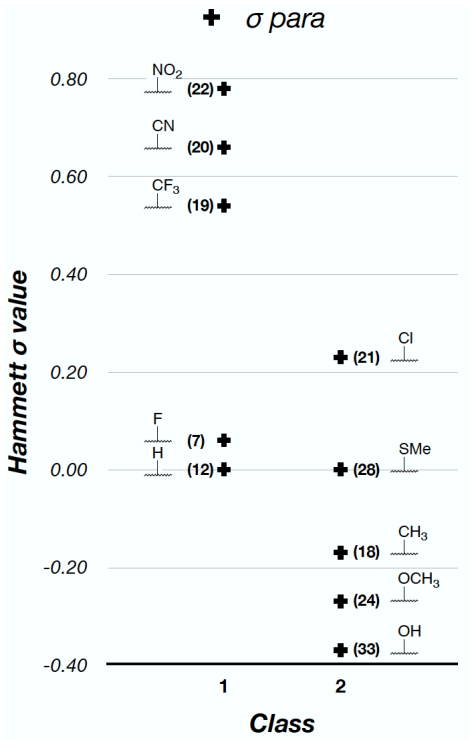

Figure 11. The effect of the stereo-electronic properties of the substituent in *para*. Active Class I and II compounds are ranked based on the Hammett σ_p values.[28]

Given that our previous studies showed that the substituent in the *para* position of the phenyl ring (C6 fragment) of triazolopyrimidines can play an important role in determining the particular cellular response (*i.e.*, Class I or II) elicited by these compounds, whereas the C7 fragment may be especially important for potency as well as ADME-PK properties,[11, 12] our exploration of SAR of triazolopyrimidines focused primarily on identifying specific features (*e.g.*, electrostatic, hydrophobic, shape) of the C6 and C7 fragments that may be preferred for Class I MT-stabilizing triazolopyrimidines. Data from the cell-based MT-stabilization assays revealed different structural and property features that appear to have a relatively high impact on the biological activity. In particular, a comparison of active congeners of either class suggests that the electrostatic characteristics of the substituent in the *para* position of the phenyl ring at C6 play an important role in determining the cellular phenotype, while the degree and pattern of fluorination can modulate potency (Figure 2). Indeed, an analysis of *in vitro* biological activity *vs* the Hammett σ values of the different substituents in *para* suggests a general trend, whereby with the sole exception of the *para*-chloro derivative, **21**, positive σ values (*e.g.,* fluorine, nitro or nitrile) are typically conducive to Class I activity, whereas σ values < 0 (*e.g.*, hydroxyl or methoxy groups) appear to be associated with Class II phenotype (Figure 11). Thus, the SAR data of the C6 fragment of triazolopyrimidines indicate that the desired Class I MT-stabilizing activity generally requires the presence of an electron-poor phenyl ring. Different fluorinated phenyl fragments can be tolerated, especially those bearing either one or two fluorine atoms in the *ortho* positions, and a *para* position that is either unsubstituted or substituted with an additional fluorine or other electron-withdrawing groups, such as nitro and nitrile.

With respect to the SAR of the fragment linked at C7, the data presented in Table 2 revealed a number of structural and property requirements for optimal MT-stabilizing activity. In particular, in addition to aliphatic amines being typically preferred (*e.g.,* over ethers or aromatic amines), a general trend emerged linking MT-stabilizing activity in cells with the lipophilic character and size of the C7 fragment (Figure 3). An interesting observation made during these studies was the fact that in specific instances the chirality

of the aliphatic amine fragment can play a role in determining the cellular phenotype elicited by the triazolopyrimidine. Although the configuration of the chiral center of the amine fragment of **3** or **7** appears to impact the potency of these compounds in the AcTub assay without affecting α-tubulin levels (*cf.,* **7** with **48**, and **3** with **45**), in selected cases, such as compounds **46** and **47**, the inversion of chiral configuration was found to cause a shift in cellular phenotype, with **46** being a Class I compound while its enantiomer, **47**, clearly produced a marked reduction (~40%) in α-Tub (Class II). Interestingly, docking studies with **46** and **47** did not reveal significant differences in binding modes that could help explain the different cellular phenotype elicited by the two enantiomers. In addition, side-by-side comparison of the cytotoxicity of enantiomers **46** (Class I) and **47** (Class II) in rapidly dividing QBI293 or HeLa cells did not reveal significant differences in IC_{50} values (Supporting Information), suggesting that both Class I and II triazolopyrimidines exhibit comparable anti-mitotic effects. These observations indicate that neither docking nor IC_{50} values in cell cytotoxicity assays should be used to predict whether a triazolopyrimidine would stabilize or disrupt the MT network. Given that such a distinction is an essential aspect driving the prioritization of candidates for neurodegenerative tauopathies, an evaluation of compounds in a cellular assay that assesses compound effect on α/β-tubulin levels as well as increases in markers of MT stabilization is ultimately a necessary step. Although such assays have some limitations, such as a relatively low-throughput and possible day-to-day variability that can be minimized by normalizing the activity of test compounds to a positive control, the SAR data generated in this study led to the identification of several characteristics that are important for Class I MT-stabilizing triazolopyrimidines. Indeed, a qualitative assessment of the combined C6 and C7 SAR data of all Class I triazolopyrimidines tested in this study, which was conducted using Activity atlas analysis,[29] identified distinct regions/characteristics that are shared by the vast majority of Class I congeners (Figure 12 A&B); these include a positive electrostatic region in the proximity of the amine fragment at C7 (indicated in red, Figure 12A), a negative electrostatic region in the proximity of the *para* position of the aryl group at C6 (cyan, Figure 12A), and two hydrophobic interaction regions near the fluorinated phenyl at C6 and the aliphatic amine fragment at C7 (yellow, Figure 12B). Furthermore, an activity cliff analysis (Figure 12C),

which highlights structural differences of similar compounds that produce a disproportionally high impact on the biological activity (*i.e.*, activity cliff regions),[30] revealed that an increase of negative electrostatic field at the *para* position of the phenyl ring (cyan), as associated with substituents like nitro and nitrile, as well as the presence of a favorable hydrophobic region in C7 (green), produce a drastic increase in MT-stabilizing activity. Collectively, these findings, combined with the development of relatively predictive models that are based on calculated binding free energies and QSAR, provide valuable insights that could facilitate the design of Class I triazolopyrimidines.

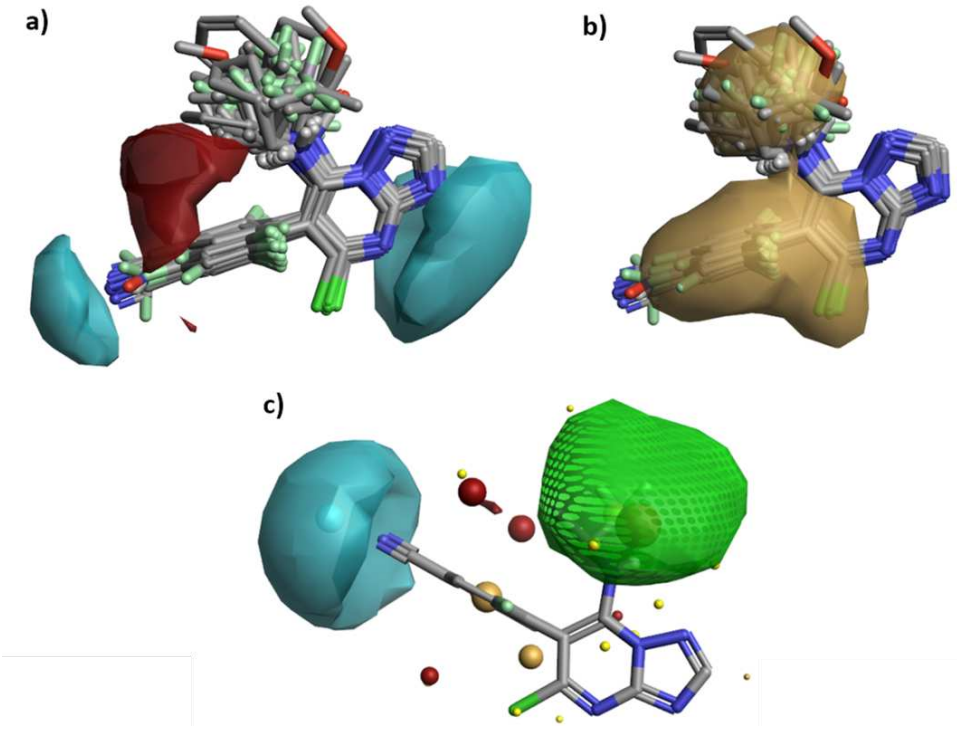

Figure 12. Activity atlas analysis revealing key features of Class I triazolopyrimidines that are necessary for MT-stabilizing activity: (a) red and cyan colors show positive and negative field regions respectively; (b) brown beige regions show hydrophobic interaction sites required for activity; (c) Activity cliffs analysis revealing a favorable hydrophobic region (green) and a favorable negative electrostatic region (cyan).

Importantly, by combining the preferred C6 and C7 fragments found in the course of these SAR studies, several new Class I triazolopyrimidine analogues have been identified (Table 3), including multiple

examples (**64**, **69** and **70**–**72**) that exhibit both improved *in vitro* activity as well as reduced lipophilic character compared to lead compound **3**. In primary cortical neurons, **69** was found to protect the MT-network against okadaic acid-induced collapse in a manner comparable to **3** (Figure 4) suggesting that these new congeners, like **3**, may be beneficial in normalizing MT-deficits in tauopathy neurons. Interestingly, although the effect of the nitrile moiety in lowering lipophilicity is well documented,[31] direct comparison of experimentally determined $\log D_{7.4}$ values of matched paired compounds bearing a nitrile moiety in the *para* position of the ring at C6 (*cf.*, **66** with **67**/**68**; **69** with **70**; and **72** with **73**) demonstrates that the fluorination state of the aromatic ring plays an equally important role as evidenced by the significantly lower $\log D_{7.4}$ values observed when both *ortho* positions are fluorinated (Figure 5). Of notice, in spite of the reduced lipophilic character of **66**, **69** and **72** compared to the corresponding 2,4,6-trifluorophenyl congeners (**3**, **60**, and **52**), these compounds retained excellent brain penetration (Table 4). Furthermore, evaluation of brain/plasma PK of **69** after i.p. injection revealed that this compound exhibits greater metabolic stability (*i.e.*, reduced clearance and increased plasma half-life) compared to existing lead (**3**). Thus, taken together, our results show that an appropriate combination of relatively bulky/lipophilic aliphatic amines at C7 with polar fluorinated cyanobenzene fragments at C6 results in Class I congeners that exhibit both improved MT-stabilizing activity in cells, as well as improved lipophilic efficiency and metabolic stability.

Conclusions.

Brain penetrant, MT-stabilizing triazolopyrimidines have produced promising results in different mouse models of AD, suggesting that compounds from this class may be considered as candidate therapeutics for neurodegenerative tauopathies. However, depending on the substitution pattern, this type of compounds can elicit very different cellular responses by either promoting MT stabilization or, conversely, disrupting MT integrity in cells. The studies presented here define the most important stereoelectronic characteristics of the C6 and C7 fragments of MT-active triazolopyrimidines that can lead to relatively potent MT-stabilizing activity in cells without reduction in cellular tubulin levels. These

results, which provide additional insight into the SAR of MT-stabilizing triazolopyrimidines, enabled both the development of predictive models as well as the design of congeners exhibiting improved properties and *in vitro* biological activity. Compounds of this type hold promise as candidate treatments for neurodegenerative tauopathies.

Experimental Section.

Materials and Methods.

All solvents were reagent grade. All reagents were purchased from Aldrich or Acros and used as received. Thin layer chromatography (TLC) was performed with 0.25 mm E. Merck precoated silica gel plates. Silica gel column chromatography was performed with silica gel 60 (particle size 0.040–0.062 mm) supplied by Silicycle and Sorbent Technologies. TLC spots were detected by viewing under a UV light. Melting points (mp) were acquired on a Mel-Temp II (model : 1001) and are uncorrected. Infrared (IR) spectra were recorded on a Bruker, model Alpha spectrometer (part number 1003271/03). Proton (^{1}H) and carbon (^{13}C) NMR spectra were recorded on a 500 MHz Bruker AMX-500 spectrometer or 600 MHz Bruker Avance III spectrometer. Fluorine (^{19}F) NMR spectra were recorded on a 500 MHz Bruker Avance II spectrometer. Chemical shifts were reported relative to solvents, Data for ^{1}H-NMR spectra are reported as follows: chemical shift (ppm, referenced to protium; s = singlet, d = doublet, t = triplet, q= quartet, quint = quintet, dd = doublet of doublets, td = triplet of doublets, ddd = doublet of doublet of doublets, bs = broad singlet, m = multiplet, coupling constant (Hz), and integration). High-resolution mass spectra were measured using an Agilent 6230 time-of-flight mass spectrometer (TOFMS) with Jet stream electrospray ionisation source (ESI). Single-crystal X-ray structure determinations were performed Bruker MicroStar with an APEX II detector, double-bounce micro-focus optics and a Cu rotating anode source. Analytical reverse-phase (Sunfire C18; 4.6 mm × 50 mm, 5 mL) high-performance liquid chromatography (HPLC) was performed with a Gilson HPLC equipped with UV and mass detector. All samples were analyzed employing a linear gradient from 10% to 90% of ACN in H_2O over 8 min and flow rate of 1 mL/min. Preparative reverse-phase HPLC purifications were performed on a Gilson

instrument employing Waters SunFire preparative C_{18} OBD columns (5 μm 19 mm × 50 mm or 19 mm × 100 mm). Purifications were carried out employing a linear gradient from 10% to 90% of ACN in H_2O for 15 min with a flow rate of 20 mL/min. All final compounds were found to be >95% pure by HPLC.

General Procedure A (synthesis of diethylmalonate derivatives):

To a suspension of NaH (60 wt % in mineral oil) (1.00 equiv) in anhydrous 1,4-dioxane (previously degassed with N_2) at 60 ˚C under N_2 was slowly added diethyl malonate (3.00 equiv) and the resulting mixture was stirred for 10 min. CuBr (1.20 equiv) and aryl bromide derivate were then added and the reaction mixture (1.75 mol/L of aryl bromide derivate) was heated to reflux overnight. The reaction mixture was then cooled to r.t., quenched with HCl 12N (1.40 equiv), filtered and washed with H_2O. The filtrate was extracted with EtOAc (×3). The combined organic extracts were washed with brine, dried over $MgSO_4$, filtered and concentrated under reduced pressure. Purification via silica gel column chromatography or preparative reverse-phase HPLC provided the desired diethylmalonate derivatives.

General procedure B (synthesis of dichloro-triazolopyrimidine derivatives):

A mixture of the appropriate diethylmalonate derivate (1.00 equiv), 3-amino-1,2,4-triazole (1.05 equiv) and tributylamine (1.05 equiv) in a sealed tube was stirred at 170 ˚C for 2 h. After cooling to 130 ˚C, the reaction mixture was diluted with toluene to reach approximately a concentration of 1.00 M of diethylmalonate derivative. The reaction was then cooled to 50 ˚C and an aqueous solution of NaOH (50% wt) (0.160 mL/mmol of diethylmalonate derivate) was added. The resulting mixture was stirred at 0 ˚C for 10 min and then filtered to obtain the triazolopyrimidine disodic salt intermediate as a solid, which was washed with cold toluene, dried and used directly without further purification. This disodic derivate (1.00 equiv) and $POCl_3$ (17.80 equiv) were mixed in a sealed tube and heated to 130 ˚C for 6 h. The reaction was then quenched with H_2O and extracted with EtOAc (×2). The combined organic extracts were washed with H_2O (×5), then brine, dried over $MgSO_4$, filtered and concentrated under reduced pressure. The resulting dichloro-triazolopyrimidine was used directly without further purification.

General procedure C (addition of the amine):

According to a reported procedure,[15] to a solution of 5,7-dichloro-6-(2,4,6-trifluorophenyl)-[1,2,4]triazolo[1,5-*a*]pyrimidine (1.0 equiv) in DMF (0.1 M) at r.t. was added the appropriate amine (1.5 – 3.0 equiv either as HCl salt or free base) followed by i-Pr_2NEt (3.0 equiv) or Et_3N (3.0 equiv), if necessary. The reaction mixture was stirred for 0.5–16 h and then diluted with H_2O. The organic layer was washed with a 1N HCl (×2), the aqueous phase was extracted with EtOAc (×3) and the combined organic layers were washed with brine (×2), dried over $MgSO_4$, filtered, and concentrated. Finally, purification via silica gel flash chromatography or by reverse-phase HPLC yielded the desired product.

General procedure D (addition of the side chain):

According to reported procedures,[15, 16] to a suspension of NaH (4.0 equiv) in a 2:1 mixture of DMSO and THF (0.35 M) was added the appropriate aminoalcohol (4.0 equiv), and the mixture was heated to 60 ˚C for 1 h. The resulting solution was treated with a solution of trifluoroarene (1.0 equiv) in a 1:1 mixture DMSO and THF (0.5 M). The reaction mixture was stirred at 60 ˚C for 3 h and monitored by LCMS. If the starting material remained after 3 h, additional aminoalcohol (4.0 equiv) and NaH (4.0 equiv) were added, sequentially, and the reaction mixture was heated for 16 h. Following complete consumption of the starting material, the reaction mixture was cooled to r.t. and diluted with H_2O and EtOAc. The organic layer was washed with H_2O and brine, and the combined aqueous layers were extracted with EtOAc (×3). The combined organic layers were dried over $MgSO_4$, filtered, and concentrated. Purification by reverse-phase HPLC provided the desired product.

(*S*)-5-Chloro-6-phenyl-*N*-(1,1,1-trifluoropropan-2-yl)-[1,2,4]triazolo[1,5-*a*]pyrimidin-7-amine (8). Following General Procedure C using 5,7-dichloro-6-phenyl-[1,2,4]triazolo[1,5-*a*]pyrimidine (0.500 g, 1.88 mmol) **(93)** and (*S*)-2-amino-1,1,1-trifluoropropane hydrochloride (0.840 g, 5.64 mmol). Purification via preparative reverse-phase chromatography provided the title compound as a white powder (0.066 g,

0.19 mmol, 10%).^{1}H NMR (500 MHz, $CDCl_3$) δ 8.40 (s, 1H), 7.62 – 7.52 (m, 3H), 7.42 – 7.36 (m, 1H), 7.35 – 7.28 (m, 1H), 5.68 (s, 1H), 4.63 (s, 1H), 1.29 (d, *J* = 6.8 Hz, 3H) ppm; ^{13}C NMR (126 MHz, $CDCl_3$) δ 157.17, 155.44, 145.72, 131.67, 131.51, 130.54, 130.09, 129.96, 129.82, 124.90 (q, *J* = 282.4 Hz), 105.26, 50.67 (q, *J* = 31.5 Hz), 15.02 (q, *J* = 1.7 Hz) ppm; IR (film) ν 3435, 1619, 1577, 1491, 1460, 1384, 1366, 1338, 1264, 1248, 1179, 1145, 1085, 1024, 955, 906, 767, 742, 702, 652, 615 cm^{-1}; HRMS (ES+) calculated for $C_{14}H_{12}ClF_3N_5$ $[M + H]^+$: 342.0728, found 342.0726.

(*S*)-5-Chloro-6-(4-fluorophenyl)-*N*-(1,1,1-trifluoropropan-2-yl)-[1,2,4]triazolo[1,5-*a*]pyrimidin-7-amine (9). Following General Procedure C using 5,7-dichloro-4-fluorophenyl-[1,2,4]triazolo[1,5-*a*]pyrimidine (0.300 g, 1.04 mmol) **(94)** and (*S*)-2-amino-1,1,1-trifluoropropane hydrochloride (0.465 g, 3.11 mmol). Purification via preparative reverse-phase chromatography provided the title compound as a white powder (0.126 g, 0.35 mmol, 34%). ^{1}H NMR (500 MHz, $CDCl_3$) δ 8.39 (s, 1H), 7.42 – 7.35 (m, 1H), 7.36 – 7.24 (m, 3H), 5.65 (s, 1H), 4.77 (s, 1H), 1.34 (d, *J* = 6.8 Hz, 3H) ppm; ^{13}C NMR (126 MHz, $CDCl_3$) δ 163.57 (d, *J* = 251.3 Hz), 157.29, 155.56, 153.93, 145.86, 133.63 (d, *J* = 8.4 Hz), 132.61 (d, *J* = 8.4 Hz), 127.57 (d, *J* = 3.7 Hz), 124.94 (q, *J* = 282.4 Hz), 117.34 (d, *J* = 22.0 Hz), 117.16 (d, *J* = 22.0 Hz), 104.31, 50.83 (q, *J* = 31.6 Hz), 15.04 (d, *J* = 2.1 Hz) ppm; IR (film) ν 3421, 1619, 1574, 1504, 1461, 1366, 1337, 1247, 1180, 1146, 1096, 1024, 957, 841, 766, 738, 610 cm^{-1}; HRMS (ES+) calculated for $C_{14}H_{10}ClF_4N_5Na$ $[M + Na]^+$: 382.0459, found 382.0464.

5-Chloro-6-(2-fluorophenyl)-*N*-(-1,1,1-trifluoropropan-2-yl)-[1,2,4]triazolo[1,5-*a*]pyrimidin-7-amine (10). Following General Procedure C using 5,7-dichloro-6-(2-fluorophenyl)-[1,2,4]triazolo[1,5-*a*]pyrimidine (0.300 g, 1.04 mmol) **(95)** and (*S*)-2-amino-1,1,1-trifluoropropane hydrochloride (0.465 g, 3.11 mmol). Purification via silica gel column chromatography (0–30% EtOAc in hexanes) provided the title compound as a white powder (0.060 g, 0.17 mmol, 16%). ^{1}H NMR (500 MHz, $CDCl_3$) mixture of diastereomers δ 8.39 (s, 1H), 7.61 – 7.52 (m, 1H), 7.40 – 7.27 (m, 3H), 6.08 – 5.49 (m, 1H), 4.95 – 4.22 (m, 1H), 1.34 (d, *J* = 6.8 Hz, 3H) ppm; ^{13}C NMR (126 MHz, $CDCl_3$) δ 161.79, 161.59, 159.80, 159.61,

157.71, 157.50, 155.50, 155.43, 154.20, 153.83, 145.83, 145.41, 133.41, 133.39, 132.79, 132.72, 132.66, 132.35, 132.34, 128.18, 128.00, 125.93, 125.76, 125.50, 125.47, 125.44, 125.41, 123.69, 123.51, 121.45, 121.27, 119.42, 119.30, 119.18, 117.21, 117.04, 116.70, 116.53, 99.20, 98.22, 51.26, 51.00, 50.75, 50.49, 50.24, 15.18, 15.16, 15.07, 15.05 ppm; IR (film) ν 3435, 1618, 1554, 1491, 1460, 1368, 1248, 1179, 1144, 1094, 1025, 960, 759, 651, 616 cm^{-1}; HRMS (ES+) calculated for $C_{14}H_{10}ClF_4N_5Na$ $[M + Na]^+$: 382.0459, found 382.0441.

(*S*)-5-Chloro-6-(2,6-difluorophenyl)-*N*-(1,1,1-trifluoropropan-2-yl)-[1,2,4]triazolo[1,5-*a*]pyrimidin-7-amine (12). Following General Procedure C using 5,7-dichloro-6-(2,6-difluorophenyl)-[1,2,4]triazolo[1,5-*a*]pyrimidine (0.280 g, 0.93 mmol) **(97)** and (*S*)-2-amino-1,1,1-trifluoropropane hydrochloride (0.417 g, 2.79 mmol). Purification via preparative reverse-phase chromatography provided the title compound as a white powder (0.024 g, 0.06 mmol, 7%). ^{1}H NMR (500 MHz, $CDCl_3$) δ 8.33 (s, 1H), 7.54 – 7.45 (m, 1H), 7.10 – 7.00 (m, 2H), 6.19 – 6.10 (m, 1H), 4.76 (s, 1H), 1.39 (d, *J* = 6.9 Hz, 3H) ppm; ^{13}C NMR (126 MHz, $CDCl_3$) δ 161.12 (dd, *J* = 252.3, 5.5 Hz), 160.82 (dd, *J* = 250.9, 5.3 Hz), 157.72, 155.26, 154.16, 145.89, 133.01 (t, *J* = 10.0 Hz), 124.59 (dd, *J* = 564.1, 282.1 Hz), 112.43 (dd, *J* = 21.5, 3.4 Hz), 112.07 (dd, *J* = 21.5, 3.6 Hz), 108.90 (t, *J* = 20.2 Hz), 92.39, 50.86 (q, *J* = 32.3 Hz), 14.98 ppm. IR (film) ν 3227, 1630, 1602, 1460, 1383, 1266, 1239, 1195, 1126, 1003, 900, 809, 765, 652, 622 cm^{-1}; HRMS (ES+) calculated for $C_{14}H_{10}ClF_5N_5$ $[M + H]^+$: 378.0539, found 378.0556.

(*S*)-5-Chloro-6-(3,5-difluorophenyl)-*N*-(1,1,1-trifluoropropan-2-yl)-[1,2,4]triazolo[1,5-*a*]pyrimidin-7-amine (13). Following General Procedure C using 5,7-dichloro-6-(3,5-difluorophenyl)-[1,2,4]triazolo[1,5-*a*]pyrimidine (0.350 g, 1.16 mmol) **(98)** and (*S*)-2-amino-1,1,1-trifluoropropane hydrochloride (0.521 g, 3.49 mmol). Purification via silica gel column chromatography (0–30% EtOAc in hexanes) provided the title compound as a white powder (0.148 g, 0.39 mmol, 34%). ^{1}H NMR (500 MHz, $CDCl_3$) δ 8.40 (s, 1H), 7.03 (dt, *J* = 8.6, 2.3 Hz, 1H), 6.96 (d, *J* = 8.3 Hz, 1H), 6.90 (d, *J* = 7.5 Hz, 1H), 5.64 (s, 1H), 4.82 (s, 1H), 1.38 (d, *J* = 6.8 Hz, 3H) ppm; ^{13}C NMR (126 MHz, $CDCl_3$) δ 163.72 (dd,

J = 253.2, 13.0 Hz), 163.66 (dd, *J* = 251.7, 11.7 Hz), 156.45, 155.71, 153.96, 145.57, 134.65 (t, *J* = 10.0 Hz), 124.85 (q, *J* = 282.4 Hz), 115.03 (dd, *J* = 21.9, 3.7 Hz), 114.04 (dd, *J* = 21.9, 3.7 Hz), 105.99 (t, *J* = 24.8 Hz), 103.18, 51.07 (q, *J* = 31.6 Hz), 15.02 (d, *J* = 1.9 Hz) ppm; IR (film) ν 3435, 1620, 1590, 1521, 1493, 1460, 1434, 1384, 1362, 1333, 1264, 1192, 1159, 1125, 1081, 1028, 987, 956, 906, 855, 763, 670, 653, 628 cm^{-1}; HRMS (ES-) calculated for $C_{14}H_8ClF_5N_5$ $[M - H]^-$ 376.0394, found 376.0376.

(*S*)-5-Chloro-6-(2,5-difluorophenyl)-*N*-(-1,1,1-trifluoropropan-2-yl)-[1,2,4]triazolo[1,5-*a*]pyrimidin-7-amine (14). Following General Procedure C using 5,7-dichloro-6-(2,5-difluorophenyl)-[1,2,4]triazolo[1,5-*a*]pyrimidine (0.400 g, 1.33 mmol) **(99)** and (*S*)-2-amino-1,1,1-trifluoropropane hydrochloride (0.596 g, 3.99 mmol). Purification via silica gel column chromatography (0–30% EtOAc in hexanes) provided the title compound as a white powder (0.020 g, 0.05 mmol, 4%). ^1H NMR (500 MHz, $CDCl_3$) mixture of diastereomers δ 8.40 (s, 1H), 7.32 – 7.24 (m, 2H), 7.15 – 7.02 (m, 1H), 6.07 – 5.46 (m, 1H), 4.71 (d, *J* = 156.9 Hz, 1H), 1.39 (d, *J* = 6.8 Hz, 3H) ppm; ^{13}C NMR (126 MHz, $CDCl_3$) mixture of diastereomers δ 159.86, 159.84, 157.90, 157.88, 157.71, 157.68, 157.28, 157.15, 155.95, 155.93, 155.76, 155.73, 155.64, 155.58, 154.21, 153.94, 145.78, 145.47, 128.12, 127.98, 125.88, 125.74, 123.64, 123.49, 121.39, 121.25, 120.68, 120.62, 120.56, 120.54, 120.50, 120.47, 120.41, 120.35, 119.99, 119.97, 119.80, 119.78, 119.54, 119.51, 119.47, 119.44, 119.35, 119.32, 119.28, 119.25, 118.91, 118.89, 118.72, 118.70, 118.52, 118.45, 118.33, 118.26, 118.00, 117.93, 117.81, 117.74, 98.19, 97.30, 51.46, 51.25, 51.21, 50.99, 50.95, 50.74, 50.70, 50.49, 15.19, 15.18, 15.09, 15.08 ppm; IR (film) ν 3441, 1622, 1494, 1461, 1424, 1383, 1251, 1182, 1145, 1092, 1025, 979, 877, 821, 775 cm^{-1}; HRMS (ES+) calculated for $C_{14}H_{10}ClF_5N_5$ $[M + H]^+$: 378.0539, found 378.0509.

(*S*)-5-Chloro-6-(3,4-difluorophenyl)-*N*-(1,1,1-trifluoropropan-2-yl)-[1,2,4]triazolo[1,5-*a*]pyrimidin-7-amine (15). Following General Procedure C using 5,7-dichloro-6-(3,4-difluorophenyl)-[1,2,4]triazolo[1,5-*a*]pyrimidine (0.150 g, 0.50 mmol) **(100)** and (*S*)-2-amino-1,1,1-trifluoropropane hydrochloride (0.223 g, 1.49 mmol). Purification via preparative reverse-phase chromatography provided

the title compound as a white powder (0.007 g, 0.02 mmol, 4%).^{1}H NMR (500 MHz, $CDCl_3$) mixture of diastereomers δ 8.42 (s, 1H), 7.45 – 7.34 (m, 1H), 7.22 – 7.05 (m, 2H), 5.71 – 5.47 (m, 1H), 5.02 – 4.63 (m, 1H), 1.37 (d, *J* = 6.9 Hz, 3H) ppm; ^{13}C NMR (126 MHz, $CDCl_3$) mixture of diastereomers δ 157.04, 157.01, 156.89, 156.88, 155.78, 155.73, 155.72, 155.66, 152.56, 152.50, 152.43, 152.38, 152.33, 152.20, 152.09, 151.96, 150.51, 150.46, 150.38, 150.35, 150.17, 150.06, 149.94, 145.95, 145.91, 145.82, 145.78, 145.74, 128.38, 128.34, 128.30, 127.36, 127.31, 127.28, 126.04, 125.99, 123.80, 123.75, 121.58, 121.55, 121.18, 121.05, 120.19, 120.17, 120.06, 120.05, 119.34, 119.29, 119.24, 119.19, 119.16, 119.02, 103.47, 103.35, 51.42, 51.35, 51.16, 51.10, 50.91, 50.84, 50.65, 50.59, 15.08 ppm; IR (film) ν 3436, 2923, 2853, 1632, 1463, 1383, 1270, 1147 cm^{-1}; HRMS (ES+) calculated for $C_{14}H_{10}ClF_5N_5$ $[M + H]^+$: 378.0539, found 378.0550.

(*S*)-5-Chloro-6-(2,3,4-trifluorophenyl)-*N*-(-1,1,1-trifluoropropan-2-yl)-[1,2,4]triazolo[1,5-*a*]pyrimidin-7-amine (16). Following General Procedure C using 5,7-dichloro-6-(2,3,4-trifluorophenyl)-[1,2,4]triazolo[1,5-*a*]pyrimidine (0.300 g, 0.94 mmol) **(101)** and (*S*)-2-amino-1,1,1-trifluoropropane hydrochloride (0.422 g, 2.82 mmol). Purification via preparative reverse-phase chromatography provided the title compound as a white powder (0.050 g, 0.13 mmol, 13%). ^{1}H NMR (500 MHz, $CDCl_3$) mixture of diastereomers δ 8.37 (s, 1H), 7.24 – 7.05 (m, 2H), 6.05 – 5.61 (m, 1H), 5.20 – 4.47 (m, 1H), 1.42 (d, *J* = 6.3 Hz, 3H) ppm; ^{13}C NMR (126 MHz, $CDCl_3$) mixture of diastereomers δ 157.56, 157.24, 155.75, 155.67, 154.40, 153.95, 153.77, 153.74, 153.69, 153.67, 153.62, 153.59, 151.74, 151.71, 151.66, 151.63, 151.58, 151.56, 151.39, 151.36, 151.31, 151.28, 151.06, 151.03, 150.98, 150.95, 149.37, 149.34, 149.29, 149.26, 149.05, 149.02, 148.97, 148.94, 146.17, 145.67, 142.19, 142.07, 141.95, 141.86, 141.74, 141.62, 140.16, 140.04, 139.91, 139.83, 139.70, 139.58, 128.20, 127.95, 127.23, 127.20, 127.18, 127.17, 127.14, 126.15, 126.14, 126.11, 126.10, 126.09, 126.08, 126.05, 125.95, 125.70, 123.71, 123.46, 121.47, 121.22, 117.07, 117.04, 116.96, 116.93, 116.91, 116.84, 116.80, 113.96, 113.92, 113.91, 113.88, 113.81, 113.78, 113.77, 113.74, 97.55, 96.47, 51.59, 51.34, 51.31, 51.08, 51.05, 50.83, 50.80, 50.55, 15.21, 15.19, 15.07, 15.06 ppm. IR (film) ν 3388, 3338, 1619, 1553, 1509, 1486, 1463, 1367, 1352, 1251, 1181, 1143, 1090,

1041, 1025, 987, 957, 906, 878, 808, 766, 738, 698, 680, 653, 619 cm^{-1}; HRMS (ES+) calculated for $C_{14}H_9ClF_6N_5$ $[M + H]^+$: 396.0445, found 396.0464.

(*S*)-5-Chloro-6-(2,4,6-trifluorobenzyl)-*N*-(1,1,1-trifluoropropan-2-yl)-[1,2,4]triazolo[1,5-*a*]pyrimidin-7-amine (17). Following General Procedure C using 5,7-dichloro-6-(2,4,6-trifluorobenzyl)-[1,2,4]triazolo[1,5-*a*]pyrimidine (0.300 g, 0.90 mmol) **(103)** and (*S*)-2-amino-1,1,1-trifluoropropane hydrochloride (0.404 g, 2.70 mmol). Purification via silica gel column chromatography (0–25% EtOAc in hexanes) provided the title compound as a white powder (0.085 g, 0.21 mmol, 23%). ^{1}H NMR (500 MHz, $CDCl_3$) δ 8.32 (s, 1H), 6.73 (t, *J* = 8.3 Hz, 2H), 6.32 – 6.12 (m, 1H), 5.23 (d, *J* = 10.2 Hz, 1H), 4.27 – 4.08 (m, 2H), 1.50 (d, *J* = 6.9 Hz, 3H) ppm; ^{13}C NMR (126 MHz, $CDCl_3$) δ 162.21 (dt, *J* = 251.1, 16.0 Hz), 161.52 (dd, *J* = 247.9, 10.9 Hz), 161.41 (dd, *J* = 248.0, 10.8 Hz), 157.36, 155.42, 154.39, 146.49, 125.14 (q, *J* = 282.1 Hz), 108.38 (td, *J* = 19.0, 4.8 Hz), 101.31 – 100.77 (m), 100.73, 51.82 (q, *J* = 31.5 Hz), 21.06, 15.30 (d, *J* = 2.2 Hz) ppm; IR (film) ν 3427, 3276, 3143, 3001, 2926, 2855, 1621, 1552, 1496, 1464, 1443, 1378, 1337, 1274, 1244, 1182, 1145, 1118, 1091, 1035, 999, 959, 910, 842, 804, 762, 734, 680, 648, 613 cm^{-1}; HRMS (ES+) calculated for $C_{15}H_{11}ClF_6N_5$ $[M + H]^+$: 410.0602, found 410.0608.

(*S*)-5-Chloro-6-(2,6-difluoro-4-methylphenyl)-*N*-(1,1,1-trifluoropropan-2-yl)-[1,2,4]triazolo[1,5-*a*]pyrimidin-7-amine (18). Following general procedure C using 5,7-dichloro-6-(2,6-difluoro-4-methylphenyl)-[1,2,4]triazolo[1,5-*a*]pyrimidine (0.050 g, 0.16 mmol) **(104)** and *(S)*-1,1,1-trifluoropropan-2-amine (0.038 g, 0.33 mmol). Purification via silica gel column chromatography (0−25% EtOAc in hexanes) provided the title compound as a white powder (0.028 g, 0.071 mmol, 65%). ^{1}H NMR (600 MHz, $CDCl_3$) δ 8.36 (s, 1H), 6.91 (d, *J* = 9.0 Hz, 2H), 6.00 – 5.94 (m, 1H), 4.73 (s, 1H), 2.45 (s, 3H), 1.39 (d, *J* = 7.0 Hz, 3H) ppm; ^{13}C NMR (150 MHz, $CDCl_3$) δ 160.75 (dd, *J* = 251.4, 7.0 Hz), 160.50 (dd, *J* = 249.9, 7.3 Hz), 158.07, 155.34, 154.11, 145.83, 144.86 (t, *J* = 10.2 Hz), 124.59 (q, *J* = 282.1 Hz), 112.93 (ddd, *J* = 65.8, 21.3, 4.0 Hz), 105.67 (t, *J* = 20.9 Hz), 92.50, 22.72 – 20.28 (m), 15.19 ppm; IR

(film) ν 1618, 1559, 1143, 840 cm^{-1}; HRMS (ES+) calculated for $C_{15}H_{12}N_5ClF_5$ $[M + H]^+$: 392.0696, found 392.0693.

(*S*)-5-Chloro-6-(2,6-difluoro-4-(trifluoromethyl)phenyl)-*N*-(1,1,1-trifluoropropan-2-yl)-[1,2,4]triazolo[1,5-*a*]pyrimidin-7-amine (19). Following General Procedure C using 5,7-dichloro-6-(2,6-difluoro-4-(trifluoromethyl)phenyl)-[1,2,4]triazolo[1,5-*a*]pyrimidine (0.350 g, 1.16 mmol) **(105)** and (*S*)-2-amino-1,1,1-trifluoropropane hydrochloride (0.389 g, 2.60 mmol). Purification via silica gel column chromatography (0–30% EtOAc in hexanes) provided the title compound as a white powder (0.240 g, 0.54 mmol, 62%). ^{1}H NMR (500 MHz, $CDCl_3$) δ 8.42 (s, 1H), 7.42 (d, *J* = 7.3 Hz, 2H), 5.87 (d, *J* = 10.5 Hz, 1H), 4.74 (s, 1H), 1.44 (d, *J* = 6.9 Hz, 3H) ppm; ^{13}C NMR (126 MHz, $CDCl_3$) δ 161.32 (dd, *J* = 255.5, 5.5 Hz), 160.96 (dd, *J* = 253.8, 5.6 Hz), 157.25, 155.74, 154.36, 145.83, 135.62 (qt, *J* = 35.0, 9.8 Hz), 124.53 (q, *J* = 280.6 Hz), 122.33 (qt, *J* = 273.4, 2.9 Hz), 112.99 (t, *J* = 20.1 Hz), 110.42 (dp, *J* = 24.9, 3.7 Hz), 109.93 (dp, *J* = 25.0, 3.8 Hz), 91.17, 51.21 (q, *J* = 32.2 Hz), 15.31 (d, *J* = 1.9 Hz) ppm; IR (film) ν 3208, 2925, 2855, 1620, 1555, 1461, 1436, 1369, 1249, 1179, 1143, 1111, 1090, 1037, 963, 909, 896, 868, 819, 767, 734, 680, 652, 612 cm^{-1}; HRMS (ES+) calculated for $C_{15}H_9ClF_8N_5$ $[M + H]^+$: 446.0413, found 446.0438.

(*S*)-4-(5-Chloro-7-((1,1,1-trifluoropropan-2-yl)amino)-[1,2,4]triazolo[1,5-*a*]pyrimidin-6-yl)-3,5-difluorobenzonitrile (20). Following general procedure C using 4-(5,7-dichloro-[1,2,4]triazolo[1,5-*a*]pyrimidin-6-yl)-3,5-difluorobenzonitrile (0.030 g, 0.09 mmol) **(106)** and (*S*)-1,1,1-trifluoropropan-2-amine (0.022 g, 0.19 mmol). Purification via silica gel column chromatography (0−40% EtOAc in hexanes) provided the title compound as a white powder (0.020 g, 0.05 mmol, 54%). ^{1}H NMR (600 MHz, $CDCl_3$) δ 8.41 (s, 1H), 7.44 (t, *J* = 7.1 Hz, 2H), 6.00 (d, *J* = 10.7 Hz, 1H), 4.77 (s, 1H), 1.45 (d, *J* = 6.9 Hz, 3H) ppm; ^{13}C NMR (150 MHz, $CDCl_3$) δ 161.28 (dd, *J* = 256.4, 5.9 Hz), 160.87 (dd, *J* = 254.7, 6.0 Hz), 156.84, 155.68, 154.32, 124.46 (q, *J* = 282.1 Hz), 116.58 (t, *J* = 11.8 Hz), 116.47 (ddd, *J* = 67.6, 25.4, 4.1 Hz), 115.79 (d, *J* = 3.5 Hz), 114.93 (t, *J* = 20.0 Hz), 90.61, 51.27 (q, *J* = 32.2 Hz), 29.83, 15.14

ppm; ^{19}F NMR (469 MHz) δ –78.31, –102.98, –105.00 ppm; IR (KBr): 2923, 2239, 1617, 1556, 1141 cm^{-1}; HRMS (ES+) calculated for $C_{15}H_9N_6ClF_5$ $[M + H]^+$: 403.0492, found 403.0486.

(*S*)-5-Chloro-6-(4-chloro-2,6-difluorophenyl)-*N*-(1,1,1-trifluoropropan-2-yl)-[1,2,4]triazolo[1,5-*a*]pyrimidin-7-amine (21). Following general procedure C using 5,7-dichloro-6-(4-chloro-2,6-difluorophenyl)-[1,2,4]triazolo[1,5-*a*]pyrimidine (0.050 g, 0.15 mmol) **(108)** and (*S*)-1,1,1-trifluoropropan-2-amine (0.035 g, 0.31 mmol). Purification via silica gel column chromatography (0−40% EtOAc in hexanes) provided the title compound as a white powder (0.035 g, 0.085 mmol, 57%). ^{1}H NMR (600 MHz, $CDCl_3$) δ 8.40 (s, 1H), 7.18 – 7.16 (m, 2H), 5.93 – 5.88 (m, 1H), 4.75 (s, 1H), 1.43 (d, J = 6.9 Hz, 3H) ppm; ^{13}C NMR (150 MHz, $CDCl_3$) δ 160.84 (ddd, J = 253.4, 48.9, 9.1 Hz), 157.67, 155.57, 154.21, 145.82, 138.62 (t, J = 14.0 Hz), 124.53 (q, J = 280.5 Hz), 114.47 – 113.17 (m), 51.00 (q, J = 32.9 Hz), 15.27 ppm. IR (film) ν 3000, 1571, 1517, 1142 cm^{-1}; HRMS (ES+) calculated for $C_{14}H_9Cl_2F_5N_5$ $[M + H]^+$: 412.0150, found 412.0146.

(*S*)-5-Chloro-6-(2,6-difluoro-4-nitrophenyl)-*N*-(1,1,1-trifluoropropan-2-yl)-[1,2,4]triazolo[1,5-*a*]pyrimidin-7-amine (22). Following general procedure C 5,7-dichloro-6-(2,6-difluoro-4-nitrophenyl)-[1,2,4]triazolo[1,5-*a*]pyrimidine (0.070 g, 0.21 mmol) **(109)** and (*S*)-1,1,1-trifluoropropan-2-amine (0.048 g, 0.42 mmol). Purification via silica gel column chromatography (0−40% EtOAc in hexanes) provided the title compound as a white powder (0.075 g, 0.18 mmol, 88%). ^{1}H NMR (600 MHz, $CDCl_3$) δ 8.41 (s, 1H), 8.00 – 7.98 (m, 2H), 5.99 (d, J = 10.6 Hz, 1H), 4.78 (s, 1H), 1.46 (d, J = 6.8 Hz, 3H) ppm; ^{13}C NMR (150 MHz, $CDCl_3$) δ 161.15 (dd, J = 257.2, 5.8 Hz), 160.73 (dd, J = 255.3, 6.1 Hz), 156.78, 155.75, 154.37, 150.43 (t, J = 10.5 Hz), 145.80, 124.47 (q, J = 282.2 Hz), 116.00 (t, J = 20.5 Hz), 108.53 (ddd, J = 61.2, 27.3, 4.0 Hz), 90.62, 51.38 (q, J = 32.1 Hz), 15.20 (d, J = 1.5 Hz) ppm; IR (film) ν 1618, 1530, 1489, 1143, 1043 cm^{-1}; HRMS (ES+) calculated for $C_{14}H_9ClF_5N_6O_2$ $[M + H]^+$: 423.0390, found 423.0384.

(*S*)-6-(4-Amino-2,6-difluorophenyl)-5-chloro-*N*-(1,1,1-trifluoropropan-2-yl)-[1,2,4]triazolo[1,5-*a*]pyrimidin-7-amine (23). To a solution of (*S*)-5-chloro-6-(2,6-difluoro-4-nitrophenyl)-*N*-(1,1,1-trifluoropropan-2-yl)-[1,2,4]triazolo[1,5-*a*]pyrimidin-7-amine (0.025 g, 0.059 mmol) **(22)** in 0.100 ml of H_2O/MeOH (1:1) was added iron powder (0.017 g, 0.30 mmol) and ammonium chloride (0.013 g, 0.24 mmol). The mixture was stirred at 80 ˚C for 2 h and then filtered and rinsed with hot methanol. The filtrate was evaporated under reduced pressure, and the resulting mixture was purified by HPLC to afford the product as a white solid (0.016 g, 0.04 mmol, 69%). ^{1}H NMR (600 MHz, $CDCl_3$) δ 8.37 (s, 1H), 6.37 (t, *J* = 9.8 Hz, 2H), 5.93 (s, 1H), 4.86 (s, 1H), 4.28 (s, 2H), 2.17 (s, 1H), 1.41 – 1.39 (m, 3H) ppm; ^{13}C NMR (150 MHz, $CDCl_3$) δ 161.86 (ddd, *J* = 246.8, 32.1, 8.7 Hz), 158.99, 155.32, 154.09, 151.02 (t, *J* = 13.9 Hz), 146.15, 130.31, 128.98, 124.72 (q, *J* = 281.8 Hz), 98.19 (ddd, *J* = 63.6, 25.1, 3.2 Hz), 97.13 (t, *J* = 21.1 Hz), 92.99, 50.71 (q, *J* = 32.4 Hz), 31.08, 15.35 ppm; IR (film) ν 3341, 1651, 1614, 1587, 1346 cm^{-1}; HRMS (ES+) calculated for $C_{14}H_{11}ClF_5N_6$ $[M + H]^+$: 393.0648, found 393.0646.

(*S*)-5-chloro-6-(2,6-difluoro-4-methoxyphenyl)-*N*-(1,1,1-trifluoropropan-2-yl)-[1,2,4]triazolo[1,5-*a*]pyrimidin-7-amine (24). To a solution of (*S*)-5-chloro-6-(2,4,6-trifluorophenyl)-*N*-(1,1,1-trifluoropropan-2-yl)-[1,2,4]triazolo[1,5-*a*]pyrimidin-7-amine (0.020 g, 0.05 mmol) **(7)** in 0.3 mL of THF, was added 0.04 ml of a 30% sodium methoxide solution in methanol at 0 °C. The reaction mixture was heated for 2 h at 60 °C in a microwave reactor, then cooled to r.t. and diluted with aqueous ammonium chloride solution. The aqueous phase was extracted with EtOAc (×3). The combined organic layers were washed with brine (×2), dried ($MgSO_4$), filtered, and concentrated. Purification by reverse-phase HPLC provided the title compound as a white solid (0.015 g, 0.036 mmol, 71% yield). ^{1}H-NMR (500 MHz; $CDCl_3$): δ 8.45 (s, 1H), 6.67 – 6.65 (m, 2H), 5.94 – 5.93 (m, 1H), 4.77 – 4.74 (m, 1H), 3.90 (s, 3H), 1.41 (d, *J* = 6.8 Hz, 3H) ppm; ^{13}C-NMR (126 MHz; $CDCl_3$): δ 163.48 (t, *J* = 13.9 Hz), 161.80 (dd, *J* = 249.9, 9.0 Hz), 161.54 (dd, *J* = 248.4, 8.9 Hz), 159.55 (q, *J* = 40.7 Hz), 158.79, 155.09, 146.15, 124.63 (q, *J* = 282.0 Hz), 100.62 (t, *J* = 21.1 Hz), 98.93 (td, *J* = 26.8, 3.0 Hz), 92.71, 56.30, 50.87 (q, *J* = 32.1 Hz), 15.32

ppm; IR (film) ν 3340, 2953, 2924, 2848, 1642, 1618, 1579, 1553, 1147 cm^{-1}; HRMS (ES+) calculated for $C_{15}H_{12}ClF_5N_5O$ $[M + H]^+$: 408.0651, found 408.0652.

(*S*)-5-Chloro-6-(4-((3-(dimethylamino)propyl)sulfinyl)-2,6-difluorophenyl)-*N*-((*S*)-1,1,1-trifluoropropan-2-yl)-[1,2,4]triazolo[1,5-*a*]pyrimidin-7-amine (26) and **(*S*)-5-Chloro-6-(4-((3-(dimethylamino)propyl)sulfonyl)-2,6-difluorophenyl)-*N*-(1,1,1-trifluoropropan-2-yl)-[1,2,4]triazolo[1,5-*a*]pyrimidin-7-amine (27).** To a solution of (*S*)-5-chloro-6-(4-((3-(dimethylamino)propyl)thio)-2,6-difluorophenyl)-*N*-(1,1,1-trifluoropropan-2-yl)-[1,2,4]triazolo[1,5-*a*]pyrimidin-7-amine (0.050 g, 0.100 mmol) **(25)** in CH_2Cl_2 (1.00 ml) was added *m*-CPBA (70%, 0.025 g, 0.100 mmol). After 2 h, the reaction mixture was concentrated under reduced pressure and purified by reverse-phase HPLC to obtain **26** (0.017 g, 0.03 mmol, 32%) and **27** (0.027 g, 0.05 mmol, 52%). **(26)**: ^{1}H NMR (600 MHz, $CDCl_3$) δ 8.37 (s, 1H), 8.19 (s, 1H), 7.02 (d, *J* = 8.0 Hz, 2H), 6.69 (s, 1H), 5.41 (s, 1H), 3.76 – 3.67 (m, 2H), 3.40 (d, *J* = 10.2 Hz, 7H), 3.22 – 3.15 (m, 2H), 2.44 – 2.37 (m, 2H), 1.43 (d, *J* = 6.9 Hz, 3H) ppm; ^{13}C NMR (150 MHz, $CDCl_3$) δ 166.95, 161.56 (dd, *J* = 253.3, 6.8 Hz), 160.98 (dd, *J* = 252.6, 6.6 Hz), 157.65, 155.36, 154.85, 146.84, 125.91 (q), 112.00 – 110.04 (m), 107.56 – 105.57 (m), 92.69, 68.14, 57.73 (d, *J* = 11.8 Hz), 51.16 (q, *J* = 31.8 Hz), 29.62 (d, *J* = 2.0 Hz), 22.63 (d, *J* = 1.7 Hz), 14.82 ppm; IR (film) ν 3053, 1589, 1535, 1178 cm^{-1}; HRMS (ES+) calculated for $C_{19}H_{21}ClF_5N_6OS$ $[M + H]^+$: 511.1101, found 511.1100. **(27)**: ^{1}H NMR (600 MHz, $CDCl_3$) mixture of diastereomers δ 8.38 (s, 1H), 8.11 (s, 1H), 7.50 (dd, *J* = 16.6, 7.4 Hz, 1H), 7.17 (d, *J* = 7.0 Hz, 0.5H), 5.88 (s, 0.5H), 5.59 (s, 0.5H), 3.86 – 3.78 (m, 1H), 3.77 – 3.70 (m, 0.5H), 3.69 – 3.62 (m, 1H), 3.36 (dd, *J* = 25.9, 3.6 Hz, 6H), 3.40 – 3.27 (m, 0.5H), 2.99 – 2.90 (m, 1H), 2.51 – 2.40 (m, 1H), 2.36 – 2.26 (m, 1H), 1.42 (dd, *J* = 6.9, 2.9 Hz, 3H) ppm; ^{13}C NMR (150 MHz, $CDCl_3$) δ 167.52, 163.09 – 161.10 (m), 161.44 (ddd, *J* = 256.9, 21.4, 4.9 Hz), 157.00, 156.86, 155.45 – 155.33 (m), 155.12, 129.28 – 119.96 (m), 112.17 (td, *J* = 20.5, 4.6 Hz), 109.28 – 107.40 (m), 92.88, 92.30, 67.84, 67.54, 58.59, 58.51, 57.34, 56.93, 52.19, 51.77, 51.29 (td, *J* = 31.8, 17.1 Hz), 15.61, 15.10, 14.68, 14.46 (d, *J* = 1.7 Hz) ppm; IR (film) ν 3285, 1589, 1535, 1142 cm^{-1}; HRMS (ES+) calculated for $C_{19}H_{21}ClF_5N_6O_2S$ $[M + H]^+$: 527.1050, found 527.1045.

(*S*)-5-Chloro-6-(2,6-difluoro-4-(methylthio)phenyl)-*N*-(1,1,1-trifluoropropan-2-yl)-[1,2,4]triazolo[1,5-*a*]pyrimidin-7-amine (28). To a suspension of sodium methanethiolate (0.331 mL, 0.71 mmol, 4 equiv) in DMSO (2 mL) at r.t. was added (*S*)-5-chloro-6-(2,4,6-trifluorophenyl)-*N*-(1,1,1-trifluoropropan-2-yl)-[1,2,4]triazolo[1,5-*a*]pyrimidin-7-amine (0.070 g, 0.18 mmol, 1 equiv) **(7)** and the mixture was heated for 3 h at 60 ˚C before it was quenched at r.t. with a saturated NH_4Cl solution. The mixture was extracted with EtOAc and the combined organic layers were washed 5 times with H_2O, dried and concentrated under reduced pressure to furnish the title compound as a white solid (0.070 g, 0.17 mmol, 93 %). ^{1}H NMR (600 MHz, $CDCl_3$) δ 8.38 (s, 1H), 6.94 – 6.92 (m, 2H), 5.92 (bs, 1H), 4.79 (bs, 1H), 2.56 (s, 3H), 1.41 (d, *J* = 6.0 Hz, 3H) ppm; ^{13}C NMR (150 MHz, $CDCl_3$) δ 161.79 (dd, *J* = 40.77, 6.0 Hz), 160.11 (dd, *J* = 39.3, 7.6 Hz), 158.15, 155.51, 154.22, 146.81 (t, *J* = 10.6 Hz), 145.95, 124.63 (q, *J* = 282.4 Hz), 109.06 (dd, *J* = 24.2, 3.0 Hz), 108.69 (dd, *J* = 24.9, 3.0 Hz), 104.03 (t, *J* = 9.0 Hz), 92.28, 50.81 (q, *J* = 18.1 Hz), 15.31, 15.10 ppm; HRMS (ES+) calculated for $C_{14}H_8N_4ClF_6O$ $[M + H]^+$: 397.0285, found 397.0279.

5-Chloro-6-(2,6-difluoro-4-(methylsulfinyl)phenyl)-*N*-((*S*)-1,1,1-trifluoropropan-2-yl)-[1,2,4]triazolo[1,5-*a*]pyrimidin-7-amine (29). To a solution of (*S*)-5-chloro-6-(2,6-difluoro-4-(methylthio)phenyl)-*N*-(1,1,1-trifluoropropan-2-yl)-[1,2,4]triazolo[1,5-*a*]pyrimidin-7-amine (0.029 g, 0.07 mmol, 1 equiv) **(28)** in CH_2Cl_2 (0.7 mL) at r.t. was added *m*-CPBA (0.012 g, 0.07 mmol, 1 equiv). After 1h the reaction was quenched with H_2O and extracted twice with EtOAc. The combined organic fractions were washed with a sat. aq. $Na_2S_2O_3$ solution, dried and concentrated under vacuum. The crude yellow material was purified by reverse phase HPLC (C18 column, H_2O/ACN 90/10 to 10/90, 15 min ramp) and lyophilized to furnish the title compound (0.021 g, 0.05 mmol, 70 %) as a white solid. ^{1}H NMR (600 MHz, $CDCl_3$) mixture of diastereomers δ 8.43 (s, 1H), 8.08 (s, 1H), 7.98 (d, *J* = 6.0 Hz, 1H), 7.58 (d, *J* = 6.0 Hz, 1.6H), 7.51 (d, *J* = 6.0 Hz, 0.4H), 7.42 (d, *J* = 9.0 Hz, 1H), 7.38 (d, *J* = 6.0 Hz, 0.4H), 7.33 (d, *J* = 6.0 Hz, 0.6H), 5.93 (bs, 0.5H), 5.87 (bs, 0.3H), 4.75 (bs, 0.4H), 4.62 (bs, 0.5H), 2.88 (s, 3H),

1.44 – 1.42 (m, 3H) ppm; HRMS (ES+) calculated for $C_{14}H_8N_4ClF_6O$ $[M + H]^+$: 440.0366, found 440.0365.

(*S*)-5-Chloro-6-(2,6-difluoro-4-(methylsulfonyl)phenyl)-*N*-(1,1,1-trifluoropropan-2-yl)-[1,2,4]triazolo[1,5-*a*]pyrimidin-7-amine (30). To a solution of (*S*)-5-chloro-6-(2,6-difluoro-4-(methylthio)phenyl)-*N*-(1,1,1-trifluoropropan-2-yl)-[1,2,4]triazolo[1,5-*a*]pyrimidin-7-amine (0.017 g, 0.04 mmol, 1 equiv) **(28)** in CH_2Cl_2 (0.7 mL) at r.t. was added 3-chlorobenzoperoxoic acid (0.021 g, 0.12 mmol, 3 equiv). After 1h the reaction was quenched with H_2O and extracted twice with EtOAc. The combined organic fractions were washed with a sat. aq. $Na_2S_2O_3$ solution, dried and concentrated under vacuum. Purification by reverse-phase HPLC (C18 column, H_2O/ACN 90/10 to 10/90, 15 min ramp) provided the title compound (0.013 g, 0.03 mmol, 71 %) as a white solid. ^{1}H NMR (600 MHz, $CDCl_3$) δ 8.43 (s, 1H), 7.73 (d, *J* = 6.0 Hz, 2H), 5.82 (d, *J* = 6.0 Hz, 1H), 4.78 (bs, 1H), 3.21 (s, 3H), 1.45 (d, *J* = 6.0Hz, 3H) ppm; HRMS (ES+) calculated for $C_{14}5H_{12}N_45ClF_5O_2S$ $[M + H]^+$: 456.0315, found 456.0311.

5-Chloro-*N*-isopropyl-6-(2,4,6-trifluorophenyl)-[1,2,4]triazolo[1,5-*a*]pyrimidin-7-amine (35). Following General Procedure C using 5,7-dichloro-6-(2,4,6-trifluorophenyl)-[1,2,4]triazolo[1,5-*a*]pyrimidine (0.064 g, 0.20 mmol) **(102)** and propan-2-amine (0.036 g, 0.60 mmol), i-Pr_2NEt (0.078 g, 0.60 mmol) and, reverse-phase HPLC purification afforded the title compound as a white solid (0.030 g, 0.09 mmol, 44% yield). ^{1}H-NMR (500 MHz; $CDCl_3$): δ 8.46 (s, 1H), 6.90 – 6.85 (m, 2H), 6.32 (d, *J* = 8.7 Hz, 1H), 3.62 – 3.60 (m, 1H), 1.19 (d, *J* = 6.4 Hz, 6H) ppm; ^{13}C-NMR (126 MHz; $CDCl_3$): δ 164.27 (dt, *J* = 254.4, 15.2 Hz), 161.64 (dd, *J* = 251.0, 8.4 Hz), 161.53 (dd, *J* = 251.0, 8.4 Hz), 159.04, 153.77, 145.89, 106.92 (td, *J* = 20.7, 4.9 Hz), 101.46 – 101.02 (m), 90.00, 46.34, 23.82 ppm; IR (film) ν 3344, 2982, 2936, 2873, 1615, 1579, 1264, 1208, 1171, 1124 cm^{-1}; HRMS (ES+) calculated for $C_{14}H_{12}ClF_3N_5$ $[M + H]^+$: 342.0733, found 342.0733.

5-Chloro-*N*-propyl-6-(2,4,6-trifluorophenyl)-[1,2,4]triazolo[1,5-*a*]pyrimidin-7-amine (36). Following general procedure C using 5,7-dichloro-6-(2,4,6-trifluorophenyl)-[1,2,4]triazolo[1,5-*a*]pyrimidine (0.030 g, 0.09 mmol) **(102)** and propan-1-amine (0.012 g, 0.20 mmol). Purification via silica gel column chromatography (0−40% EtOAc in hexanes) provided the title compound as a white powder (0.020 g, 0.06 mmol, 62%). ^{1}H NMR (600 MHz, $CDCl_3$) δ 8.33 (s, 1H), 6.84 – 6.82 (m, 2H), 6.48 (t, *J* = 5.9 Hz, 1H), 2.98 (q, *J* = 6.7 Hz, 2H), 1.57 (h, *J* = 7.3 Hz, 2H), 0.85 (t, *J* = 7.4 Hz, 4H) ppm; ^{13}C NMR (150 MHz, $CDCl_3$) δ 163.93 (dt, *J* = 253.7, 15.4 Hz), 161.77 (ddd, *J* = 250.6, 14.9, 8.5 Hz), 158.16, 155.07, 153.65, 146.36, 107.18 (td, *J* = 20.8, 4.9 Hz), 101.12 – 100.62 (m), 88.91, 45.31, 29.83, 23.33, 11.04 ppm; IR (film) ν 2923, 1573, 1439, 1122 cm^{-1}; HRMS (ES+) calculated for $C_{14}H_{12}N_5ClF_3$ $[M + H]^+$: 342.0728, found 342.0725.

5-Chloro-*N*-*iso*butyl-6-(2,4,6-trifluorophenyl)-[1,2,4]triazolo[1,5-*a*]pyrimidin-7-amine (37). Following general procedure C using 5,7-dichloro-6-(2,4,6-trifluorophenyl)-[1,2,4]triazolo[1,5-*a*]pyrimidine (0.030 g, 0.09 mmol) **(102)** and 2-methylpropan-1-amine (0.014 g, 0.20 mmol). Purification via silica gel column chromatography (0−40% EtOAc in hexanes) provided the title compound as a white powder (0.027 g, 0.08 mmol, 81%). ^{1}H NMR (600 MHz, $CDCl_3$) δ 8.33 (s, 1H), 6.88 – 6.81 (m, 2H), 6.56 (t, *J* = 6.1 Hz, 1H), 2.84 (t, *J* = 6.5 Hz, 2H), 1.77 – 1.70 (m, 1H), 0.84 (d, *J* = 6.7 Hz, 8H) ppm; ^{13}C NMR (150 MHz, $CDCl_3$) δ 164.05 (dt, *J* = 253.8, 15.1 Hz), 161.72 (ddd, *J* = 250.4, 14.9, 8.4 Hz), 158.13, 155.05, 153.63, 146.42, 107.31 (td, *J* = 20.8, 4.8 Hz), 102.26 – 98.14 (m), 88.95, 50.83, 29.05, 19.79 ppm; IR (film) ν 2961, 2924, 1637, 1577, 1434 cm^{-1}; HRMS (ES+) calculated for $C_{15}H_{14}N_5ClF_3$ $[M + H]^+$: 356.0884, found 356.0887.

5-Chloro-6-(2,4,6-trifluorophenyl)-[1,2,4]triazolo[1,5-*a*]pyrimidin-7-ol (38). *This compound has been obtained as a side product form the attempt of synthetizing 5-chloro-N-isobutyl-N-(2,2,2-trifluoroethyl)-6-(2,4,6-trifluorophenyl)-[1,2,4]triazolo[1,5-a]pyrimidin-7-amine*. Following General Procedure C using5,7-dichloro-6-(2,4,6-trifluorophenyl)-[1,2,4]triazolo[1,5-*a*]pyrimidine (0.064 g, 0.20 mmol) **(102)**,

2-methyl-*N*-(2,2,2-trifluoroethyl)propan-1-amine hydrochloride (0.115 g, 0.60 mmol) and i-Pr_2NEt (0.139 mL, 0.80 mmol). Purification via preparative reverse-phase HPLC provided the title compound (0.023 g, 0.08 mmol, 38%). ^{1}H-NMR (500 MHz; MeOD): δ 8.74 (s, 1H), 6.97 (dd, *J* = 8.7, 7.8 Hz, 2H) ppm; ^{13}C NMR (126 MHz; MeOD): δ 164.78 (dt, *J* = 250.7, 16.4 Hz), 162.77 (ddd, *J* = 248.8, 15.2, 9.5 Hz), 159.40, 156.62, 108.75 (td, *J* = 21.2, 4.8 Hz), 102.66, 101.52 – 101.06 (m) ppm; IR (film) ν 3446, 2789, 2684, 2549, 1683, 1667, 1655, 1635, 1616, 1600, 1558, 1532 cm^{-1}.

***N*-(5-Chloro-6-(2,4,6-trifluorophenyl)-[1,2,4]triazolo[1,5-*a*]pyrimidin-7-yl)isobutyramide (39).** To a solution of 5-chloro-6-(2,4,6-trifluorophenyl)-[1,2,4]triazolo[1,5-*a*]pyrimidin-7-amine (0.035 g, 0.12 mmol, 1.00 equiv) **(102)** in anhydrous CH_2Cl_2 (0.450 mL) was added Et_3N (0.022 mL, 0.15 mmol, 1.30 equiv) and DMAP (0.001 g, 0.01 mmol, 0.10 equiv) under N_2 and the resulting solution was stirred at 0 ˚C. *Iso*butyryl chloride (0.015 mL, 0.14 mmol, 1.20 equiv) was slowly added and the reaction was stirred at 0 ˚C for 30 min and r.t. for 18 h. Then, Et_3N (0.022 mL, 0.15 mmol, 1.30 equiv) and *iso*butyryl chloride (0.015 mL, 0.14 mmol, 1.20 equiv) were added and the reaction was stirred at r.t. for 2 h. The reaction mixture was then concentrated under reduced pressure. Purification via preparative reverse-phase HPLC provided the title compound (0.023 g, 0.06 mmol, 53%). ^{1}H NMR (500 MHz, $CDCl_3$) δ 8.72 (s, 1H), 8.47 (s, 1H), 6.81 (t, *J* = 8.1 Hz, 2H), 2.66 (hept, *J* = 6.9 Hz, 1H), 1.12 (d, *J* = 6.9 Hz, 6H) ppm; ^{13}C NMR (126 MHz, $CDCl_3$) δ 173.47, 163.85 (dt, *J* = 252.8, 15.4 Hz), 160.51 (dd, *J* = 251.6, 9.0 Hz), 160.39 (dd, *J* = 251.7, 8.9 Hz), 158.48, 156.09, 153.73, 141.44, 107.40 (td, *J* = 19.8, 4.9 Hz), 104.48, 100.85 (td, *J* = 26.1, 3.4 Hz), 36.73, 19.10 ppm; IR (film) ν 3415, 2974, 1732, 1618, 1515, 1487, 1440, 1384, 1263, 1230, 1153, 1126, 1040, 997, 842, 738, 669 cm^{-1}; HRMS (ES+) calculated for $C_{15}H_{11}ClF_3N_5NaO$ $[M + Na]^+$: 392.0502, found 392.0488.

5-Chloro-*N*-phenyl-6-(2,4,6-trifluorophenyl)-[1,2,4]triazolo[1,5-*a*]pyrimidin-7-amine (40). To a solution of 5,7-dichloro-6-(2,4,6-trifluorophenyl)-[1,2,4]triazolo[1,5-*a*]pyrimidine (0.053 g, 0.17 mmol) **(102)** and aniline (0.015 mL, 0.17 mmol) in DMF (1.67 mL) was added K_2CO_3 (0.046 g, 0.33 mmol) and

the resulting mixture was stirred for 24 h at 30 ˚C. The reaction mixture was then diluted with H_2O. The organic layer was washed with a 1N HCl (×2), the aqueous phase was extracted with EtOAc (×3) and the combined organic layers were washed with brine (×2), dried over $MgSO_4$, filtered, and concentrated. Purification via silica gel column chromatography (0–40% EtOAc in hexanes) provided the title compound as a white powder (0.049 g, 0.13 mmol, 78%). ^{1}H NMR (500 MHz, $CDCl_3$) δ 8.43 (s, 1H), 8.24 (s, 1H), 7.16 – 7.11 (m, 3H), 7.10 – 7.00 (m, 2H), 6.36 (t, *J* = 8.2 Hz, 2H) ppm; ^{13}C NMR (126 MHz, $CDCl_3$) δ 164.69 (dt, *J* = 255.2, 15.1 Hz), 161.57 (ddd, *J* = 253.8, 15.0, 8.2 Hz), 161.32 (ddd, *J* = 251.3, 14.9, 8.2 Hz), 158.29, 155.56, 153.98, 146.56, 124.53 (q, *J* = 283.5 Hz), 101.86 (td, *J* = 25.8, 4.1 Hz), 101.36 (td, *J* = 25.2, 2.4 Hz), 90.99, 58.99 (q, *J* = 29.4 Hz), 28.34, 19.81, 16.74 ppm; IR (film) ν 3423, 1638, 1613, 1563, 1491, 1440, 1335, 1261, 1197, 1122, 1036, 998, 940, 840, 766, 694, 668 cm^{-1}; HRMS (ES+) calculated for $C_{17}H_{10}ClF_3N_5$ $[M + H]^+$: 376.0571, found 376.0571.

***N*-Benzyl-5-chloro-6-(2,4,6-trifluorophenyl)-[1,2,4]triazolo[1,5-*a*]pyrimidin-7-amine (41).** Following General Procedure C using 5,7-dichloro-6-(2,4,6-trifluorophenyl)-[1,2,4]triazolo[1,5-*a*]pyrimidine (0.064 g, 0.20 mmol) **(102)** and benzylamine (0.064 g, 0.60 mmol), reverse-phase HPLC purification afforded the title compound as a yellow solid (0.024 g, 0.06 mmol, 31% yield). ^{1}H-NMR (500 MHz; $CDCl_3$): δ 8.45 (s, 1H), 7.33 – 7.31 (m, 3H), 7.08 – 7.06 (m, *J* = 6.5, 2.7 Hz, 2H), 6.89 – 6.88 (m, 1H), 6.89 – 6.86 (m, 1H), 6.72 (dd, *J* = 8.5, 6.8 Hz, 2H), 4.33 (d, *J* = 5.9 Hz, 2H) ppm; ^{13}C-NMR (126 MHz; $CDCl_3$): δ 164.32 (dt, *J* = 254.1, 15.1 Hz), 164.01 , 161.77 (ddd, *J* = 250.8, 14.9, 8.2 Hz), 159.63 (q, *J* = 40.8 Hz), 159.26, 154.03, 146.40, 135.30, 129.28, 128.75, 126.77, 106.56 (td, *J* = 20.7, 4.8 Hz), 101.15 – 100.70 (m), 90.43, 47.76 ppm; IR (film) ν 3352, 3268, 3113, 3067, 3033, 2928, 1642, 1617, 1595, 1575, 1495, 1441, 1124, 1036 cm^{-1}; HRMS (ES+) calculated for $C_{18}H_{12}ClF_3N_5$ $[M + H]^+$: 390.0733, found 390.0730.

5-Chloro-6-(2,4,6-trifluorophenyl)-7-((1,1,1-trifluoropropan-2-yl)oxy)-[1,2,4]triazolo[1,5-*a*]pyrimidine (42). To sodium hydride (60%, 0.015 g, 0.38 mmol) suspended in THF (3 ml) was added

1,1,1-trifluoropropan-2-ol (0.034 mL, 0.38 mmol) and the resulting mixture was stirred for 2 h while heated to reflux. 5,7-dichloro-6-(2,4,6-trifluorophenyl)-[1,2,4]triazolo[1,5-*a*]pyrimidine (0.100 g, 0.31 mmol) **(102)** was then added at r.t.. The reaction mixture was stirred for 20 min before the reaction was quenched with H_2O (5 ml) and extracted with EtOAc (×3). The combined organic layers were dried over $MgSO_4$, filtered, and concentrated under reduced pressure. Purification via silica gel column chromatography (0−40% EtOAc in hexanes) provided the title compound (0.046 g, 0.11 mmol, 37%). ^{1}H NMR (600 MHz, $CDCl_3$) δ 8.51 (s, 1H), 6.89 – 6.77 (m, 2H), 6.21 – 6.12 (m, 1H), 1.63 (d, *J* = 6.6 Hz, 4H) ppm; ^{13}C NMR (150 MHz, $CDCl_3$) δ 164.14 (dt, *J* = 253.1, 15.2 Hz), 161.12 (ddd, *J* = 252.7, 15.1, 8.7 Hz), 160.86 (ddd, *J* = 251.3, 15.0, 8.6 Hz), 158.43, 156.71, 155.59 (d, *J* = 43.8 Hz), 151.92, 123.23 (q, *J* = 281.1 Hz), 104.10 (td, *J* = 20.5, 4.9 Hz), 102.40 – 98.42 (m), 76.02 (q, *J* = 32.7, 31.8 Hz), 14.07, 12.80 ppm; IR (film) ν 2925, 2854, 1606, 1517, 1493 cm^{-1}; HRMS (ES+) calculated for $C_{14}H_8N_4ClF_6O$ $[M + H]^+$: 397.0285, found 397.0279.

5-Chloro-*N*-(1,1-difluoropropan-2-yl)-6-(2,4,6-trifluorophenyl)-[1,2,4]triazolo[1,5-*a*]pyrimidin-7-amine (43). Following General Procedure C using 5,7-dichloro-6-(2,5-difluorophenyl)-[1,2,4]triazolo[1,5-*a*]pyrimidine (0.053 g, 0.17 mmol) **(102)**, 1,1-difluoropropan-2-amine hydrochloride (0.045 g, 0.34 mmol) and Et_3N (0.093 mL, 0.67 mmol). Purification via silica gel column chromatography (0–30% EtOAc in hexanes) provided the title compound as a white powder (0.035 g, 0.09 mmol, 56%). ^{1}H NMR (500 MHz, $CDCl_3$) δ 8.37 (s, 1H), 6.89 (t, *J* = 7.9 Hz, 2H), 6.00 (d, *J* = 8.2 Hz, 1H), 5.75 (td, *J* = 55.4, 1.6 Hz, 1H), 4.32 (bs, 1H), 1.31 (d, *J* = 6.8 Hz, 3H) ppm; ^{13}C NMR (151 MHz, $CDCl_3$) δ 164.46 (dt, *J* = 254.9, 15.1 Hz), 161.5 (ddd, *J* = 250.66, 8.4, 5.4 Hz), 161.41 (ddd, *J* = 252.17, 8.3, 5.3 Hz), 157.94, 155.46, 154.22, 114.59 (t, *J* = 246.2 Hz), 105.90 (td, *J* = 20.5, 4.8 Hz), 101.54 (dtd, *J* = 29.9, 25.9, 4.1 Hz), 90.88, 51.09 (t, *J* = 24.16 Hz), 42.38 (t, *J* = 552.1 Hz), 29.82, 14.61 (t, *J* = 3.8 Hz) ppm; IR (film) ν 1613, 1578, 1552, 1527, 1492, 1461, 1440, 1360, 1263, 1124, 1208, 1171, 1134, 1122, 1100, 1083 cm^{-1}; HRMS (ES+) calculated for $C_{15}H_{10}ClF_5N_4$ $[M + H]^+$: 378.0539, found 378.0537.

5-Chloro-*N*-(1-fluoropropan-2-yl)-6-(2,4,6-trifluorophenyl)-[1,2,4]triazolo[1,5-*a*]pyrimidin-7-amine (44). Following General Procedure C using 5,7-dichloro-6-(2,5-difluorophenyl)-[1,2,4]triazolo[1,5-*a*]pyrimidine (0.073 g, 0.23 mmol) **(102)**, 1-fluoropropan-2-amine hydrochloride (0.053 g, 0.47 mmol) and Et_3N (0.130 mL, 0.91 mmol). Purification via silica gel column chromatography (0–30% EtOAc in hexanes) provided the title compound as a white powder (0.059 g, 0.16 mmol, 72%). ^{1}H NMR (600 MHz, $CDCl_3$) δ 8.35 (s, 1H), 6.93 – 6.83 (m, 2H), 6.26 (d, *J* = 8.1 Hz, 1H), 4.37 (ddd, *J* = 66, 9.6, 3.5 Hz, 1H), 4.29 (ddd, *J* = 66, 9.6, 4.3 Hz, 1H), 4.01 (bs, 1H), 1.26 (d, *J* = 6.8 Hz, 3H) ppm; ^{13}C NMR (151 MHz, $CDCl_3$) δ 164.29 (dt, *J* = 254.6, 15.2 Hz), 161.53 (ddd, *J* = 250.7, 14.9, 8.3, Hz), 161.52 (ddd, *J* = 249.9, 14.9, 8.3, Hz), 157.98, 155.28, 154.08, 146.19, 106.53 (td, *J* = 20.7, 4.7 Hz), 101.39 (tdd, *J* = 25.9, 9.1, 4.1 Hz), 90.03, 85.42 (d, *J* = 175.2 Hz), 49.79 (d, *J* = 19.6 Hz), 17.59 (d, *J* = 5.3 Hz), 14.32 ppm; IR (film) ν 1639, 1611, 1594, 1580, 1492, 1468, 1440, 1358, 1239, 1207, 1171 cm^{-1}; HRMS (ES+) calculated for $C_{15}H_{11}ClF_4N_4$ $[M + H]^+$: 360.0634, found 360.0636.

(*S*)-5-chloro-*N*-(3-methylbutan-2-yl)-6-(2,4,6-trifluorophenyl)-[1,2,4]triazolo[1,5-*a*]pyrimidin-7-amine (45). Following General Procedure C using 5,7-dichloro-6-(2,4,6-trifluorophenyl)-[1,2,4]triazolo[1,5-*a*]pyrimidine (0.119 g, 0.37 mmol) **(102)** and (*S*)-3-methylbutan-2-amine (0.090 mL, 0.78 mmol). Purification via silica gel column chromatography (0–15% EtOAc in hexanes) provided the title compound as a white powder (0.099 g, 0.27 mmol, 72%). The spectroscopic properties of the compound were identical to those reported for its enantiomer, **3**.[11]

(*R*)-5-Chloro-*N*-(1,1,1-trifluoro-3-methylbutan-2-yl)-6-(2,4,6-trifluorophenyl)-[1,2,4]triazolo[1,5-*a*]pyrimidin-7-amine (46). Following General Procedure C using 5,7-dichloro-6-(2,4,6-trifluorophenyl)-[1,2,4]triazolo[1,5-*a*]pyrimidine (0.123 g, 0.38 mmol) **(102)** and (*R*)-1,1,1-trifluoro-3-methyl-2-butylamine (0.152 mL, 1.15 mmol). Purification via silica gel column chromatography (0–15% EtOAc in hexanes) provided the title compound as a white powder (0.056 g, 0.13 mmol, 35%). ^{1}H NMR (500 MHz, $CDCl_3$) δ 8.41 (s, 1H), 7.01 – 6.77 (m, 2H), 6.28 (s, 1H), 3.96 (s, 1H), 2.26 – 2.09 (m, 1H), 1.03 (d,

J = 6.9 Hz, 3H), 0.97 (d, *J* = 6.8 Hz, 3H) ppm; ^{13}C NMR (126 MHz, $CDCl_3$) δ 164.69 (dt, *J* = 255.2, 15.1 Hz), 161.57 (ddd, *J* = 253.8, 15.0, 8.2 Hz), 161.32 (ddd, *J* = 251.3, 14.9, 8.2 Hz), 158.29, 155.56, 153.98, 146.56, 124.53 (q, *J* = 283.5 Hz), 101.86 (td, *J* = 25.8, 4.1 Hz), 101.36 (td, *J* = 25.2, 2.4 Hz), 90.99, 58.99 (q, *J* = 29.4 Hz), 28.34, 19.81, 16.74 ppm; IR (film) ν 3339, 2972, 2928, 1618, 1562, 1493, 1442, 1364, 1264, 1170, 1126, 1090, 1039, 999, 937, 911, 846, 768, 734, 705, 653 cm^{-1}; HRMS (ES+) calculated for $C_{16}H_{12}ClF_6N_5Na$ $[M + Na]^+$: 446.0583, found 446.0598.

(*S*)-5-Chloro-*N*-(1,1,1-trifluoro-3-methylbutan-2-yl)-6-(2,4,6-trifluorophenyl)-[1,2,4]triazolo[1,5-*a*]pyrimidin-7-amine (47). Following General Procedure C using 5,7-dichloro-6-(2,4,6-trifluorophenyl)-[1,2,4]triazolo[1,5-*a*]pyrimidine (0.123 g, 0.38 mmol) **(102)** and (*S*)-1,1,1-trifluoro-3-methyl-2-butylamine (0.152 mL, 1.15 mmol). Purification via silica gel column chromatography (0–15% EtOAc in hexanes) provided the title compound as a white powder (0.039 g, 0.09 mmol, 24%). ^{1}H NMR (500 MHz, $CDCl_3$) δ 8.41 (s, 1H), 6.99 – 6.84 (m, 2H), 6.29 (s, 1H), 3.98 (s, 1H), 2.24 – 2.10 (m, *J* = 6.7 Hz, 1H), 1.03 (d, *J* = 6.8 Hz, 3H), 0.97 (d, *J* = 6.8 Hz, 3H) ppm; ^{13}C NMR (126 MHz, $CDCl_3$) δ 164.63 (dt, *J* = 255.2, 15.0 Hz), 161.50 (ddd, *J* = 253.8, 14.9, 8.2 Hz), 161.25 (ddd, *J* = 251.3, 14.9, 8.2 Hz), 158.23, 155.49, 153.90, 146.50, 124.47 (q, *J* = 283.5 Hz), 101.80 (td, *J* = 25.8, 4.2 Hz), 101.30 (td, *J* = 27.1, 26.1, 3.7 Hz), 90.92, 58.93 (q, *J* = 29.4 Hz), 28.28, 19.75, 16.68 ppm; IR (film) ν 3339, 2972, 2930, 1618, 1562, 1493, 1459, 1442, 1364, 1264, 1170, 1126, 1090, 1066, 1038, 999, 938, 846, 768, 738, 704, 628 cm^{-1}; HRMS (ES+) calculated for $C_{16}H_{13}ClF_6N_5$ $[M + H]^+$: 424.0758, found 424.0762.

(*R*)-5-Chloro-6-(2,4,6-trifluorophenyl)-*N*-(1,1,1-trifluoropropan-2-yl)-[1,2,4]triazolo[1,5-*a*]pyrimidin-7-amine (48). Following General Procedure A using (*R*)-1,1,1-trifluoropropan-2-amine hydrochloride (0.090 g, 0.60 mmol), i-Pr_2NEt (0.078 g, 0.60 mmol) and 5,7-dichloro-6-(2,4,6-trifluorophenyl)-[1,2,4]triazolo[1,5-*a*]pyrimidine (0.064 g, 0.20 mmol) **(102)**. Purification via reverse-phase HPLC afforded the title compound as a white solid (0.017 g, 0.04 mmol, 21% yield). ^{1}H-NMR (500 MHz; $CDCl_3$): δ 8.39 (s, 1H), 6.91 (dd, *J* = 8.4, 7.1 Hz, 2H), 5.92 (d, *J* = 10.3 Hz, 1H), 4.73 (s, 1H), 1.43

(d, J = 6.9 Hz, 3H) ppm; ^{13}C-NMR (126 MHz; $CDCl_3$): δ 164.64 (dt, J = 255.3, 15.1 Hz), 161.65 (ddd, J = 253.4, 15.1, 8.2 Hz), 161.32 (ddd, J = 251.7, 14.9, 8.2 Hz), 157.97, 155.60, 154.26, 145.97, 124.57 (q, J = 282.0 Hz), 105.51 (td, J = 20.7, 4.8 Hz), 101.61 (dtd, J = 52.6, 26.1, 4.0 Hz), 91.50, 51.02 (q, J = 32.2 Hz), 15.30 ppm; IR (film) ν 3335, 3205, 2924, 2852, 1621, 1558, 1272, 1251, 1175, 1145, 1120 cm^{-1}; HRMS (ES+) calculated for $C_{14}H_9ClF_6N_5$ $[M + H]^+$: 396.0451, found 396.0451.

7-(Azetidin-1-yl)-5-chloro-6-(2,4,6-trifluorophenyl)-[1,2,4]triazolo[1,5-*a*]pyrimidine (49). Following General Procedure C using 5,7-dichloro-6-(2,4,6-trifluorophenyl)-[1,2,4]triazolo[1,5-*a*]pyrimidine (0.064 g, 0.20 mmol) **(102)** and azetidine (0.034 g, 0.60 mmol). Purification via reverse-phase HPLC afforded the title compound as a white solid (0.005 g, 0.02 mmol, 8% yield). ^{1}H-NMR (500 MHz; $CDCl_3$): δ 8.34 (s, 1H), 6.84 – 6.79 (m, 2H), 4.49 – 4.45 (m, 4H), 2.37 (quintet, J = 7.9 Hz, 2H) ppm; ^{13}C-NMR (126 MHz; $CDCl_3$): δ 164.10 (dt, J = 253.9, 15.2 Hz), 162.35 (dd, J = 249.8, 8.2 Hz), 162.23 (dd, J = 249.7, 8.4 Hz), 158.12, 155.06, 155.04, 154.45, 146.35, 106.96 (td, J = 21.0, 4.6 Hz), 100.80 – 100.36 (m), 89.00, 56.73, 29.86, 17.36 ppm; IR (film) ν 2957, 2924, 2852, 1594, 1558, 1455, 1255, 1167, 1120, 1041 cm^{-1}; HRMS (ES+) calculated for $C_{14}H_9ClF_3N_5$ $[M + H]^+$: 340.0577, found 340.0573.

5-Chloro-7-(pyrrolidin-1-yl)-6-(2,4,6-trifluorophenyl)-[1,2,4]triazolo[1,5-*a*]pyrimidine (50). Following General Procedure C using 5,7-dichloro-6-(2,4,6-trifluorophenyl)-[1,2,4]triazolo[1,5-*a*]pyrimidine (0.064 g, 0.20 mmol) **(102)** and pyrrolidine (0.043 g, 0.60 mmol). Purification by reverse-phase HPLC afforded the title compound as a yellow solid (0.009 g, 0.03 mmol, 14% yield). ^{1}H-NMR (500 MHz; $CDCl_3$): δ 8.37 (s, 1H), 6.81 (dd, J = 8.4, 6.9 Hz, 2H), 3.71 (t, J = 6.5 Hz, 4H), 1.91 (dt, J = 6.2, 3.3 Hz, 4H) ppm; ^{13}C-NMR (126 MHz; $CDCl_3$): δ 163.80 (dt, J = 252.3, 14.5 Hz), 161.66 (dd, J = 248.1, 7.1 Hz), 161.55 (dd, J = 249.6, 8.3 Hz), 158.54, 155.74, 154.26, 148.57, 109.66 (td, J = 20.7, 4.9 Hz), 100.94 – 100.50 (m), 92.85, 53.27, 25.94 ppm; IR (film) ν 3444, 1636, 1594, 1537, 1455, 1333, 1253, 1123 cm^{-1}. HRMS (ES+) calculated for $C_{15}H_{12}ClF_3N_5$ $[M + H]^+$: 354.0733, found 354.0723.

5-Chloro-7-(piperidin-1-yl)-6-(2,4,6-trifluorophenyl)-[1,2,4]triazolo[1,5-*a*]pyrimidine (51). Following General Procedure C using 5,7-dichloro-6-(2,4,6-trifluorophenyl)-[1,2,4]triazolo[1,5-*a*]pyrimidine (0.064 g, 0.20 mmol) **(102)** and piperidine (0.051 g, 0.60 mmol). Purification via reverse-phase HPLC afforded the title compound as a yellow solid (0.012 g, 0.03 mmol, 17% yield). ^{1}H-NMR (500 MHz; $CDCl_3$): δ 8.40 (s, 1H), 6.86 (dd, *J* = 8.4, 7.3 Hz, 2H), 3.27 (bs, 4H), 1.64 (bs, 6H) ppm; ^{13}C-NMR (126 MHz; $CDCl_3$): δ 163.71 (dt, *J* = 252.8, 15.4 Hz), 161.19 (dd, *J* = 250.3, 8.7 Hz), 161.08 (dd, *J* = 250.1, 8.8 Hz), 158.24, 155.29, 151.15, 108.64 (td, *J* = 20.2, 4.8 Hz), 101.30 – 100.86 (m), 98.10, 51.13, 25.98, 23.71 ppm; IR (film) ν 2945, 2929, 2857, 1595, 1558, 1538, 1506, 1446, 1361, 1121, 1035 cm^{-1}; HRMS (ES+) calculated for $C_{16}H_{14}ClF_3N_5$ $[M + H]^+$: 368.0890, found 368.0877.

7-(Azepan-1-yl)-5-chloro-6-(2,4,6-trifluorophenyl)-[1,2,4]triazolo[1,5-*a*]pyrimidine (52). Following General Procedure C using 5,7-dichloro-6-(2,4,6-trifluorophenyl)-[1,2,4]triazolo[1,5-*a*]pyrimidine (0.197 g, 0.62 mmol) **(102)** and azepane (0.184 g, 1.85 mmol). Purification via silica gel column chromatography (0–15% EtOAc in hexanes) provided the title compound as a white powder (0.057 g, 0.15 mmol, 24%). ^{1}H NMR (500 MHz, $CDCl_3$) δ 8.36 (s, 1H), 6.85 (t, *J* = 8.1 Hz, 2H), 3.45 – 3.39 (m, 4H), 1.76 – 1.67 (m, 4H), 1.65 – 1.58 (m, 4H) ppm; ^{13}C NMR (126 MHz, $CDCl_3$) δ 163.64 (dt, *J* = 253.0, 15.4 Hz), 161.10 (dd, *J* = 250.2, 8.8 Hz), 160.98 (dd, *J* = 250.3, 8.8 Hz), 158.21, 155.45, 155.08, 152.31, 109.08 (td, *J* = 20.4, 5.0 Hz), 102.17 – 100.48 (m), 98.50, 53.70, 28.28, 28.23 ppm; IR (film) ν 3436, 2932, 2858, 1637, 1593, 1525, 1492, 1443, 1357, 1284, 1259, 1231, 1200, 1171, 1152, 1125, 1100, 1035, 998, 968, 931, 842, 776, 760, 732, 656, 636, 614 cm^{-1}; HRMS (ES+) calculated for $C_{17}H_{16}ClF_3N_5$ $[M + H]^+$: 382.1041, found 382.1031.

7-(Azocan-1-yl)-5-chloro-6-(2,4,6-trifluorophenyl)-[1,2,4]triazolo[1,5-*a*]pyrimidine (53). Following general procedure C using 5,7-dichloro-6-(2,4,6-trifluorophenyl)-[1,2,4]triazolo[1,5-*a*]pyrimidine (0.191 g, 0.60 mmol) **(102)** and azocane (0.142 g, 1.26 mmol). Purification via silica gel column chromatography (0–20% EtOAc in hexanes) provided the title compound as a white powder (0.177 g, 0.45 mmol, 75%).

^{1}H NMR (500 MHz, $CDCl_3$) δ 8.32 (s, 1H), 6.81 (t, *J* = 7.9 Hz, 2H), 3.49 – 3.38 (m, 4H), 1.78 – 1.15 (m, 10H) ppm; ^{13}C NMR (126 MHz, $CDCl_3$) δ 163.63 (dt, *J* = 253.5, 15.2 Hz), 160.93 (dd, *J* = 250.6, 8.9 Hz), 160.81 (dd, *J* = 250.5, 8.7 Hz), 158.19, 155.50, 154.73, 151.18, 108.91 (td, *J* = 20.2, 4.8 Hz), 102.27 – 100.10 (m), 98.25, 51.91, 27.67, 26.77, 24.36 ppm; IR (film) ν 3450, 2927, 2860, 1637, 1593, 1529, 1494, 1440, 1375, 1356, 1266, 1230, 1212, 1171, 1151, 1124, 1091, 1035, 998, 967, 914, 846, 761, 735, 656, 636, 612 cm^{-1}; HRMS (ES+) calculated for $C_{18}H_{18}ClF_3N_5$ $[M + H]^+$: 396.1197, found 396.1201.

5-Chloro-*N*-cyclopropyl-6-(2,4,6-trifluorophenyl)-[1,2,4]triazolo[1,5-*a*]pyrimidin-7-amine (55). Following General Procedure C using 5,7-dichloro-6-(2,4,6-trifluorophenyl)-[1,2,4]triazolo[1,5-*a*]pyrimidine (0.064 g, 0.20 mmol) **(102)**, cyclopropanamine (0.057 g, 0.60 mmol) and i-Pr_2NEt (0.078 g, 0.60 mmol). Purification via reverse-phase HPLC afforded the title compound as a beige solid (0.021 g, 0.06 mmol, 30% yield). ^{1}H-NMR (500 MHz; $CDCl_3$): δ 8.34 (s, 1H), 6.84 – 6.80 (m, 3H), 2.36 – 2.33 (m, 1H), 0.68 – 0.65 (m, 2H), 0.48 – 0.44 (m, 2H) ppm; ^{13}C-NMR (126 MHz; $CDCl_3$): δ 163.93 (dt, *J* = 252.6, 13.5 Hz), 162.00 (dd, *J* = 249.8, 8.5 Hz), 161.88 (dd, *J* = 250.1, 9.0 Hz), 158.41, 155.18, 153.53, 147.23, 147.17, 108.06 (td, *J* = 20.8, 5.0 Hz), 100.71 – 100.27 (m), 89.74, 89.70, 25.70, 25.56, 9.00, 8.96 ppm; IR (film) ν 3361, 3260, 3104, 2919, 1597, 1576, 1494, 1441, 1264, 1123, 1032 cm^{-1}; HRMS (ES+) calculated for $C_{14}H_{19}ClF_3N_5$ $[M + H]^+$: 340.0577, found 340.0574.

5-Chloro-*N*-cyclobutyl-6-(2,4,6-trifluorophenyl)-[1,2,4]triazolo[1,5-*a*]pyrimidin-7-amine (56). Following general procedure C using 5,7-dichloro-6-(2,4,6-trifluorophenyl)-[1,2,4]triazolo[1,5-*a*]pyrimidine (0.030 g, 0.09 mmol) **(102)** and cyclobutanamine (0.014 g, 0.20 mmol). Purification via silica gel column chromatography (0−40% EtOAc in hexanes) provided the title compound as a white powder (0.025 g, 0.07 mmol, 75%). ^{1}H NMR (600 MHz, $CDCl_3$) δ 8.35 (s, 1H), 6.85 – 6.81 (m, 2H), 6.61 (d, *J* = 7.5 Hz, 1H), 3.71 (q, *J* = 7.7 Hz, 1H), 2.08 – 1.94 (m, 4H), 1.80 – 1.73 (m, 1H), 1.60 – 1.51 (m, 1H), 1.24 (s, 1H) ppm; ^{13}C NMR (150 MHz, $CDCl_3$) δ 164.03 (dt, *J* = 253.8, 15.4 Hz), 161.71 (ddd, *J* = 250.5, 15.1, 8.4 Hz), 158.22, 155.04, 145.33, 120.10 , 102.32 – 99.71 (m), 89.07, 48.80, 31.96, 14.62

ppm; IR (film) 3285, 2838, 2178, 1571 cm^{-1}; HRMS (ES+) calculated for $C_{15}H_{12}ClF_3N_5$ $[M + H]^+$: 354.0728, found 354.0726.

5-Chloro-*N*-cyclopentyl-6-(2,4,6-trifluorophenyl)-[1,2,4]triazolo[1,5-*a*]pyrimidin-7-amine (57). Following general procedure C using 5,7-dichloro-6-(2,4,6-trifluorophenyl)-[1,2,4]triazolo[1,5-*a*]pyrimidine (0.030 g, 0.09 mmol) **(102)** and cyclopentanamine (0.017 g, 0.20 mmol). Purification via silica gel column chromatography (0−40% EtOAc in hexanes) provided the title compound as a white powder (0.027 g, 0.07 mmol, 78%). ^{1}H NMR (600 MHz, $CDCl_3$) δ 8.31 (s, 1H), 6.84 – 6.81 (m, 2H), 6.42 (d, *J* = 8.3 Hz, 1H), 3.63 (s, 1H), 1.82 – 1.59 (m, 4H), 1.62 – 1.38 (m, 4H) ppm. ^{13}C NMR (150 MHz, $CDCl_3$) δ 163.99 (dt, *J* = 253.7, 15.2 Hz), 161.66 (ddd, *J* = 250.5, 15.0, 8.4 Hz), 158.19, 154.93, 145.81, 101.30 – 100.53 (m), 88.98, 55.11, 34.64, 23.92 ppm; IR (film) ν 3195, 2838, 1678, 1553 cm^{-1}; HRMS (ES+) calculated for $C_{16}H_{14}N_5ClF_3$ $[M + H]^+$: 368.0884, found 368.0881.

5-Chloro-*N*-cyclohexyl-6-(2,4,6-trifluorophenyl)-[1,2,4]triazolo[1,5-*a*]pyrimidin-7-amine (58). Following general procedure C using 5,7-dichloro-6-(2,4,6-trifluorophenyl)-[1,2,4]triazolo[1,5-*a*]pyrimidine (0.100 g, 0.31 mmol) **(102)** and cyclohexanamine (0.094 g, 0.94 mmol). Purification via silica gel column chromatography (0–40% EtOAc in hexanes) provided the title compound as a white powder (0.119 g, 0.31 mmol, 99%). ^{1}H NMR (500 MHz, $CDCl_3$) δ 8.33 (s, 1H), 6.92 – 6.81 (m, 2H), 6.37 (d, *J* = 8.7 Hz, 1H), 3.14 – 2.98 (m, 1H), 1.86 – 1.77 (m, 2H), 1.74 – 1.64 (m, 2H), 1.53 (dt, *J* = 13.2, 3.8 Hz, 1H), 1.30 – 1.18 (m, 2H), 1.12 (tdd, *J* = 12.9, 9.8, 6.1 Hz, 1H), 1.01 – 0.85 (m, 2H) ppm; ^{13}C NMR (126 MHz, $CDCl_3$) δ 164.08 (dt, *J* = 253.8, 15.1 Hz), 161.76 (dd, *J* = 250.7, 8.5 Hz), 161.65 (dd, *J* = 250.7, 8.4 Hz), 158.12, 155.00, 153.74, 145.59, 107.50 (td, *J* = 20.7, 4.8 Hz), 102.70 – 97.55 (m), 88.82, 52.94, 34.06, 24.92, 24.75 ppm; IR (film) ν 3341, 3103, 2934, 2856, 2239, 1636, 1610, 1578, 1492, 1439, 1367, 1341, 1313, 1263, 1207, 1159, 1125, 1036, 998, 976, 957, 930, 844, 766, 733, 655, 627 cm^{-1}; HRMS (ES+) calculated for $C_{17}H_{16}ClF_3N_5$ $[M + H]^+$: 382.1041, found 382.1054.

5-Chloro-*N*-neopentyl-6-(2,4,6-trifluorophenyl)-[1,2,4]triazolo[1,5-*a*]pyrimidin-7-amine (59). Following General Procedure C using 5,7-dichloro-6-(2,4,6-trifluorophenyl)-[1,2,4]triazolo[1,5-*a*]pyrimidine (0.050 g, 0.16 mmol) **(102)** and 2,2-dimethylpropan-1-amine (0.039 mL, 0.33 mmol). Purification via silica gel column chromatography (0–30% EtOAc in hexanes) provided the title compound as a white powder (0.033 g, 0.09 mmol, 57%). ^{1}H NMR (500 MHz, $CDCl_3$) δ 8.33 (s, 1H), 6.85 (dd, *J* = 8.0, 7.2 Hz, 2H), 6.45 (s, 1H), 2.80 (d, *J* = 5.7 Hz, 2H), 0.88 (s, 9H) ppm; ^{13}C NMR (126 MHz, $CDCl_3$) δ 164.63 (dt, *J* = 255.2, 15.0 Hz), 161.50 (ddd, *J* = 253.8, 14.9, 8.2 Hz), 161.25 (ddd, *J* = 251.3, 14.9, 8.2 Hz), 158.23, 155.49, 153.90, 146.50, 124.47 (q, *J* = 283.5 Hz), 101.80 (td, *J* = 25.8, 4.2 Hz), 101.30 (td, *J* = 27.1, 26.1, 3.7 Hz), 90.92, 58.93 (q, *J* = 29.4 Hz), 28.28, 19.75, 16.68 ppm; IR (film) ν 2959, 1636, 1611, 1573, 1495, 1438, 1358, 1263, 1250, 1124, 1036, 998, 843 766, 533 cm^{-1}; HRMS (ES+) calculated for $C_{16}H_{15}ClF_3N_5$ $[M + H]^+$: 370.1041, found 370.1039.

(*S*)-5-Chloro-*N*-(3,3-dimethylbutan-2-yl)-6-(2,4,6-trifluorophenyl)-[1,2,4]triazolo[1,5-*a*]pyrimidin-7-amine (60). Following General Procedure C using 5,7-dichloro-6-(2,4,6-trifluorophenyl)-[1,2,4]triazolo[1,5-*a*]pyrimidine (0.100 g, 0.31 mmol) **(102)** and (*S*)-3,3-dimethylbutan-2-amine (0.088 mL, 0.66 mmol). Purification via silica gel column chromatography (0–30% EtOAc in hexanes) provided the title compound as a white powder (0.094 g, 0.24 mmol, 78%). ^{1}H NMR (500 MHz, $CDCl_3$) δ 8.31 (s, 1H), 6.92 – 6.74 (m, 2H), 6.44 (s, 1H), 3.08 (s, 1H), 1.00 (d, *J* = 6.7 Hz, 4H), 0.82 (s, 11H) ppm; ^{13}C NMR (126 MHz, $CDCl_3$) δ 164.07 (dt, *J* = 254.0, 15.2 Hz), 161.52 (ddd, *J* = 250.8, 14.8, 8.4 Hz), 161.27 (ddd, *J* = 250.6, 14.9, 8.4 Hz), 158.13, 154.94, 153.61, 146.25, 107.54 (td, *J* = 20.6, 5.1 Hz), 101.51 – 100.58 (m), 88.60, 58.07, 34.72, 25.78, 16.58 ppm; IR (film) ν 1608, 1578, 1490, 1438, 1354, 1264, 1252, 1124, 999, 767, 623, 540 cm^{-1}; HRMS (ES+) calculated for $C_{17}H_{17}ClF_3N_5$ $[M + H]^+$: 384.1197, found 384.1198.

(*R*)-5-Chloro-*N*-(3,3-dimethylbutan-2-yl)-6-(2,4,6-trifluorophenyl)-[1,2,4]triazolo[1,5-*a*]pyrimidin-7-amine (61). Following General Procedure C using 5,7-dichloro-6-(2,4,6-trifluorophenyl)-[1,2,4]triazolo[1,5-*a*]pyrimidine (0.150 g, 0.47 mmol) **(102)** and (*R*)-3,3-dimethylbutan-2-amine (0.132

mL, 0.99 mmol). Purification via silica gel column chromatography (0–30% EtOAc in hexanes) provided the title compound as a white powder (0.157 g, 0.86 mmol, 87%). The spectroscopic properties of the compound were identical to those reported for **60**.

5-Chloro-7-(3,3,3-trifluoro-2-methylpropyl)-6-(2,4,6-trifluorophenyl)-[1,2,4]triazolo[1,5-*a*]pyrimidine (62). To a solution of *tert*-butyl 2-(5-chloro-6-(2,4,6-trifluorophenyl)-[1,2,4]triazolo[1,5-*a*]pyrimidin-7-yl)-4,4,4-trifluoro-3-methylbutanoate (0.026 g, 0.05 mmol, 1 equiv) **(112)** in CH_2Cl_2 (2 mL) at r.t. was added 2,2,2-trifluoroacetic acid (0.125 mL, 1.60 mmol, 30 equiv). The mixture was stirred 16 h at r.t. and then diluted with CH_2Cl_2 and quenched with a saturated $NaHCO_3$ solution. The aqueous layer was then extracted with CH_2Cl_2 and the combined organic layers were dried over $MgSO_4$, filtered and concentrated under reduced pressure. Purification via preparative reverse-phase HPLC (C18 column, 20 ml/min, 10 min ramp, 10 to 90% ACN/H_2O + 0.1% formic acid, tr = 8.5 min) provided the title compound (0.014 g, 0.04 mmol, 68 %) as a tan solid. ^{1}H NMR (600 MHz, $CDCl_3$) δ 8.56 (s, 1H), 6.92 – 6.88 (m, 2H), 3.34 (dd, *J* = 13.9, 6.2 Hz, 1H), 3.22 (m, 1H), 3.05 (dd, *J* = 13.9, 8.4 Hz, 1H), 1.03 (d, *J* = 7.0 Hz, 4H) ppm; ^{13}C NMR (151 MHz, $CDCl_3$) δ 164.45 (dt, 256.7, 18.1 Hz), 160.86 (ddd, 252.2, 15.1, 9.1 Hz), 160.61 (ddd, 250.7, 15.1, 9.06 Hz), 157.19, 157.02, 154.03, 148.77, 127.25 (q, 280.11 Hz) 112.29, 106.39 (td, 21.14, 4.9 Hz), 101.48 (dtd, *J* = 30.1, 25.9, 4.1 Hz), 35.37 (q, *J* = 27.6 Hz), 30.65, 12.88 ppm; IR (film) ν 1639, 1609, 1599, 1516, 1495, 1442, 1278, 1265, 1207, 1186, 1172, 1146, 1122, 1039, 999 cm^{-1}; HRMS (ES+) calculated for $C_{15}H_9ClF_6N_4$ $[M + H]^+$: 395.0493, found 395.0486.

(*S*)-4-(5-Chloro-7-((1,1,1-trifluoropropan-2-yl)amino)-[1,2,4]triazolo[1,5-*a*]pyrimidin-6-yl)-3-fluorobenzonitrile (63). Following general procedure C using 4-(5,7-dichloro-[1,2,4]triazolo[1,5-*a*]pyrimidin-6-yl)-3-fluorobenzonitrile (0.040 g, 0.13 mmol) **(107)** and *(S)*-1,1,1-trifluoropropan-2-amine (0.031 g, 0.27 mmol). Purification by reverse-phase HPLC provided the title compound as a white powder (0.031 g, 0.07 mmol, 54%). ^{1}H NMR (600 MHz, $CDCl_3$) mixture of diastereomers δ 8.41 (s, 1H), 7.68 (ddd, *J* = 7.8, 3.8, 1.5 Hz, 1H), 7.61 (ddd, *J* = 8.4, 3.8, 1.5 Hz, 1H), 7.57 (t, *J* = 7.4 Hz, 1H), 7.50 (t, *J* =

7.3 Hz, 1H), 5.94 (d, *J* = 11.0 Hz, 1H), 5.57 (d, *J* = 10.8 Hz, 1H), 4.97 (s, 1H), 4.50 (s, 1H), 1.40 (d, *J* = 6.9 Hz, 3H) ppm; ^{13}C NMR (150 MHz, $CDCl_3$) δ 161.29 (d, *J* = 52.0 Hz), 159.61 (d, *J* = 50.4 Hz), 156.65 (d, *J* = 24.9 Hz), 155.72 (d, *J* = 11.0 Hz), 154.20 (d, *J* = 57.5 Hz), 145.65 (d, *J* = 62.8 Hz), 135.00 (d, *J* = 2.0 Hz), 133.84 (d, *J* = 2.2 Hz), 129.21 (d, *J* = 4.2 Hz), 124.97 (dd, *J* = 16.2, 13.1 Hz), 124.67 (qd, *J* = 282.3, 34.7 Hz), 120.62 (dd, *J* = 74.3, 25.2 Hz), 116.67 (d, *J* = 2.8 Hz), 116.33 (dd, *J* = 9.3, 5.2 Hz), 97.66, 96.61, 51.26 (dq, *J* = 37.9, 31.8 Hz), 15.13, 14.99 ppm; HRMS (ES+) calculated for $C_{15}H_{10}ClF_4N_6$ $[M + H]^+$: 385.0586, found 385.0589.

(*R*)-5-Chloro-6-(2,6-difluorophenyl)-*N*-(3-methylbutan-2-yl)-[1,2,4]triazolo[1,5-*a*]pyrimidin-7-amine (64). Following General Procedure C using 5,7-dichloro-6-(3,5-difluorophenyl)-[1,2,4]triazolo[1,5-*a*]pyrimidine (0.048 g, 0.16 mmol) **(97)** and (*R*)-3-methylbutan-2-amine (0.028 g, 0.32 mmol). Purification via silica gel column chromatography (0−30% EtOAc in hexanes) provided the title compound as a white powder (0.049 g, 0.14 mmol, 87%). ^{1}H NMR (600 MHz, $CDCl_3$) δ 8.32 (s, 1H), 7.54 – 7.49 (m, 1H), 7.09 – 7.06 (m, 2H), 6.34 (bs, 1H), 3.12 (bs, 1H), 1.61 (oct, *J* = 6 Hz, 1H), 1.03 (d, *J* = 6 Hz, 3H), 0.77 (d, *J* = 6 Hz, 3H), 0.74 (d, *J* = 6 Hz, 3H) ppm; ^{13}C NMR (150 MHz, $CDCl_3$) δ 160.77 (dt, *J* = 250.66, 5.3 Hz), 158.04, 154.89 (d, *J* = 4.5 Hz), 153.65, 145.94, 132.38 – 132.22 (m), 110.93 (t, *J* = 21.1 Hz), 112.08 – 111.81 (m), 89.78, 54.76, 33.65, 33.63, 18.21 (q, 3Hz), 18.00 (q, *J* = 7.6 Hz), 17.80 (q, *J* = 3 Hz) ppm; HRMS (ES+) calculated for $C_{18}H_{17}ClFN_6$ $[M + H]^+$: 352.1135, found 352.1135.

(*R*)-5-chloro-6-(2-fluorophenyl)-*N*-(3-methylbutan-2-yl)-[1,2,4]triazolo[1,5-*a*]pyrimidin-7-amine (65). Following General Procedure C using 5,7-dichloro-6-(2-fluorophenyl)-[1,2,4]triazolo[1,5-*a*]pyrimidine (0.046 g, 0.16 mmol) **(95)** and (*R*)-3-methylbutan-2-amine (0.028 g, 0.32 mmol). Purification via silica gel column chromatography (0−30% EtOAc in hexanes) provided the title compound as a white powder (0.017 g, 0.051 mmol, 31%). ^{1}H NMR (600 MHz, $CDCl_3$) mixture of diastereomers δ 8.33 (s, 1H), 7.52 (q, *J* = 6 Hz, 1H), 7.36 – 7.29 (m, *2*H), 7.24 (t, *J* = 6 Hz, 1H), 6.19 (bs, 1H), 3.15 (bs, 1H), 1.02 (d, *J* = 6 Hz, 1.5H), 0.96 (d, *J* = 6 Hz, 1.5H), 0.77 (t, *J* = 6 Hz, 3H), 0.74 (d, *J* =

6 Hz, 1.5H), 0.72 (d, J = 6 Hz, 1.5H) ppm; ^{13}C NMR (150 MHz, $CDCl_3$) δ 160.83 (dd, J = 250.66, 9 Hz), 158.26 (d, J = 12.1 Hz), 153.91, 152.70, 146.02, 133.61, 133.61, 132.98, 132.06 (t, J = 8.3 Hz), 124.94 (d, J = 4.5 Hz), 124.89 (d, J = 3.0 Hz), 120.96 (d, J = 25.7 Hz), 120.85 (dd, J = 21.9, 1.6 Hz), 97.14, 96.99, 54.75, 54.59, 33.77, 33.47, 18.28, 17.98, 17.81, 17.73, 17.62 ppm; HRMS (ES+) calculated for $C_{18}H_{17}ClFN_6$ $[M + H]^+$: 334.1229, found 334.1227.

***(R)*-4-(5-Chloro-7-((3-methylbutan-2-yl)amino)-[1,2,4]triazolo[1,5-*a*]pyrimidin-6-yl)-3,5-difluorobenzonitrile (66).** Following general procedure C using 4-(5,7-dichloro-[1,2,4]triazolo[1,5-*a*]pyrimidin-6-yl)-3,5-difluorobenzonitrile (0.030 g, 0.09 mmol) **(106)** and *(R)*-3-methylbutan-2-amine (0.017 g, 0.19 mmol). Purification by reverse-phase HPLC provided the title compound as a white powder (0.028 g, 0.07 mmol, 81%). ^{1}H NMR (600 MHz, DMSO-d_6) δ 8.62 (s, 1H), 8.11 (t, J = 7.8 Hz, 2H), 7.88 (s, 1H), 1.78 (dq, J = 13.9, 6.8 Hz, 1H), 1.10 (d, J = 6.6 Hz, 3H), 0.74 (dd, J = 6.8, 2.9 Hz, 6H) ppm; ^{13}C NMR (151 MHz, DMSO-d_6) δ 160.71 (dd, J = 249.2, 6.8 Hz), 160.38 (dd, J = 249.5, 6.3 Hz), 155.02, 146.81 , 117.00 (ddd, J = 26.3, 12.6, 3.9 Hz), 116.48 (d, J = 3.5 Hz), 114.83 (t, J = 12.8 Hz) ppm; ^{19}F NMR (469 MHz) δ –103.93 (d, J = 9.9 Hz), –104.42 (d, J = 9.9 Hz) ppm; IR (film) ν 2966, 2220, 1690, 1562, 1422, 1204 cm^{-1}; HRMS (ES+) calculated for $C_{17}H_{16}ClF_2N_6$ $[M + H]^+$: 377.1088, found 377.1089.

(*R*)-4-(5-chloro-7-((3-methylbutan-2-yl)amino)-[1,2,4]triazolo[1,5-*a*]pyrimidin-6-yl)-3-fluorobenzonitrile (67) and (68). Following general procedure C using 4-(5,7-dichloro-[1,2,4]triazolo[1,5-*a*]pyrimidin-6-yl)-3-fluorobenzonitrile (0.048 g, 0.15 mmol) **(107)** and (*R*)-3-methylbutan-2-amine (0.037 g, 0.42 mmol). Purification via silica gel column chromatography provided atropoisomer **67** as a white solid (0.029 g, 0.08 mmol, 39%) and atroposiomer **68** (0.023 g, 0.06 mmol, 30%). Recrystallization of **68** from CH_2Cl_2, followed by single crystal diffraction (m.p. 143.7 – 145.2) permitted the structural assignment of the two atropoisomers (see Supporting Material). **68** ^{1}H NMR (600 MHz, $CDCl_3$) δ 8.35 (s, 1H), 7.63 (dd, J = 12.0, 3.0 Hz, 1H), 7.56 (dd, J = 12.0, 3.0 Hz, 1H), 7.53 (t, J = 9.0 Hz, 1H), 6.29 (d, J = 12.0 Hz, 1H), 3.00 (bs, 1H), 1.64 (oct, J = 6.0 Hz, 1H), 0.99 (d, J = 6 Hz, 3H),

0.80 (d, J = 6 Hz, 3H), 0.77 (d, J = 6 Hz, 3H) ppm; ^{13}C NMR (150 MHz, $CDCl_3$) δ 161.37, 159.70, 156.91, 155.15, 153.15, 145.67, 134.39, 128.71, 128.69, 127.13 (d, J = 16.6 Hz), 120.02 (d, J = 25.7 Hz), 116.98, 115.50 (d, J = 9.1 Hz), 94.53, 55.04, 33.48, 18.16, 17.80, 17.14 ppm. **67** ^{1}H NMR (600 MHz, $CDCl_3$) δ 8.35 (s, 1H), 7.63 (dd, J = 12.0, 3.0 Hz, 1H), 7.56 (dd, J = 12.0, 3.0 Hz, 1H), 7.52 (t, J = 9.0 Hz, 1H), 6.30 (bs, 1H), 3.05 (bs, 1H), 1.61 (oct, J = 6.0 Hz, 1H), 1.05 (d, J = 6 Hz, 3H), 0.79 (d, J = 6 Hz, 3H), 0.75 (d, J = 6 Hz, 3H) ppm; ^{13}C NMR (150 MHz, $CDCl_3$) δ 161.40, 159.73, 156.90, 155.19, 153,57, 145.67, 135.08, 134.40 (d, J = 3.0 Hz), 128.55 (d, J = 4.5 Hz), 127.03 (d, J = 15.1 Hz), 120.22 (d, J = 25.7 Hz), 117.01, 115.45 (d, J = 9.1 Hz), 94.37, 54.85, 33.80, 18.20, 17.90, 17.82 ppm; IR (film) ν 2963, 2220, 1608, 1570, 1260, 1156 cm^{-1}; HRMS (ES+) calculated for $C_{18}H_{17}ClFN_6$ $[M + H]^+$: 359.1182, found 359.1184.

(*R*)-4-(5-Chloro-7-((3,3-dimethylbutan-2-yl)amino)-[1,2,4]triazolo[1,5-*a*]pyrimidin-6-yl)-3,5-difluorobenzonitrile (69). Following general procedure C using 4-(5,7-dichloro-[1,2,4]triazolo[1,5-*a*]pyrimidin-6-yl)-3,5-difluorobenzonitrile (0.020 g, 0.06 mmol) **(106)** and (*R*)-3,3-dimethylbutan-2-amine (0.013 g, 0.13 mmol). Purification by reverse-phase HPLC provided the title compound as a white powder (0.018 g, 0.05 mmol, 75%). ^{1}H NMR (600 MHz, $CDCl_3$) δ 8.36 (s, 1H), 7.45 – 7.41 (m, 2H), 6.52 (d, J = 10.8 Hz, 1H), 2.94 (s, 1H), 1.02 (d, J = 6.7 Hz, 3H), 0.84 (s, 9H) ppm; ^{13}C NMR (150 MHz, $CDCl_3$) δ 161.33 (dd, J = 253.8, 6.2 Hz), 161.05 (dd, J = 253.8, 6.2 Hz), 157.12, 155.22, 146.03, 116.22 (d, J = 4.0 Hz), 116.13 – 115.95 (m), 115.95 – 115.82 (m), 58.57, 34.93, 25.86, 16.56 ppm; ^{19}F NMR (469 MHz) δ –103.70 (d, J = 4.7 Hz), –104.31 (d, J = 4.7 Hz) ppm; HRMS (ES+) calculated for $C_{18}H_{18}ClF_2N_6$ $[M + H]^+$: 391.1244, found 391.1241.

(*R*)-4-(5-Chloro-7-((3,3-dimethylbutan-2-yl)amino)-[1,2,4]triazolo[1,5-*a*]pyrimidin-6-yl)-3-fluorobenzonitrile (70). Following general procedure C using 4-(5,7-dichloro-[1,2,4]triazolo[1,5-*a*]pyrimidin-6-yl)-3-fluorobenzonitrile (0.040 g, 0.13 mmol) **(107)** and *(R)*-3,3-dimethylbutan-2-amine (0.028 g, 0.27 mmol). Purification by reverse-phase HPLC provided the title compound as a white powder

(0.027 g, 0.07 mmol, 56%). ^{1}H NMR (600 MHz, $CDCl_3$) mixture of diastereomers δ 8.41 – 8.34 (m, 1H), 7.67 – 7.61 (m, 1H), 7.60 – 7.55 (m, 1H), 7.55 – 7.49 (m, 1H), 6.37 (s, 1H), 2.94 – 2.89 (m, 1H), 1.01 (d, *J* = 6.7 Hz, 1H), 0.94 (d, *J* = 6.7 Hz, 2H), 0.82 (s, 5H), 0.81 (s, 4H) ppm; ^{13}C NMR (150 MHz, $CDCl_3$) δ 161.71 – 159.28 (m), 156.76, 156.67, 145.96, 135.28 (d, *J* = 2.4 Hz), 133.96 (d, *J* = 2.3 Hz), 128.65 (d, *J* = 4.1 Hz), 128.43 (d, *J* = 4.1 Hz), 119.96 (dd, *J* = 37.6, 25.4 Hz), 116.86 (d, *J* = 2.8 Hz), 115.42 (dd, *J* = 16.7, 9.3 Hz), 94.27, 94.14, 58.27, 58.07, 35.01, 34.82, 25.77 (d, *J* = 1.9 Hz), 16.42 (d, *J* = 2.2 Hz) ppm; HRMS (ES+) calculated for $C_{18}H_{19}ClFN_6$ $[M + H]^+$: 373.1338, found 373.1338.

4-(5-chloro-7-((1*R*,3*s*,5*S*)-3-methoxy-8-azabicyclo[3.2.1]octan-8-yl)-[1,2,4]triazolo[1,5-*a*]pyrimidin-6-yl)-3,5-difluorobenzonitrile (71). Following general procedure C using 4-(5,7-dichloro-[1,2,4]triazolo[1,5-*a*]pyrimidin-6-yl)-3,5-difluorobenzonitrile (0.100 g, 0.31 mmol) **(106)**, (1*R*,3*R*,5*S*)-3-methoxy-8-azabicyclo[3.2.1]octane hydrochloride (0.082 g, 0.46 mmol) and Et_3N (0.094 g, 0.92 mmol). Purification by reverse-phase HPLC provided the title compound as a white powder (0.112 g, 0.26 mmol, 85%). ^{1}H NMR (600 MHz, $CDCl_3$) δ 8.28 (s, 1H), 7.39 (d, *J* = 5.9 Hz, 2H), 4.57 (s, 2H), 3.45 (s, 1H), 3.23 (s, 3H), 2.13 (d, *J* = 7.4 Hz, 2H), 2.00 (d, *J* = 14.9 Hz, 2H), 1.92 (d, *J* = 14.7 Hz, 2H), 1.80 – 1.74 (m, 2H) ppm; ^{13}C NMR (150 MHz, $CDCl_3$) δ 161.66 (d, *J* = 6.6 Hz), 159.98 (d, *J* = 6.6 Hz), 156.99, 155.05, 146.39, 118.79, 116.34, 116.30, 116.18, 116.15, 116.11, 115.16 (t, *J* = 11.8 Hz), 92.08, 73.33, 62.34, 59.30, 56.53, 36.34, 27.98 ppm; HRMS (ES+) calculated for $C_{20}H_{18}ClF_2N_6O$ $[M + H]^+$: 431.1188, found 431.1193.

4-(7-(Azepan-1-yl)-5-chloro-[1,2,4]triazolo[1,5-*a*]pyrimidin-6-yl)-3,5-difluorobenzonitrile (72). Following general procedure C using 4-(5,7-dichloro-[1,2,4]triazolo[1,5-*a*]pyrimidin-6-yl)-3,5-difluorobenzonitrile (0.020 g, 0.06 mmol) **(106)** and azepane (0.013 g, 0.13 mmol). Purification by reverse-phase HPLC provided the title compound as a white powder (0.015 g, 0.04 mmol, 63%). ^{1}H NMR (600 MHz, $CDCl_3$) δ 8.38 (s, 1H), 7.40 (d, *J* = 6.0 Hz, 2H), 3.45 – 3.39 (m, 4H), 1.78 – 1.70 (m, 4H), 1.64 – 1.60 (m, 4H) ppm; ^{13}C NMR (150 MHz, $CDCl_3$) δ 160.74 (dd, *J* = 253.4, 6.6 Hz), 157.14, 155.26,

152.10, 118.61 (t, J = 19.7 Hz), 116.30 – 115.97 (m), 115.12 (t, J = 11.9 Hz), 97.32, 53.99, 51.22, 28.27, 28.17, 27.28, 27.07 ppm; ^{19}F NMR (469 MHz) δ –105.22 ppm; IR (film) ν 2928, 2857, 2238, 1589, 1515, 1422 cm^{-1}; HRMS (ES+) calculated for $C_{18}H_{16}ClF_2N_6$ [M + H]$^+$: 389.1088, found 389.1085.

4-(7-(Azepan-1-yl)-5-chloro-[1,2,4]triazolo[1,5-*a*]pyrimidin-6-yl)-3-fluorobenzonitrile (73).

Following general procedure C using 4-(5,7-dichloro-[1,2,4]triazolo[1,5-*a*]pyrimidin-6-yl)-3-fluorobenzonitrile (0.040 g, 0.13 mmol) **(107)** and azepane (0.027 g, 0.27 mmol). Purification by reverse-phase HPLC provided the title compound as a white powder (0.027 g, 0.07 mmol, 56%). ^{1}H NMR (600 MHz, $CDCl_3$) δ 8.34 (s, 1H), 7.61 (dd, J = 7.9, 1.6 Hz, 1H), 7.53 (dd, J = 8.7, 1.6 Hz, 1H), 7.48 (t, J = 7.5 Hz, 1H), 3.38 – 3.33 (m, 4H), 1.71 (dq, J = 8.0, 4.2 Hz, 4H), 1.60 (p, J = 3.0 Hz, 4H) ppm; ^{13}C NMR (150 MHz, $CDCl_3$) δ 160.85, 159.18, 156.93, 155.27, 155.18, 151.61, 134.44 (d, J = 2.8 Hz), 128.60 (d, J = 3.9 Hz), 128.48, 120.11, 119.94, 117.09 (d, J = 2.8 Hz), 114.68 (d, J = 9.2 Hz), 103.59, 54.05, 28.27, 28.03 ppm; IR (film) ν 2926, 2235, 1589, 1519, 1446 cm^{-1}; HRMS (ES+) calculated for $C_{18}H_{17}ClFN_6$ [M + H]$^+$: 371.1182, found 371.1180.

4-(7-(Azocan-1-yl)-5-chloro-[1,2,4]triazolo[1,5-*a*]pyrimidin-6-yl)-3,5-difluorobenzonitrile (74).

Following general procedure C using 4-(5,7-dichloro-[1,2,4]triazolo[1,5-*a*]pyrimidin-6-yl)-3,5-difluorobenzonitrile (0.054 g, 0.17 mmol) **(106)** and azocane (0.019 g, 0.17 mmol). Purification via silica gel column chromatography provided the title compound as a white solid (0.031 g, 0.08 mmol, 46%). ^{1}H NMR (600 MHz, $CDCl_3$) δ 8.29 (s, 1H), 7.30 (d, J = 6.0 Hz, 2H), 3.36 (t, J = 5.7 Hz, 5H), 1.62 (t, J = 5.8 Hz, 5H), 1.52 (t, J = 5.5 Hz, 6H), 1.44 (d, J = 6.0 Hz, 2H) ppm; ^{13}C NMR (151 MHz, $CDCl_3$) δ 160.68 (dd, J = 253.6, 6.5 Hz), 157.23, 155.73, 155.12, 151.06, 118.55 (t, J = 19.8 Hz), 116.38, 116.34, 116.23, 116.19, 115.23 (t, J = 11.8 Hz), 97.29, 52.24, 27.72, 26.80, 24.44 ppm; HRMS (ES+) calculated for $C_{18}H_{17}ClFN_6$ [M + H]$^+$: 403.1244, found 403.1240.

4-(7-(Azocan-1-yl)-5-chloro-[1,2,4]triazolo[1,5-*a*]pyrimidin-6-yl)-3-fluorobenzonitrile (75). Following general procedure C using 4-(5,7-dichloro-[1,2,4]triazolo[1,5-*a*]pyrimidin-6-yl)-3-fluorobenzonitrile (0.048 g, 0.15 mmol) **(107)** and azocane (0.035 g, 0.30 mmol). Purification via silica gel column chromatography provided the title compound as a white solid (0.032 g, 0.08 mmol, 53%). ^{1}H NMR (600 MHz, $CDCl_{3,}$) mixture of diastereomers δ 8.59 (s, 0.4H), 8.42 (s, 0.3H), 7.80 – 7.77 (m, 0.6H), 7.30 (d, *J* = 6 Hz, 0.3H), 7.16 (d, *J* = 12 Hz, 0.4H), 3.41 (t, *J* = 6 Hz, 1.2H), 3.32 (bs, 1.8H), 3.04 (bs, 1.8H), 1.70 – 1.41 (m, 10H) ppm; HRMS (ES+) calculated for $C_{18}H_{17}ClFN_6$ $[M + H]^+$: 385.1338, found 385.1332.

Diethyl 2-phenylmalonate (76). Following General Procedure A using diethyl malonate (6.122 g, 38.20 mmol) and bromobenzene (2.002 g, 12.70mmol). Purification via silica gel column chromatography (0–8% EtOAc in hexanes) provided the title compound as a colorless oil (0.833 g, 3.53 mmol, 28%). ^{1}H NMR (500 MHz, $CDCl_3$) δ 7.50 – 7.31 (m, 5H), 4.61 (s, 1H), 4.45 – 4.01 (m, 4H), 1.26 (t, *J* = 7.1 Hz, 6H); ^{13}C NMR (126 MHz, $CDCl_3$) δ 168.30, 132.94, 129.40, 128.73, 128.33, 61.94, 58.12, 14.16 ppm; IR (film) ν 3450, 1731, 1638, 1455, 1368, 1305, 1217, 1147, 1029, 700 cm^{-1}; HRMS (ES+) calculated for $C_{13}H_{16}NaO_4$ $[M + Na]^+$: 259.0946, found 259.0952.

Diethyl 2-(4-fluorophenyl)malonate (77). Following General Procedure A using diethyl malonate (5.491 g, 34.30 mmol) and 1-bromo-4-fluorobenzene (2.000 g, 11.40 mmol). Purification via silica gel column chromatography (8/8/84 EtOAc/CH_2Cl_2/ hexanes) provided the title compound as a colorless oil (0.818 g, 3.22 mmol, 28%). ^{1}H NMR (500 MHz, $CDCl_3$) δ 7.41 – 7.36 (m, 2H), 7.07 – 7.01 (m, 2H), 4.59 (s, 1H), 4.27 – 4.14 (m, 4H), 1.25 (t, *J* = 7.1 Hz, 6H) ppm; ^{13}C NMR (126 MHz, $CDCl_3$) δ 168.10, 162.72 (d, *J* = 246.9 Hz), 131.11 (d, *J* = 8.3 Hz), 128.70 (d, *J* = 3.4 Hz), 115.59 (d, *J* = 21.6 Hz), 61.99, 57.18, 14.07 ppm; IR (film) ν 3451, 2985, 2940, 1733, 1607, 1467, 1447, 1369, 1302, 1223, 1157, 1096, 1031, 841, 806, 753 cm^{-1}; HRMS (ES+) calculated for $C_{13}H_{15}FNaO_4$ $[M + Na]^+$: 277.0852, found 277.0861.

Diethyl 2-(2-fluorophenyl)malonate (78). Following General Procedure A using diethyl malonate (5.491 g, 34.30 mmol) and 1-bromo-2-fluorobenzene (2.000 g, 11.40 mmol). Purification via silica gel column chromatography (0–8% EtOAc in hexanes) provided the title compound as a colorless oil (1.411 g, 5.55 mmol, 49%). ^{1}H NMR (500 MHz, $CDCl_3$) δ 7.47 (td, *J* = 7.6, 1.8 Hz, 1H), 7.34 – 7.28 (m, 1H), 7.16 (t, *J* = 7.6 Hz, 1H), 7.07 (t, *J* = 9.1 Hz, 1H), 4.98 (s, 1H), 4.23 (p, *J* = 7.0 Hz, 4H), 1.27 (t, *J* = 7.1 Hz, 6H) ppm; ^{13}C NMR (126 MHz, $CDCl_3$) δ 167.66, 160.59 (d, *J* = 247.6 Hz), 130.54 (d, *J* = 3.0 Hz), 130.04 (d, *J* = 8.3 Hz), 124.34 (d, *J* = 3.7 Hz), 120.51 (d, *J* = 14.5 Hz), 115.51 (d, *J* = 22.2 Hz), 62.09, 50.61 (d, *J* = 3.3 Hz), 14.07 ppm; IR (film) ν 3458, 2984, 2940, 2907, 1737, 1617, 1589, 1494, 1458, 1369, 1303, 1232, 1149, 1094, 1030, 952, 860, 815, 756, 697cm^{-1}; HRMS (ES+) calculated for $C_{13}H_{15}FNaO_4$ $[M + Na]^+$: 277.0852, found 277.0858.

Diethyl 2-(2,4-difluorophenyl)malonate (79). Following General Procedure A using diethyl malonate (5.000 g, 31.10 mmol) and 1-bromo-2,4-difluorobenzene (2.000 g, 10.30 mmol). Purification via silica gel column chromatography (0–5% EtOAc in hexanes) provided the title compound as a colorless oil (1.907 g, 6.98 mmol, 68%). ^{1}H NMR (500 MHz, $CDCl_3$) δ 7.47 (td, *J* = 8.5, 6.3 Hz, 1H), 6.89 (td, *J* = 7.4, 3.8 Hz, 1H), 6.82 (td, *J* = 8.5, 2.5 Hz, 1H), 4.91 (s, 1H), 4.29 – 4.15 (m, 4H), 1.25 (t, *J* = 7.1 Hz, 6H) ppm; ^{13}C NMR (126 MHz, $CDCl_3$) δ 167.46, 162.83 (dd, *J* = 249.9, 12.2 Hz), 160.68 (dd, *J* = 250.0, 12.1 Hz), 131.58 (dd, *J* = 9.8, 4.5 Hz), 116.52 (dd, *J* = 14.6, 4.0 Hz), 111.64 (dd, *J* = 21.4, 3.7 Hz), 103.88 (t, *J* = 25.8 Hz), 62.17, 49.97 (d, *J* = 2.7 Hz), 14.01 ppm; IR (film) ν 3449, 1737, 1624, 1508, 1291, 1220, 1144, 1031, 970, 851 cm^{-1}; HRMS (ES+) calculated for $C_{13}H_{15}F_2O_4$ $[M + H]^+$: 273.0938, found 273.0946.

Diethyl 2-(2,6-difluorophenyl)malonate (80). Following General Procedure A using diethyl malonate (4.981 g, 31.10 mmol) and 2-bromo-1,3-difluorobenzene (2.000 g, 10.30 mmol). Purification via preparative reverse-phase HPLC provided the title compound as a colorless oil (2.082 g, 7.64 mmol, 74%). ^{1}H NMR (500 MHz, $CDCl_3$) δ 7.34 – 7.27 (m, 1H), 6.93 (t, *J* = 8.1 Hz, 2H), 4.97 (s, 1H), 4.26 (q, *J* = 7.1 Hz, 4H), 1.27 (t, *J* = 7.1 Hz, 6H) ppm; ^{13}C NMR (126 MHz, $CDCl_3$) δ 167.05, 161.29 (dd, *J* =

250.6, 7.1 Hz), 130.27 (t, J = 11.9 Hz), 111.75 (t, J = 25.6 Hz), 111.65 (dd, J = 20.6, 4.6 Hz), 62.38, 47.32, 14.05 ppm; IR (film) ν 3460, 2985, 1746, 1628, 1595, 1471, 1370, 1303, 1274, 1236, 1157, 1096, 1035, 1003, 788, 698 cm^{-1}; HRMS (ES+) calculated for $C_{13}H_{14}F_2NaO_4$ $[M + Na]^+$: 295.0758, found 295.0757.

Diethyl 2-(3,5-difluorophenyl)malonate (81). Following General Procedure A using diethyl malonate (5.000 g, 31.10 mmol) and 1-bromo-3,5-difluorobenzene (2.000 g, 10.30 mmol). Purification via silica gel column chromatography (0–5% EtOAc in hexanes) provided the title compound as a colorless oil (1.462 g, 5.36 mmol, 52%). ^{1}H NMR (500 MHz, $CDCl_3$) δ 6.99 – 6.93 (m, 2H), 6.76 (tt, J = 8.9, 2.4 Hz, 1H), 4.57 (s, 1H), 4.28 – 4.13 (m, 4H), 1.25 (t, J = 7.1 Hz, 6H) ppm; ^{13}C NMR (126 MHz, $CDCl_3$) δ 167.20, 162.86 (dd, J = 248.7, 12.9 Hz), 136.08 (t, J = 9.9 Hz), 112.63 (dd, J = 20.7, 6.0 Hz), 103.87 (t, J = 25.2 Hz), 62.26, 57.35 (t, J = 1.9 Hz), 14.00 ppm; IR (film) ν 3450, 2986, 1736, 1626, 1601, 1465, 1369, 1305, 1234, 1154, 1121, 1037, 995, 867, 738, 675 cm^{-1}; HRMS (ES+) calculated for $C_{13}H_{14}F_2NaO_4$ $[M + Na]^+$: 295.0758, found 295.0745.

Diethyl 2-(2,5-difluorophenyl)malonate (82). Following General Procedure A using diethyl malonate (5.000 g, 31.10 mmol) and 2-bromo-1,4-difluorobenzene (2.000 g, 10.30 mmol). Purification via silica gel column chromatography (0–10% EtOAc in hexanes) provided the title compound as a colorless oil (1.767 g, 6.46 mmol, 62%). ^{1}H NMR (500 MHz, $CDCl_3$) δ 7.25 – 7.19 (m, 1H), 7.06 – 6.95 (m, 2H), 4.94 (s, 1H), 4.29 – 4.17 (m, 4H), 1.26 (t, J = 7.1 Hz, 6H) ppm; ^{13}C NMR (126 MHz, $CDCl_3$) δ 167.10, 158.54 (dd, J = 242.3, 2.5 Hz), 156.62 (dd, J = 243.9, 2.5 Hz), 121.84 (dd, J = 17.0, 8.4 Hz), 117.20 (dd, J = 25.5, 3.2 Hz), 116.59 (dd, J = 15.0, 8.8 Hz), 116.39 (dd, J = 16.3, 8.6 Hz), 62.29, 50.35 (d, J = 2.7 Hz), 14.02 ppm; IR (film) ν 3452, 2986, 1737, 1631, 1499, 1369, 1303, 1226, 1154, 1031, 877, 819, 739 cm^{-1}; HRMS (ES+) calculated for $C_{13}H_{14}F_2NaO_4$ $[M + Na]^+$: 295.0758, found 295.0755.

Diethyl 2-(3,4-difluorophenyl)*malonate* (83). Following General Procedure A using diethyl malonate (5.002 g, 31.10 mmol) and 4-bromo-1,2-difluorobenzene (2.001 g, 10.30 mmol). Purification via

preparative reverse-phase HPLC provided the title compound as an orange oil (0.530 g, 1.95 mmol, 19%). ^{1}H NMR (500 MHz, $CDCl_3$) δ 7.33 – 7.28 (m, 1H), 7.18 – 7.07 (m, 2H), 4.56 (d, *J* = 2.9 Hz, 1H), 4.28 – 4.17 (m, 4H), 1.27 (td, *J* = 7.3, 2.2 Hz, 6H) ppm; ^{13}C NMR (126 MHz, $CDCl_3$) δ 167.67, 150.35 (dd, *J* = 272.8, 12.7 Hz), 150.35 (dd, *J* = 224.7, 12.6 Hz), 129.67 (dd, *J* = 6.2, 4.0 Hz), 125.77 (dd, *J* = 6.5, 3.7 Hz), 118.63 (d, *J* = 18.4 Hz), 117.34 (d, *J* = 17.4 Hz), 62.24, 57.00, 14.05 ppm; IR (film) ν 3450, 2986, 1734, 1613, 1520, 1441, 1369, 1287, 1154, 1032, 773 cm^{-1}; HRMS (ES+) calculated for $C_{13}H_{15}F_2O_4$ $[M + H]^+$: 273.0938, found 273.0941.

Diethyl 2-(2,3,4-trifluorophenyl)malonate (84). Following General Procedure A using diethyl malonate (4.560 g, 28.44 mmol) and 1-bromo-2,3,4-trifluorobenzene (2.000 g, 9.48 mmol). Purification via silica gel column chromatography (0–8% EtOAc in hexanes) provided the title compound as a colorless oil (1.621 g, 5.58 mmol, 59%). ^{1}H NMR (500 MHz, $CDCl_3$) δ 7.28 – 7.19 (m, 1H), 7.00 (tdd, *J* = 9.2, 7.0, 2.1 Hz, 1H), 4.90 (s, 1H), 4.29 – 4.19 (m, 4H), 1.28 (t, *J* = 7.1 Hz, 6H) ppm; ^{13}C NMR (126 MHz, $CDCl_3$) δ 166.98, 151.11 (ddd, *J* = 251.2, 9.8, 3.2 Hz), 149.78 (ddd, *J* = 251.2, 10.7, 3.4 Hz), 139.90 (dt, *J* = 251.5, 15.5 Hz), 124.30 (dt, *J* = 7.9, 3.9 Hz), 118.08 (dd, *J* = 11.8, 4.0 Hz), 112.31 (dd, *J* = 17.6, 3.9 Hz), 62.40, 50.06, 14.01 ppm; IR (film) ν 3405, 2986, 1738, 1617, 1513, 1490, 1370, 1305, 1243, 1151, 1033, 992, 865, 810, 672 cm^{-1}; HRMS (ES+) calculated for $C_{13}H_{13}F_3NaO_4$ $[M + Na]^+$: 313.0664, found 313.0663.

Diethyl 2-(2,4,6-trifluorophenyl)malonate (85). Following General Procedure A using diethyl malonate (8.408 g, 52.5 mmol) and 2-bromo-1,3,5-trifluorobenzene (3.692 g, 17.5 mmol). Purification via silica gel column chromatography (0−8% EtOAc in hexanes) provided the title compound as a white powder (2.542 g, 8.75 mmol, 50% yield). ^{1}H-NMR (500 MHz; $CDCl_3$): δ 6.74 – 6.68 (m, 2H), 4.89 (s, 1H), 4.29 – 4.23 (m, 4H), 1.28 (t, J = 7.1 Hz, 6H) ppm; ^{13}C NMR (126 MHz, $CDCl_3$) δ 166.68, 162.78 (dt, *J* = 250.7, 15.1 Hz), 161.5 (dd, *J* = 250.7, 15.1 Hz), 161.44 (dd, *J* = 252.2, 15.1 Hz), 107.25 (dt, *J* = 18.1, 4.5 Hz), 100.81 – 100.43 (m), 62.41, 46.95, 14.04 ppm; LCMS: $[M + H]^+$: 291.

Diethyl 2-(2,4,6-trifluorobenzyl)malonate (86). To a suspension of NaH (60 wt % in mineral oil) (0.462 g, 11.56 mmol, 1.30 equiv) in anhydrous DMF (8.5 mL) at 0 °C under N_2 was slowly added diethyl malonate (1.712 g, 10.67 mmol, 1.20 equiv). After addition, the reaction was stirred at 0 °C for 10 min. Then, 2-(bromomethyl)-1,3,5-trifluorobenzene (2.001 g, 8.89 mmol, 1.00 equiv) in solution in anhydrous DMF (8.5 mL) was slowly added and the reaction was stirred at 0 °C for 1 h. Then, the reaction was quenched with saturated solution of NH_4Cl and H_2O (85 mL) was added. The mixture was extracted with EtOAc (×3). The combined organic extracts were washed with brine, then dried over $MgSO_4$, filtered and concentrated under reduced pressure. Purification via silica gel column chromatography (0–5% EtOAc in hexanes) provided the title compound as a colorless oil (2.43 g, 7.99 mmol, 90%). ^{1}H NMR (500 MHz, $CDCl_3$) δ 7.28 – 7.19 (m, 1H), 7.04 – 6.95 (m, 1H), 4.90 (s, 1H), 4.29 – 4.19 (m, 4H), 1.28 (t, *J* = 7.1 Hz, 6H) ppm; ^{13}C NMR (126 MHz, $CDCl_3$) δ 168.33, 161.72 (dd, *J* = 248.9, 11.3 Hz), 161.70 (dt, *J* = 248.9, 16.0, 15.5 Hz), 161.60 (dd, *J* = 249.0, 11.2 Hz), 109.78 (td, *J* = 20.1, 4.7 Hz), 100.35 – 99.84 (m), 61.63, 51.10, 21.45 (t, *J* = 2.3 Hz), 13.90 ppm; IR (film) ν 3437, 1733, 1639, 1499, 1444, 1371, 1304, 1239, 1153, 1048, 838, 617 cm^{-1}; HRMS (ES+) calculated for $C_{14}H_{15}F_3NaO_4$ $[M + Na]^+$: 327.0820, found 327.0818.

Diethyl 2-(2,6-difluoro-4-methylphenyl)malonate (87). Following General Procedure A using diethyl malonate (4.180 g, 26.10 mmol) and 2-bromo-1,3-difluoro-5-methylbenzene (1.800 g, 8.69 mmol). Purification via silica gel column chromatography (0−8% EtOAc in hexanes) provided the title compound as a colorless oil (2.005 g, 6.99 mmol, 80%). ^{1}H NMR (600 MHz, $CDCl_3$) δ 6.67 – 6.65 (m, 2H), 4.83 (d, *J* = 3.0 Hz, 1H), 4.20 – 4.14 (m, 4H), 2.27 (d, *J* = 3.2 Hz, 3H), 1.22 – 1.17 (m, 6H) ppm; ^{13}C NMR (150 MHz, $CDCl_3$) δ 166.89, 160.75 (dd, *J* = 249.1, 8.1 Hz), 141.32, 115.89 – 110.83 (m), 107.42 (t, *J* = 18.8 Hz), 61.99, 46.98, 21.23 (d, *J* = 1.9 Hz), 13.87 ppm; IR (film) ν 3000, 1678, 1106, 1017 cm^{-1}. LCMS: $[M + H]^+$: 287.

Diethyl 2-(2,6-difluoro-4-(trifluoromethyl)phenyl)malonate (88). Following General Procedure A using diethyl malonate (2.160 g, 13.50 mmol) and 1,2,3-trifluoro-5-(trifluoromethyl)benzene (0.900 g, 4.50 mmol). Purification via silica gel column chromatography (0–5% EtOAc in hexanes) provided the title compound as a colorless oil (0.620 g, 1.82 mmol, 40%). ^{1}H NMR (500 MHz, $CDCl_3$) δ 7.23 (d, *J* = 7.3 Hz, 2H), 4.99 (s, 1H), 4.27 (dt, *J* = 7.4, 6.5 Hz, 4H), 1.29 (t, *J* = 7.1 Hz, 6H) ppm; ^{13}C NMR (126 MHz, $CDCl_3$) δ 166.12, 161.21 (dd, *J* = 252.9, 7.4 Hz), 132.89 (qt, *J* = 34.8, 10.3 Hz), 122.63 (qt, *J* = 272.6, 3.3 Hz), 114.85 (t, *J* = 18.5 Hz), 109.41 (ddt, *J* = 26.3, 7.4, 3.8 Hz), 62.69, 47.34, 14.07 ppm; IR (film) ν 3083, 2987, 1755, 1061, 1442, 1365, 1306, 1240, 1177, 1138, 1080, 1031, 910, 867, 719, 702 cm^{-1}; HRMS (ES+) calculated for $C_{14}H_{13}F_5NaO_4$ $[M + Na]^+$: 363.0632, found 363.0631.

Diethyl 2-(4-cyano-2,6-difluorophenyl)malonate (89). A mixture of 3,4,5-trifluorobenzonitrile (1.000 g, 6.37 mmol, 1 equiv), potassium carbonate (1.760 g, 12.70 mmol, 2.00 equiv), and diethyl malonate (1.031 g, 6.43 mmol, 1.01 equiv) in DMF (6.37 ml) under N_2 was stirred at 65 ˚C until starting material was consumed as determined by TLC. The reaction mixture was cooled to r.t., washed with 1M HCl (50 mL), and extracted with EtOAc (×3). The organic layers were combined, washed with satd. aq. NaCl, dried over Na_2SO_4, filtered, and concentrated under reduced pressure. Purification via silica gel column chromatography (0−30% EtOAc in hexanes) provided the title compound as a white solid (1.408 g, 4.69 mmol, 73%). ^{1}H NMR (600 MHz, $CDCl_3$) δ 7.30 (d, *J* = 7.0 Hz, 2H), 5.01 (s, 1H), 4.31 – 4.24 (m, 4H), 1.29 (t, *J* = 7.4 Hz, 6H) ppm; ^{13}C NMR (150 MHz, $CDCl_3$) δ 165.54, 161.02 (dd, *J* = 254.0, 7.8 Hz), 116.78 (t, *J* = 18.5 Hz), 116.20 (t, *J* = 3.4 Hz), 115.94 – 115.48 (m), 113.88 (t, *J* = 12.4 Hz), 62.60, 47.24, 13.87 ppm; IR (film) ν 2856, 2178, 1695 cm^{-1}; LCMS: $[M + H]^+$: 298.

Diethyl 2-(4-cyano-2-fluorophenyl)malonate (90). To a dry flask, under nitrogen, was added 3,4-difluorobenzonitrile (4.000 g, 28.81 mmol, 1 equiv), K_2CO_3 (7.954 g, 57.51 mmol, 2.00 equiv), diethyl malonate (4.660 g, 29.10 mmol, 1.01 equiv), and anhydrous DMF (24 ml) and was heated at 65 ˚C until starting material was consumed based on TLC. The reaction mixture was cooled to r.t. and added to a

separatory funnel containing 50 ml of 1 N HCl. The mixture was extracted with EtOAc (×3), and the combined organic layers were washed with H_2O and satd. aq. NaCl. The organic layer was dried over anh. Na_2SO_4, filtered, and concentrated under reduced pressure. Purification via silica gel column chromatography (0−30% EtOAc in hexanes) provided the title compound as a colorless oil (6.734 g, 24.10 mmol, 84%). ^{1}H NMR (600 MHz, $CDCl_3$) δ 7.64 (t, *J* = 7.6 Hz, 1H), 7.47 (dd, *J* = 8.0, 1.6 Hz, 1H), 7.38 (dd, *J* = 9.2, 1.6 Hz, 1H), 4.98 (s, 1H), 4.28 – 4.18 (m, 4H), 1.26 (t, *J* = 7.2 Hz, 6H) ppm; ^{13}C NMR (150 MHz, $CDCl_3$) δ 166.55, 160.04 (d, *J* = 252.0 Hz), 131.98 (d, *J* = 3.5 Hz), 128.26 (d, *J* = 4.0 Hz), 126.21 (d, *J* = 14.4 Hz), 119.23 (d, *J* = 26.0 Hz), 117.28 (d, *J* = 2.9 Hz), 113.71 (d, *J* = 9.8 Hz), 62.55, 50.44 (d, *J* = 2.9 Hz), 14.00 ppm; IR (film) ν 2984, 2236, 1733, 1219 cm^{-1}; LCMS: $[M + H]^+$: 280.

Diethyl 2-(4-chloro-2,6-difluorophenyl)malonate (91). Following General Procedure A using diethyl malonate (6.390 g, 39.57 mmol) and 2-bromo-5-chloro-1,3-difluorobenzene (3.000 g, 13.19 mmol). Purification via silica gel column chromatography (0−8% EtOAc in hexanes) provided the title compound as a colorless oil (1.424 g, 4.63 mmol, 35%). ^{1}H NMR (600 MHz, $CDCl_3$) δ 6.96 – 6.93 (m, 2H), 4.89 (s, 1H), 4.24 (q, *J* = 7.2 Hz, 4H), 1.28 – 1.24 (m, 6H) ppm; ^{13}C NMR (150 MHz, $CDCl_3$) δ 166.40, 161.05 (dd, *J* = 252.7, 8.8 Hz), 135.40 (t, *J* = 13.4 Hz), 113.18 – 112.42 (m), 109.85 (t, *J* = 18.8 Hz), 62.4, 47.07, 14.01 ppm; IR (film) ν 2838, 1678, 1642, 1249 cm^{-1}; LCMS: $[M + H]^+$: 308.

Diethyl 2-(2,6-difluoro-4-nitrophenyl)malonate (92). A mixture of 1,2,3-trifluoro-5-nitrobenzene (1.000 g, 5.65 mmol, 1 equiv), potassium carbonate (1.562 g, 11.29 mmol, 2.00 equiv), and diethyl malonate (0.914 g, 5.71 mmol, 1.01 equiv), in DMF (6.37 ml) under N_2 was stirred at 65 ˚C until starting material was consumed as indicated by TLC. The reaction mixture was cooled to r.t. and washed with 1N HCl (50 mL) and extracted with EtOAc (×3). The organic layers were combined, washed with satd. aq. NaCl, dried over Na_2SO_4, filtered, and concentrated under reduced pressure. Purification via silica gel column chromatography (0−30% EtOAc in hexanes) provided the title compound as a white solid (1.536 g, 4.85 mmol, 86%). ^{1}H NMR (600 MHz, $CDCl_3$) δ 7.84 (d, *J* = 7.2 Hz, 2H), 5.00 (s, 1H), 4.27 (q, *J* = 7.1

Hz, 4H), 1.28 (t, J = 7.2 Hz, 6H) ppm; ^{13}C NMR (150 MHz, $CDCl_3$) δ 165.55, 160.93 (dd, J = 254.8, 7.7 Hz), 148.60 (t, J = 11.2 Hz), 118.05 (t, J = 18.7 Hz), 108.15 – 107.61 (m), 62.84, 47.49, 14.04 ppm.

5,7-Dichloro-6-phenyl-[1,2,4]triazolo[1,5-*a*]pyrimidine (93). Following General Procedure B using diethyl 2-phenylmalonate (0.780 g, 3.30 mmol) **(76)** and 3-amino-1,2,4-triazole (0.292 g, 3.47 mmol). Then using the intermediate sodium 6-phenyl-[1,2,4]triazolo[1,5-*a*]pyrimidine-5,7-bis(olate) (0.740 g, 2.71 mmol) and $POCl_3$ (7.410 g, 48.46 mmol) to obtain the title compound as a brown solid (0.527 g, 1.99 mmol, 73%). ^{1}H NMR (500 MHz, $CDCl_3$) δ 8.56 (s, 1H), 7.58 – 7.51 (m, 3H), 7.38 – 7.34 (m, 2H) ppm; ^{13}C NMR (126 MHz, $CDCl_3$) δ 156.93, 156.65, 153.35, 139.90, 131.72, 130.07, 129.95, 129.16, 124.01 ppm; IR (film) ν 3437, 1637, 1458, 1383, 1267, 1205, 1180, 867, 802, 764, 740, 698, 652 cm^{-1}; HRMS (ES+) calculated for $C_{11}H_7Cl_2N_4$ $[M + H]^+$: 265.0042, found 265.0043.

5,7-Dichloro-6-(4-fluorophenyl)-[1,2,4]triazolo[1,5-*a*]pyrimidine (94). Following General Procedure B using diethyl 2-(4-fluorophenyl)malonate (0.700 g, 2.75 mmol) **(77)** and 3-amino-1,2,4-triazole (0.242 g, 2.89 mmol). Then using the intermediate sodium 6-(4-fluorophenyl)-[1,2,4]triazolo[1,5-*a*]pyrimidine-5,7-bis(olate) (0.760 g, 2.61 mmol) and $POCl_3$ (7.150 g, 46.45 mmol) to obtain the title compound as a brown solid (0.481 g, 1.70 mmol, 67%). ^{1}H NMR (500 MHz, $CDCl_3$) δ 8.53 (s, 1H), 7.36 (dd, J = 8.4, 5.2 Hz, 2H), 7.29 – 7.20 (m, 2H) ppm; ^{13}C NMR (126 MHz, $CDCl_3$) δ 163.47 (d, J = 250.9 Hz), 156.95, 156.53, 153.29, 140.05, 132.18 (d, J = 8.6 Hz), 127.59 (d, J = 3.7 Hz), 123.03, 116.43 (d, J = 21.9 Hz) ppm; IR (film) ν 3421, 1600, 1529, 1504, 1460, 1330, 1267, 1229, 1203, 1183, 1160, 1089, 1024, 899, 837, 790 cm^{-1}; HRMS (ES+) calculated for $C_{11}H_6Cl_2FN_4$ $[M + H]^+$: 282.9948, found 282.9945.

5,7-Dichloro-6-(2-fluorophenyl)-[1,2,4]triazolo[1,5-*a*]pyrimidine (95). Following General Procedure B using diethyl 2-(2-fluorophenyl)malonate (0.700 g, 2.75 mmol) **(78)** and 3-amino-1,2,4-triazole (0.242 g, 2.89 mmol). Then using the intermediate sodium 6-(2-fluorophenyl)-[1,2,4]triazolo[1,5-*a*]pyrimidine-5,7-bis(olate) (0.760 g, 2.61 mmol) and $POCl_3$ (7.150 g, 46.45 mmol) to obtain the title compound as a

brown solid (0.572 g, 2.02 mmol, 77%). ^{1}H NMR (500 MHz, $CDCl_3$) δ 8.54 (t, *J* = 3.3 Hz, 1H), 7.59 – 7.51 (m, 1H), 7.38 – 7.29 (m, 2H), 7.28 – 7.20 (m, 1H) ppm; ^{13}C NMR (126 MHz, $CDCl_3$) δ 159.79 (d, *J* = 249.6 Hz), 156.94, 156.57, 153.53, 140.57, 132.48 (d, *J* = 8.2 Hz), 131.78 (d, *J* = 1.8 Hz), 124.85 (d, *J* = 3.7 Hz), 119.39 (d, *J* = 15.9 Hz), 118.45, 116.38 (d, *J* = 21.1 Hz) ppm; IR (film) ν 3436, 1598, 1492, 1463, 1425, 1366, 1330, 1263, 1221, 1196, 1131, 1099, 1033, 900, 822, 792, 755, 652 cm^{-1}; HRMS (ES+) calculated for $C_{11}H_5Cl_2FN_4Na$ $[M + Na]^+$: 304.9768, found 304.9772.

5,7-Dichloro-6-(2,4-difluorophenyl)-[1,2,4]triazolo[1,5-*a*]pyrimidine (96). Following General Procedure B using diethyl 2-(2,4-difluorophenyl)malonate (0.800 g, 2.94 mmol) **(79)** and 3-amino-1,2,4-triazole (0.260 g, 3.09 mmol). Then using the intermediate sodium 6-(2,4-difluorophenyl)-[1,2,4]triazolo[1,5-*a*]pyrimidine-5,7-bis(olate) (0.800 g, 2.60 mmol) and $POCl_3$ (7.080 g, 46.23 mmol) to obtain the title compound as a brown solid (0.455 g, 1.51 mmol, 58%). ^{1}H NMR (500 MHz, $CDCl_3$) δ 8.50 (s, 1H), 7.39 – 7.32 (m, 1H), 7.06 (td, *J* = 8.3, 2.5 Hz, 1H), 6.99 (td, *J* = 9.1, 2.5 Hz, 1H) ppm; ^{13}C NMR (126 MHz, $CDCl_3$) δ 164.23 (dd, *J* = 253.6, 11.8 Hz), 160.18 (dd, *J* = 252.2, 12.3 Hz), 156.94, 156.47, 153.47, 140.79, 132.91 (dd, *J* = 10.1, 3.4 Hz), 117.55, 115.54 (dd, *J* = 16.1, 4.1 Hz), 112.47 (dd, *J* = 21.9, 3.7 Hz), 104.96 (t, *J* = 25.4 Hz) ppm; IR (film) ν 3451, 1600, 1503, 1464, 1424, 1368, 1335, 1267, 1196, 1143, 1128, 1092, 1022, 969, 890, 851, 796, 765, 735, 652, 631 cm^{-1}; HRMS (ES+) calculated for $C_{11}H_5Cl_2F_2N_4$ $[M + H]^+$: 300.9854, found 300.9850.

5,7-Dichloro-6-(2,6-difluorophenyl)-[1,2,4]triazolo[1,5-*a*]pyrimidine (97). Following General Procedure B using diethyl 2-(2,6-difluorophenyl)malonate (0.800 g, 2.94 mmol) **(80)** and 3-amino-1,2,4-triazole (0.260 g, 3.09 mmol). Then using the intermediate sodium 6-(2,6-difluorophenyl)-[1,2,4]triazolo[1,5-*a*]pyrimidine-5,7-bis(olate) (0.600 g, 1.90 mmol) and $POCl_3$ (5.310 g, 34.70 mmol) to obtain the title compound as a brown solid (0.290 g, 0.96 mmol, 49%). ^{1}H NMR (500 MHz, $CDCl_3$) δ 8.59 (d, *J* = 1.4 Hz, 1H), 7.61 – 7.52 (m, 1H), 7.11 (t, *J* = 7.9 Hz, 2H) ppm; ^{13}C NMR (126 MHz, $CDCl_3$) δ 160.23 (dd, *J* = 252.0, 5.7 Hz), 157.17, 156.65, 153.87, 141.38, 133.06 (t, *J* = 10.2 Hz), 113.14, 112.16

(dd, J = 20.4, 4.2 Hz), 109.07 (t, J = 19.9 Hz) ppm; IR (film) ν 3427, 1629, 1602, 1460, 1384, 1266, 1194, 1003899, 806, 765, 652 cm^{-1}; HRMS (ES+) calculated for $C_{11}H_5Cl_2F_2N_4$ [M + H]$^+$: 300.9854, found 300.9866.

5,7-Dichloro-6-(3,5-difluorophenyl)-[1,2,4]triazolo[1,5-*a*]pyrimidine (98). Following General Procedure B using diethyl 2-(3,5-difluorophenyl)malonate (0.700 g, 2.57 mmol) **(81)** and 3-amino-1,2,4-triazole (0.227 g, 2.70 mmol). Then using the intermediate sodium 6-(3,5-difluorophenyl)-[1,2,4]triazolo[1,5-*a*]pyrimidine-5,7-bis(olate) (0.700 g, 2.27 mmol) and $POCl_3$ (6.200 g, 40.51 mmol) to obtain the title compound as a brown solid (0.422 g, 1.40 mmol, 62%). ^{1}H NMR (500 MHz, $CDCl_3$) δ 8.60 (s, 1H), 7.02 (tt, J = 8.8, 2.4 Hz, 1H), 6.97 – 6.89 (m, 2H) ppm; ^{13}C NMR (126 MHz, $CDCl_3$) δ 163.29 (dd, J = 251.5, 12.6 Hz), 157.31, 155.74, 153.47, 140.16, 134.33 (t, J = 10.3 Hz), 121.84, 113.71 (dd, J = 19.6, 6.9 Hz), 105.89 (t, J = 25.0 Hz) ppm; IR (film) ν 3434, 1628, 1595, 1460, 1435, 1121, 987, 833 cm^{-1}; HRMS (ES+) calculated for $C_{11}H_5Cl_2F_2N_4$ [M + H]$^+$: 300.9854, found 300.9871.

5,7-Dichloro-6-(2,5-difluorophenyl)-[1,2,4]triazolo[1,5-*a*]pyrimidine (99). Following General Procedure B using diethyl 2-(2,5-difluorophenyl)malonate (0.800 g, 2.94 mmol) **(82)** and 3-amino-1,2,4-triazole (0.259 g, 3.09 mmol). Then using the intermediate sodium 6-(2,5-difluorophenyl)-[1,2,4]triazolo[1,5-*a*]pyrimidine-5,7-bis(olate) (0.800 g, 2.60 mmol) and $POCl_3$ (7.080 g, 46.23 mmol) to obtain the title compound as a brown solid (0.443 g, 1.47 mmol, 57%). ^{1}H NMR (500 MHz, $CDCl_3$) δ 8.58 (s, 1H), 7.28 – 7.23 (m, 2H), 7.11 – 7.07 (m, 1H) ppm; ^{13}C NMR (126 MHz, $CDCl_3$) δ 158.60 (dd, J = 245.1, 2.5 Hz), 157.24, 156.21, 156.03 (dd, J = 245.9, 2.7 Hz), 153.68, 140.80, 120.50 (dd, J = 18.7, 8.8 Hz), 119.24 (dd, J = 23.9, 8.4 Hz), 118.42 (dd, J = 25.1, 2.2 Hz), 117.80 (dd, J = 24.2, 8.7 Hz), 117.43 ppm; IR (film) ν 3421, 1642, 1492, 1458, 1432, 1383, 1253, 1203, 1092, 1025, 858, 822, 775, 699, 651 cm^{-1}; HRMS (ES+) calculated for $C_{11}H_5Cl_2F_2N_4$ [M + H]$^+$: 300.9854, found 300.9857.

5,7-Dichloro-6-(3,4-difluorophenyl)-[1,2,4]triazolo[1,5-*a*]pyrimidine (100). Following General Procedure B using diethyl 2-(3,4-difluorophenyl)malonate (0.456 g, 1.67 mmol) **(83)** and 3-amino-1,2,4-triazole (0.147 g, 1.73 mmol). Then using the intermediate sodium 6-(3,4-difluorophenyl)-[1,2,4]triazolo[1,5-*a*]pyrimidine-5,7-bis(olate) (0.400 g, 1.30 mmol) and $POCl_3$ (2.982 g, 23.11 mmol) to obtain the title compound as a brown solid (0.183 g, 0.61 mmol, 40%). ^{1}H NMR (500 MHz, $CDCl_3$) δ 8.57 (s, 1H), 7.41 – 7.32 (m, 1H), 7.26 – 7.21 (m, 1H), 7.16 – 7.11 (m, 1H) ppm; ^{13}C NMR (126 MHz, $CDCl_3$) δ 157.20, 156.17, 153.39, 151.41 (dd, *J* = 252.7, 11.8 Hz), 150.60 (dd, *J* = 251.2, 12.8 Hz), 140.27, 128.21 (dd, *J* = 6.6, 4.6 Hz), 126.97 (dd, *J* = 6.7, 3.9 Hz), 122.03, 119.74 (d, *J* = 18.4 Hz), 118.49 (d, *J* = 17.9 Hz) ppm; IR (film) ν 3377, 2918, 1606, 1460, 1383, 1269, 1180, 1120, 861, 793, 652 cm^{-1}; HRMS (ES+) calculated for $C_{11}H_5Cl_2F_2N_4$ $[M + H]^+$: 300.9854, found 300.9859.

5,7-Dichloro-6-(2,3,4-trifluorophenyl)-[1,2,4]triazolo[1,5-*a*]pyrimidine (101). Following General Procedure B using diethyl 2-(2,3,4-trifluorophenyl)malonate (0.800 g, 2.75 mmol) **(84)** and 3-amino-1,2,4-triazole (0.242 g, 2.89 mmol). Then using the intermediate sodium 6-(2,3,4-trifluorophenyl)-[1,2,4]triazolo[1,5-*a*]pyrimidine-5,7-bis(olate) (0.740 g, 2.67 mmol) and $POCl_3$ (6.151 g, 40.33 mmol) to obtain the title compound as a brown solid (0.367 g, 1.15 mmol, 43%). ^{1}H NMR (500 MHz, $CDCl_3$) δ 8.59 (s, 1H), 7.24 – 7.16 (m, 1H), 7.16 – 7.09 (m, 1H) ppm; ^{13}C NMR (126 MHz, $CDCl_3$) δ 157.39, 156.24, 153.75, 152.71 (ddd, *J* = 254.7, 9.8, 3.0 Hz), 149.54 (ddd, *J* = 253.6, 10.9, 3.6 Hz), 141.10, 140.64 (dt, *J* = 254.7, 15.1 Hz), 125.78 (ddd, *J* = 8.0, 4.4, 1.7 Hz), 117.08 (dd, *J* = 12.9, 4.0 Hz), 116.70 (d, *J* = 2.3 Hz), 113.42 (dd, *J* = 18.0, 3.9 Hz) ppm; IR (film) ν 3387, 1601, 1485, 1458, 1383, 1343, 1274, 12010, 1180, 1053, 1024, 963, 915, 859, 820, 790, 761, 689, 650 cm^{-1}; HRMS (ES+) calculated for $C_{11}H_4Cl_2F_3N_4$ $[M + H]^+$: 318.9760, found 319.9764.

5,7-Dichloro-6-(2,4,6-trifluorophenyl)-[1,2,4]triazolo[1,5-*a*]pyrimidine (102). Following General Procedure B using diethyl 2-(2,4,6-trifluorophenyl)malonate (3.66 g, 12.58 mmol) **(85)** and 3-amino-1,2,4-triazole (1.07 g, 12.83 mmol). Then using the intermediate sodium 6-(2,3,4-trifluorophenyl)-

[1,2,4]triazolo[1,5-*a*]pyrimidine-5,7-bis(olate) (2.000 g, 6.29 mmol) and $POCl_3$ (17.20 g, 112.0 mmol) to obtain the title compound as a brown solid (1.00 g, 3.14 mmol, 50%). ^1H NMR (500 MHz, $CDCl_3$) δ 8.62(s, 1H), 6.91 (t, *J* = 6.0 Hz, 2H) ppm; ^{13}C NMR (126 MHz, $CDCl_3$) δ 164.60 (dt, *J* = 253.7, 16.6 Hz), 160.77 (dd, *J* = 252.9, 9.1 Hz), 160.67 (dd, *J* = 252.9, 9.1 Hz), 157.36, 156.69, 141.67, 112.36, 105.67 (dt, *J* = 19.6, 4.5 Hz), 101.63 – 101.26 (m) ppm.

5,7-Dichloro-6-(2,4,6-trifluorobenzyl)-[1,2,4]triazolo[1,5-*a*]pyrimidine (103). Following General Procedure B using diethyl 2-(2,4,6-trifluorobenzyl)malonate (0.800 g, 2.63 mmol) **(86)** and 3-amino-1,2,4-triazole (0.232 g, 2.76 mmol). Then using the intermediate sodium 6-(2,4,6-trifluorobenzyl)-[1,2,4]triazolo[1,5-*a*]pyrimidine-5,7-bis(olate) (0.700 g, 2.06 mmol) and $POCl_3$ (5.610 g, 36.60 mmol) to obtain the title compound as a brown solid (0.355 g, 1.07 mmol, 52%). ^1H NMR (500 MHz, $CDCl_3$) δ 8.40 (s, 1H), 6.59 (t, *J* = 8.5 Hz, 2H), 4.27 (s, 2H) ppm; ^{13}C NMR (126 MHz, $CDCl_3$) δ 161.93 (dt, *J* = 250.5, 16.0 Hz), 161.44 (dd, *J* = 249.9, 10.6 Hz), 161.33 (dd, *J* = 249.8, 10.7 Hz), 156.68, 156.48, 152.67, 140.34, 118.92, 108.12 (td, *J* = 18.5, 4.8 Hz), 102.62 – 96.83 (m), 23.49 (t, *J* = 2.4 Hz) ppm; IR (film) ν 3408, 1633, 1471, 1266, 1118, 1038 cm^{-1}; HRMS (ES+) calculated for $C_{12}H_6Cl_2F_3N_4$ $[M + H]^+$: 332.9916, found 332.9906.

5,7-Dichloro-6-(2,6-difluoro-4-methylphenyl)-[1,2,4]triazolo[1,5-*a*]pyrimidine (104). Following General Procedure B using diethyl 2-(2,6-difluoro-4-methylphenyl)malonate (0.800 g, 2.79 mmol) **(87)** and 3-amino-1,2,4-triazole (0.247 g, 2.93 mmol). Then using the intermediate sodium 6-(2,6-difluoro-4-methylphenyl)-[1,2,4]triazolo[1,5-*a*]pyrimidine-5,7-bis(olate) (0.500 g, 1.55 mmol) and $POCl_3$ (4.240 g, 27.60 mmol) to obtain the title compound as a brown solid (0.334 g, 1.06 mmol, 68%). ^1H NMR (600 MHz, $CDCl_3$) δ 8.59 (s, 1H), 6.92 (d, *J* = 8.5 Hz, 2H), 2.46 (s, 3H) ppm; ^{13}C NMR (150 MHz, $CDCl_3$) δ 159.92 (dd, *J* = 251.1, 6.6 Hz), 157.07, 157.01, 153.85, 144.81 (d, *J* = 19.7 Hz), 141.44, 113.44, 112.74 (dd, *J* = 20.7, 3.5 Hz), 106.01 (d, *J* = 39.9 Hz), 21.88 (d, *J* = 1.9 Hz) ppm; IR (film) ν 3071, 1606, 1571, 1356 cm^{-1}; LCMS: $[M + H]^+$: 317.

5,7-Dichloro-6-(2,6-difluoro-4-(trifluoromethyl)phenyl)-[1,2,4]triazolo[1,5-*a*]pyrimidine (105). Following General Procedure B using diethyl 2-(2,6-difluoro-4-(trifluoromethyl)phenyl)malonate (0.600 g, 1.76 mmol) **(88)** and 3-amino-1,2,4-triazole (0.156 g, 1.85 mmol). Then using the intermediate sodium 6-(2,6-difluoro-4-(trifluoromethyl)phenyl)-[1,2,4]triazolo[1,5-*a*]pyrimidine-5,7-bis(olate) (0.600 g, 1.60 mmol) and $POCl_3$ (4.350 g, 28.41 mmol) to obtain the title compound as a brown solid (0.392 g, 1.07 mmol, 66%). ^{1}H NMR (500 MHz, $CDCl_3$) δ 8.62 (s, 1H), 7.47 (d, *J* = 7.2 Hz, 2H) ppm; ^{13}C NMR (126 MHz, $CDCl_3$) δ 160.16 (dd, *J* = 254.8, 5.8 Hz), 157.22, 155.50, 153.81, 141.35, 135.19 (qt, *J* = 35.3, 34.6, 9.5 Hz), 122.14 (qt, *J* = 273.3, 3.2 Hz), 112.72 (t, *J* = 19.7 Hz), 111.49, 110.18 – 109.25 (m) ppm; IR (film) ν 3435, 1633, 1603, 1466, 1437, 1364, 1266, 1250, 1179, 1137, 1038, 916, 868, 801, 766, 705, 653 cm^{-1}; HRMS (ES-) calculated for $C_{12}H_3Cl_2F_4N_4$ $[M - F]^-$: 348.9676, found 348.9662.

4-(5,7-Dichloro-[1,2,4]triazolo[1,5-*a*]pyrimidin-6-yl)-3,5-difluorobenzonitrile (106). Following General Procedure B using diethyl 2-(4-cyano-2,6-difluorophenyl)malonate (0.500 g, 1.68 mmol) **(89)** and 3-amino-1,2,4-triazole (0.148 g, 1.77 mmol). Then using the intermediate sodium 6-(4-cyano-2,6-difluorophenyl)-[1,2,4]triazolo[1,5-*a*]pyrimidine-5,7-bis(olate) (0.400 g, 1.20 mmol) and $POCl_3$ (3.280 g, 21.41 mmol) to obtain the title compound as a brown solid (0.210 g, 1.20 mmol, 53%). ^{1}H NMR (600 MHz, $CDCl_3$) δ 8.65 (s, 1H), 7.47 (d, *J* = 6.2 Hz, 2H) ppm; ^{13}C NMR (150 MHz, $CDCl_3$) δ 161.21 (d, *J* = 6.4 Hz), 159.51 (d, *J* = 6.2 Hz), 157.66, 155.57, 116.85, 116.62 – 116.30 (m), 115.86 (t, *J* = 3.5 Hz), 114.64 (t, *J* = 19.6 Hz) ppm; IR (film) ν 3087, 2195, 1571, 1338, 1195 cm^{-1}; LCMS: $[M + H]^+$: 327.

4-(5,7-Dichloro-[1,2,4]triazolo[1,5-*a*]pyrimidin-6-yl)-3-fluorobenzonitrile (107). Following General Procedure B using diethyl 2-(4-cyano-2,6-difluorophenyl)malonate (0.500 g, 1.68 mmol) **(90)** and 3-amino-1,2,4-triazole (0.148 g, 1.77 mmol). Then using the intermediate sodium 6-(4-cyano-2-fluorophenyl)-[1,2,4]triazolo[1,5-*a*]pyrimidine-5,7-bis(olate) (3.000 g, 9.52 mmol) and $POCl_3$ (26.000 g, 169.00 mmol) to obtain the title compound as a brown solid (1.970 g, 9.52 mmol, 67%). ^{1}H NMR (600

MHz, $CDCl_3$) δ 8.61 (s, 1H), 7.68 (dd, *J* = 7.9, 1.5 Hz, 1H), 7.61 (dd, *J* = 8.6, 1.5 Hz, 1H), 7.54 (t, *J* = 7.4 Hz, 1H) ppm;^{13}C NMR (150 MHz, $CDCl_3$) δ 160.47 , 158.79, 157.48, 155.52, 153.79, 140.73, 133.32, 128.86 (d, *J* = 4.6 Hz), 124.68 (d, *J* = 15.7 Hz), 120.42 (d, *J* = 24.9 Hz), 116.76 (d, *J* = 2.9 Hz), 116.69, 116.36 (d, *J* = 9.3 Hz) ppm.

5,7-Dichloro-6-(4-chloro-2,6-difluorophenyl)-[1,2,4]triazolo[1,5-*a*]pyrimidine (108). Following General Procedure B using diethyl 2-(4-chloro-2,6-difluorophenyl)malonate (1.2 g, 3.91 mmol) **(91)** and 3-amino-1,2,4-triazole (0.350 g, 4.10 mmol). Then using the intermediate sodium 6-(4-chloro-2,6-difluorophenyl)-[1,2,4]triazolo[1,5-*a*]pyrimidine-5,7-bis(olate) (1.000 g, 2.92 mmol) and $POCl_3$ (7.970 g, 52.00 mmol) to obtain the title compound as a brown solid (0.710 g, 2.12 mmol, 73%). ^{1}H NMR (600 MHz, $CDCl_3$) δ 8.62 (s, 1H), 7.18 (d, *J* = 7.1 Hz, 2H) ppm; ^{13}C NMR (150 MHz, $CDCl_3$) δ 161.29 – 159.09 (m), 157.36, 156.45, 153.95, 141.55, 138.63 (t, *J* = 13.0 Hz), 113.78 – 113.35 (m), 112.29, 108.08 (t, *J* = 20.0 Hz) ppm; IR (film) ν 3106, 1642, 1427, 1391, 1071 cm^{-1}; LCMS: $[M + H]^+$: 336.

5,7-Dichloro-6-(2,6-difluoro-4-nitrophenyl)-[1,2,4]triazolo[1,5-*a*]pyrimidine (109). Following General Procedure B using diethyl 2-(2,6-difluoro-4-nitrophenyl)malonate (0.500 g, 1.58 mmol) **(92)** and 3-amino-1,2,4-triazole (0.139 g, 1.65 mmol). Then using the intermediate sodium 6-(2,6-difluoro-4-nitrophenyl)-[1,2,4]triazolo[1,5-*a*]pyrimidine-5,7-bis(olate) (0.150 g, 0.43 mmol) and $POCl_3$ (1.160 g, 7.56 mmol) to obtain the title compound as a brown solid (0.100 g, 0.29 mmol, 68%). ^{1}H NMR (600 MHz, $CDCl_3$) δ 8.64 (s, 1H), 8.04 (d, *J* = 6.8 Hz, 2H) ppm; ^{13}C NMR (150 MHz, $CDCl_3$) δ 160.22 (dd), 157.70, 156.90, 155.39, 154.08, 150.51 (d, *J* = 10.5 Hz), 141.48, 116.12 – 115.19 (m), 111.63, 108.69 – 108.36 (m) ppm; IR (film) ν 2916, 2848, 1698, 1601, 1532 cm^{-1}; LCMS: $[M + H]^+$: 347.

Methyl 2-(5-chloro-6-(2,4,6-trifluorophenyl)-[1,2,4]triazolo[1,5-*a*]pyrimidin-7-yl)-4,4,4-trifluoro-3-methylbutanoate (110). To a solution of HMDS (0.101 g, 0.63 mmol, 1 equiv) in THF (0.632 mL) at – 78 ˚C was added *n*-butyllithium (0.369 mL, 0.63 mmol, 1 equiv) and the mixture was stirred at 0 ˚C for 1

h. Then methyl 4,4,4-trifluoro-3-methylbutanoate (0.117 g, 0.69 mmol, 1.1 equiv) was added dropwise at –78 ˚C and the reaction mixture was stirred for 1 h. Then a solution of 5,7-dichloro-6-(2,4,6-trifluorophenyl)-[1,2,4]triazolo[1,5-*a*]pyrimidine (0.200 g, 0.63 mmol, 1 equiv) **(102)** in THF (0.500 mL) was added at –78 ˚C and resulting mixture was stirred for 2.5 h prior to quenching of the reaction with 1M HCl. The aqueous layer was then extracted EtOAc (×2) and washed with sat. aq. NaCl, dried and concentrated under reduced pressure. Purification via silica gel chromatography using hexanes /EtOAc (5–20%) provided the product (0.200 g, 0.44 mmol, 70 %) as a white solid. ^{1}H NMR (600 MHz, $CDCl_3$) mixture of diastereomers δ 8.53 (d, *J* = 6.6 Hz, 1H), 6.94 – 6.86 (m, 2H), 4.04 (d, *J* = 7.4 Hz, 1H), 3.92 – 3.85 (m, 1H), 3.62 (d, *J* = 10.4 Hz, 3H), 1.38 (d, *J* = 6.6 Hz, 1H), 0.80 (d, *J* = 7.4 Hz, 2H) ppm; HRMS (ES+) calculated for $C_{17}H_{12}ClF_6N_4O_2$ $[M + H]^+$: 453.0547, found 453.0542.

7,9-Difluoro-10-(3,3,3-trifluoro-2-methylpropyl)benzofuro[2,3-d][1,2,4]triazolo[1,5-*a*]pyrimidine (111). Methyl 2-(5-chloro-6-(2,4,6-trifluorophenyl)-[1,2,4]triazolo[1,5-*a*]pyrimidin-7-yl)-4,4,4-trifluoro-3-methylbutanoate (0.020 g, 0.04 mmol, 1 equiv) **(110)**, LiCl (0.002 g, 0.04 mmol, 1 equiv), and DMSO (0.100 mL) were stirred at 130 ˚C for 3 h (microwave irradiation). The reaction mixture was then diluted in water and extracted with EtOAc (×3) and the combined organic layers were washed with brine (×2), dried over $MgSO_4$, filtered, and concentrated. Purification by reverse-phase HPLC provided the title compound as a white solid (0.012 g, 0.03 mmol, 76%). X-ray quality crystals were obtained by slow evaporation from a CH_2Cl_2/Pentane solution: m.p. (CH_2Cl_2/Pentane) 103.4–107.4. ^{1}H NMR (600 MHz, $CDCl_3$) δ 8.55 (s, 1H), 8.01 (s, 1H), 7.01 (ddd, *J* = 11.0, 9.3, 2.2 Hz, 1H), 6.86 – 6.79 (m, 3H), 4.11 – 4.05 (m, 2H), 3.88 – 3.78 (m, 2H), 3.30 (p, *J* = 7.3 Hz, 1H), 3.20 (dd, *J* = 13.9, 5.8 Hz, 2H), 3.05 (dt, *J* = 15.1, 7.6 Hz, 2H), 2.79 (dd, *J* = 14.0, 8.7 Hz, 2H), 1.20 (d, *J* = 7.0 Hz, 3H), 1.02 (d, *J* = 7.0 Hz, 3H) ppm; ^{13}C NMR (150 MHz, $CDCl_3$) δ 165.15 – 164.48 (m), 163.01 (d, *J* = 15.1 Hz), 162.26 – 160.00 (m), 158.41, 156.38, 152.47, 150.91, 145.88, 143.80, 127.47 (dd, *J* = 279.5, 28.1 Hz), 108.69, 106.96, 106.21 – 104.64 (m), 102.08 – 100.00 (m), 97.85 (dd, *J* = 27.4, 4.6 Hz), 36.01 (q, *J* = 28.3, 27.6 Hz), 30.84, 29.86 ppm; HRMS (ES+) calculated for $C_{15}H_9F_5N_4O$ $[M + H]^+$: 357.0769, found 357.0768.

***tert*-Butyl-2-(5-chloro-6-(2,4,6-trifluorophenyl)-[1,2,4]triazolo[1,5-*a*]pyrimidin-7-yl)-4,4,4-trifluoro-3-methylbutanoate (112).** To a solution of HMDS (0.054 g, 0.33 mmol, 1.6 equiv) in THF (3 mL) at –78 °C was added *n*-butyllithium (0.180 mL, 0.33 mmol, 1.6 equiv) and the mixture was stirred at 0 °C for 30 min. Then *tert*-butyl 4,4,4-trifluoro-3-methylbutanoate (0.066 g, 0.31 mmol, 1.5 equiv) was added dropwise at –78 °C and the mixture was stirred at this temperature for 1 h. Finally, a solution of 5,7-dichloro-6-(2,4,6-trifluorophenyl)-[1,2,4]triazolo[1,5-*a*]pyrimidine (0.066 g, 0.21 mmol, 1 equiv) **(102)** in THF (0.500 mL) was added at –78 °C. After stirring for 2.5 h at this temperature, the reaction was quenched with a 1M HCl solution. The aqueous layer was then extracted twice with EtOAc and the combined organic layers were washed with brine, dried and concentrated under reduced pressure. Purification via silica gel chromatography using a hexanes/EtOAc gradient (95/05 to 80/20) provided *tert*-butyl 2-(5-chloro-6-(2,4,6-trifluorophenyl)-[1,2,4]triazolo[1,5-*a*]pyrimidin-7-yl)-4,4,4-trifluoro-3-methylbutanoate (0.026 g, 0.05 mmol, 25 %) as a white solid. ^{1}H NMR (600 MHz, $CDCl_3$) mixture of diastereomers δ 8.56 (s, 0.6H), 8.55 (s, 0.4H), 6.91 – 6.87 (m, 2H), 4.14 – 4.04 (m, 0.4H), 3.95 – 3.83 (m, 1.2H), 3.72 (d, 0.4H), 1.38 (d, J = 6.7 Hz, 1.3H), 1.27 (s, 3.5H), 1.25 (s, 6.8H), 0.80 (d, J = 7.0 Hz, 2H) ppm; IR (film) ν 2922, 2852, 1598, 1736, 1493, 1460, 1441, 1371, 1271, 1252, 1201, 1182, 1173, 1142, 1040 cm^{-1}; HRMS (ES+) calculated for $C_{20}H_{18}ClF_6N_4O_2$ $[M + H]^+$: 495.1017, found 495.1010.

Computational Studies. The X-ray crystal structure of the tubulin in complex with a triazolopyrimidine was downloaded from the Protein Data Bank and completed with MAESTRO (Schrödinger Release 2019–3),[32] waters and other co-crystallised molecules were removed, except for the ligand and GDP. Predicting protonation states of protein residues was calculated considering a temperature of 300K and a pH of 7, while the molecules were prepared considering the ionization states at pH 7±2. A 12 Å docking grid (inner-box 10 Å and outer-box 20 Å) was prepared using as centroid the co-crystallised ligand. The docking studies were performed using Glide SP precision keeping the default parameters and setting, and it was combined with "molecular mechanics generalized Born surface area" (MMGBSA), implemented

in the Prime module from Maestro, to re-score the 3 output docking poses of each compound. Only the best MMGBSA score and pose for each compound were plotted in the graph, and correlated with the normalized activity, expressed as the log of the average of the activity at 1 and 10 μM in the AcTub assay, relative to positive control (**5**).

The 3D-QSAR field-based and activity atlas model were constructed using Forge software (Cresset Inc., Cambridgeshire, UK).[33] Firstly, the molecular structures of each compound were subjected to a field-based alignment to the co-crystallized compound, which was used as reference structure. This method is based on 3D-shape and electrostatic potential similarity calculated by the alignment and superposition between the reference compound and the compounds in the database according to their electrostatic distribution and volume occupied. Field point-based descriptors were used for building the 3D-QSAR model after the alignment of 52 Class I compounds with known activity. The activity was computed using the log of the average of the activity at 1 and 10 μM in the AcTub assay and defined as the dependent variable. The derived QSAR model was assessed by the leave-one-out (LOO) technique to optimize the activity-prediction model. Activity atlas was used to acquire qualitative information of the field and steric contributions significant for the activity.

Molecular Operating Environment (MOE) 2019.10 was used to visualize the structures and acquire the images,[34] while GraphPad software[35] and DataWarrior[36] were used for the statistical analysis.

QBI293 Cell and neuronal Acetyl-tubulin and α-Tubulin Determinations. Compound-induced changes in acetylated-tubulin and α-tubulin in QBI293 cells or primary mouse neurons was as previously described.[5, 11] Briefly, QBI293 cells were maintained in Dulbecco's Modified Eagle's Medium containing 10% fetal bovine serum (FBS), 2 mM L-glutamine (Mediatech), 50 units/ml penicillin, and 50 μg/ml streptomycin. For compound testing, cells were dissociated with trypsin/EDTA and plated at a density of 6 x 105 cells/well in 6-well plates. After overnight incubation, the medium was aspirated and fresh medium containing vehicle or test compound was added. After 4 h incubation, whole-cell extracts were prepared from the QBI293 cells as described.[5, 11] The supernatant fraction from each sample was collected and

analyzed for protein content by BCA assay.[11] The acetyl-tubulin and α-tubulin enzyme-linked immunosorbent assays (ELISA) were performed on the supernatant fraction as previously described.[11] The amount of acetyl- and α-tubulin protein in each sample was extrapolated using standard curves generated from serial dilutions with known acetyl- or α-tubulin preparations of known concentrations. Acetyl-tubulin levels were determined in a similar fashion in mouse cortical neuron cultures plated at 6 x 10^5 cells/well in 6-well plates, essentially as previously described for rat cortical neurons.[11] After 10 days of growth, the neurons were treated for 8 hours with 15 nM okadaic acid in the presence or absence of test compound (1 or 10 μM) or vehicle (0.25% DMSO), and homogenates were prepared for determination of acetyl-tubulin levels as previously described.[11]

Acetyl-tubulin staining of rat cortical neuron cultures treated with test compounds in the absence or presence of okadaic acid. Rat cortical neurons were grown in 24-well plates on coverslips for 10 days as previously described.[11] The cultures were then treated for 8 hours with or without 15 nM okadaic acid in the presence or absence of test compounds (1 μM), with methods as described.[11] Finally, the cultures were prepared for acetyl-tubulin staining as previously discussed.[11]

Determination of Plasma and Brain Drug Concentrations. All animal protocols were approved by the University of Pennsylvania Institutional Animal Care and Use Committee (IACUC). Test compounds were administered to groups of three 2–3-month old female CD-1 mice (Charles River). For standard single time-point brain and plasma determinations, mice were injected i.p. with a single dose of 5 mg/kg compound dissolved in DMSO. In some instances, mice were cassette-dosed via i.p. administration with 2–3 compounds concurrently, each at 2.5 mg/kg. One hour following compound administration, mice were euthanized following an IACUC-approved protocol. Whole brain hemispheres were homogenized in 10 mM ammonium acetate, pH 5.7 (50%, w/v), using a hand-held sonic homogenizer. Plasma was obtained from blood collected in 0.5 M EDTA solution and centrifuged for 10 min at 4,500 x g at 4 ˚C.

Compound levels with plasma and brain homogenates were determined essentially as previously described[10, 11] either in-house or at a contract laboratory (Inotiv, Inc.).

Associated Content: NMR spectra of test compounds; X-ray crystal structures of compounds **68** (CCDC 1995770) and **111** (CCDC 2003391), Authors will release the atomic coordinates and experimental data upon article publication; the SMILES string structures along the full data set in tabular form (csv file format). This material is available free of charge via the Internet at http://pubs.acs.org.

Author Information: Kurt R. Brunden (email: kbrunden@upenn.edu) and Carlo Ballatore (email: cballatore@health.ucsd.edu).

Acknowledgments. Financial support for this work has been provided by the NIH/NIA (AG061173, AG044332).

Abbreviations Used: *AcTub*, acetylated α-tubulin; *m-CPBA*, *meta*-chloroperbenzoic acid; *MMGBSA*, molecular mechanics generalized Born surface-area; *MT*, microtubule; *NFTs,* neurofibrillary tangles; *NTs*, neuropil threads; *Tg*, transgenic.

References

1. Lee, V. M. Y.; Goedert, M.; Trojanowski, J. Q. Neurodegenerative tauopathies. *Annu. Rev. Neurosci.* **2001,** 24, 1121-1159.
2. Ballatore, C.; Lee, V. M. Y.; Trojanowski, J. Q. Tau-mediated neurodegeneration in Alzheimer's disease and related disorders. *Nat. Rev. Neurosci.* **2007,** 8, 663-672.
3. Sadleir, K. R.; Kandalepas, P. C.; Buggia-Prevot, V.; Nicholson, D. A.; Thinakaran, G.; Vassar, R. Presynaptic dystrophic neurites surrounding amyloid plaques are sites of microtubule disruption, BACE1 elevation, and increased Abeta generation in Alzheimer's disease. *Acta neuropathol.* **2016**, 132, 235-256.
4. Lee, V. M. Y.; Daughenbaugh, R.; Trojanowski, J. Q. Microtubule stabilizing drugs for the treatment of Alzheimers-disease. *Neurobiol. Aging* **1994,** 15, S87-S89.
5. Brunden, K. R.; Zhang, B.; Carroll, J.; Yao, Y.; Potuzak, J. S.; Hogan, A. M.; Iba, M.; James, M. J.; Xie, S. X.; Ballatore, C.; Smith, A. B., III; Lee, V. M.; Trojanowski, J. Q. Epothilone D improves microtubule density, axonal integrity, and cognition in a transgenic mouse model of tauopathy. *J. Neurosci.* **2010,** 30, 13861-13866.
6. Makani, V.; Zhang, B.; Han, H.; Yao, Y.; Lassalas, P.; Lou, K.; Paterson, I.; Lee, V. M. Y.; Trojanowski, J. Q.; Ballatore, C.; Smith, A. B., III; Brunden, K. R. Evaluation of the brain-penetrant microtubule-stabilizing agent, dictyostatin, in the PS19 tau transgenic mouse model of tauopathy. *Acta Neuropathol. Commun.* **2016,** 4, 1-12.
7. Zhang, B.; Carroll, J.; Trojanowski, J. Q.; Yao, Y.; Iba, M.; Potuzak, J. S.; Hogan, A. M.; Xie, S. X.; Ballatore, C.; Smith, A. B., III; Lee, V. M.; Brunden, K. R. The microtubule-stabilizing agent, epothilone D, reduces axonal dysfunction, neurotoxicity, cognitive deficits, and Alzheimer-like pathology in an interventional study with aged tau transgenic mice. *J. Neurosci.* **2012,** 32, 3601-3611.
8. Barten, D. M.; Fanara, P.; Andorfer, C.; Hoque, N.; Wong, P. Y. A.; Husted, K. H.; Cadelina, G. W.; DeCarr, L. B.; Yang, L.; Liu, L.; Fessler, C.; Protassio, J.; Riff, T.; Turner, H.; Janus, C. G.; Sankaranarayanan, S.; Polson, C.; Meredith, J. E.; Gray, G.; Hanna, A.; Olson, R. E.; Kim, S. H.; Vite,

G. D.; Lee, F. Y.; Albright, C. F. Hyperdynamic microtubules, cognitive deficits, and pathology are improved in tau transgenic mice with low doses of the microtubule-stabilizing agent BMS-241027 *J. Neurosci*. **2012,** 32, 7137–7145.

9. Ballatore, C.; Brunden, K. R.; Trojanowski, J. Q.; Lee, V. M.; Smith, A. B., III. Non-naturally occurring small molecule microtubule-stabilizing agents: a potential tactic for CNS-directed therapies. *ACS Chem. Neurosci*. **2017,** 8, 5-7.
10. Lou, K.; Yao, Y.; Hoye, A. T.; James, M. J.; Cornec, A. S.; Hyde, E.; Gay, B.; Lee, V. M.; Trojanowski, J. Q.; Smith, A. B., III; Brunden, K. R.; Ballatore, C. Brain-penetrant, orally bioavailable microtubule-stabilizing small molecules are potential candidate therapeutics for Alzheimer's disease and related tauopathies. *J. Med. Chem*. **2014,** 57, 6116-6127.
11. Kovalevich, J.; Cornec, A. S.; Yao, Y.; James, M.; Crowe, A.; Lee, V. M.; Trojanowski, J. Q.; Smith, A. B.; Ballatore, C.; Brunden, K. R. Characterization of brain-penetrant pyrimidine-containing molecules with differential microtubule-stabilizing activities developed as potential therapeutic agents for Alzheimer's disease and related tauopathies. *J. Pharmacol. Exp. Ther*. **2016,** 357, 432-450.
12. Zhang, B.; Yao, Y.; Cornec, A.-S.; Oukoloff, K.; James, M. J.; Koivula, P.; Trojanowski, J. Q.; Smith, A. B., III; Lee, V. M.-Y.; Ballatore, C.; Brunden, K. R. A brain-penetrant triazolopyrimidine enhances microtubule-stability, reduces axonal dysfunction and decreases tau pathology in a mouse tauopathy model. *Mol. Neurodegener*. **2018,** 13, 59.
13. Sáez-Calvo, G.; Sharma, A.; Balaguer, F. d. A.; Barasoain, I.; Rodríguez-Salarichs, J.; Olieric, N.; Muñoz-Hernández, H.; Berbís, M. Á.; Wendeborn, S.; Peñalva, M. A.; Matesanz, R.; Canales, Á.; Prota, A. E.; Jímenez-Barbero, J.; Andreu, J. M.; Lamberth, C.; Steinmetz, M. O.; Díaz, J. F. Triazolopyrimidines are microtubule-stabilizing agents that bind the vinca inhibitor site of tubulin. *Cell Chem. Biol*. **2017,** 24, 737-750 e6.
14. Yao, Y.; Nzou, G.; Alle, T.; Tsering, W.; Maimaiti, S.; Trojanowski, J. Q.; Lee, V. M.; Ballatore, C.; Brunden, K. Correction of microtubule defects within Aβ plaque-associated dystrophic axons results in lowered Aβ release and plaque deposition. *Alzheimer's Dement*. **2020**, 16, 1345-1357.

15. Zhang, N.; Ayral-Kaloustian, S.; Nguyen, T.; Afragola, J.; Hernandez, R.; Lucas, J.; Gibbons, J.; Beyer, C. Synthesis and SAR of [1,2,4]triazolo[1,5-a]pyrimidines, a class of anticancer agents with a unique mechanism of tubulin inhibition. *J. Med. Chem.* **2007,** 50, 319-327.
16. Zhang, N.; Ayral-Kaloustian, S.; Nguyen, T.; Hernandez, R.; Lucas, J.; Discafani, C.; Beyer, C. Synthesis and SAR of 6-chloro-4-fluoroalkylamino-2-heteroaryl-5-(substituted)phenylpyrimidines as anti-cancer agents. *Bioorg. Med. Chem.* **2009,** 17, 111-118.
17. Ayral-Kaloustian, S.; Zhang, N.; Beyer, C. Cevipabulin (TTI-237): preclinical and clinical results for a novel antimicrotubule agent. *Methods Find. Exp. Clin. Pharmacol.* **2009,** 31, 443-447.
18. Wang-Gillam, A.; Arnold, S. M.; Bukowski, R. M.; Rothenberg, M. L.; Cooper, W.; Wang, K. K.; Gauthier, E.; Lockhart, A. C. A phase I dose escalation study of TTI-237 in patients with advanced malignant solid tumors. *Invest. New Drugs* **2012,** 30, 266-272.
19. Fukushima, N.; Furuta, D.; Hidaka, Y.; Moriyama, R.; Tsujiuchi, T. Post-translational modifications of tubulin in the nervous system. *J. Neurochem.* **2009,** 109, 683-693.
20. Cornec, A. S.; James, M. J.; Kovalevich, J.; Trojanowski, J. Q.; Lee, V. M.; Smith, A. B., III; Ballatore, C.; Brunden, K. R. Pharmacokinetic, pharmacodynamic and metabolic characterization of a brain retentive microtubule (MT)-stabilizing triazolopyrimidine. *Bioorg. Med. Chem. Lett.* **2015,** 25, 4980-4982.
21. Gomez, L.; Massari, M. E.; Vickers, T.; Freestone, G.; Vernier, W.; Ly, K.; Xu, R.; McCarrick, M.; Marrone, T.; Metz, M.; Yan, Y. G.; Yoder, Z. W.; Lemus, R.; Broadbent, N. J.; Barido, R.; Warren, N.; Schmelzer, K.; Neul, D.; Lee, D.; Andersen, C. B.; Sebring, K.; Aertgeerts, K.; Zhou, X.; Tabatabaei, A.; Peters, M.; Breitenbucher, J. G. Design and synthesis of novel and selective phosphodiesterase 2 (PDE2a) inhibitors for the treatment of memory disorders. *J. Med. Chem.* **2017,** 60, 2037-2051.
22. Krapcho P. A; E., C. The Krapcho dealkoxycarbonylation reaction of esters with α-electron-withdrawing substituents. *Org. React.* **2013**, 81, 1-536.

23. Oukoloff, K.; Kovalevich, J.; Cornec, A. S.; Yao, Y.; Owyang, Z. A.; James, M.; Trojanowski, J. Q.; Lee, V. M.; Smith, A. B., III; Brunden, K. R.; Ballatore, C. Design, synthesis and evaluation of photoactivatable derivatives of microtubule (MT)-active [1,2,4]triazolo[1,5-a]pyrimidines. *Bioorg. Med. Chem. Lett.* **2018,** 28, 2180-2183.

24. Wang, E.; Sun, H.; Wang, J.; Wang, Z.; Liu, H.; Zhang, J. Z. H.; Hou, T. End-point binding free energy calculation with MM/PBSA and MM/GBSA: strategies and applications in drug design. *Chem. Rev.* **2019,** 119, 9478-9508.

25. Tosco, P.; Mackey, M. Lessons and successes in the use of molecular fields. In *Comprehensive medicinal chemistry III*; Chackalamannil, S., Rotella, D, Ward. S. E., Eds.; Elsevier: 2017; Vol. 3-8, p 253-296.

26. Ballatore, C.; Brunden, K. R.; Huryn, D. M.; Trojanowski, J. Q.; Lee, V. M. Y.; Smith, A. B., III Microtubule stabilizing agents as potential treatment for alzheimer's disease and related neurodegenerative tauopathies. *J. Med. Chem.* **2012,** 55, 8979-8996.

27. Beyer, C. F.; Zhang, N.; Hernandez, R.; Vitale, D.; Lucas, J.; Nguyen, T.; Discafani, C.; Ayral-Kaloustian, S.; Gibbons, J. J. TTI-237: a novel microtubule-active compound with in vivo antitumor activity. *Cancer Res.* **2008,** 68, 2292-300.

28. Hansch, C.; Leo, A.; Taft, R. W. A survey of Hammett substituent constants and resonance and field parameters. *Chem. Rev.* **1991,** 91, 165-195.

29. Activity Atlas, Forge, Version 10.6.0; Cresset: Litlington, Cambridgeshire, https://www.cresset-group.com/software/forge/ (accessed November 17, 2020).

30. Stumpfe, D.; Bajorath, J. Exploring activity cliffs in medicinal chemistry. *J. Med. Chem.* **2012,** 55, 2932-2942.

31. Fleming, F. F.; Yao, L.; Ravikumar, P. C.; Funk, L.; Shook, B. C. Nitrile-containing pharmaceuticals: efficacious roles of the nitrile pharmacophore. *J. Med. Chem.* **2010,** 53, 7902-7917.

32. Schrödinger, L. Schrödinger, LLC, New York, NY, 2019 https://www.schrodinger.com (accessed Nov 17, 2020).

33. 3D QSAR, Forge, Version 10.6.0; Cresset: Litlington, Cambridgeshire https://www.cresset-group.com/software/forge/ (accessed Nov 17, 2020).
34. Molecular Operating Environment (MOE), Montreal, QC, Canada, H3A 2R7, 2019 http://www.chemcomp.com (acessed Nov 17, 2020).
35. GraphPad Prism Version 8.00 for Windows, GraphPad Software, La Jolla California USA, https://www.graphpad.com (acessed Nov 17, 2020).
36. Sander, T.; Freyss, J.; Von Korff, M.; Rufener, C. DataWarrior: an open-source program for chemistry aware data visualization and analysis. *J. Chem. Inf. Model.* **2015,** 55, 460-473.
37. Brunden, K. R.; Yao, Y.; Potuzak, J. S.; Ferrer, N. I.; Ballatore, C.; James, M. J.; Hogan, A. M.; Trojanowski, J. Q.; Smith, A. B., III; Lee, V. M. The characterization of microtubule-stabilizing drugs as possible therapeutic agents for Alzheimer's disease and related tauopathies. *Pharmacol. Res.* **2011,** 63, 341-351.

TABLE OF CONTENT GRAPHIC.

SAR of microtubule stabilizing triazolopyrimidines

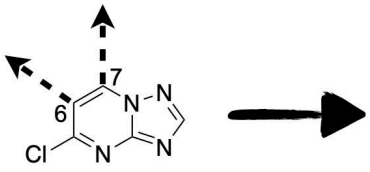

68 compounds

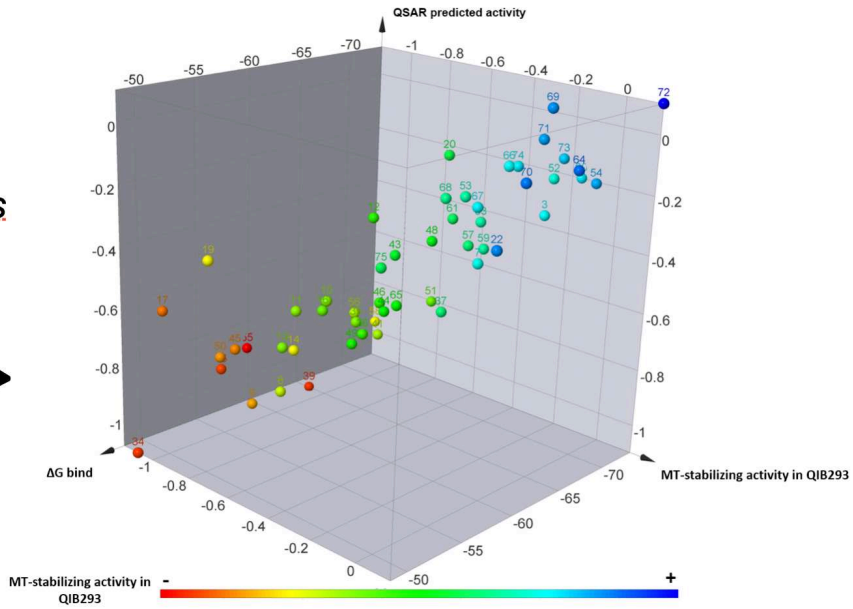

Supporting Information

Evaluation of Structure-Activity Relationship of Microtubule (MT)-Targeting 1,2,4-Triazolo[1,5-*a*]pyrimidines Identifies New Candidates for Neurodegenerative Tauopathies.

Killian Oukoloff,[a] Goodwell Nzou,[b] Carmine Varricchio,[c] Bobby Lucero,[d] Thibault Alle,[a] Jane Kovalevich,[b] Ludovica Monti,[a] Anne-Sophie Cornec,[c] Yuemang Yao,[b] Michael J. James,[b] John Q. Trojanowski,[b] Virginia M.-Y. Lee,[b] Amos B. Smith III,[c] Andrea Brancale,[c] Kurt R. Brunden[b,*] and Carlo Ballatore[a,*]

[a]Skaggs School of Pharmacy and Pharmaceutical Sciences, University of California, San Diego, 9500 Gilman Drive, La Jolla, CA 92093; [b]Center for Neurodegenerative Disease Research, Perelman School of Medicine, University of Pennsylvania, 3600 Spruce St., Philadelphia, PA 19104; [c]Cardiff School of Pharmacy and Pharmaceutical Sciences, Cardiff, King Edward VII Avenue, Cardiff CF103NB, UK; [d]Department of Chemistry & Biochemistry, University of California San Diego, 9500 Gilman Drive, La Jolla, CA, 92093, USA;[e]Department of Chemistry, School of Arts and Sciences, University of Pennsylvania, 231 South 34th St., Philadelphia, PA 19104-6323.

Table of contents

Table S-1: HeLa/QBI293 cell cytotoxicity assay of selected compounds

Cpd#	Structure	HeLa IC_{50} (nM)	QBI293 IC_{50} (nM)
Taxol	-	1.45 ± 0.083	1.40 ± 0.129
Vinblastine	-	3.11 ± 0.252	1.93 ± 0.286
7	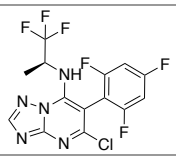	50.8 ± 0.051	102 ± 0.120
6	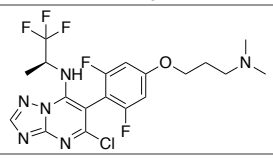	10.1 ± 0.066	21.2 ± 0.101
3	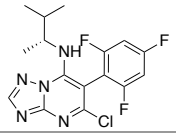	51.9 ± 0.081	84.0 ± 0.141
46	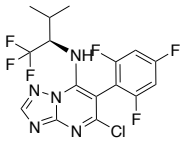	80.7 ± 0.080	186 ± 0.142
47	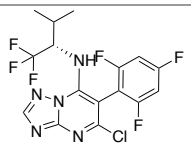	75.4 ± 0.077	236 ± 0.138
5 (Cevipabulin)	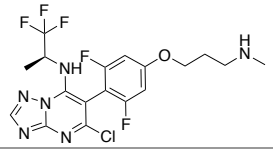	12.8 ± 0.117	28.0 ± 0.168

Experimental section

HeLa/QBI293 cells cytotoxicity assay

The CellTiter-Glo® luminescent cell viability assay (G7572; Promega) was employed to measure the ability of test compounds to inhibit cancer cell proliferation. Compounds in 100% DMSO stocks were diluted in 50 µL medium in 96-well plates (Corning 3903) such that the final DMSO

concentration was 1%. Eight-point dose response assays were set up. HeLa or QBI293 cells were then diluted to $1x10^5$ cells/mL in medium and dispensed into the previously prepared 96-well plates at 50 µL per well. After 48 h incubation at 37°C and 5% CO_2, cells were lysed by the addition of 100 µL/well of Cell-titer Glo®. Plates were read on the 2104 EnVision® multilabel plate reader (PerkinElmer). The activity of test compounds was normalized against controls from the same plate. ED_{50} values, *i.e.*, the concentration of drug required to inhibit cell growth by 50%, were calculated using GraphPad Prism software, version 8.3.0 for macOS. Each assay was performed as three experimental replicates and means ± SD values are shown.

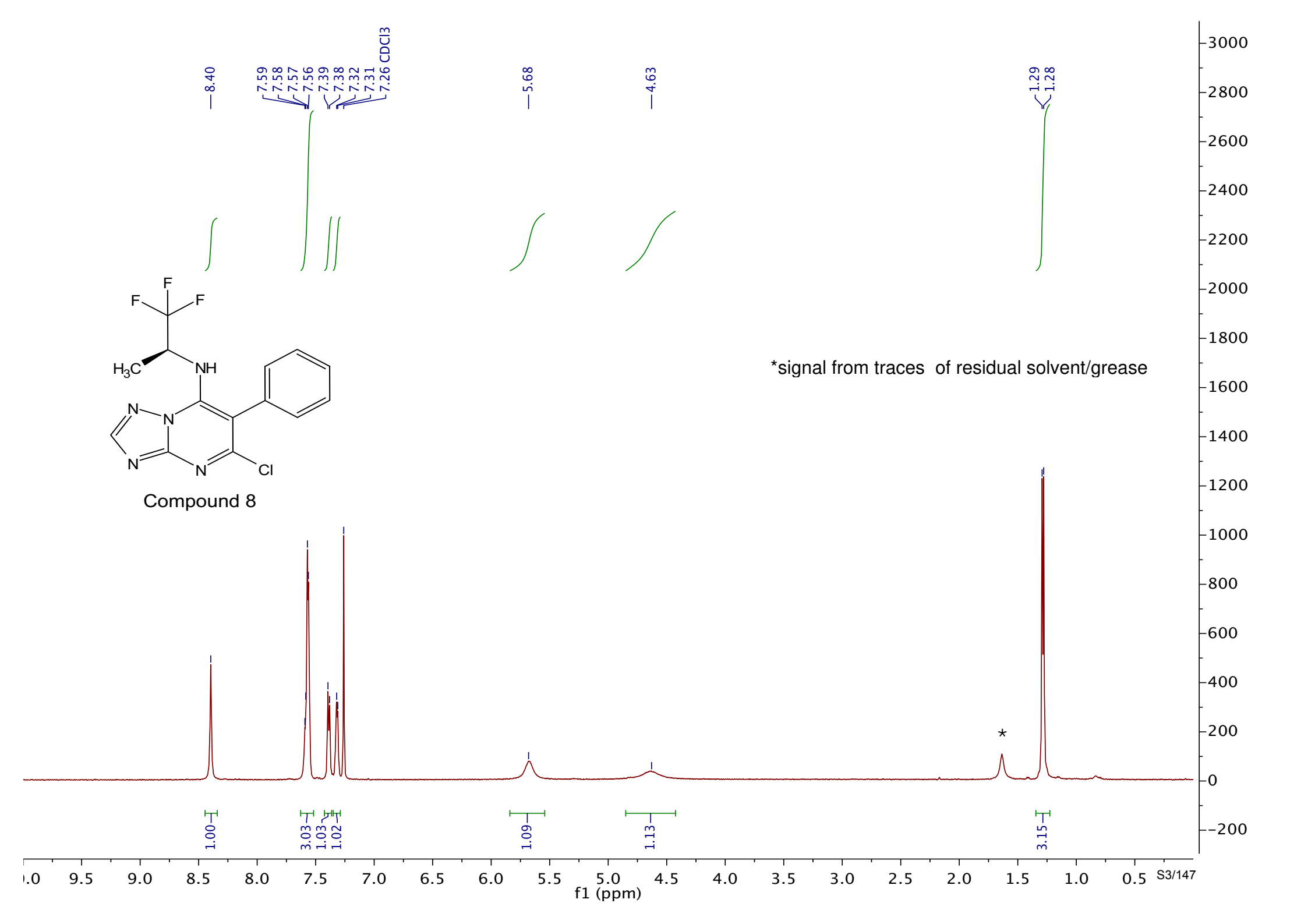
8.40
7.59
7.58
7.57
7.56
7.39
7.38
7.32
7.31
7.26 CDCl3
5.68
4.63
1.29
1.28
F
F
F
H3C
NH
N
N
N
N
Cl
Compound 8
*signal from traces of residual solvent/grease
*
1.00
3.03
1.03
1.02
1.09
1.13
3.15
f1 (ppm)
S3/147

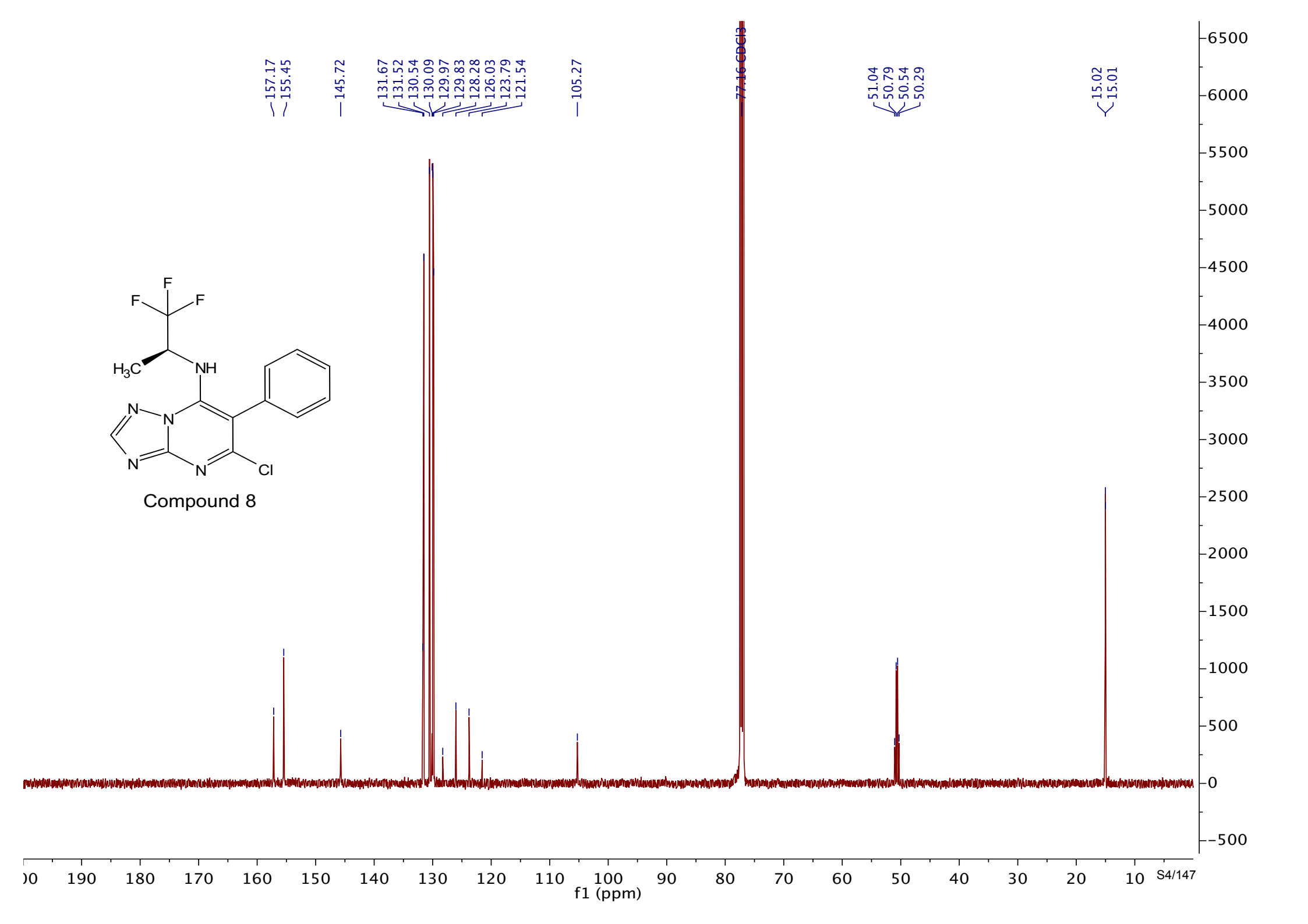
157.17
155.45
145.72
131.67
131.52
130.54
130.09
129.97
129.83
128.28
126.03
123.79
121.54
105.27
77.16 CDCl3
51.04
50.79
50.54
50.29
15.02
15.01
F
F
F
H3C
NH
N
N
N
N
Cl
Compound 8
f1 (ppm)
S4/147

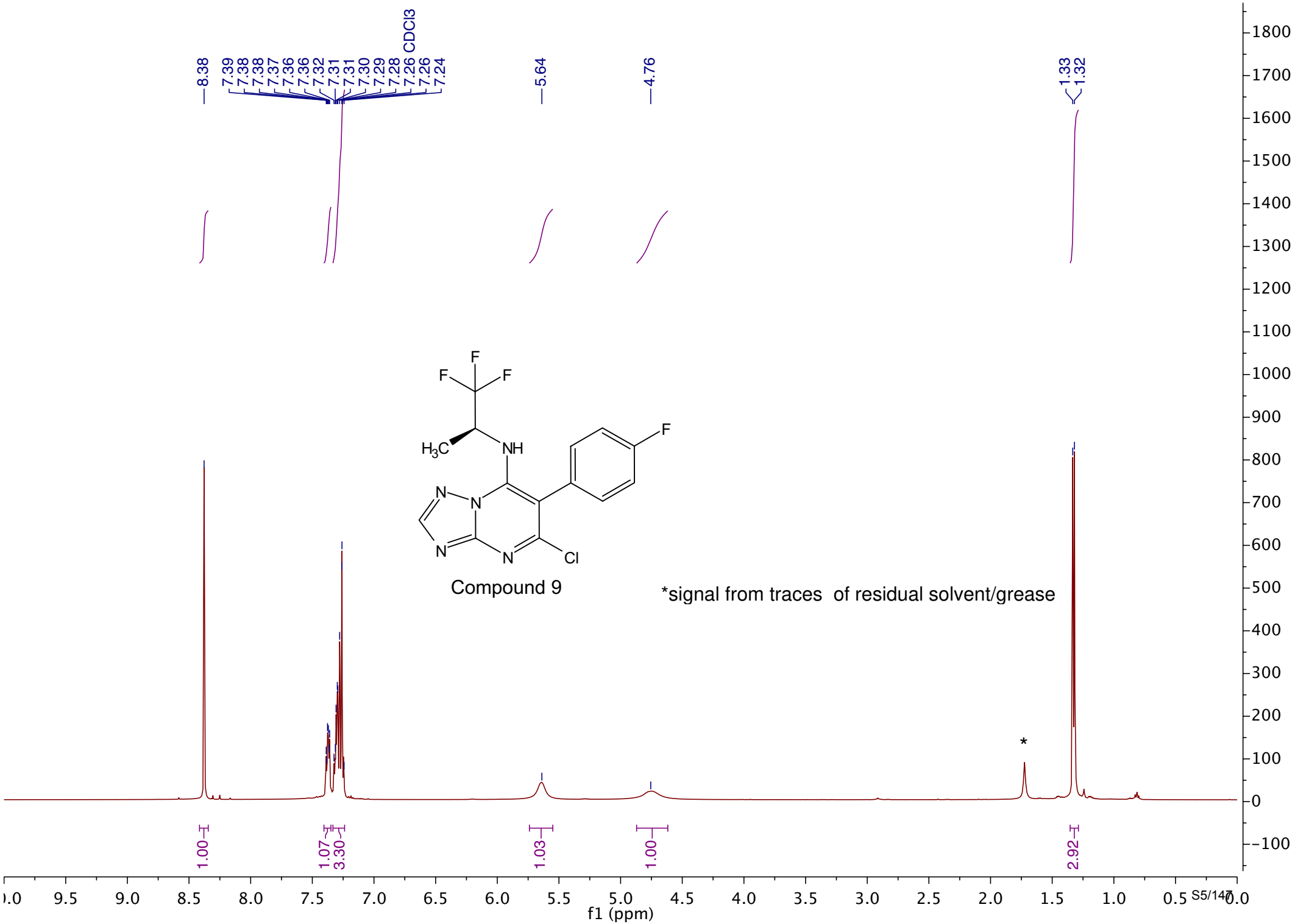
8.38
7.39
7.38
7.38
7.37
7.36
7.36
7.32
7.31
7.31
7.30
7.29
7.28
CDCl3
7.26
7.26
7.24
5.64
4.76
1.33
1.32
F
F
F
H3C
NH
N
N
N
N
Cl
F
Compound 9
*signal from traces of residual solvent/grease
*
1.00
1.07
3.30
1.03
1.00
2.92
f1 (ppm)

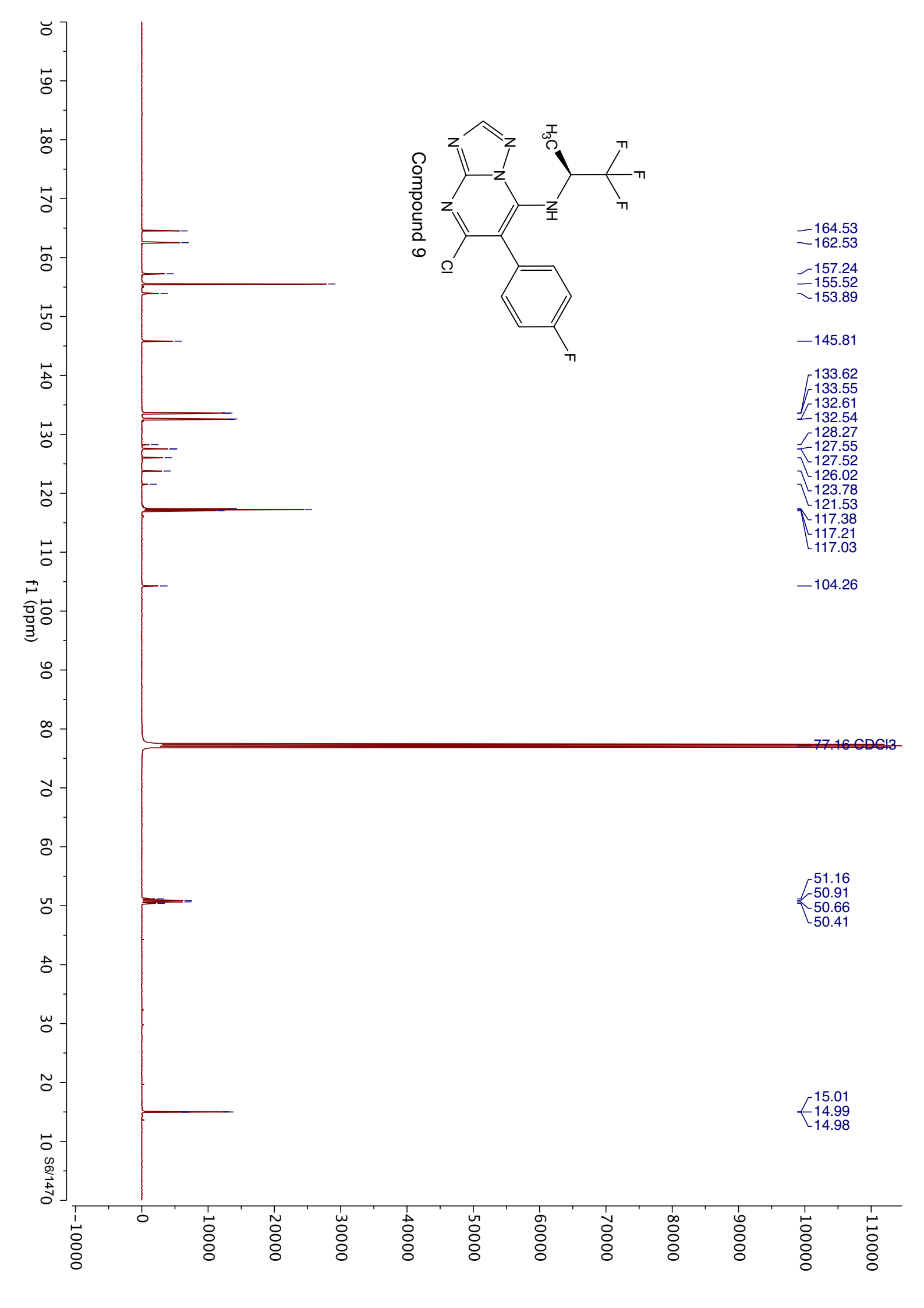
Compound 9
164.53
162.53
157.24
155.52
153.89
145.81
133.62
133.55
132.61
132.54
128.27
127.55
127.52
126.02
123.78
121.53
117.38
117.21
117.03
104.26
77.16 CDCl3
51.16
50.91
50.66
50.41
15.01
14.99
14.98
f1 (ppm)
S6/1470

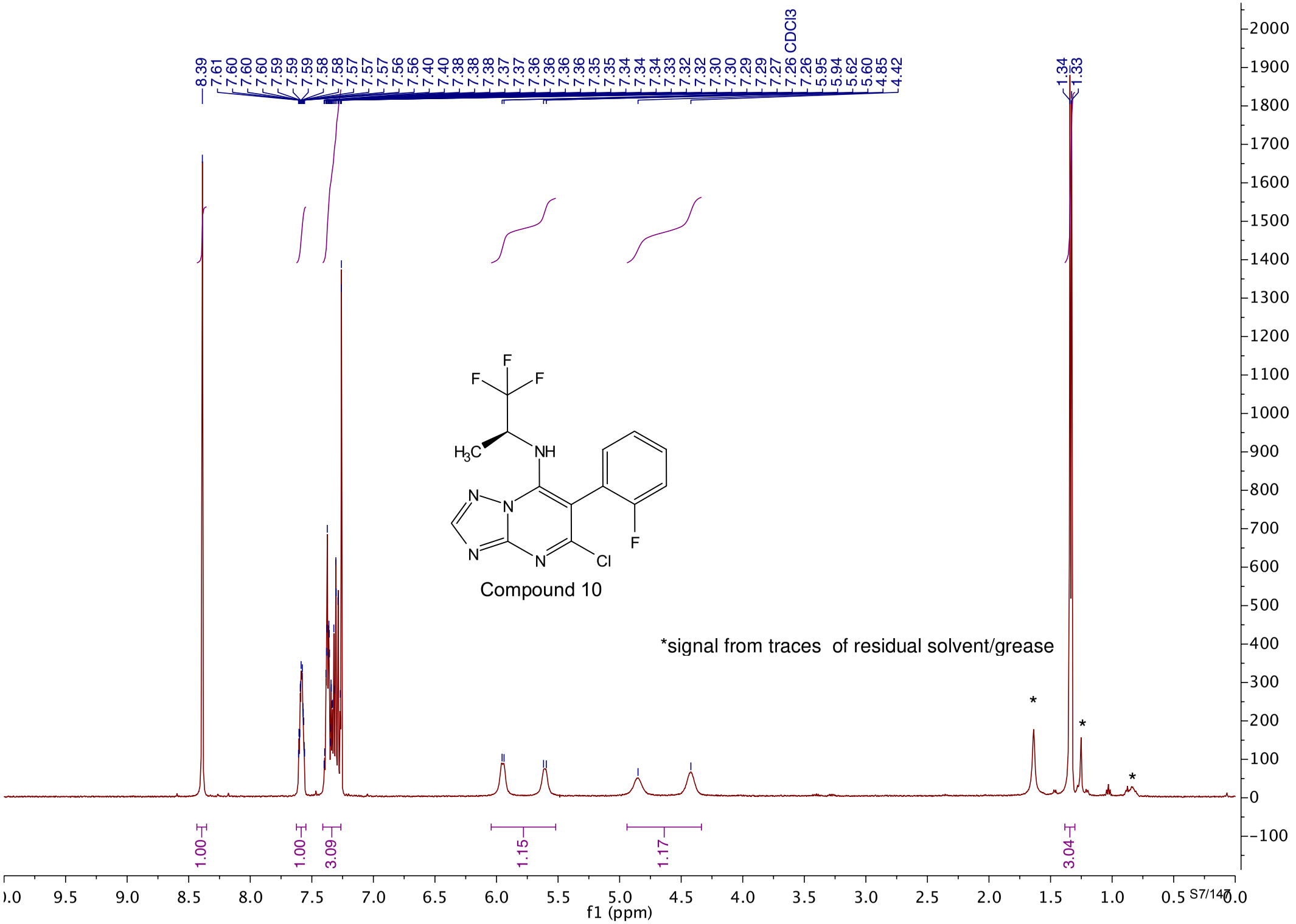
8.39
7.61
7.60
7.60
7.60
7.59
7.59
7.59
7.58
7.58
7.57
7.57
7.57
7.56
7.56
7.40
7.38
7.38
7.38
7.37
7.37
7.36
7.36
7.36
7.35
7.35
7.34
7.34
7.34
7.33
7.32
7.30
7.30
7.29
7.29
7.27
7.26 CDCl3
7.26
5.95
5.94
5.62
5.60
4.85
4.42
1.34
1.33
F
F
F
H3C
NH
N
N
N
N
Cl
F
Compound 10
*signal from traces of residual solvent/grease
1.00
1.00
3.09
1.15
1.17
3.04
f1 (ppm)
S7/147

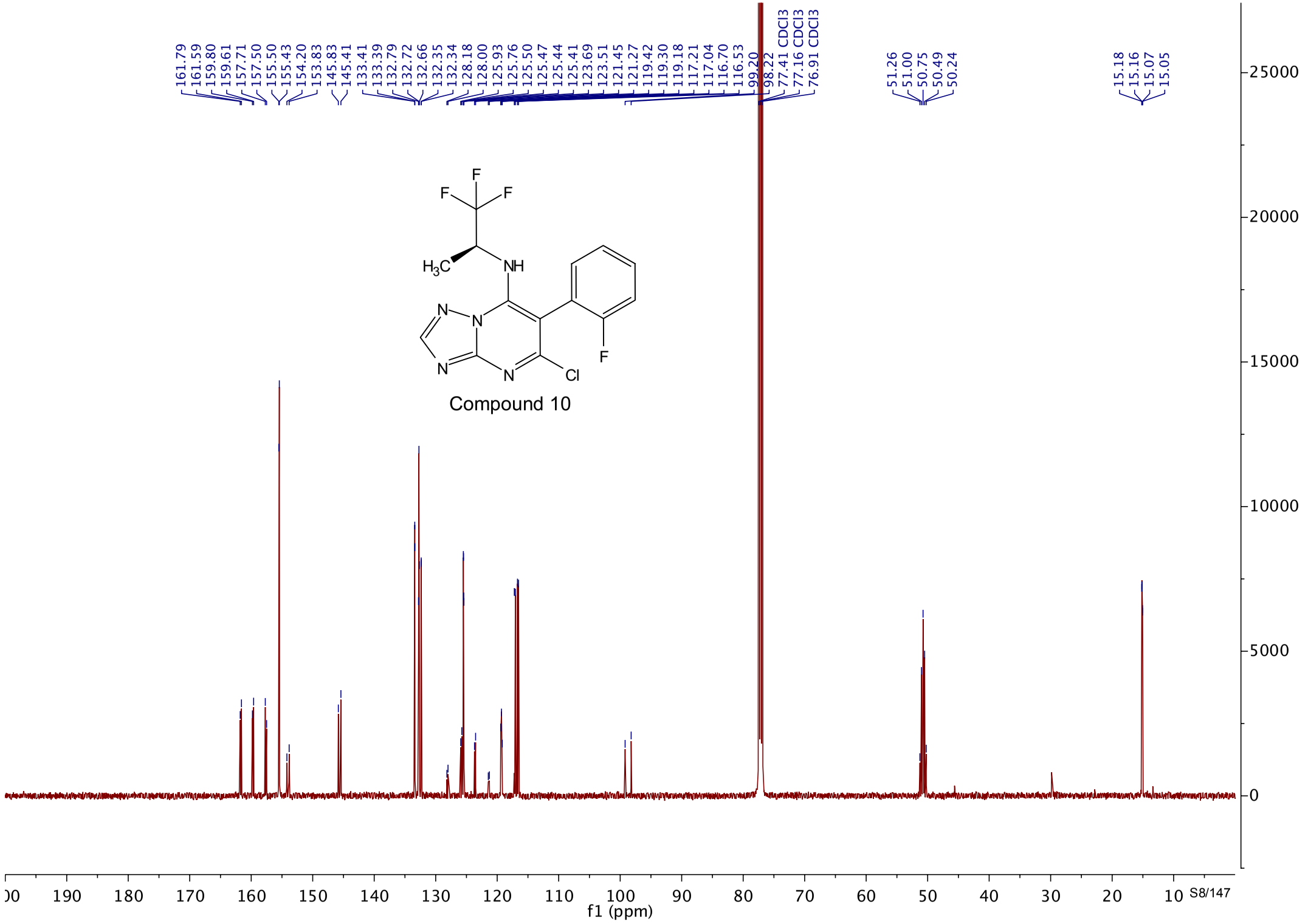
161.79
161.59
159.80
159.61
157.71
157.50
155.50
155.43
154.20
153.83
145.83
145.41
133.41
133.39
132.79
132.72
132.66
132.35
132.34
128.18
128.00
125.93
125.76
125.50
125.47
125.44
125.41
123.69
123.51
121.45
121.27
119.42
119.30
119.18
117.21
117.04
116.70
116.53
99.20
98.22
77.41 CDCl3
77.16 CDCl3
76.91 CDCl3
51.26
51.00
50.75
50.49
50.24
15.18
15.16
15.07
15.05
F
F
F
H3C
NH
N
N
N
N
Cl
F
Compound 10
25000
20000
15000
10000
5000
0
190
180
170
160
150
140
130
120
110
100
90
80
70
60
50
40
30
20
10
f1 (ppm)
S8/147

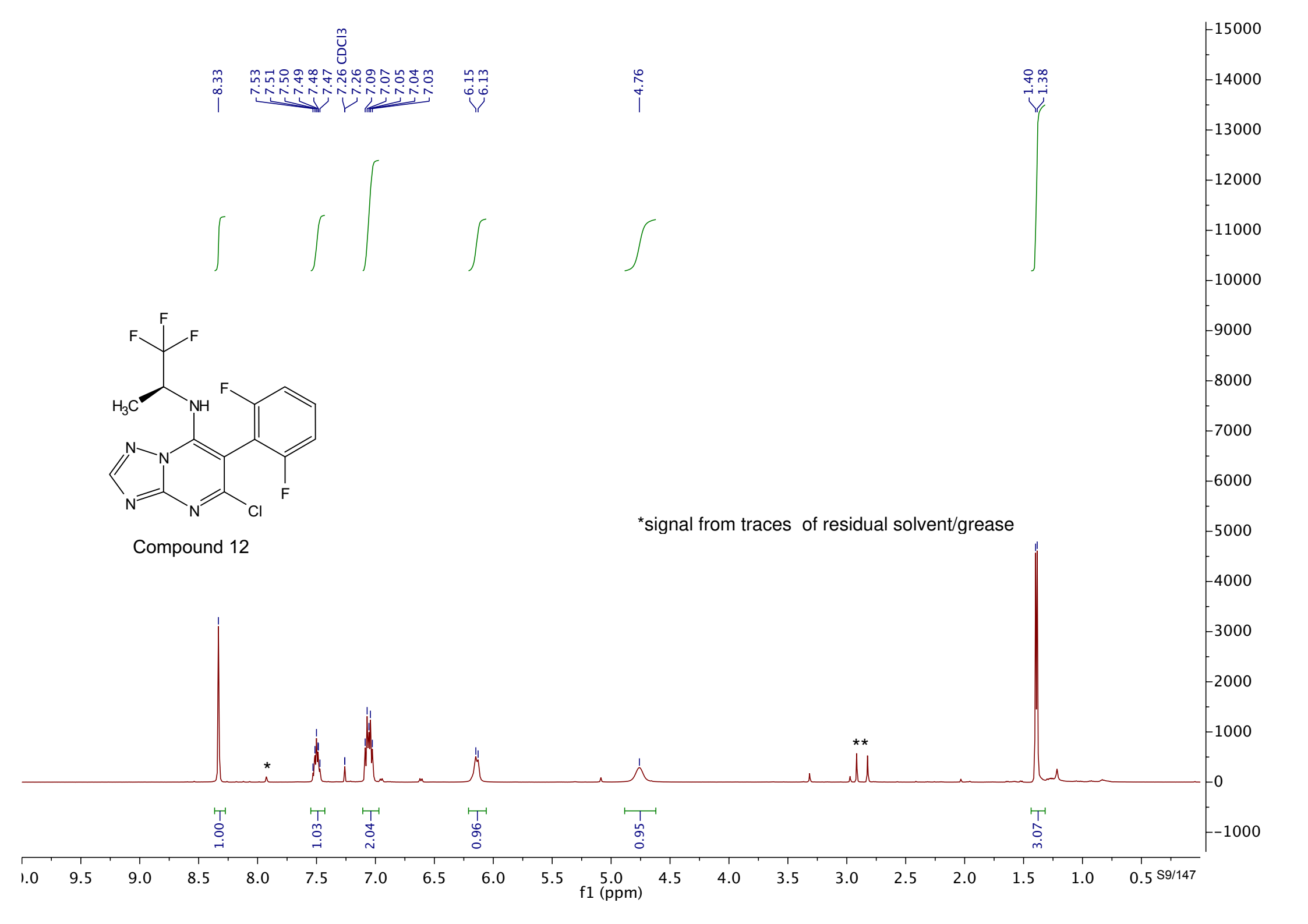
8.33
7.53
7.51
7.50
7.49
7.48
7.47
7.26 CDCl3
7.26
7.09
7.07
7.05
7.04
7.03
6.15
6.13
4.76
1.40
1.38
F
F
F
H3C
NH
F
N
N
N
N
Cl
Compound 12
*signal from traces of residual solvent/grease
*
**
1.00
1.03
2.04
0.96
0.95
3.07
f1 (ppm)
S9/147

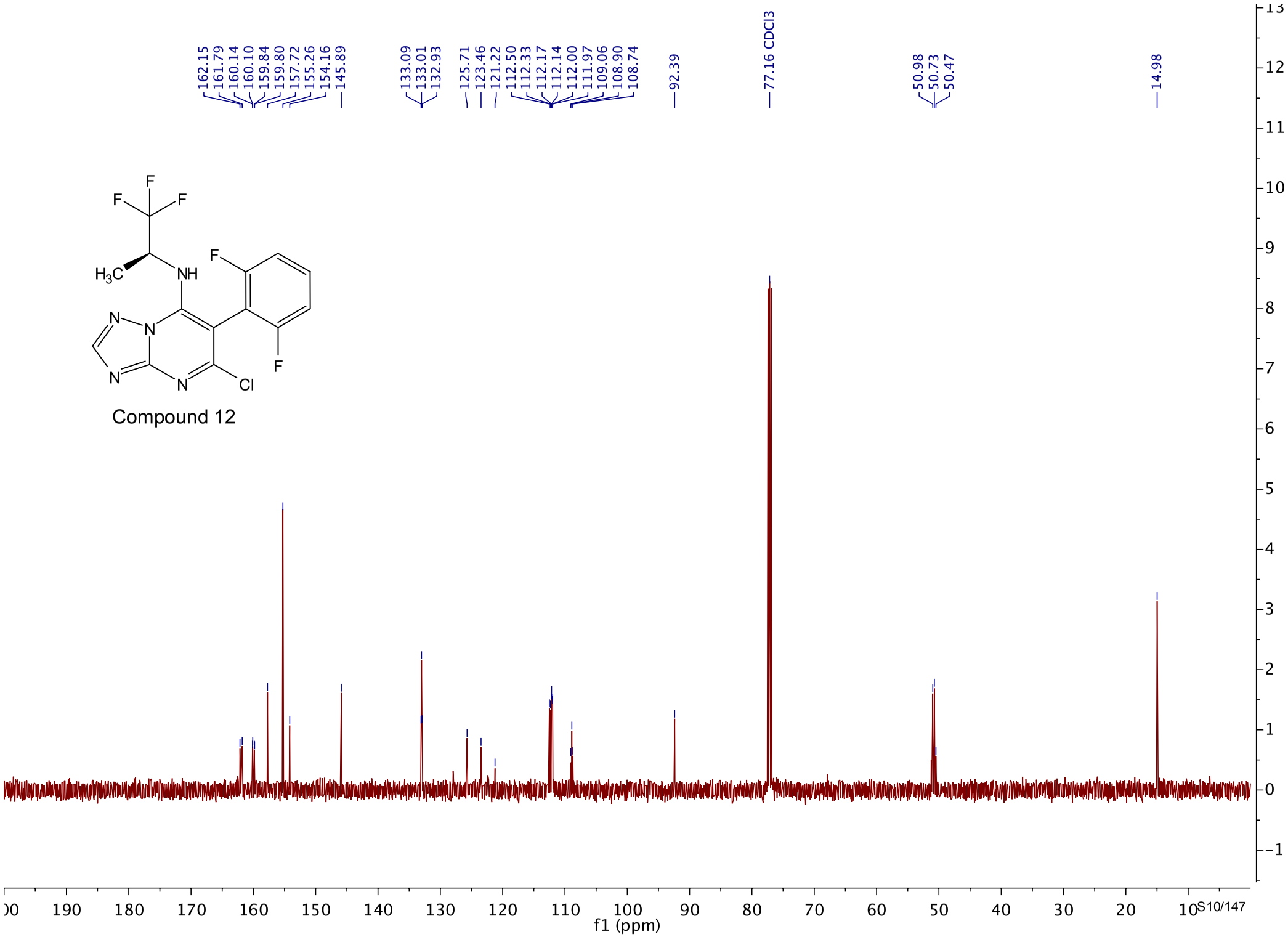
162.15
161.79
160.14
160.10
159.84
159.80
157.72
155.26
154.16
145.89
133.09
133.01
132.93
125.71
123.46
121.22
112.50
112.33
112.17
112.14
112.00
111.97
109.06
108.90
108.74
92.39
77.16 CDCl3
50.98
50.73
50.47
14.98
F
F
F
H3C
NH
F
N
N
N
N
Cl
F
Compound 12
f1 (ppm)
S10/147

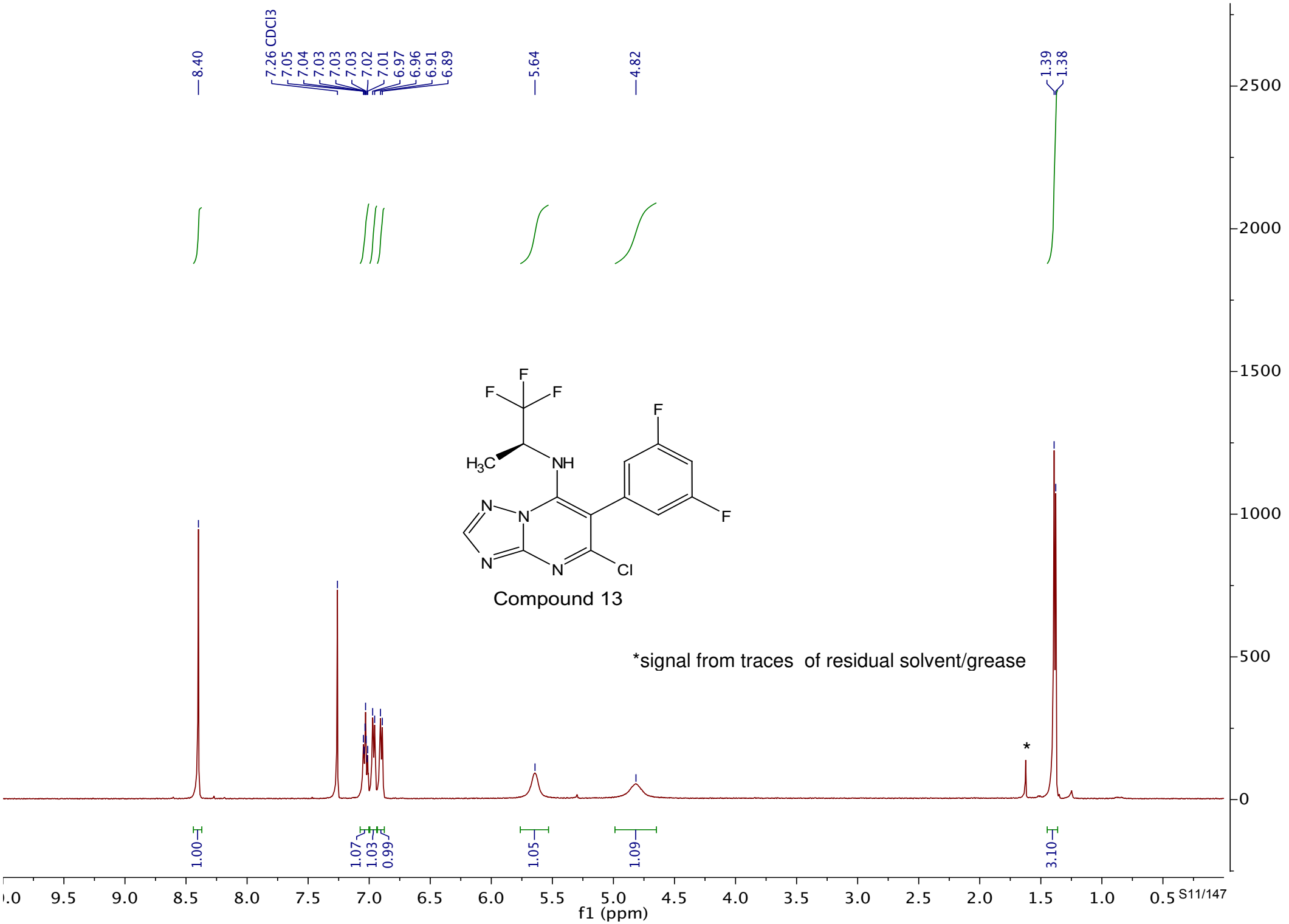
8.40
7.26 CDCl3
7.05
7.04
7.03
7.03
7.03
7.02
7.01
6.97
6.96
6.91
6.89
5.64
4.82
1.39
1.38
F
F
F
H3C
NH
F
N
N
N
N
Cl
Compound 13
*signal from traces of residual solvent/grease
*
1.00
1.07
1.03
0.99
1.05
1.09
3.10
2500
2000
1500
1000
500
0
f1 (ppm)
S11/147

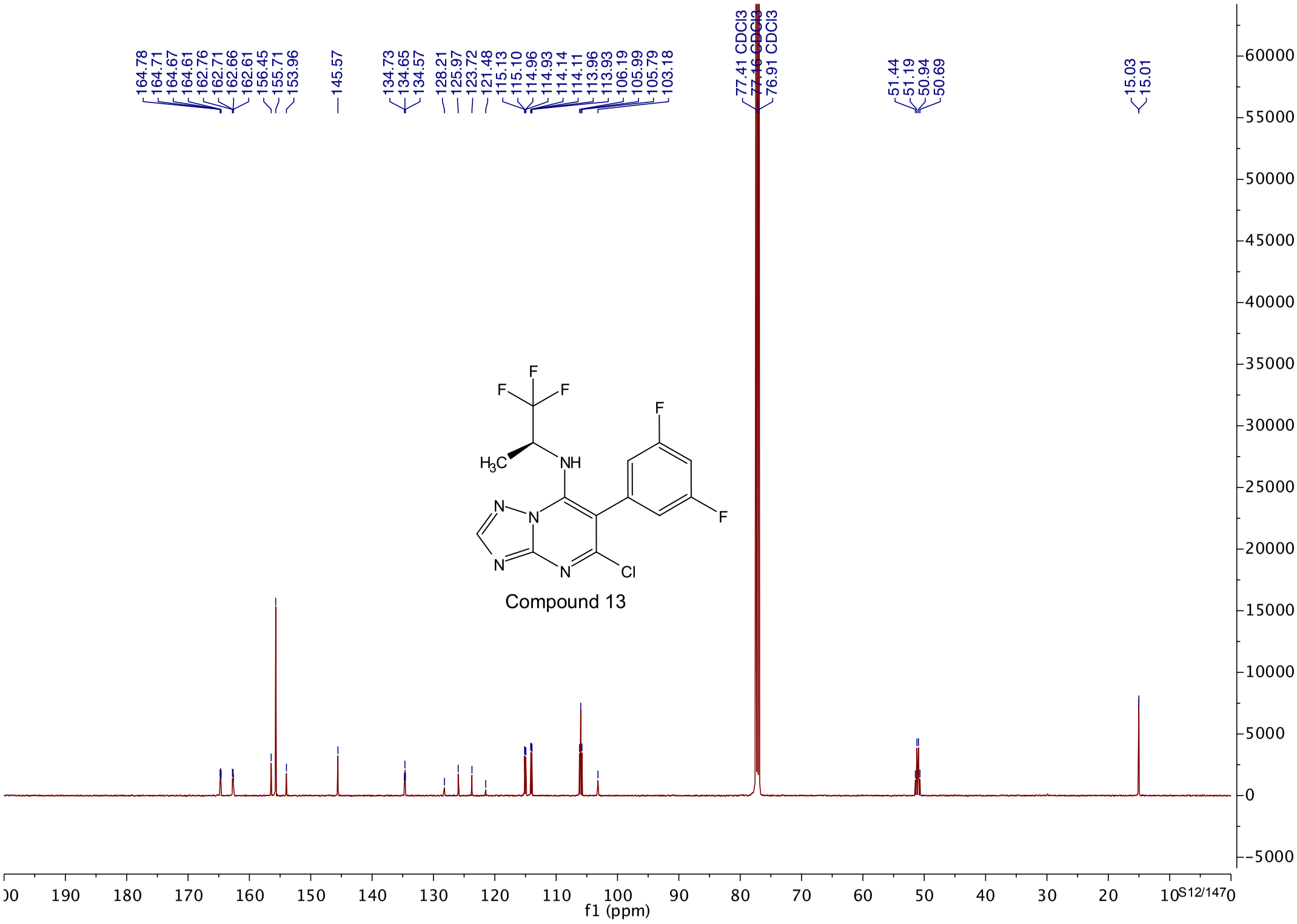
164.78
164.71
164.67
164.61
162.76
162.71
162.66
162.61
156.45
155.71
153.96
145.57
134.73
134.65
134.57
128.21
125.97
123.72
121.48
115.13
115.10
114.96
114.93
114.14
114.11
113.96
113.93
106.19
105.99
105.79
103.18
77.41 CDCl3
77.16 CDCl3
76.91 CDCl3
51.44
51.19
50.94
50.69
15.03
15.01
F
F
F
H3C
NH
F
N
N
N
N
Cl
Compound 13
60000
55000
50000
45000
40000
35000
30000
25000
20000
15000
10000
5000
0
-5000
190
180
170
160
150
140
130
120
110
100
90
80
70
60
50
40
30
20
10
f1 (ppm)

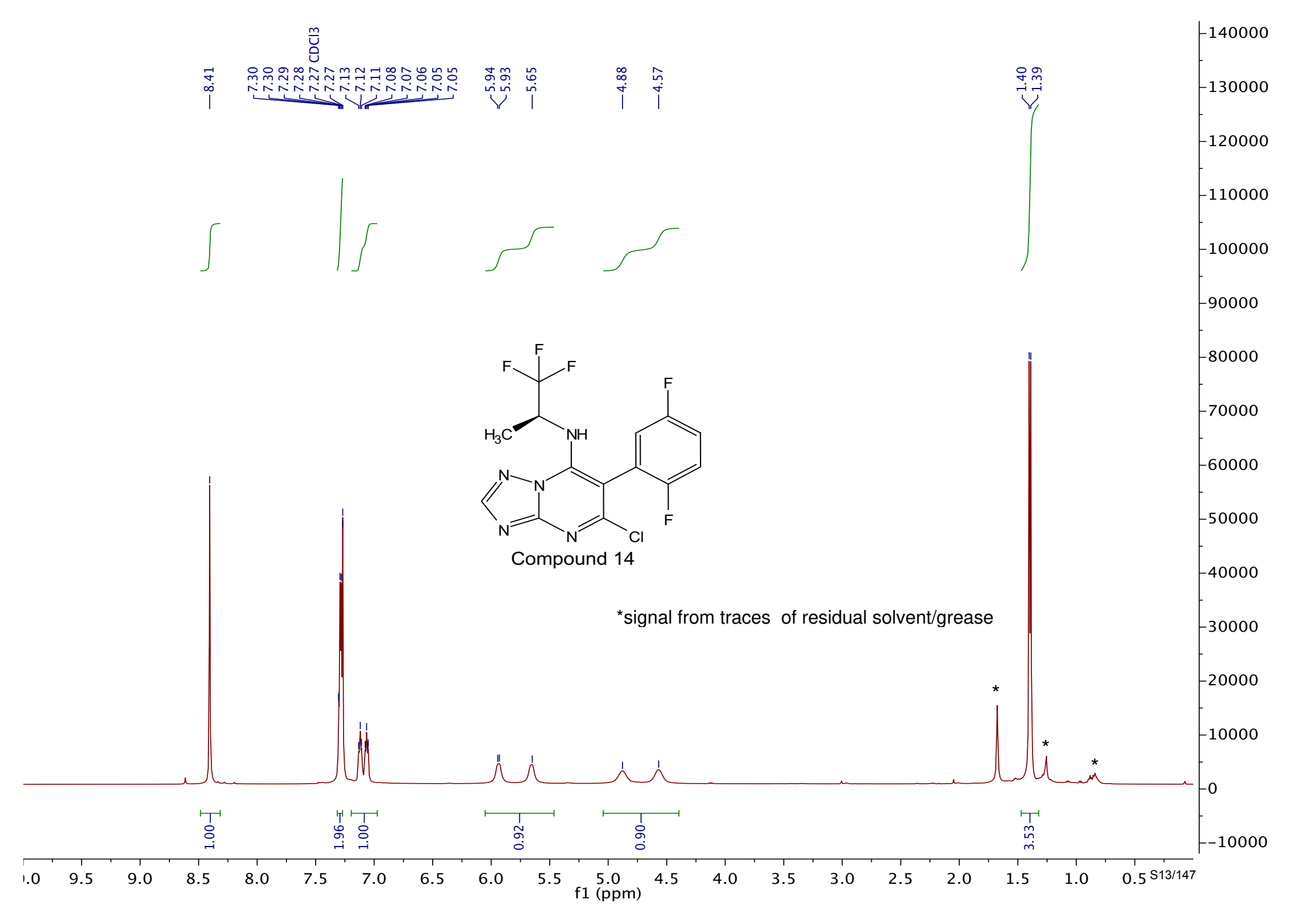
8.41
7.30
7.30
7.29
7.28
7.27 CDCl3
7.27
7.13
7.12
7.11
7.08
7.07
7.06
7.05
7.05
5.94
5.93
5.65
4.88
4.57
1.40
1.39
F
F
F
F
H3C
NH
N
N
N
N
Cl
Compound 14
*signal from traces of residual solvent/grease
1.00
1.96
1.00
0.92
0.90
3.53
f1 (ppm)

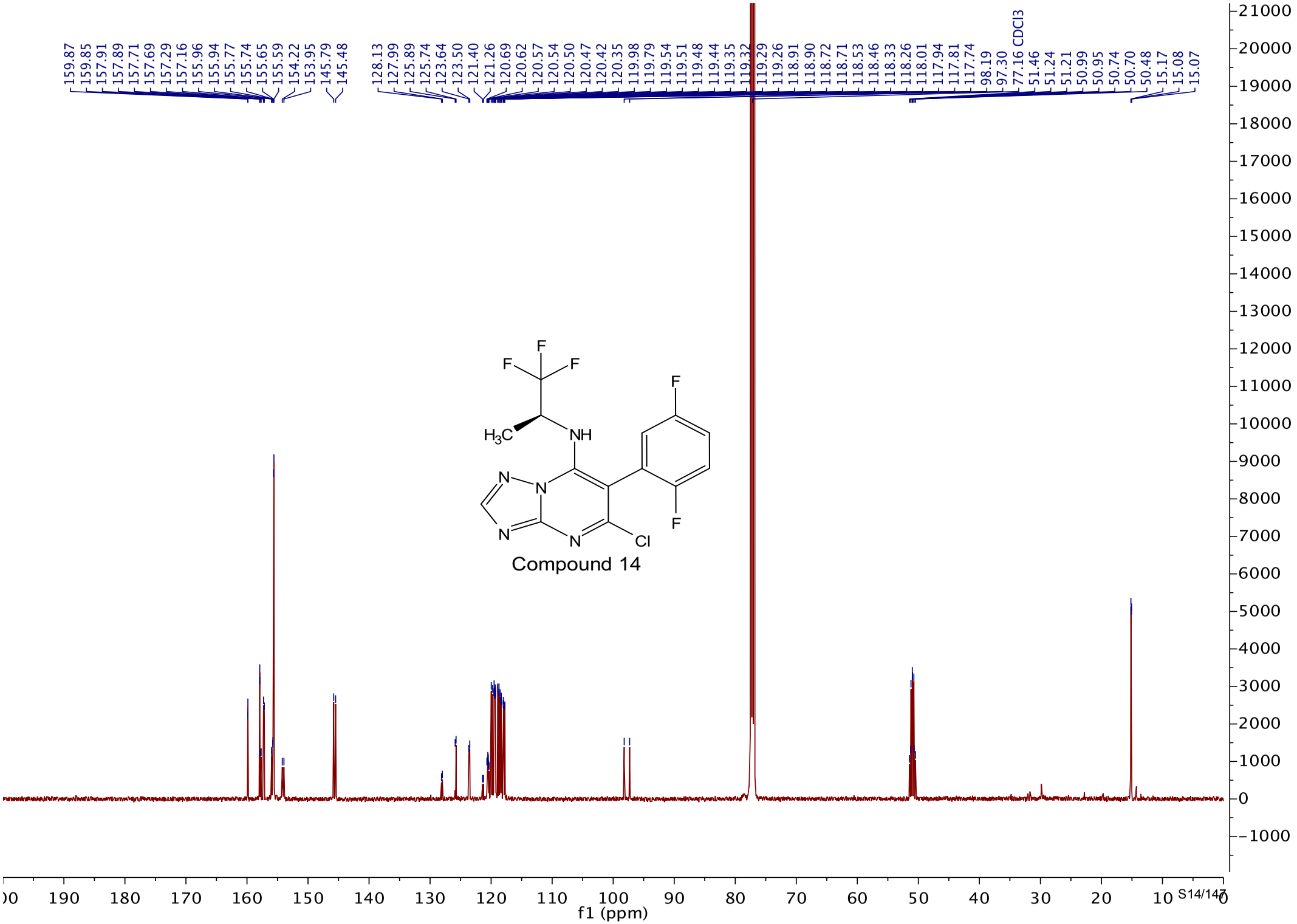
159.87
159.85
157.91
157.89
157.71
157.69
157.29
157.16
155.96
155.94
155.77
155.74
155.65
155.59
154.22
153.95
145.79
145.48
128.13
127.99
125.89
125.74
123.64
123.50
121.40
121.26
120.69
120.62
120.57
120.54
120.50
120.47
120.42
120.35
119.98
119.79
119.54
119.51
119.48
119.44
119.35
119.32
119.29
119.26
118.91
118.90
118.72
118.71
118.53
118.46
118.33
118.26
118.01
117.94
117.81
117.74
98.19
97.30
77.16 CDCl3
51.46
51.24
51.21
50.99
50.95
50.74
50.70
50.48
15.17
15.08
15.07
F
F
F
F
H3C
NH
N
N
N
N
Cl
F
Compound 14
21000
20000
19000
18000
17000
16000
15000
14000
13000
12000
11000
10000
9000
8000
7000
6000
5000
4000
3000
2000
1000
0
-1000
190
180
170
160
150
140
130
120
110
100
90
80
70
60
50
40
30
20
10
0
f1 (ppm)

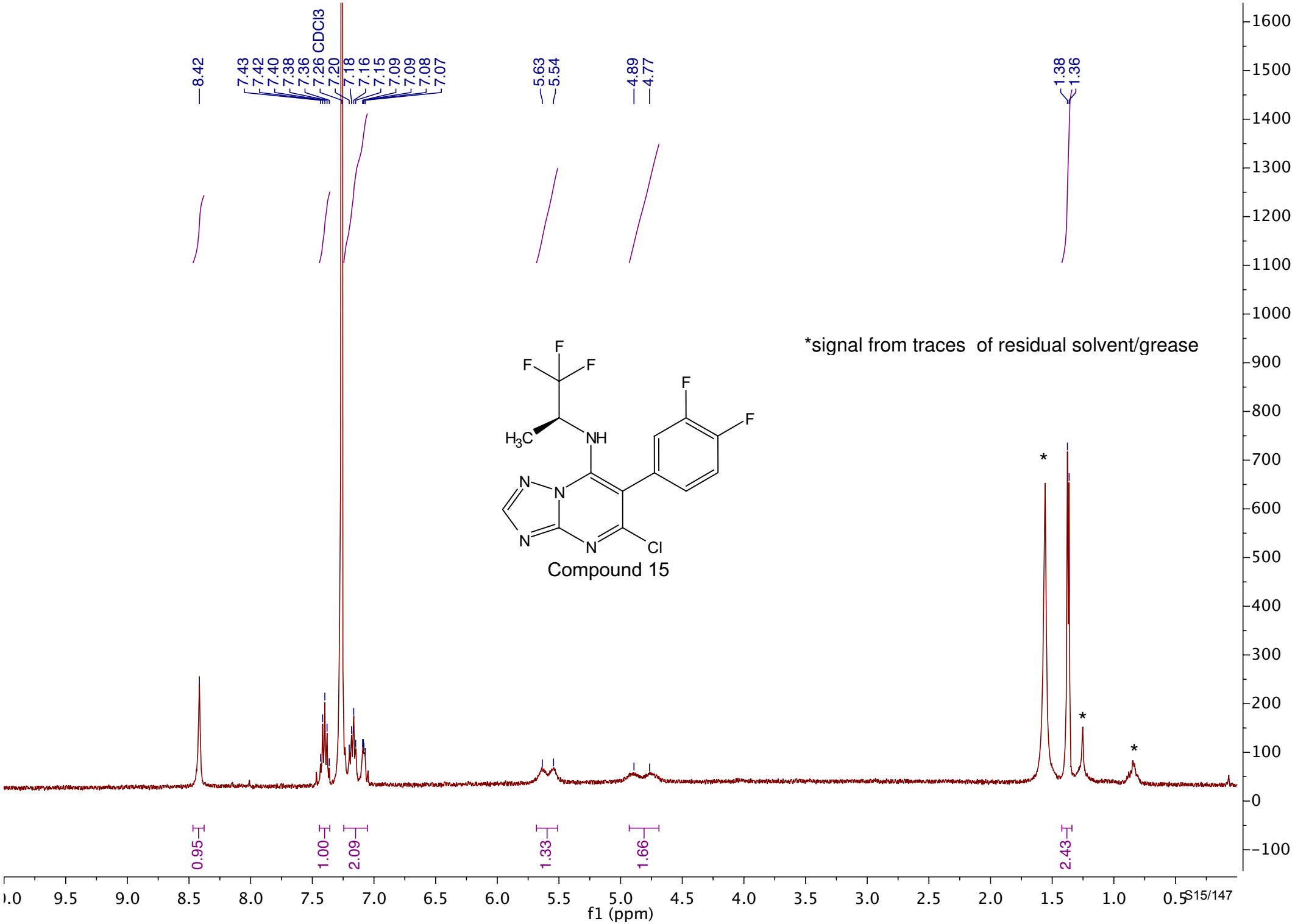
8.42
7.43
7.42
7.40
7.38
7.36
CDCl3
7.26
7.20
7.18
7.16
7.15
7.09
7.09
7.08
7.07
5.63
5.54
4.89
4.77
1.38
1.36
*signal from traces of residual solvent/grease
Compound 15
0.95
1.00
2.09
1.33
1.66
2.43
f1 (ppm)
S15/147

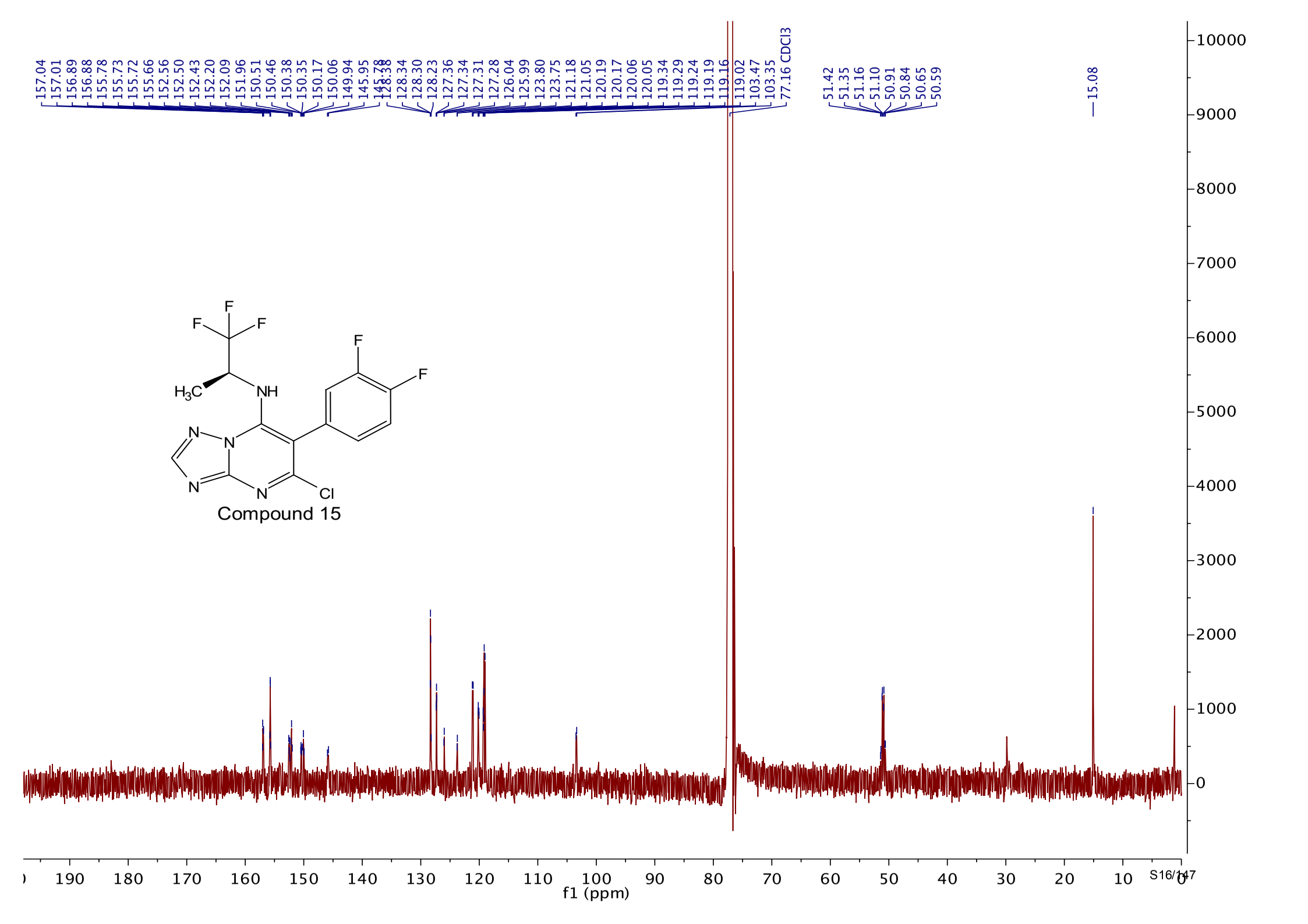
157.04
157.01
156.89
156.88
155.78
155.73
155.72
155.66
152.56
152.50
152.43
152.20
152.09
151.96
150.51
150.46
150.38
150.35
150.17
150.06
149.94
145.95
128.34
128.30
128.23
127.36
127.34
127.31
127.28
126.04
125.99
123.80
123.75
121.18
121.05
120.19
120.17
120.06
120.05
119.34
119.29
119.24
119.19
119.16
119.02
103.47
103.35
77.16 CDCl3
51.42
51.35
51.16
51.10
50.91
50.84
50.65
50.59
15.08
F
F
F
F
F
H3C
NH
N
N
N
N
Cl
Compound 15
10000
9000
8000
7000
6000
5000
4000
3000
2000
1000
0
190
180
170
160
150
140
130
120
110
100
90
80
70
60
50
40
30
20
10
0
f1 (ppm)
S16/147

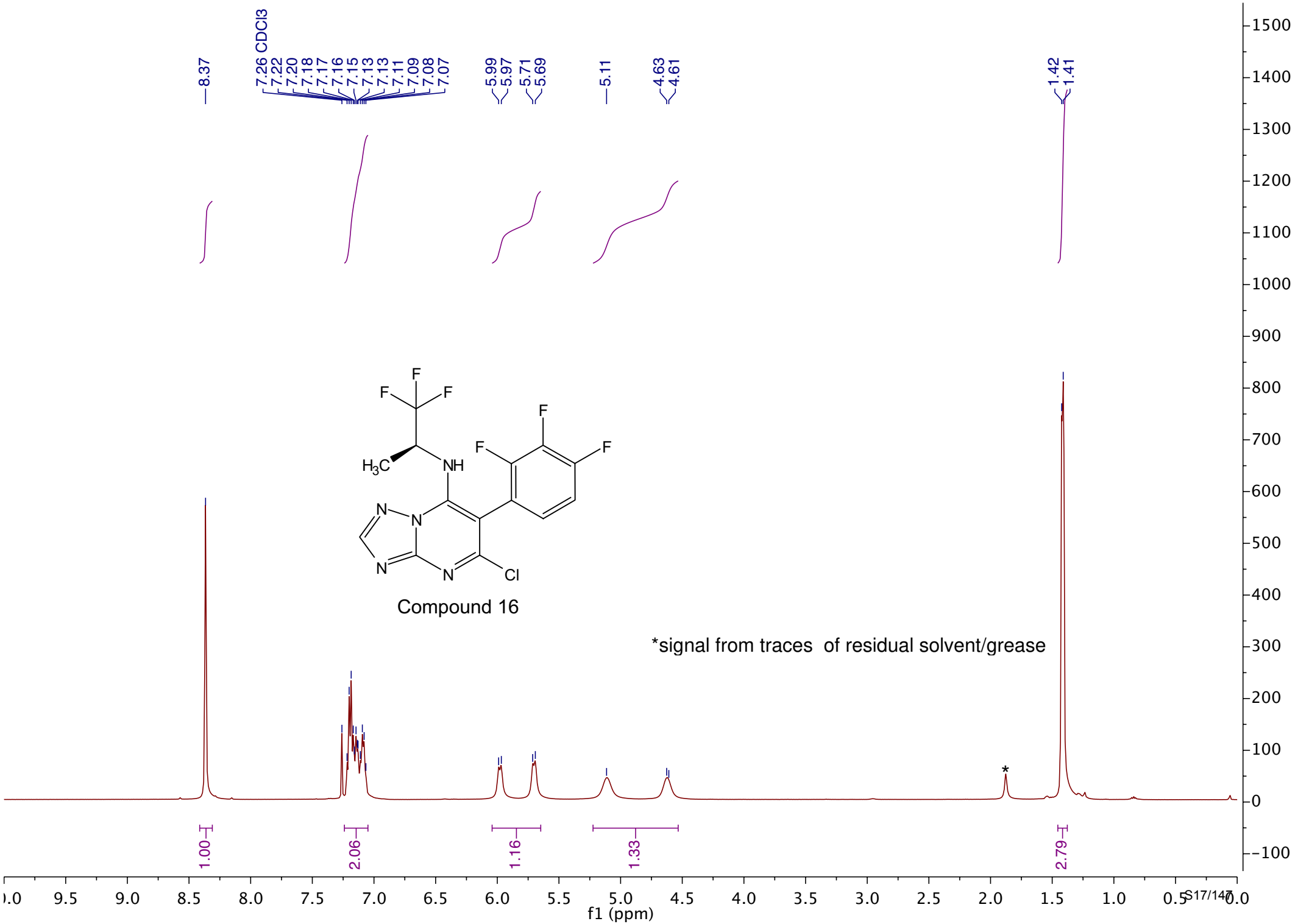
7.26 CDCl3
8.37
7.22
7.20
7.18
7.17
7.16
7.15
7.13
7.13
7.11
7.09
7.08
7.07
5.99
5.97
5.71
5.69
5.11
4.63
4.61
1.42
1.41
F
F
F
H3C
NH
F
F
F
N
N
N
N
Cl
Compound 16
*signal from traces of residual solvent/grease
1.00
2.06
1.16
1.33
2.79
f1 (ppm)
S17/147

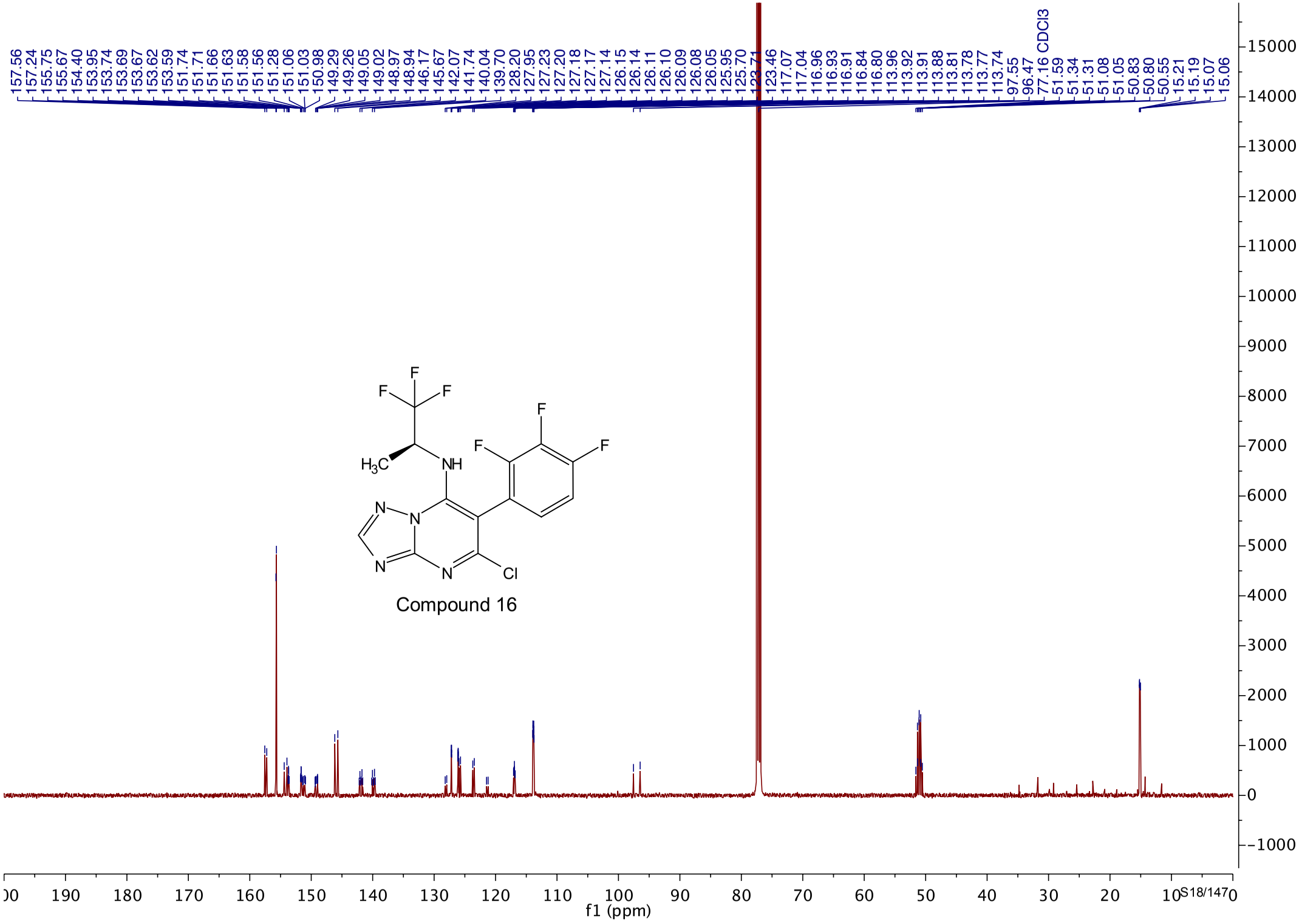
157.56
157.24
155.75
155.67
154.40
153.95
153.74
153.69
153.67
153.62
153.59
151.74
151.71
151.66
151.63
151.58
151.56
151.28
151.06
151.03
150.98
149.29
149.26
149.05
149.02
148.97
148.94
146.17
145.67
142.07
141.74
140.04
139.70
128.20
127.95
127.23
127.20
127.18
127.17
127.14
126.15
126.14
126.11
126.10
126.09
126.08
126.05
125.95
125.70
123.71
123.46
117.07
117.04
116.96
116.93
116.91
116.84
116.80
113.96
113.92
113.91
113.88
113.81
113.78
113.77
113.74
97.55
96.47
77.16 CDCl3
51.59
51.34
51.31
51.08
51.05
50.83
50.80
50.55
15.21
15.19
15.07
15.06
F
F
F
F
F
F
H3C
NH
N
N
N
N
Cl
Compound 16
15000
14000
13000
12000
11000
10000
9000
8000
7000
6000
5000
4000
3000
2000
1000
0
-1000
190
180
170
160
150
140
130
120
110
100
90
80
70
60
50
40
30
20
10
f1 (ppm)
S18/147

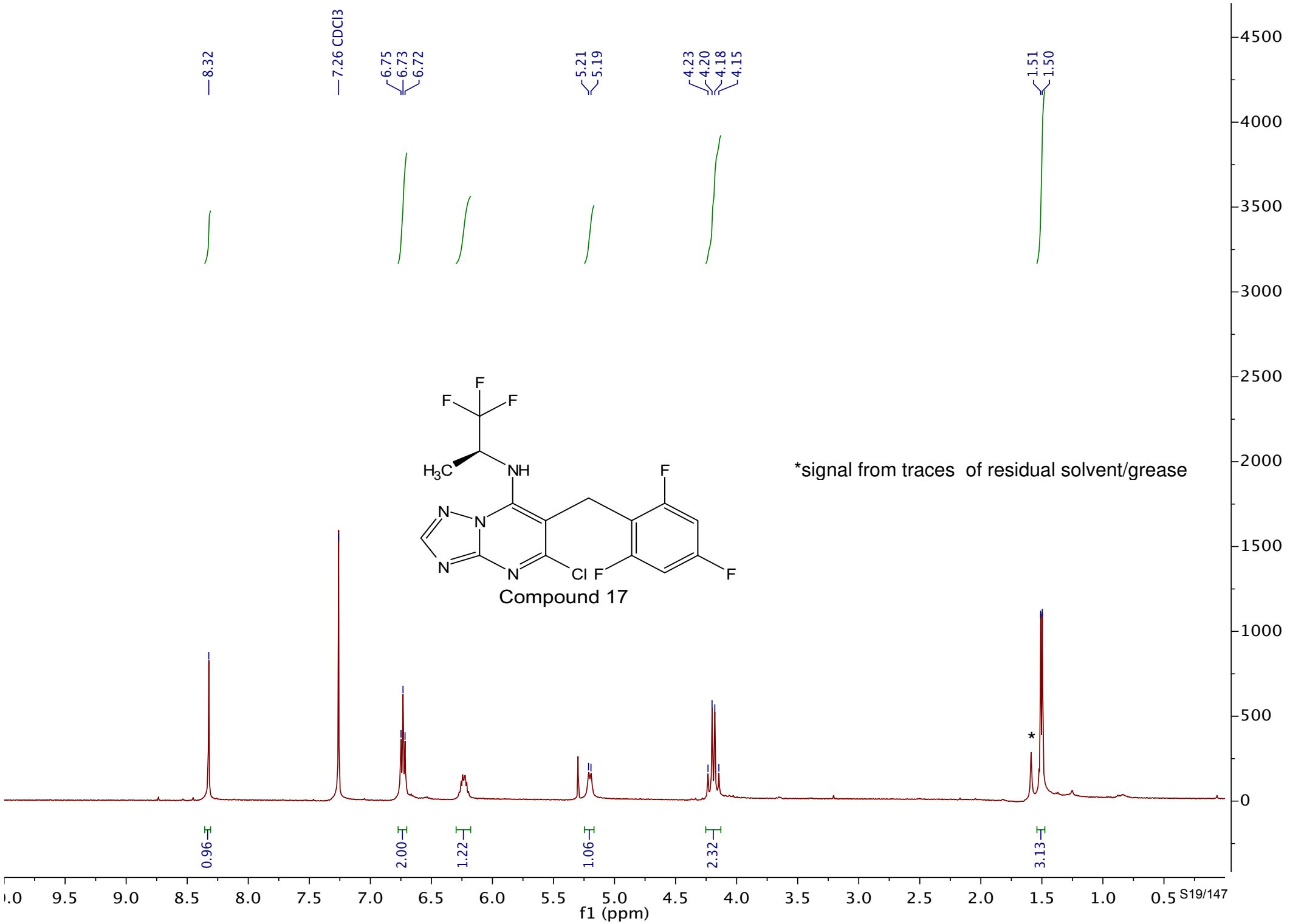
8.32
7.26 CDCl3
6.75
6.73
6.72
5.21
5.19
4.23
4.20
4.18
4.15
1.51
1.50
F
F
F
H3C
NH
F
N
N
N
N
Cl F
F
Compound 17
*signal from traces of residual solvent/grease
0.96
2.00
1.22
1.06
2.32
3.13
f1 (ppm)
S19/147

Compound 17
f1 (ppm)
S20/147
163.34
163.22
163.09
162.62
162.56
162.54
162.51
162.47
162.44
162.42
162.36
161.35
161.22
161.09
160.59
160.57
160.54
160.50
160.47
160.45
160.39
157.44
157.37
155.49
155.43
154.46
154.40
146.56
146.49
128.51
126.33
126.26
124.02
121.78
108.57
108.55
108.51
108.46
108.42
108.40
108.36
108.31
108.25
108.21
101.31
101.29
101.25
101.23
101.19
101.11
101.09
101.07
101.04
101.02
101.00
100.92
100.88
100.86
100.82
100.80
100.79
100.73
77.16 CDCl3
52.26
52.19
52.01
51.94
51.76
51.69
51.44
21.11
21.05
15.36
15.34
15.29
15.28

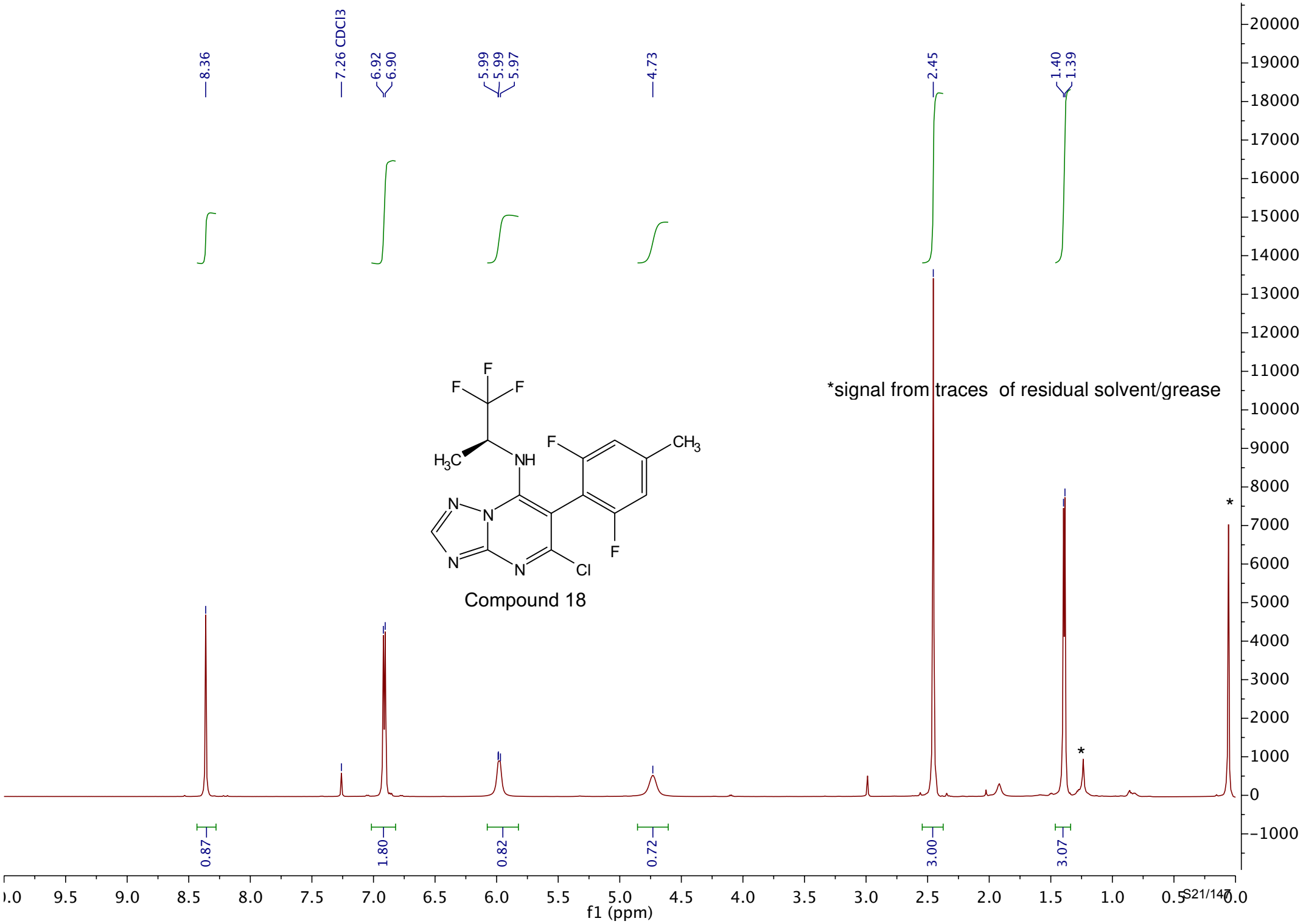
8.36
7.26 CDCl3
6.92
6.90
5.99
5.99
5.97
4.73
2.45
1.40
1.39
F
F
F
H3C
NH
F
CH3
N
N
N
N
Cl
F
*signal from traces of residual solvent/grease
Compound 18
0.87
1.80
0.82
0.72
3.00
3.07
f1 (ppm)
S21/147

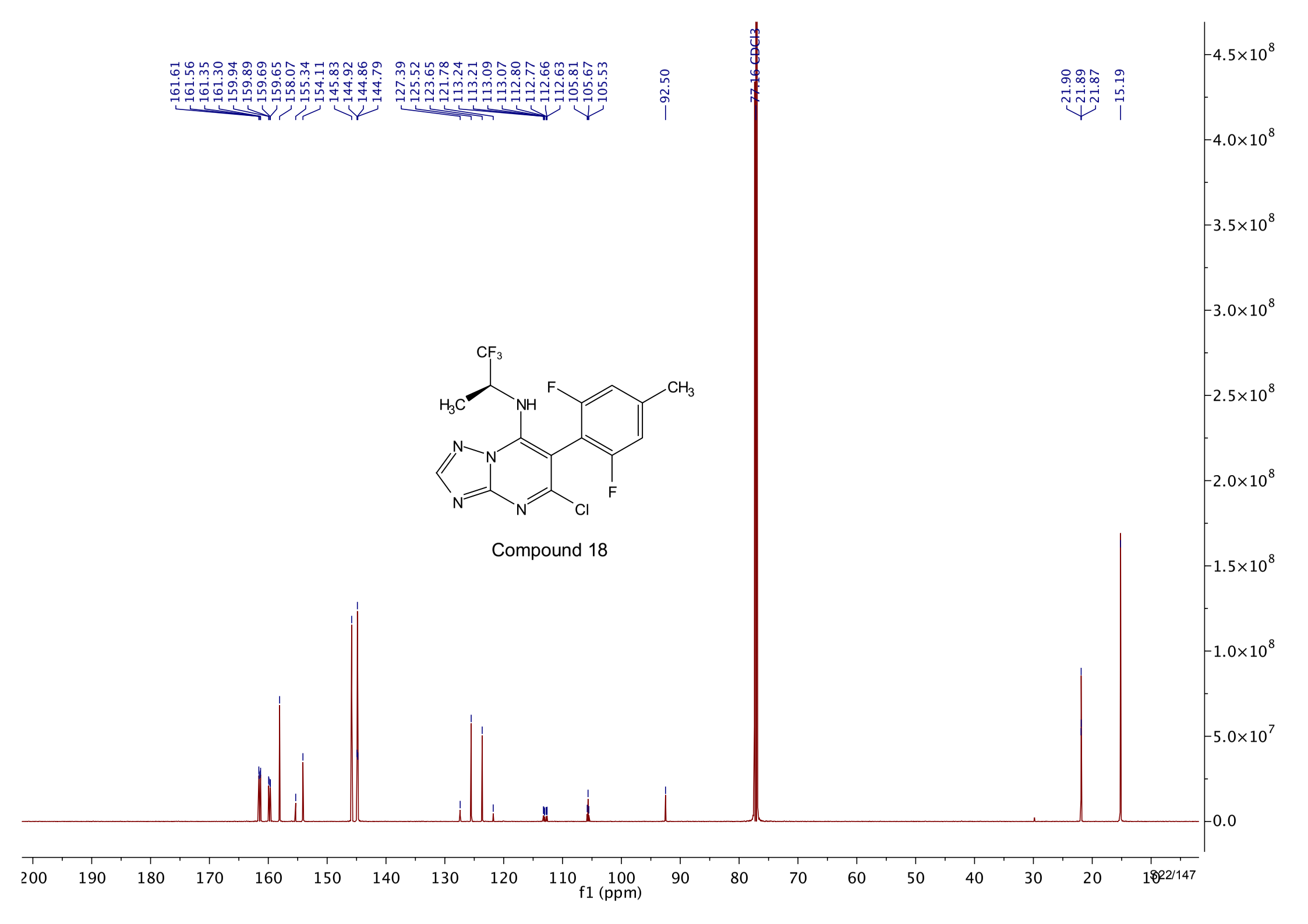
161.61
161.56
161.35
161.30
159.94
159.89
159.69
159.65
158.07
155.34
154.11
145.83
144.92
144.86
144.79
127.39
125.52
123.65
121.78
113.24
113.21
113.09
113.07
112.80
112.77
112.66
112.63
105.81
105.67
105.53
92.50
77.16 CDCl3
21.90
21.89
21.87
15.19
CF3
H3C
NH
F
CH3
N
N
N
N
Cl
F
Compound 18
4.5×10^8
4.0×10^8
3.5×10^8
3.0×10^8
2.5×10^8
2.0×10^8
1.5×10^8
1.0×10^8
5.0×10^7
0.0
200
190
180
170
160
150
140
130
120
110
100
90
80
70
60
50
40
30
20
10
f1 (ppm)

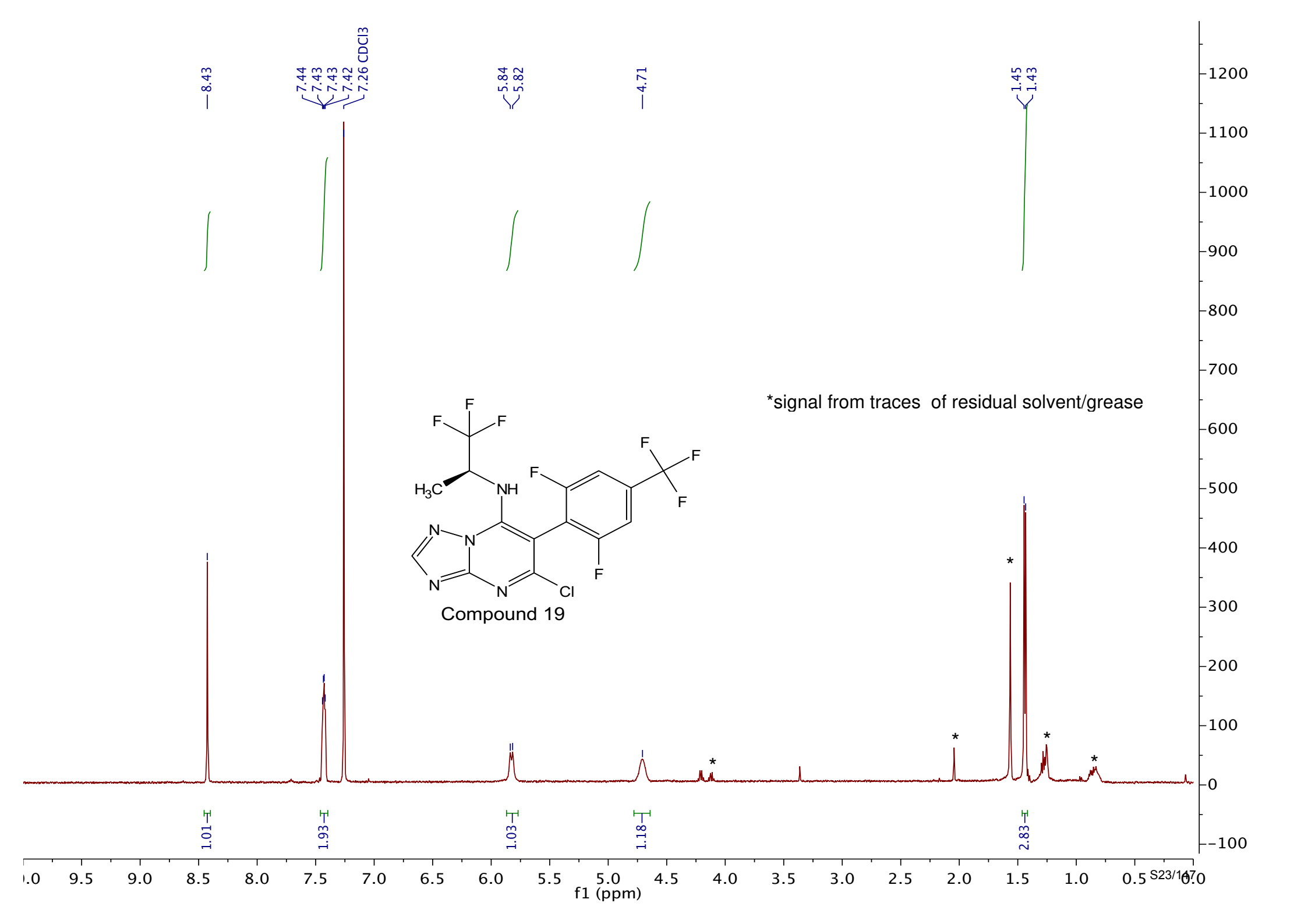
8.43
7.44
7.43
7.43
7.42
7.26 CDCl3
5.84
5.82
4.71
1.45
1.43
*signal from traces of residual solvent/grease
Compound 19
1.01
1.93
1.03
1.18
2.83
f1 (ppm)

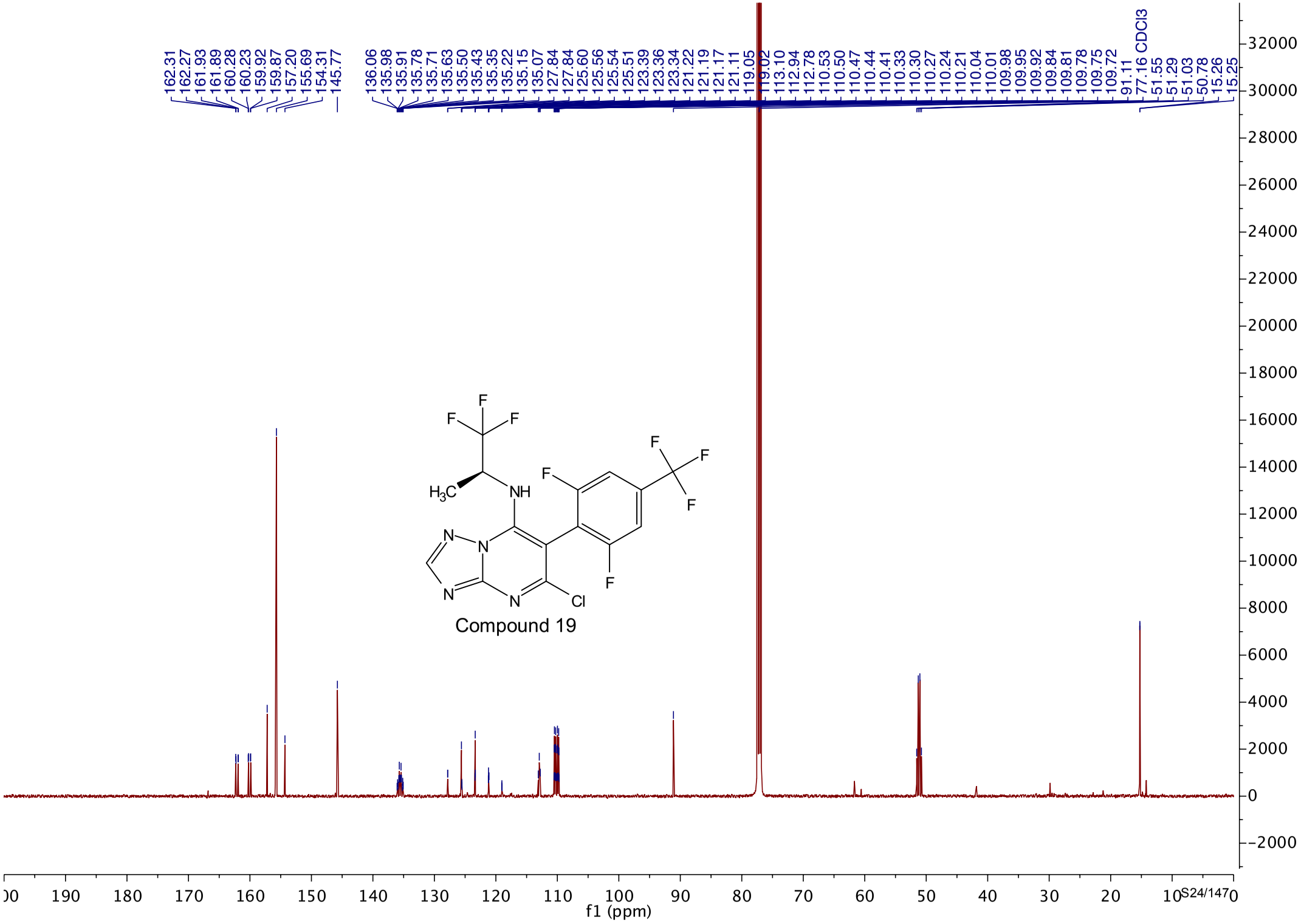
162.31
162.27
161.93
161.89
160.28
160.23
159.92
159.87
157.20
155.69
154.31
145.77
136.06
135.98
135.91
135.78
135.71
135.63
135.50
135.43
135.35
135.22
135.15
135.07
127.84
127.84
125.60
125.56
125.54
125.51
123.39
123.36
123.34
121.22
121.19
121.17
121.11
119.05
119.02
113.10
112.94
112.78
110.53
110.50
110.47
110.44
110.41
110.33
110.30
110.27
110.24
110.21
110.04
110.01
109.98
109.95
109.92
109.84
109.81
109.78
109.75
109.72
91.11
77.16 CDCl3
51.55
51.29
51.03
50.78
15.26
15.25
F
F
F
H3C
NH
N
N
N
N
Cl
F
F
F
F
Compound 19
32000
30000
28000
26000
24000
22000
20000
18000
16000
14000
12000
10000
8000
6000
4000
2000
0
-2000
190
180
170
160
150
140
130
120
110
100
90
80
70
60
50
40
30
20
10
f1 (ppm)

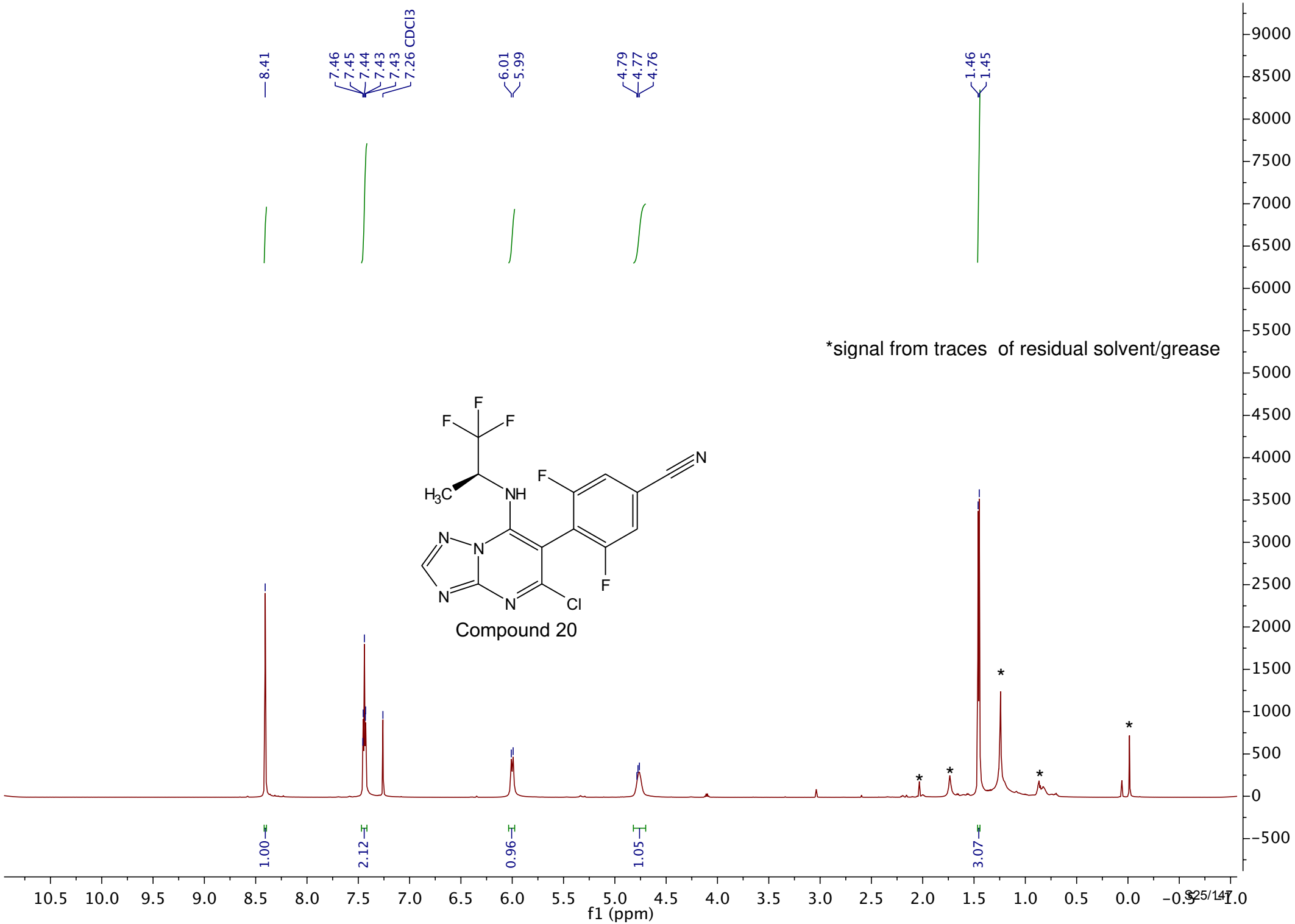
8.41
7.46
7.45
7.44
7.43
7.43
7.26 CDCl3
6.01
5.99
4.79
4.77
4.76
1.46
1.45
*signal from traces of residual solvent/grease
F
F
F
H3C
NH
F
N
N
N
N
N
Cl
F
Compound 20
1.00
2.12
0.96
1.05
3.07
f1 (ppm)

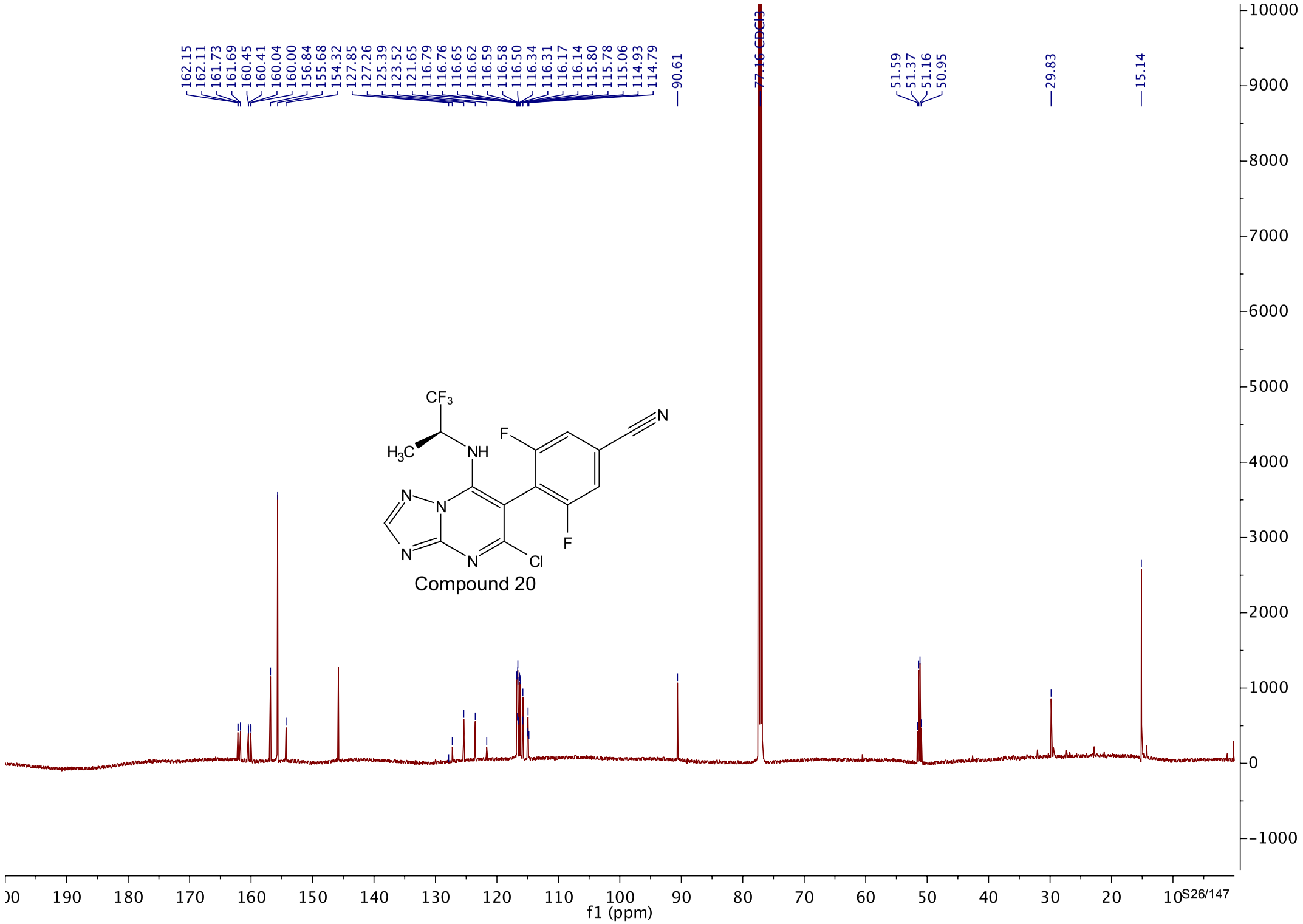
162.15
162.11
161.73
161.69
160.45
160.41
160.04
160.00
156.84
155.68
154.32
127.85
127.26
125.39
123.52
121.65
116.79
116.76
116.65
116.62
116.59
116.58
116.50
116.34
116.31
116.17
116.14
115.80
115.78
115.06
114.93
114.79
90.61
77.16 CDCl3
51.59
51.37
51.16
50.95
29.83
15.14
CF3
H3C
NH
F
N
N
N
N
Cl
F
Compound 20
10000
9000
8000
7000
6000
5000
4000
3000
2000
1000
0
-1000
f1 (ppm)

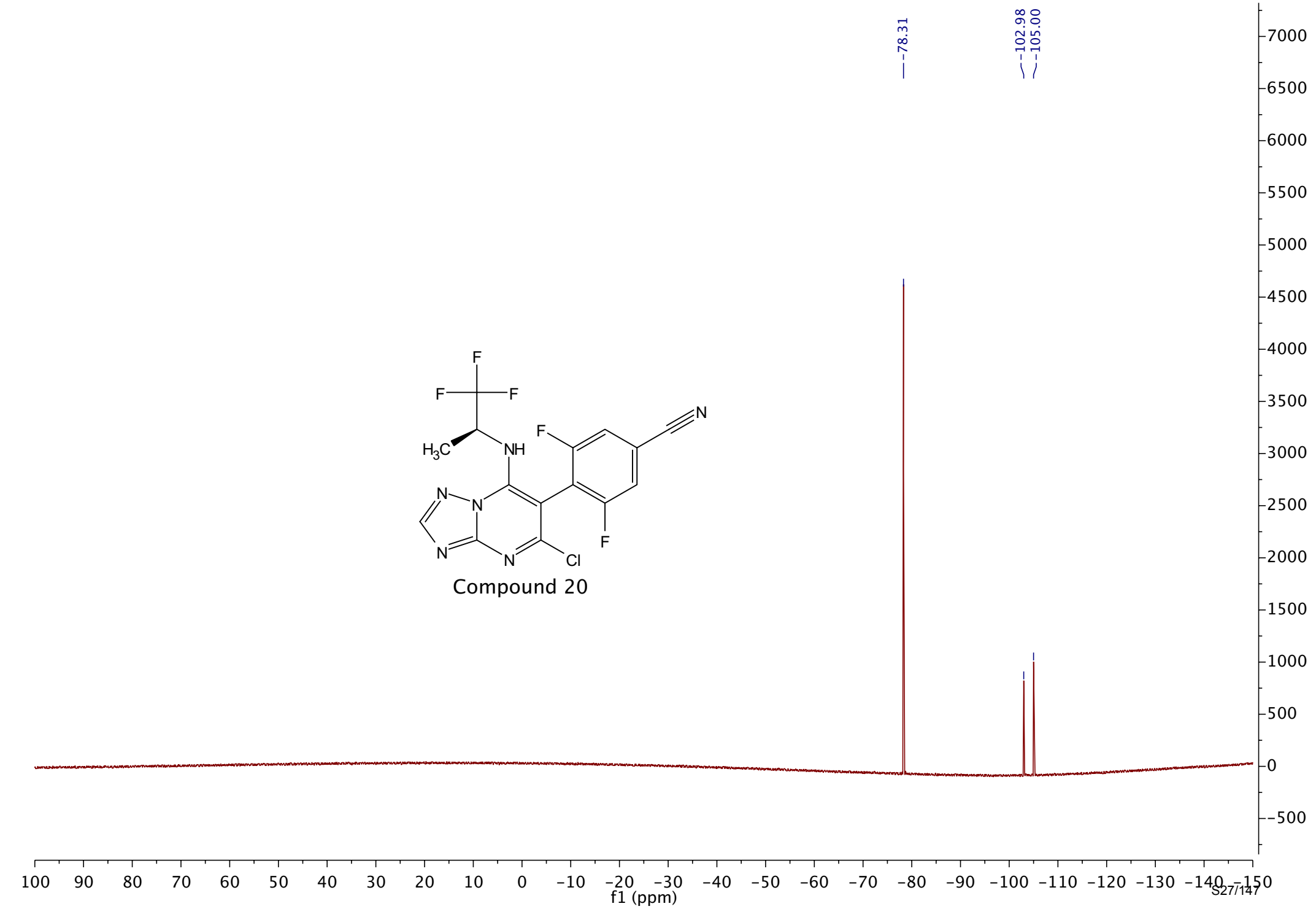
-78.31
-102.98
-105.00
7000
6500
6000
5500
5000
4500
4000
3500
3000
2500
2000
1500
1000
500
0
-500
100 90 80 70 60 50 40 30 20 10 0 -10 -20 -30 -40 -50 -60 -70 -80 -90 -100 -110 -120 -130 -140 -150
f1 (ppm)
F
F
F
H3C
NH
F
N
N
N
N
Cl
F
N

Compound 20

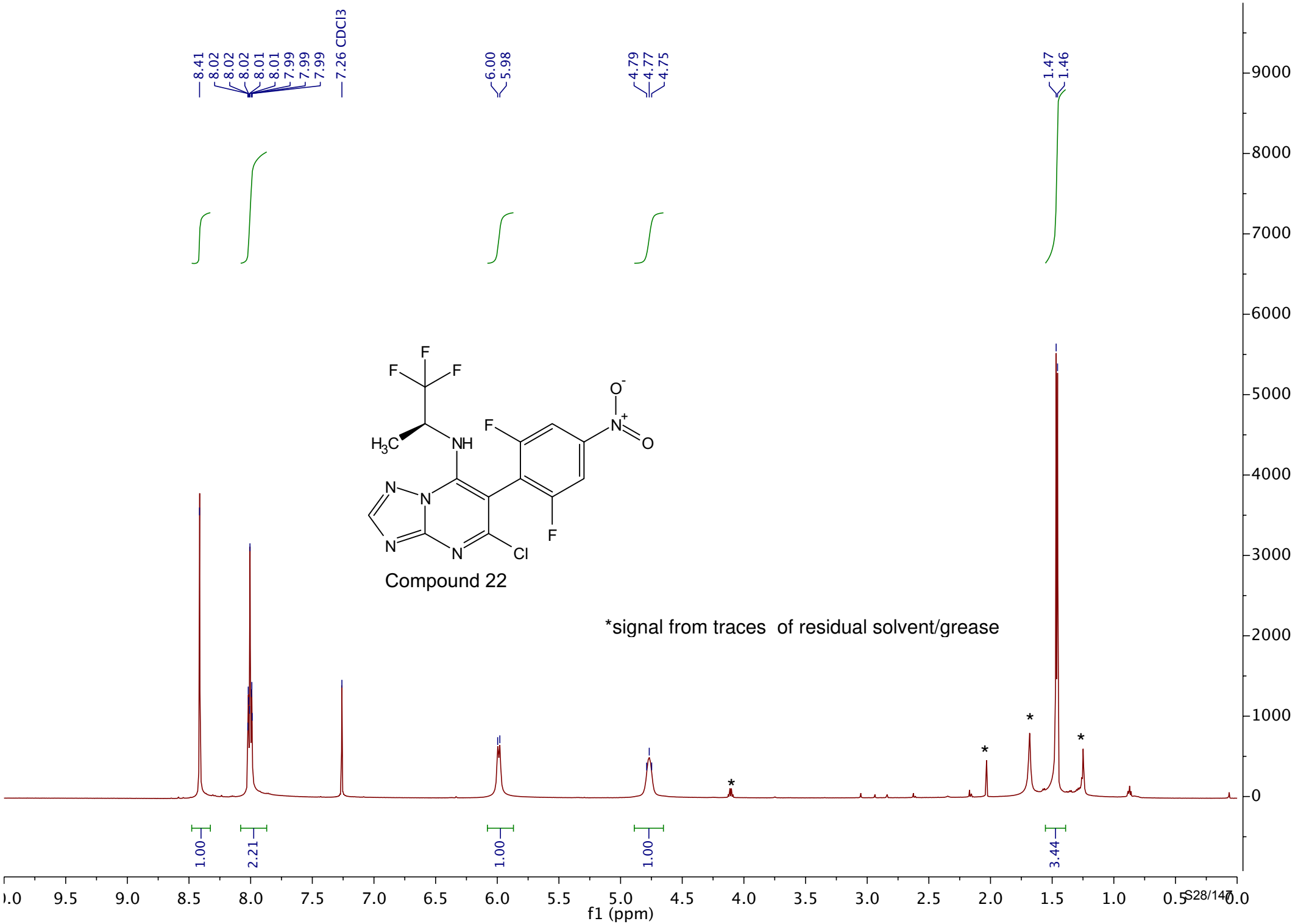
8.41
8.02
8.02
8.02
8.01
8.01
7.99
7.99
7.99
7.26 CDCl3
6.00
5.98
4.79
4.77
4.75
1.47
1.46
F
F
F
H3C
NH
N
N
N
N
Cl
F
F
O-
N+
O
Compound 22
*signal from traces of residual solvent/grease
1.00
2.21
1.00
1.00
3.44
f1 (ppm)

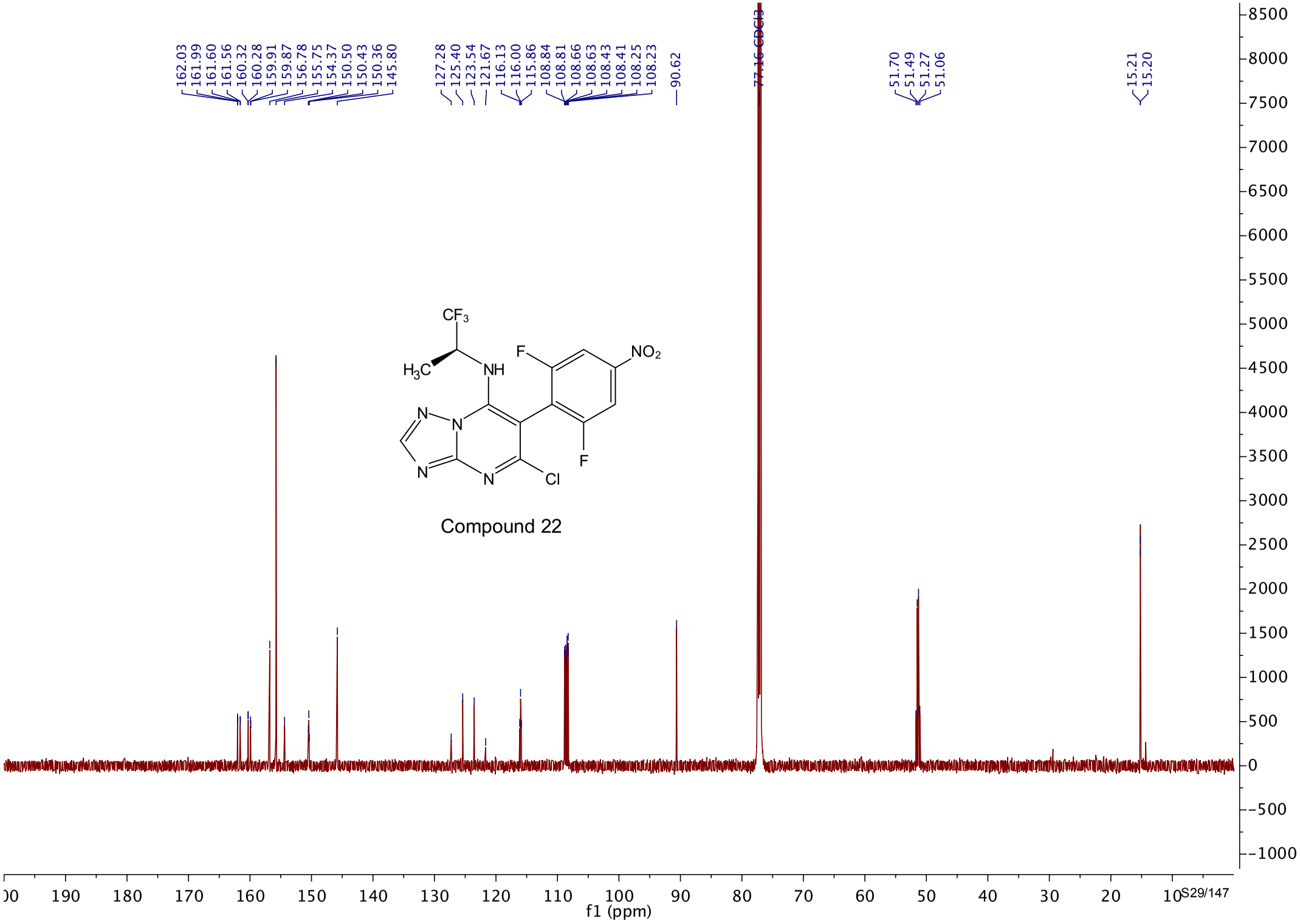
162.03
161.99
161.60
161.56
160.32
160.28
159.91
159.87
156.78
155.75
154.37
150.50
150.43
150.36
145.80
127.28
125.40
123.54
121.67
116.13
116.00
115.86
108.84
108.81
108.66
108.63
108.43
108.41
108.25
108.23
90.62
77.16 CDCl3
51.70
51.49
51.27
51.06
15.21
15.20
CF3
H3C
NH
F
NO2
N
N
N
N
Cl
F
Compound 22
8500
8000
7500
7000
6500
6000
5500
5000
4500
4000
3500
3000
2500
2000
1500
1000
500
0
-500
-1000
190
180
170
160
150
140
130
120
110
100
90
80
70
60
50
40
30
20
10
f1 (ppm)
S29/147

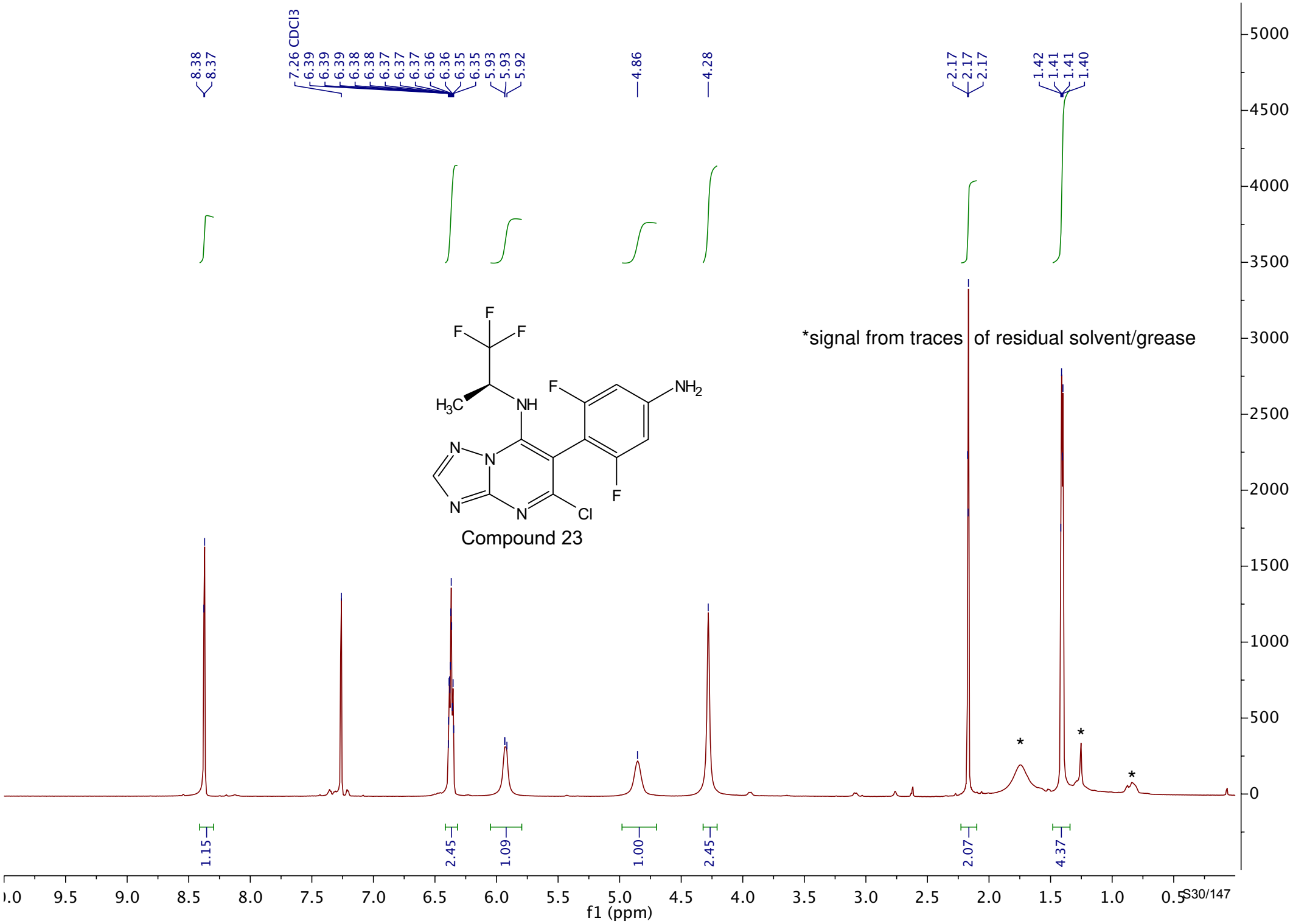
8.38
8.37
7.26 CDCl3
6.39
6.39
6.39
6.38
6.38
6.37
6.37
6.37
6.36
6.36
6.35
6.35
5.93
5.93
5.92
4.86
4.28
2.17
2.17
2.17
1.42
1.41
1.41
1.40
F
F
F
H3C
NH
F
NH2
N
N
N
N
Cl
F
Compound 23
*signal from traces of residual solvent/grease
1.15
2.45
1.09
1.00
2.45
2.07
4.37
f1 (ppm)
S30/147

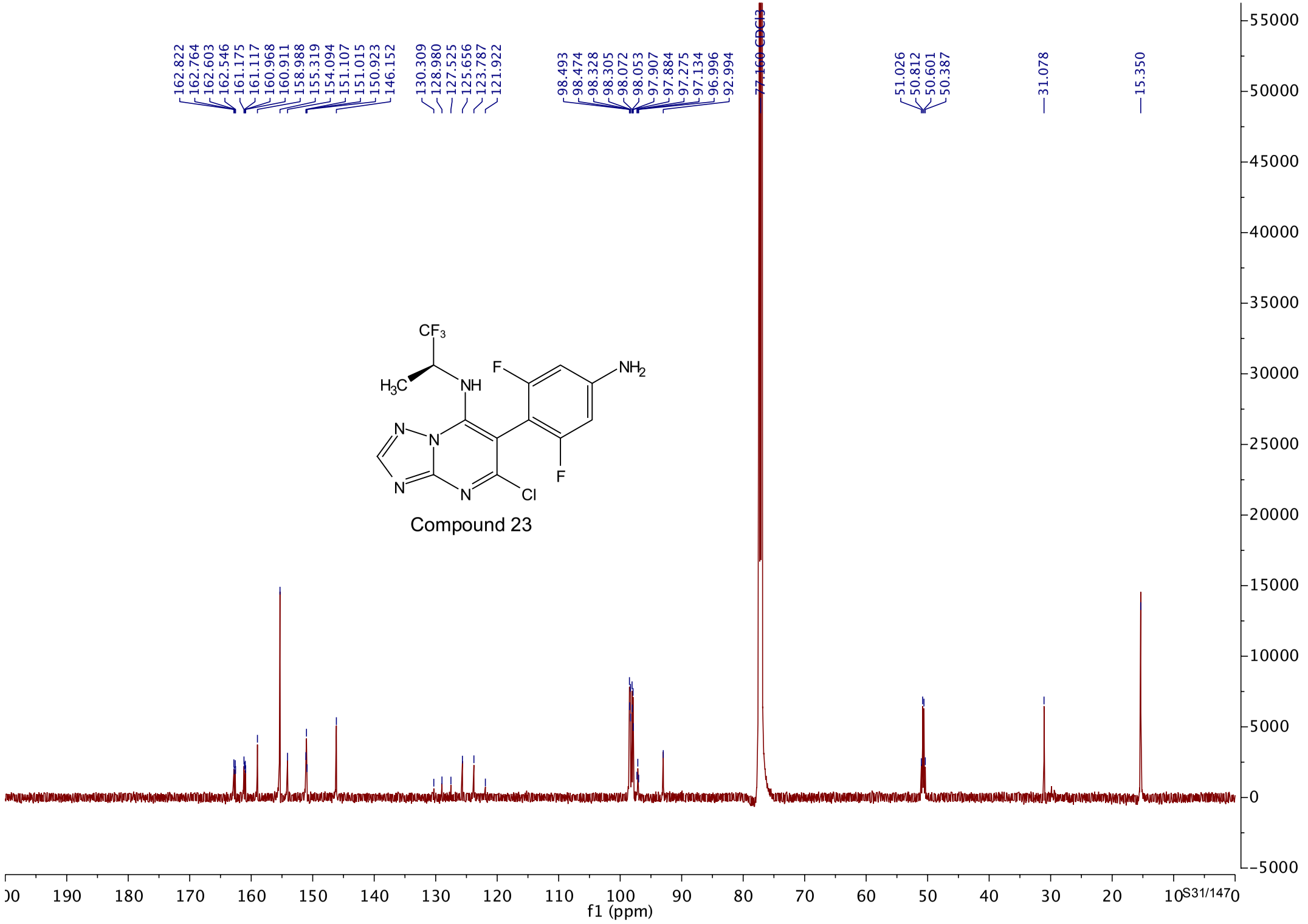
162.822
162.764
162.603
162.546
161.175
161.117
160.968
160.911
158.988
155.319
154.094
151.107
151.015
150.923
146.152
130.309
128.980
127.525
125.656
123.787
121.922
98.493
98.474
98.328
98.305
98.072
98.053
97.907
97.884
97.275
97.134
96.996
92.994
77.160 CDCl3
51.026
50.812
50.601
50.387
31.078
15.350
CF3
H3C
NH
F
NH2
N
N
N
N
Cl
F
Compound 23
55000
50000
45000
40000
35000
30000
25000
20000
15000
10000
5000
0
-5000
190
180
170
160
150
140
130
120
110
100
90
80
70
60
50
40
30
20
10
f1 (ppm)
S31/147

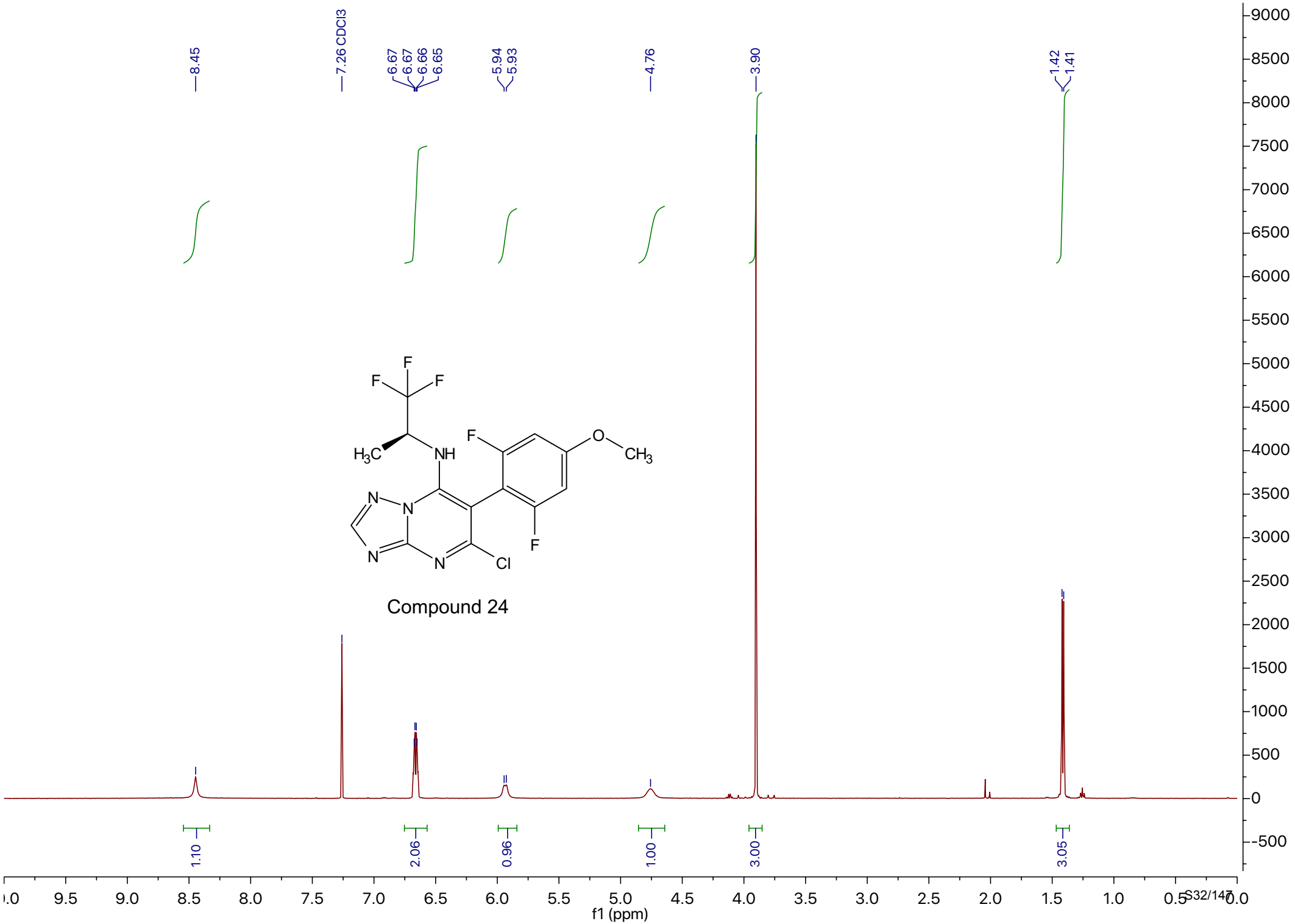
8.45
7.26 CDCl3
6.67
6.67
6.66
6.65
5.94
5.93
4.76
3.90
1.42
1.41
F
F
F
H3C
NH
F
O
CH3
N
N
N
N
Cl
F
Compound 24
1.10
2.06
0.96
1.00
3.00
3.05
f1 (ppm)

Compound 24
163.60
163.49
163.38
162.84
162.77
162.57
162.50
160.85
160.78
160.60
160.53
159.72
159.40
158.80
155.09
146.16
128.00
125.76
123.52
121.27
100.79
100.63
100.46
99.17
99.14
98.97
98.94
98.92
98.74
98.71
92.71
77.16 CDCl3
56.30
51.25
51.00
50.74
50.49
15.32
15.31
f1 (ppm)
S33/147

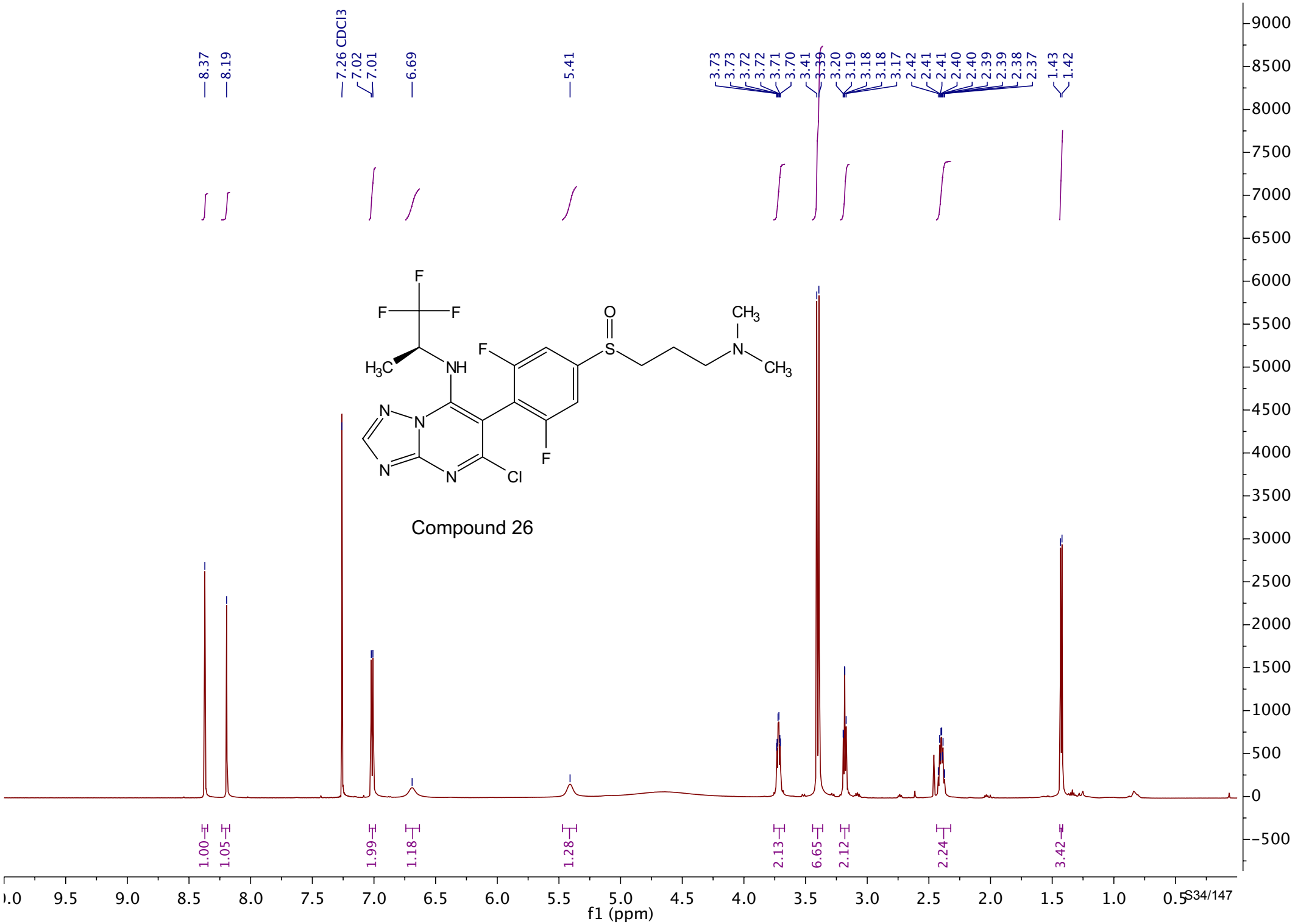
8.37
8.19
7.26 CDCl3
7.02
7.01
6.69
5.41
3.73
3.73
3.72
3.72
3.71
3.70
3.41
3.39
3.20
3.19
3.18
3.18
3.17
2.42
2.41
2.41
2.40
2.40
2.39
2.39
2.38
2.37
1.43
1.42
F
F
F
H3C
NH
F
O
S
CH3
N
CH3
N
N
N
N
Cl
F
Compound 26
1.00
1.05
1.99
1.18
1.28
2.13
6.65
2.12
2.24
3.42
f1 (ppm)
S34/147

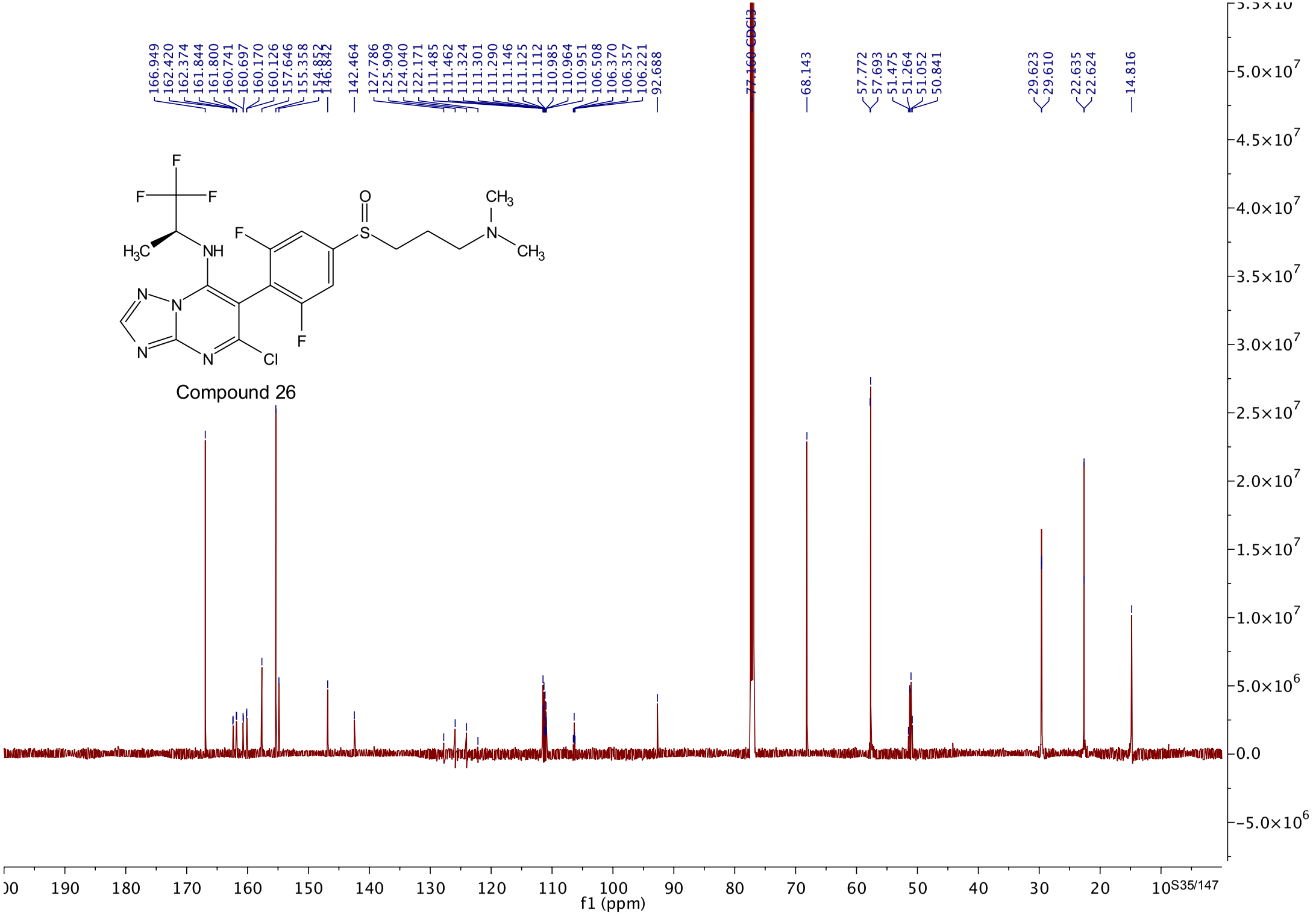
166.949
162.420
162.374
161.844
161.800
160.741
160.697
160.170
160.126
157.646
155.358
154.852
154.842
146.842
142.464
127.786
125.909
124.040
122.171
111.485
111.462
111.324
111.301
111.290
111.146
111.125
111.112
110.985
110.964
110.951
106.508
106.370
106.357
106.221
92.688
77.160 CDCl3
68.143
57.772
57.693
51.475
51.264
51.052
50.841
29.623
29.610
22.635
22.624
14.816
F
F
F
H3C
NH
N
N
N
N
Cl
F
F
O
S
CH3
N
CH3
Compound 26
5.5×10^7
5.0×10^7
4.5×10^7
4.0×10^7
3.5×10^7
3.0×10^7
2.5×10^7
2.0×10^7
1.5×10^7
1.0×10^7
5.0×10^6
0.0
-5.0×10^6
190
180
170
160
150
140
130
120
110
100
90
80
70
60
50
40
30
20
10
f1 (ppm)

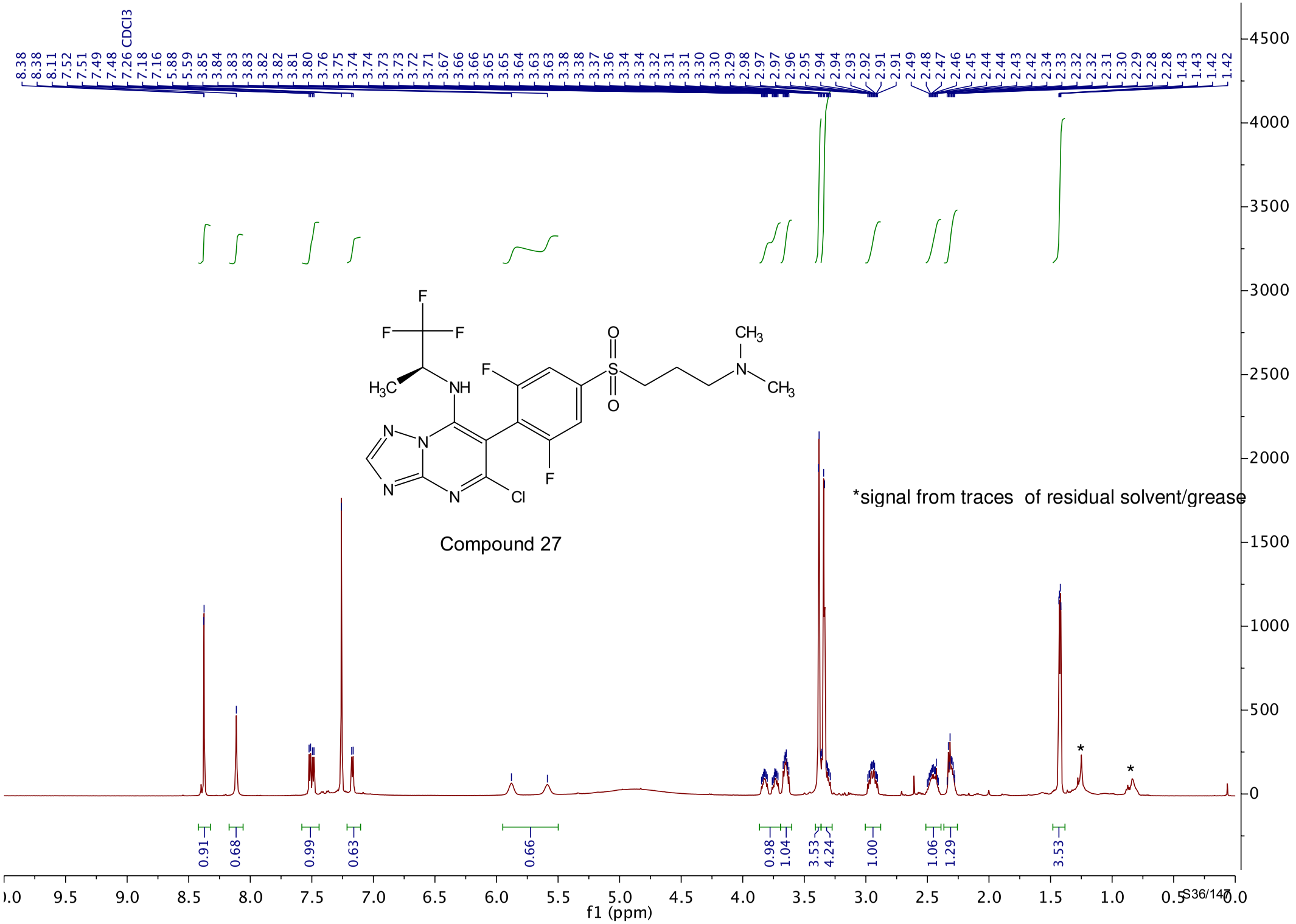
CDCl3
8.38 8.38 8.11 7.52 7.51 7.49 7.48 7.26 7.18 7.16 5.88 5.59 3.85 3.84 3.83 3.83 3.82 3.82 3.81 3.80 3.76 3.75 3.74 3.74 3.73 3.73 3.72 3.71 3.67 3.66 3.66 3.65 3.65 3.64 3.63 3.63 3.38 3.38 3.37 3.36 3.34 3.34 3.32 3.31 3.31 3.30 3.30 3.29 2.98 2.97 2.97 2.96 2.95 2.94 2.94 2.93 2.92 2.91 2.91 2.49 2.48 2.47 2.46 2.45 2.44 2.44 2.43 2.42 2.34 2.33 2.32 2.32 2.31 2.30 2.29 2.28 2.28 1.43 1.43 1.42 1.42
F
F
F
H3C
NH
N
N
N
N
Cl
F
F
O
S
O
CH3
N
CH3
Compound 27
*signal from traces of residual solvent/grease
0.91 0.68 0.99 0.63 0.66 0.98 1.04 3.53 4.24 1.00 1.06 1.29 3.53
f1 (ppm)
S36/147

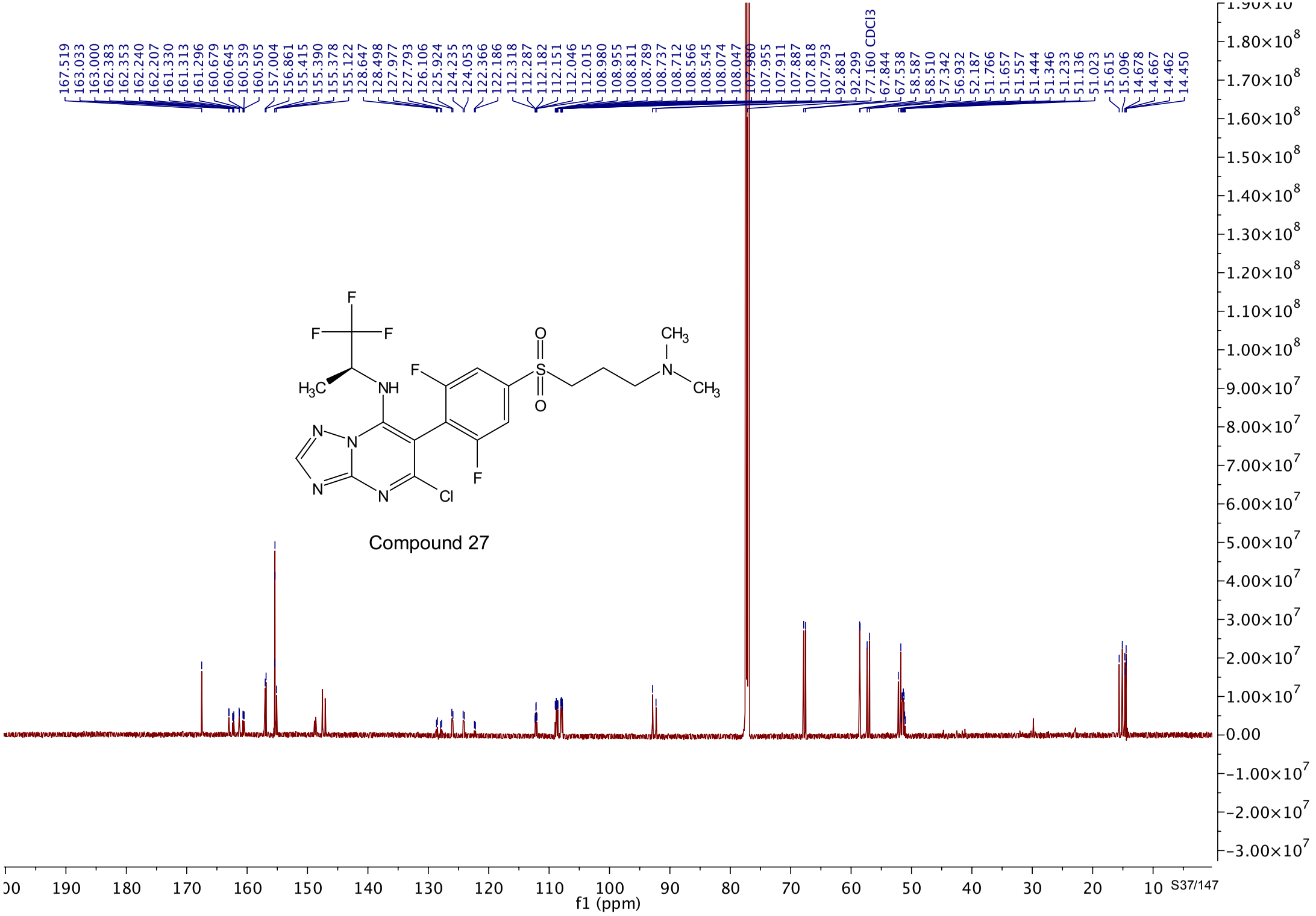
167.519
163.033
163.000
162.383
162.353
162.240
162.207
161.330
161.313
161.296
160.679
160.645
160.539
160.505
157.004
156.861
155.415
155.390
155.378
155.122
128.647
128.498
127.977
127.793
126.106
125.924
124.235
124.053
122.366
122.186
112.318
112.287
112.182
112.151
112.046
112.015
108.980
108.955
108.811
108.789
108.737
108.712
108.566
108.545
108.074
108.047
107.980
107.955
107.911
107.887
107.818
107.793
92.881
92.299
77.160 CDCl3
67.844
67.538
58.587
58.510
57.342
56.932
52.187
51.766
51.657
51.557
51.444
51.346
51.233
51.136
51.023
15.615
15.096
14.678
14.667
14.462
14.450
1.90×10^8
1.80×10^8
1.70×10^8
1.60×10^8
1.50×10^8
1.40×10^8
1.30×10^8
1.20×10^8
1.10×10^8
1.00×10^8
9.00×10^7
8.00×10^7
7.00×10^7
6.00×10^7
5.00×10^7
4.00×10^7
3.00×10^7
2.00×10^7
1.00×10^7
0.00
-1.00×10^7
-2.00×10^7
-3.00×10^7
F
F
F
H3C
NH
F
O
S
O
CH3
N
CH3
N
N
N
N
Cl
F
Compound 27
200
190
180
170
160
150
140
130
120
110
100
90
80
70
60
50
40
30
20
10
f1 (ppm)
S37/147

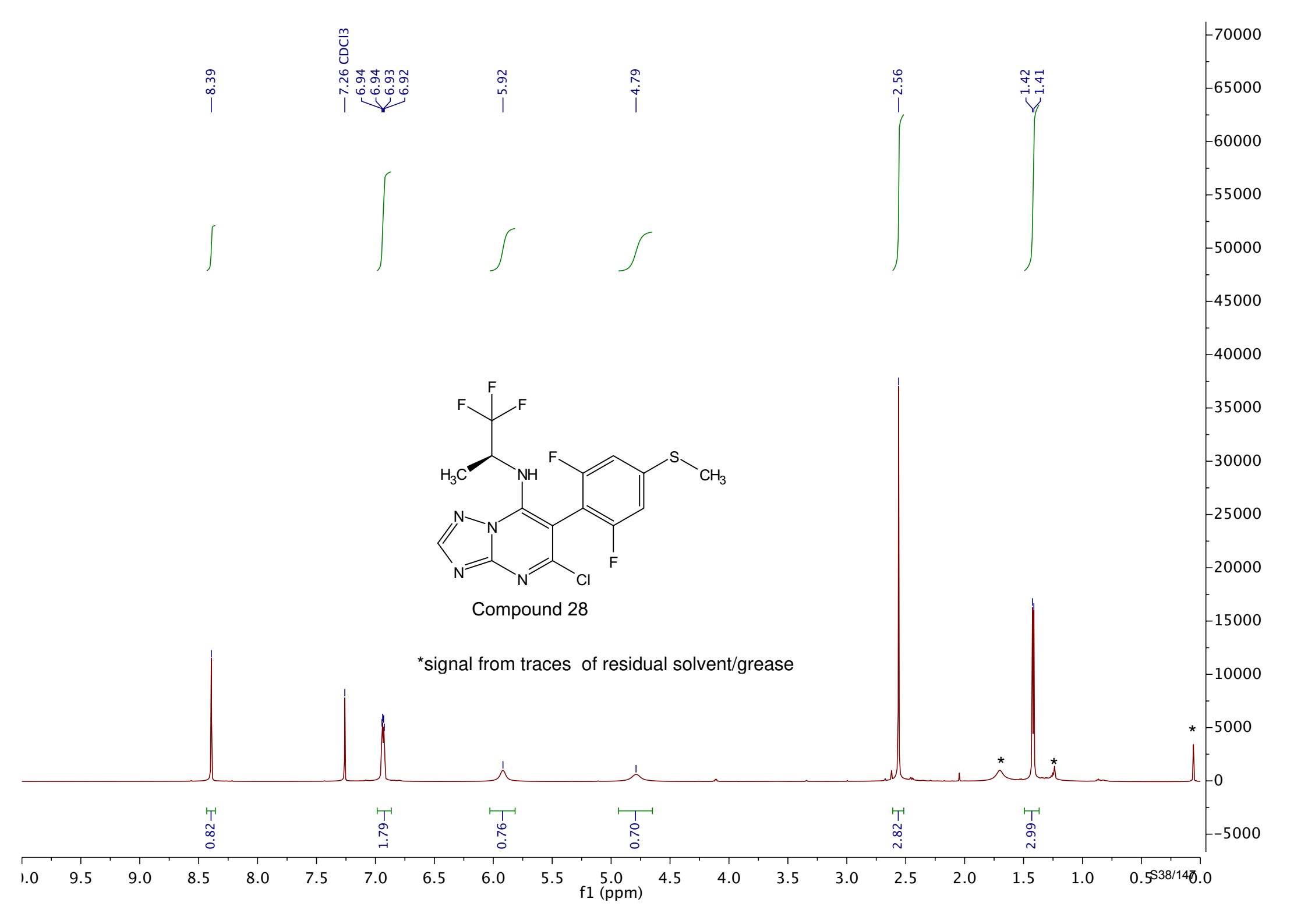
8.39
7.26 CDCl3
6.94
6.94
6.93
6.92
5.92
4.79
2.56
1.42
1.41
F
F
F
H3C
NH
F
S
CH3
N
N
N
N
Cl
F
Compound 28
*signal from traces of residual solvent/grease
0.82
1.79
0.76
0.70
2.82
2.99
f1 (ppm)
S38/147

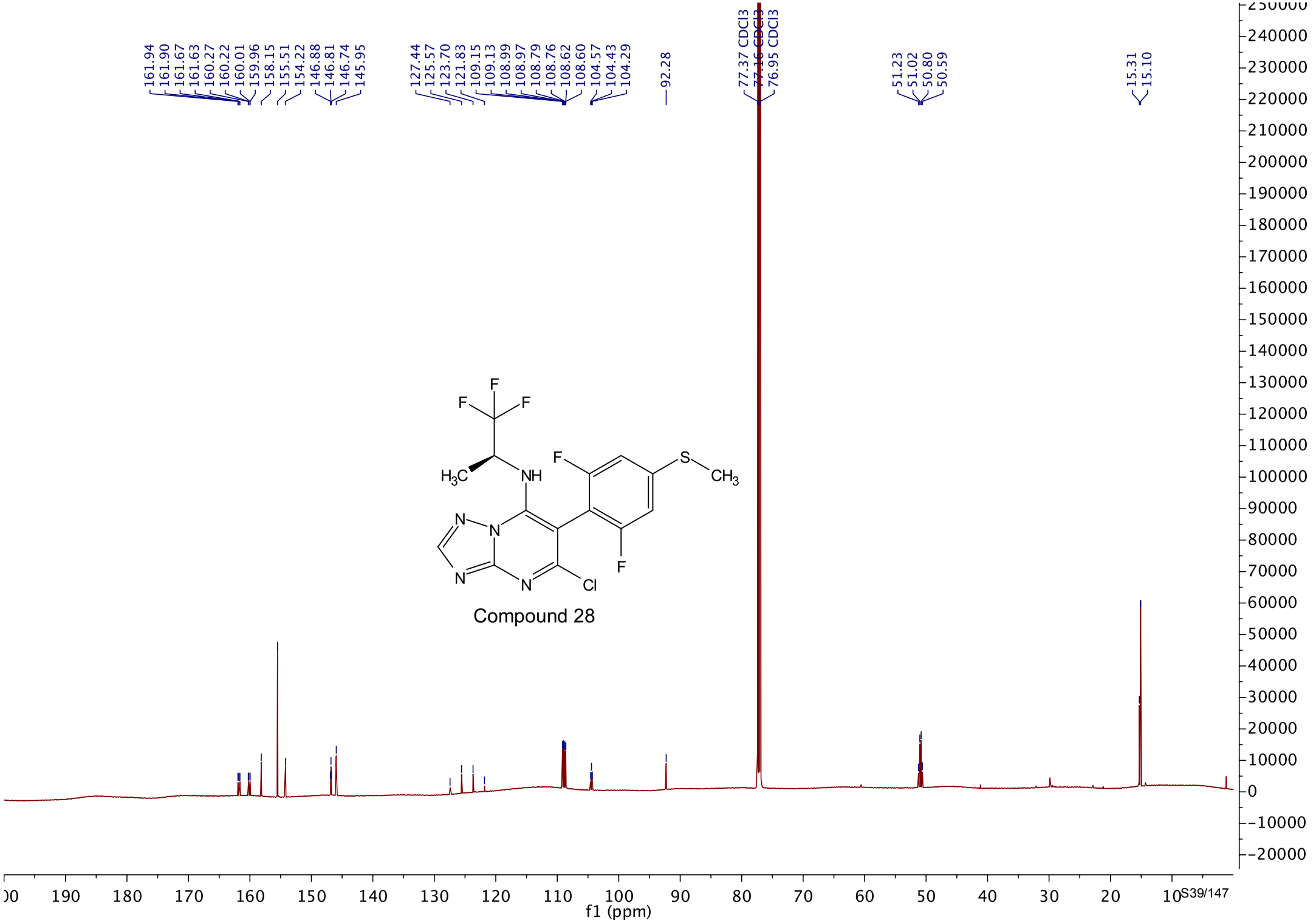
161.94
161.90
161.67
161.63
160.27
160.22
160.01
159.96
158.15
155.51
154.22
146.88
146.81
146.74
145.95
127.44
125.57
123.70
121.83
109.15
109.13
108.99
108.97
108.79
108.76
108.62
108.60
104.57
104.43
104.29
92.28
77.37 CDCl3
77.16 CDCl3
76.95 CDCl3
51.23
51.02
50.80
50.59
15.31
15.10
F
F
F
H3C
NH
F
S
CH3
N
N
N
N
Cl
F
Compound 28
f1 (ppm)

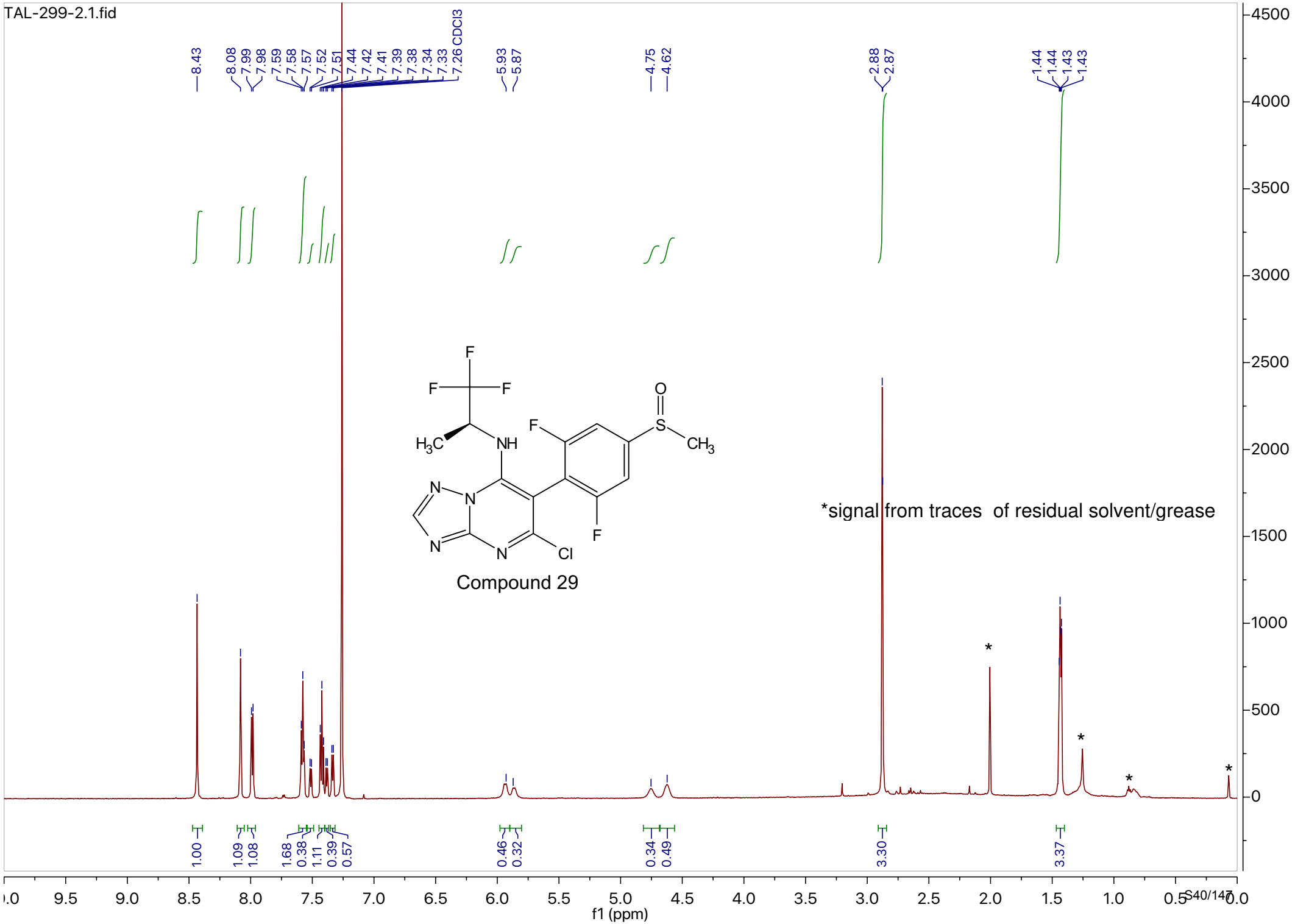
TAL-299-2.1.fid
8.43
8.08
7.99
7.98
7.59
7.58
7.57
7.52
7.51
7.44
7.42
7.41
7.39
7.38
7.34
7.33
7.26 CDCl3
5.93
5.87
4.75
4.62
2.88
2.87
1.44
1.44
1.43
1.43
F
F
F
H3C
NH
F
O
S
CH3
N
N
N
N
Cl
F
Compound 29
*signal from traces of residual solvent/grease
1.00
1.09
1.08
1.68
0.38
1.11
0.39
0.57
0.46
0.32
0.34
0.49
3.30
3.37
f1 (ppm)

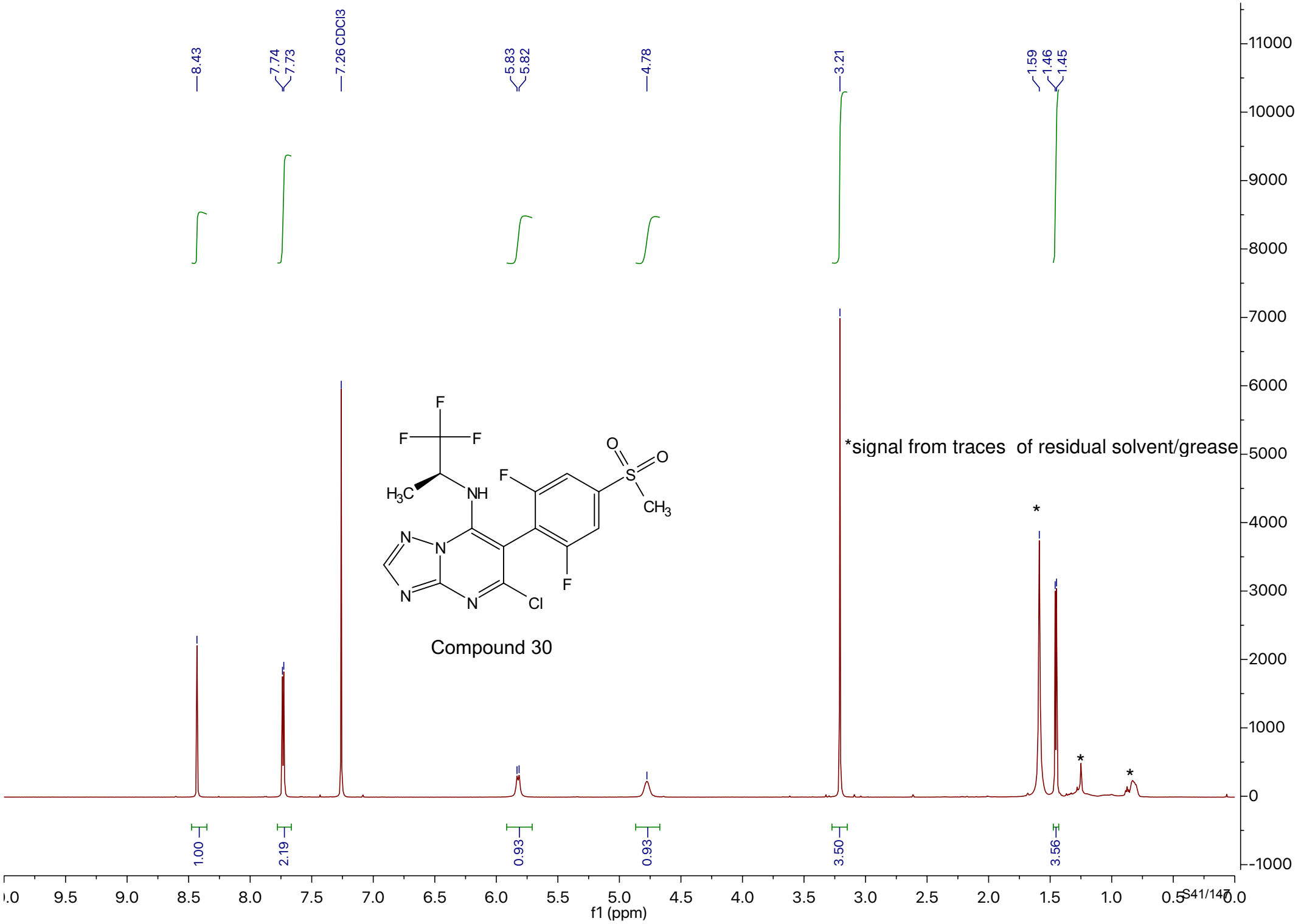
8.43
7.74
7.73
7.26 CDCl3
5.83
5.82
4.78
3.21
1.59
1.46
1.45
*signal from traces of residual solvent/grease
Compound 30
1.00
2.19
0.93
0.93
3.50
3.56
f1 (ppm)

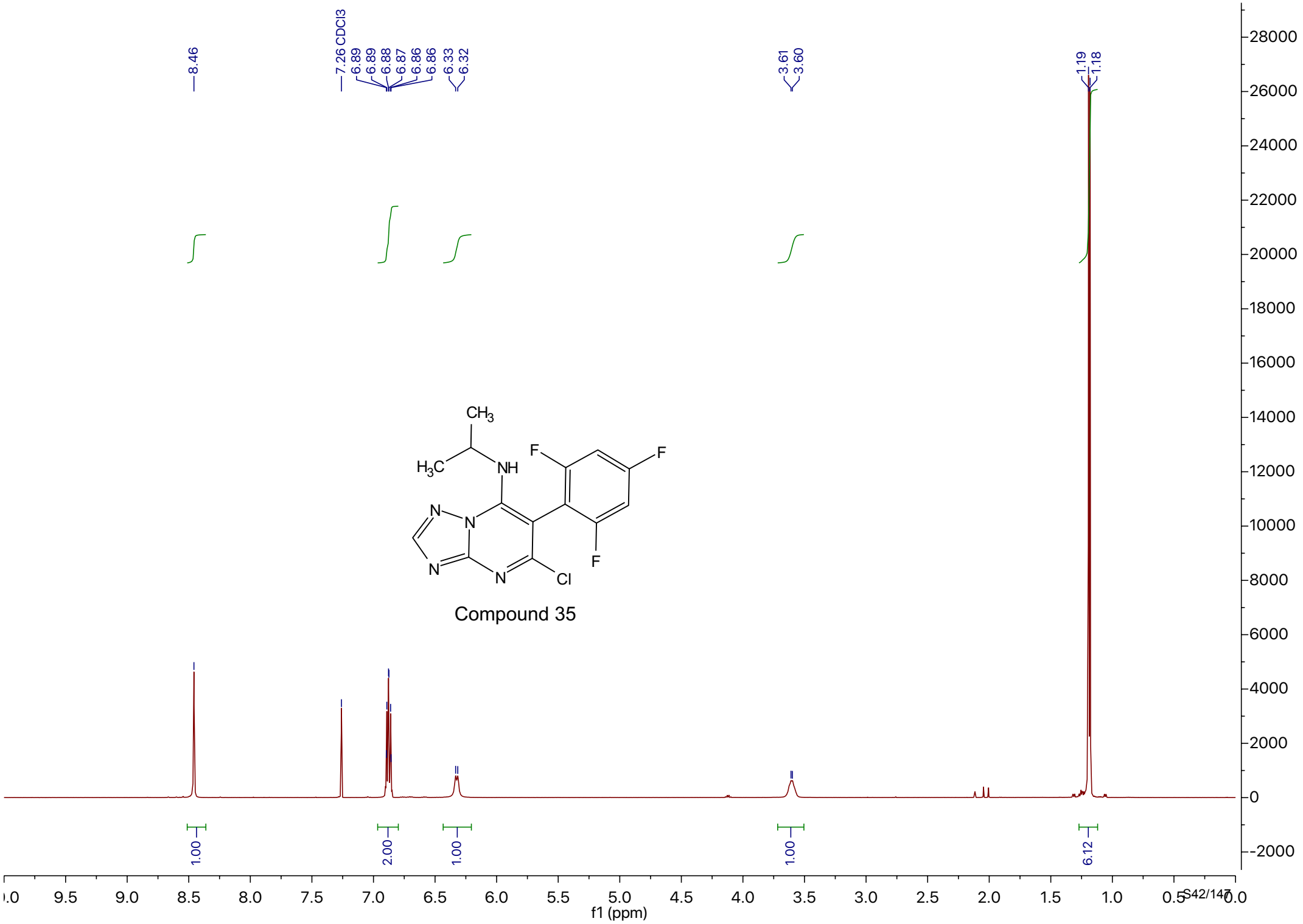
8.46
7.26 CDCl3
6.89
6.89
6.88
6.87
6.86
6.86
6.33
6.32
3.61
3.60
1.19
1.18
CH3
H3C
NH
F
F
F
N
N
N
N
Cl
Compound 35
1.00
2.00
1.00
1.00
6.12
f1 (ppm)

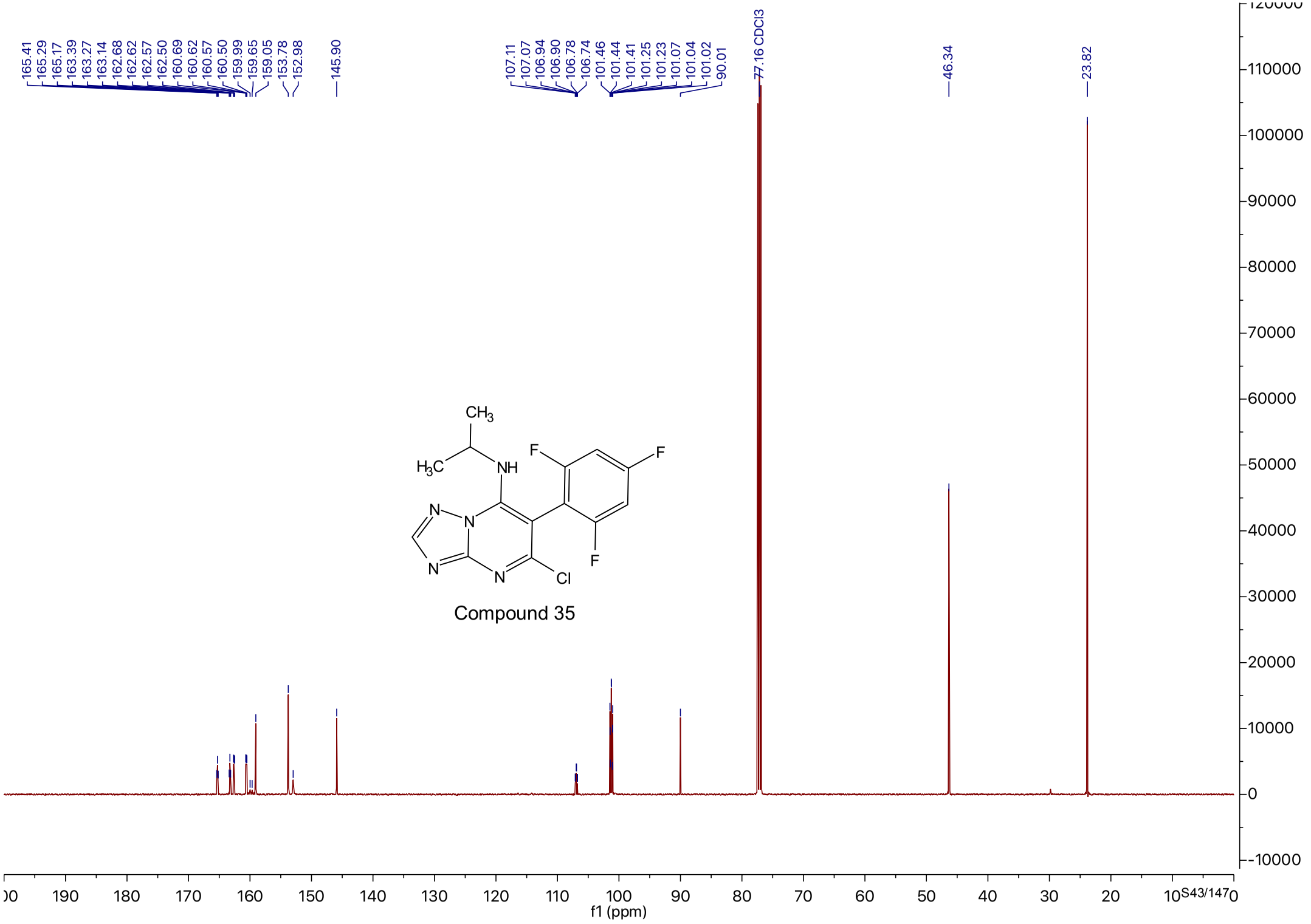
165.41
165.29
165.17
163.39
163.27
163.14
162.68
162.62
162.57
162.50
160.69
160.62
160.57
160.50
159.99
159.65
159.05
153.78
152.98
145.90
107.11
107.07
106.94
106.90
106.78
106.74
101.46
101.44
101.41
101.25
101.23
101.07
101.04
101.02
90.01
77.16 CDCl3
46.34
23.82
CH3
H3C
NH
F
F
F
N
N
N
N
Cl
Compound 35
f1 (ppm)

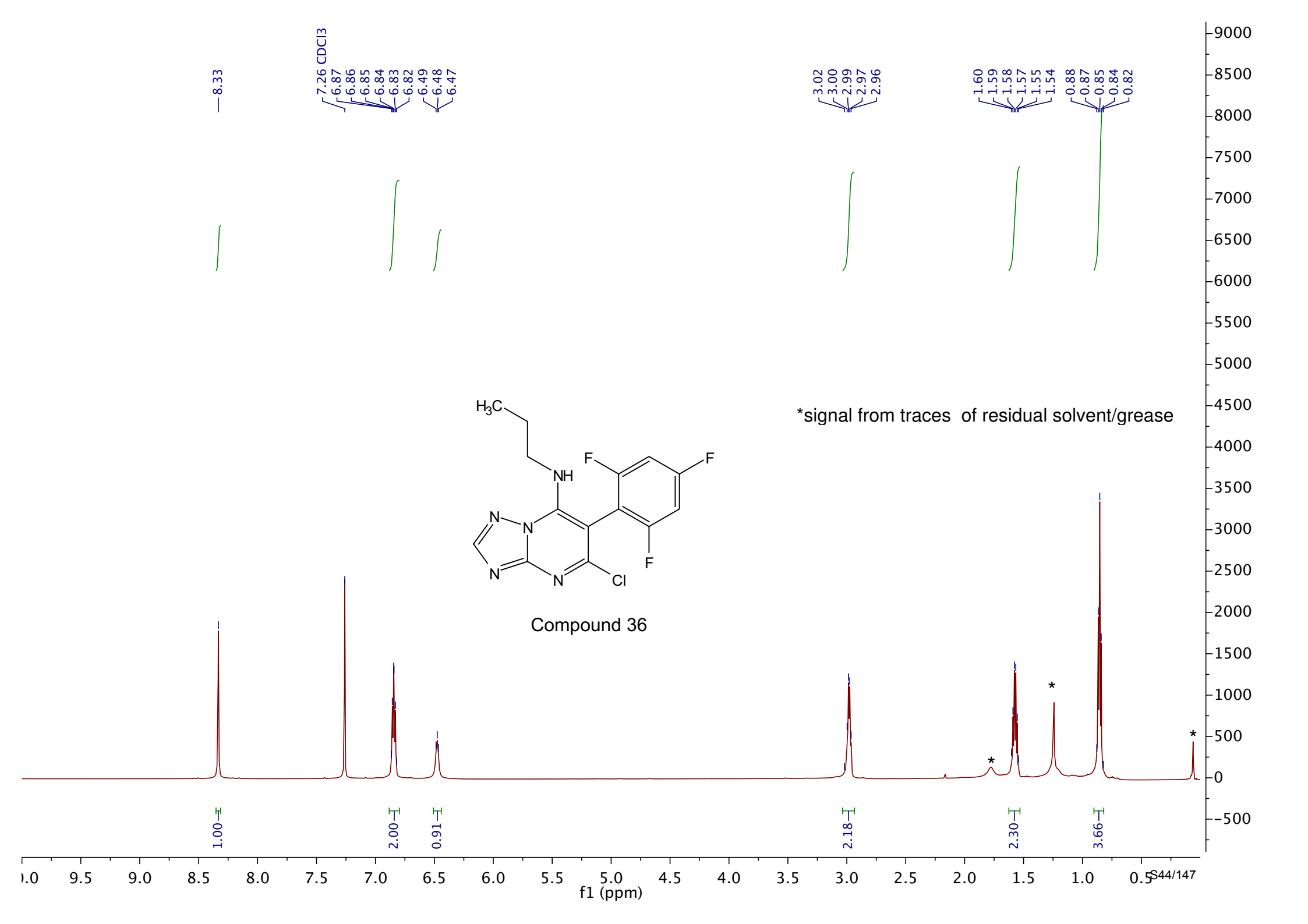
8.33
7.26 CDCl3
6.87
6.86
6.85
6.84
6.83
6.82
6.49
6.48
6.47
3.02
3.00
2.99
2.97
2.96
1.60
1.59
1.58
1.57
1.55
1.54
0.88
0.87
0.85
0.84
0.82
H3C
NH
F
F
F
N
N
N
N
Cl
*signal from traces of residual solvent/grease
Compound 36
1.00
2.00
0.91
2.18
2.30
3.66
f1 (ppm)
S44/147

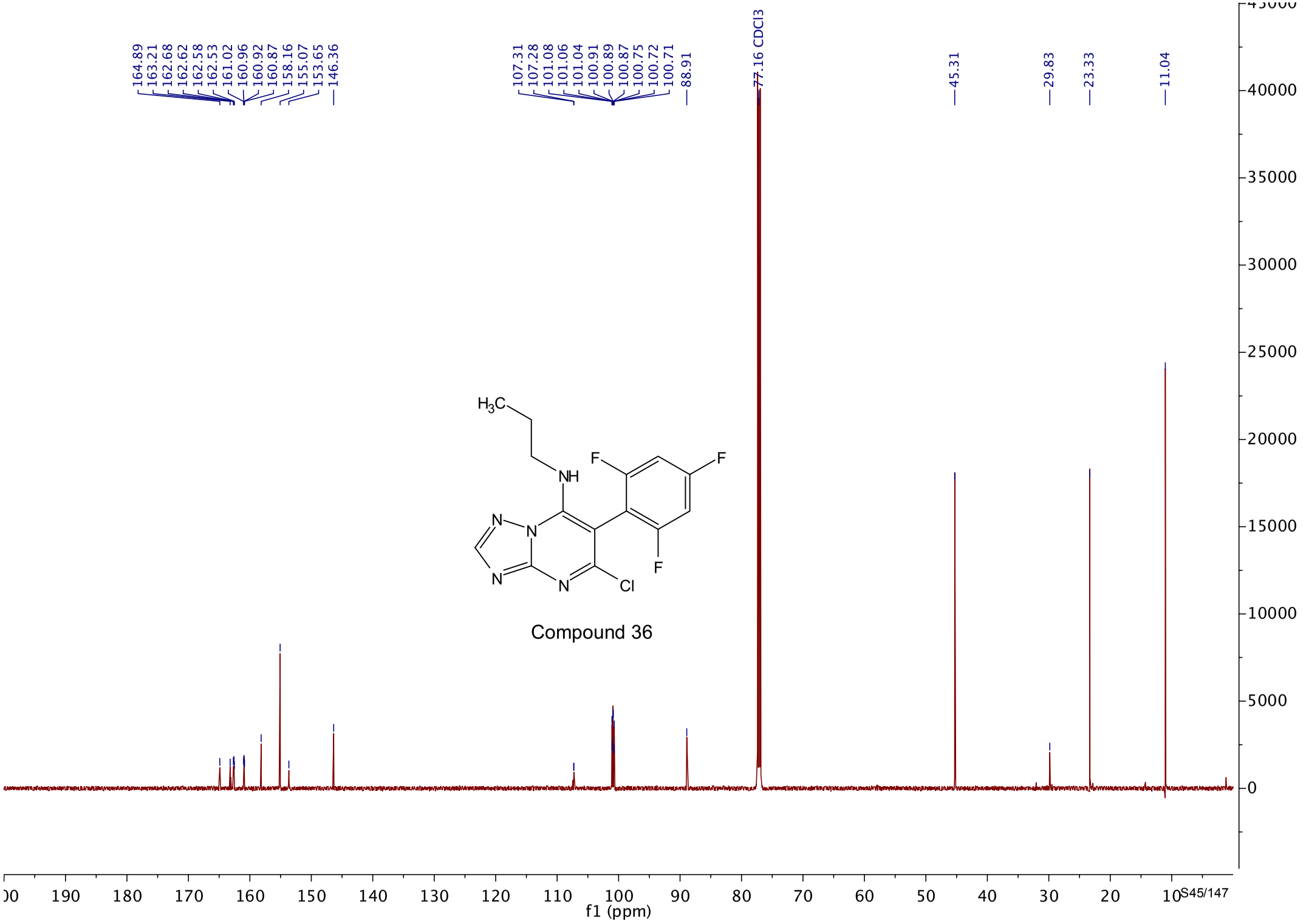
164.89
163.21
162.68
162.62
162.58
162.53
161.02
160.96
160.92
160.87
158.16
155.07
153.65
146.36
107.31
107.28
101.08
101.06
101.04
100.91
100.89
100.87
100.75
100.72
100.71
88.91
77.16 CDCl3
45.31
29.83
23.33
11.04
H3C
NH
F
F
F
N
N
N
N
Cl
Compound 36
45000
40000
35000
30000
25000
20000
15000
10000
5000
0
f1 (ppm)
S45/147

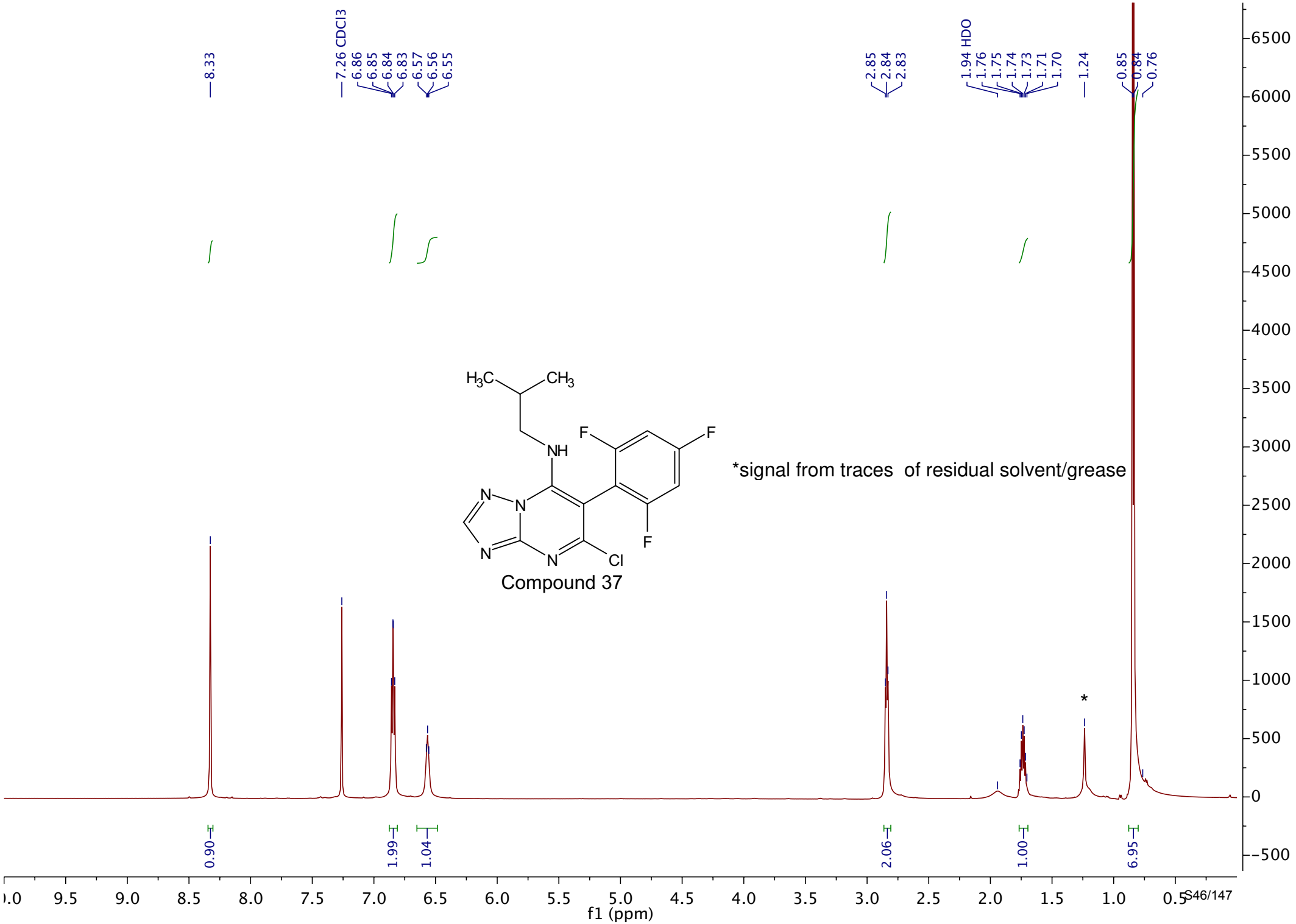
8.33
7.26 CDCl3
6.86
6.85
6.84
6.83
6.57
6.56
6.55
2.85
2.84
2.83
1.94 HDO
1.76
1.75
1.74
1.73
1.71
1.70
1.24
0.85
0.84
0.76
H3C
CH3
NH
F
F
F
N
N
N
N
Cl
*signal from traces of residual solvent/grease
Compound 37
0.90
1.99
1.04
2.06
1.00
6.95
f1 (ppm)
S46/147

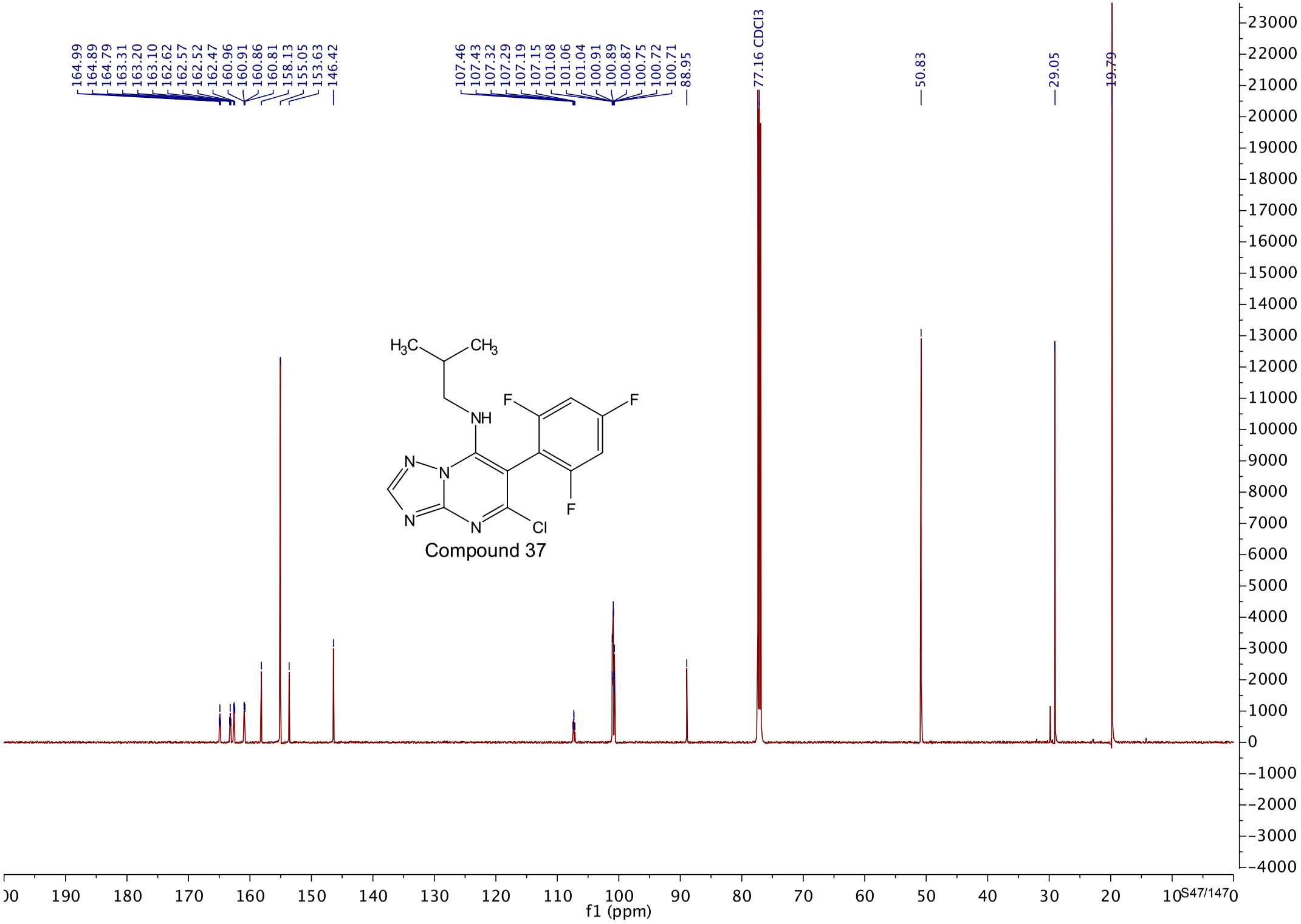
164.99
164.89
164.79
163.31
163.20
163.10
162.62
162.57
162.52
162.47
160.96
160.91
160.86
160.81
158.13
155.05
153.63
146.42
107.46
107.43
107.32
107.29
107.19
107.15
101.08
101.06
101.04
100.91
100.89
100.87
100.75
100.72
100.71
88.95
77.16 CDCl3
50.83
29.05
19.79
H3C
CH3
NH
F
F
F
N
N
N
N
Cl
Compound 37
f1 (ppm)
S47/147

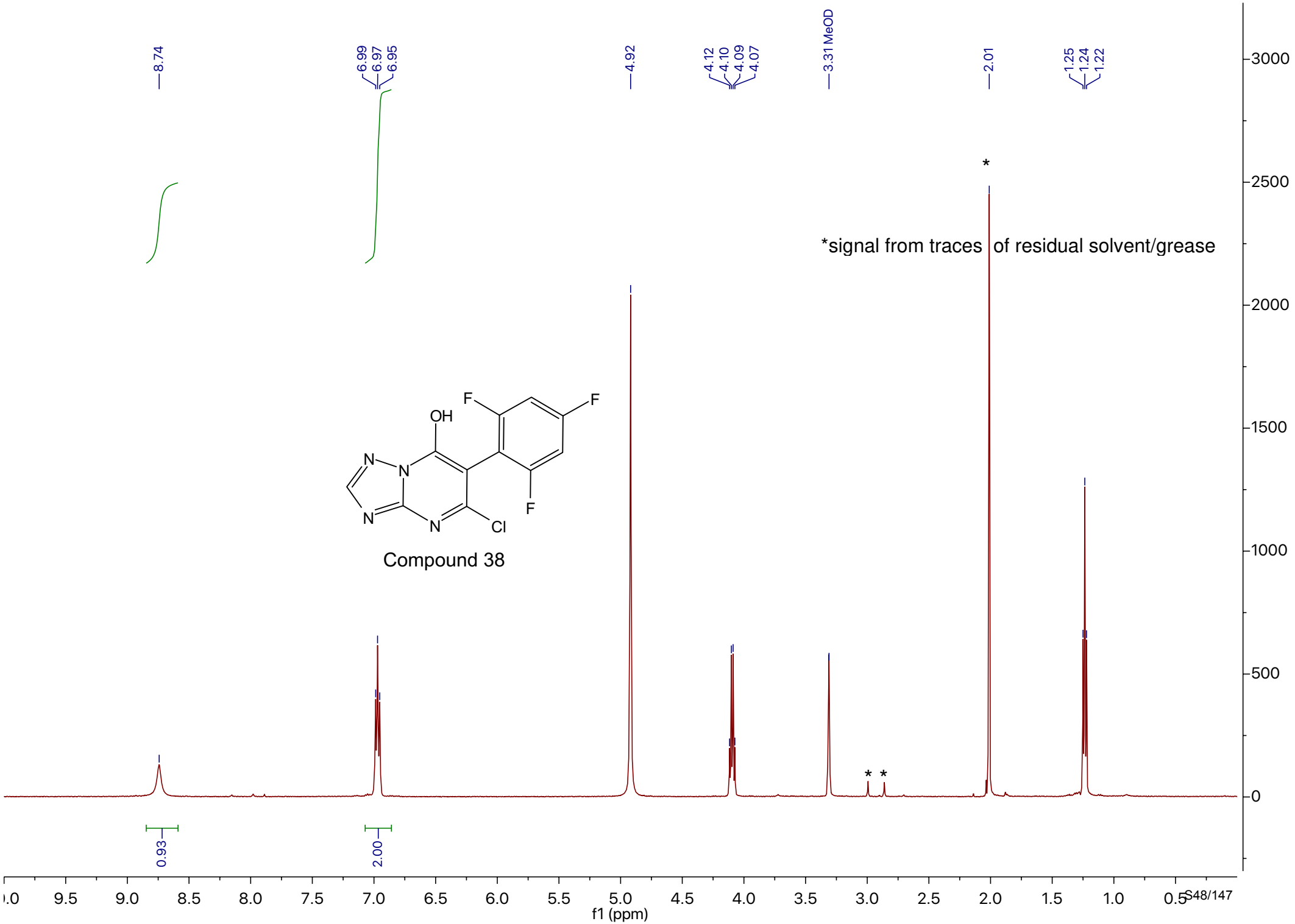
8.74
6.99
6.97
6.95
4.92
4.12
4.10
4.09
4.07
3.31 MeOD
2.01
1.25
1.24
1.22
*signal from traces of residual solvent/grease
F
F
OH
N
N
N
N
F
Cl
Compound 38
0.93
2.00
f1 (ppm)
S48/147

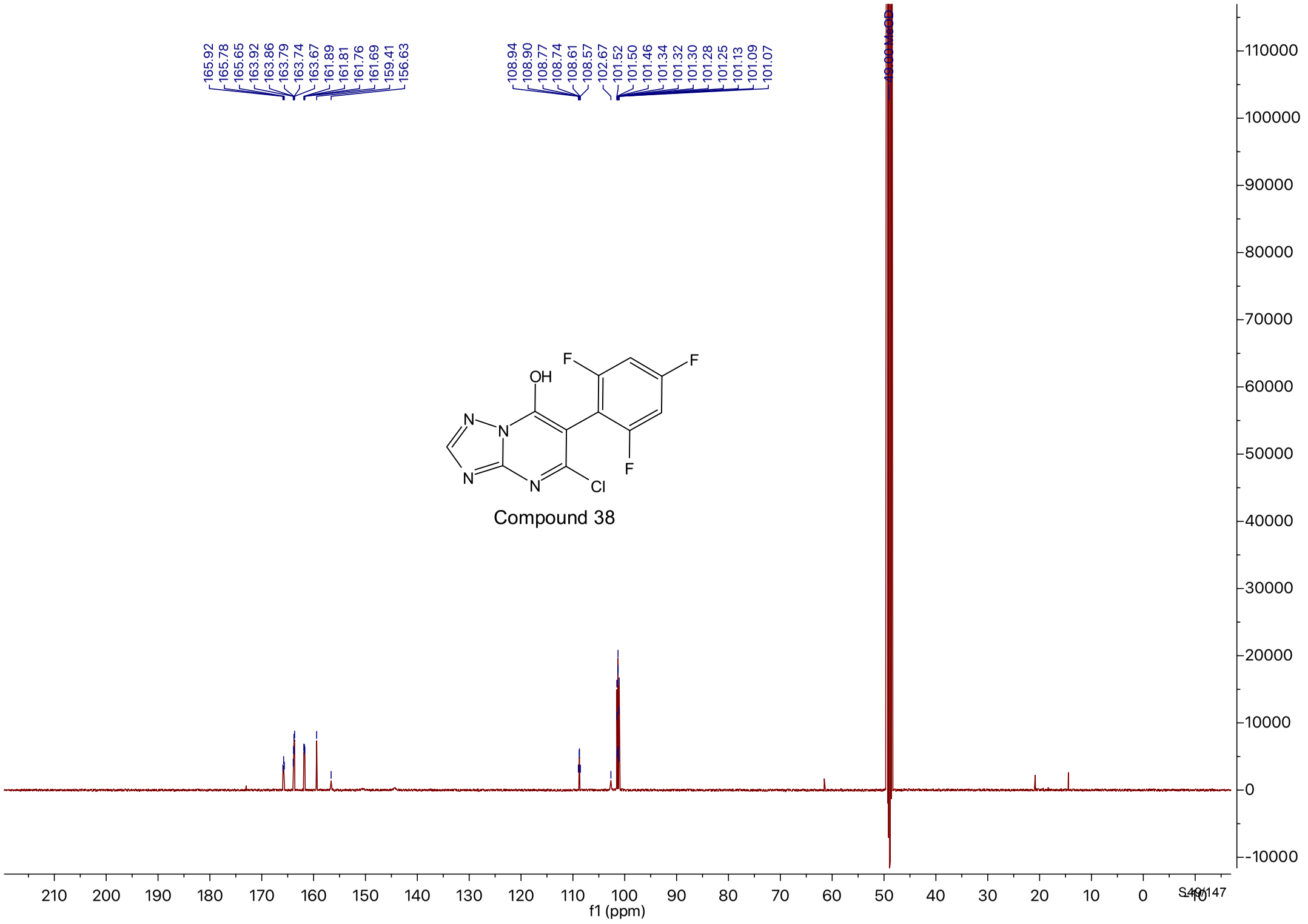
165.92
165.78
165.65
163.92
163.86
163.79
163.74
163.67
161.89
161.81
161.76
161.69
159.41
156.63
108.94
108.90
108.77
108.74
108.61
108.57
102.67
101.52
101.50
101.46
101.34
101.32
101.30
101.28
101.25
101.13
101.09
101.07
49.00 MeOD
F
F
OH
N
N
N
N
F
Cl
110000
100000
90000
80000
70000
60000
50000
40000
30000
20000
10000
0
-10000
210
200
190
180
170
160
150
140
130
120
110
100
90
80
70
60
50
40
30
20
10
0
-10
f1 (ppm)

Compound 38

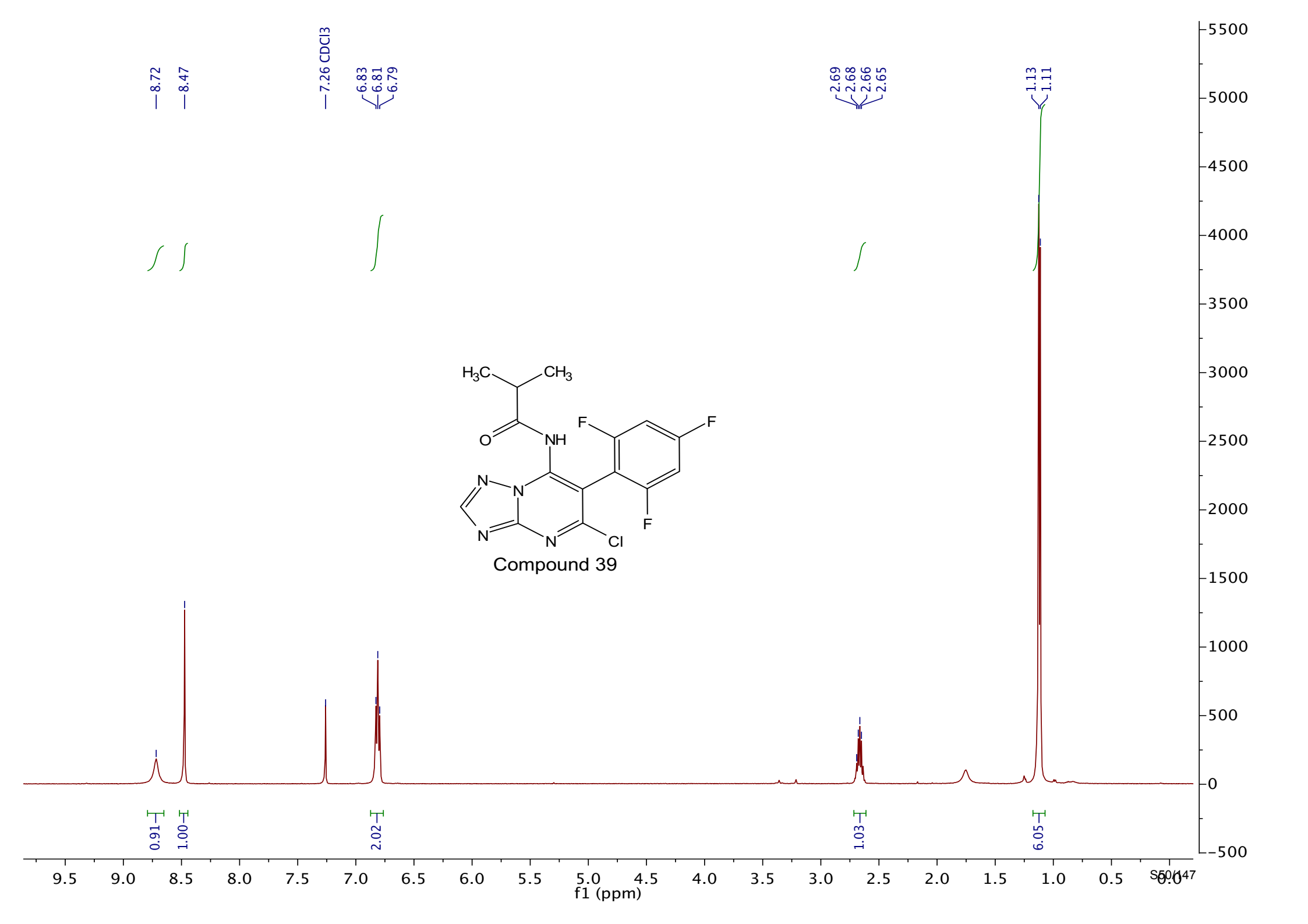
8.72
8.47
7.26 CDCl3
6.83
6.81
6.79
2.69
2.68
2.66
2.65
1.13
1.11
H3C
CH3
O
NH
F
F
F
N
N
N
N
Cl
Compound 39
0.91
1.00
2.02
1.03
6.05
f1 (ppm)
S50/147

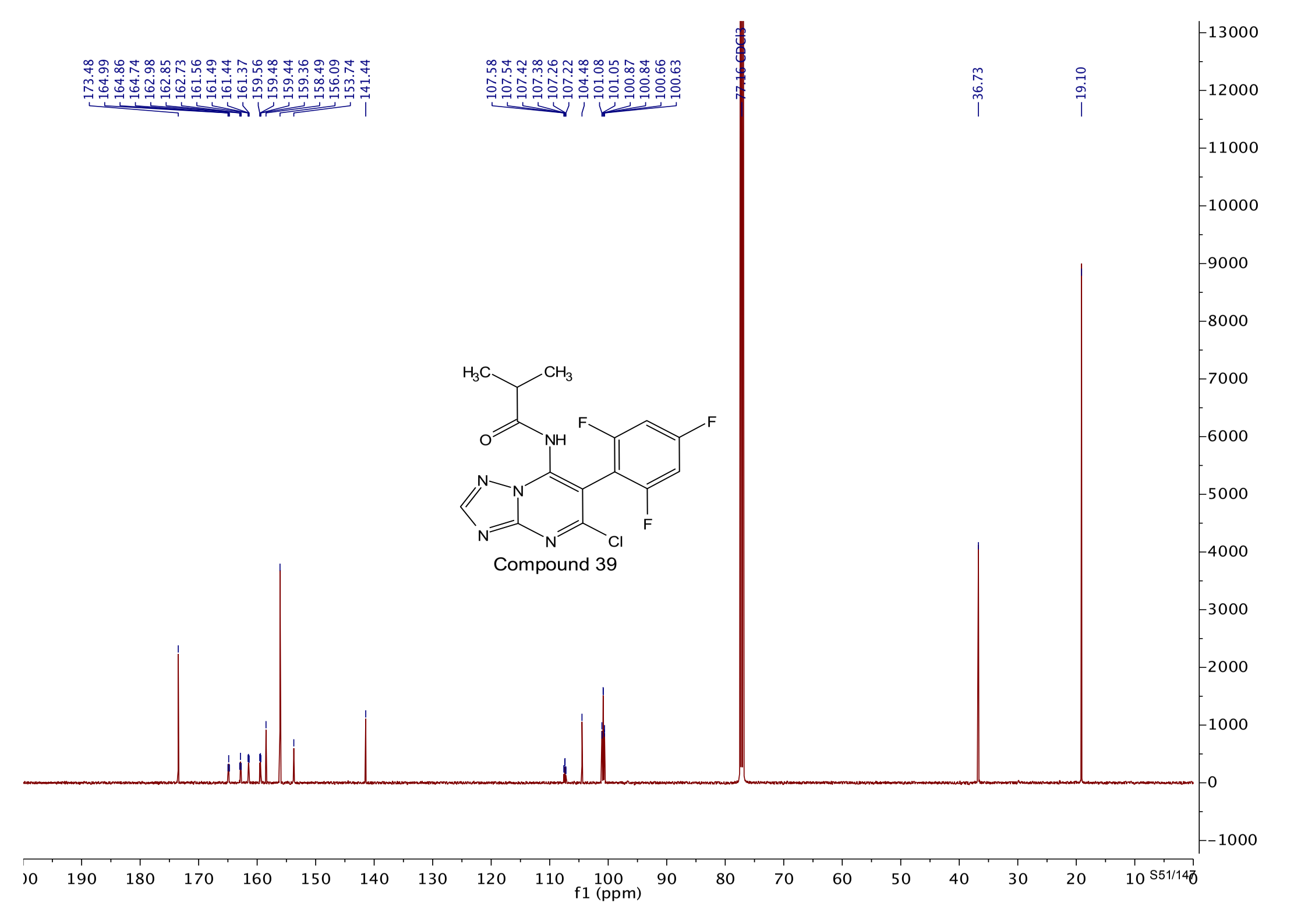
173.48
164.99
164.86
164.74
162.98
162.85
162.73
161.56
161.49
161.44
161.37
159.56
159.48
159.44
159.36
158.49
156.09
153.74
141.44
107.58
107.54
107.42
107.38
107.26
107.22
104.48
101.08
101.05
100.87
100.84
100.66
100.63
77.16 CDCl3
36.73
19.10
H3C
CH3
O
NH
F
F
F
N
N
N
N
Cl
Compound 39
f1 (ppm)
S51/147

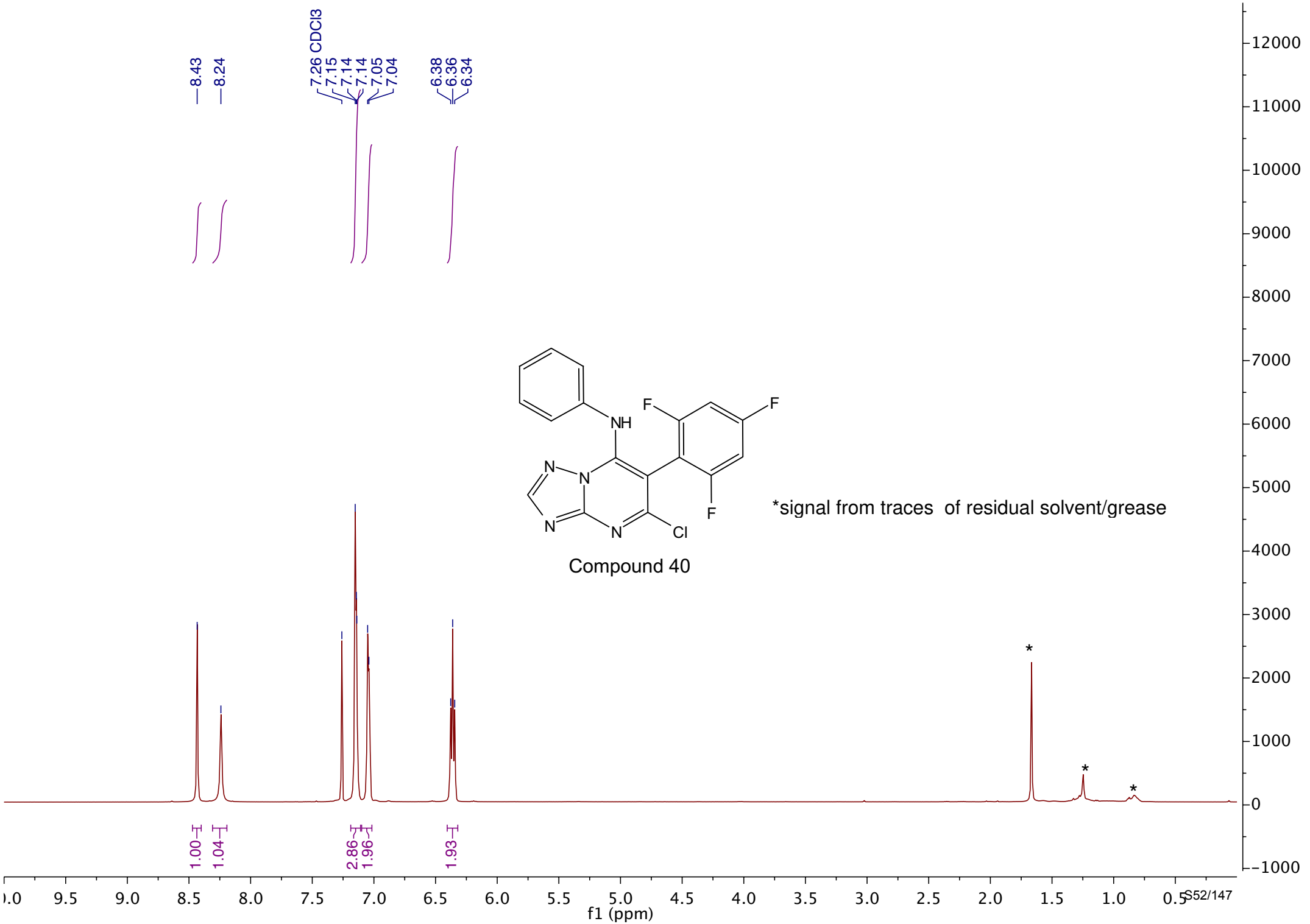

Compound 40

*signal from traces of residual solvent/grease

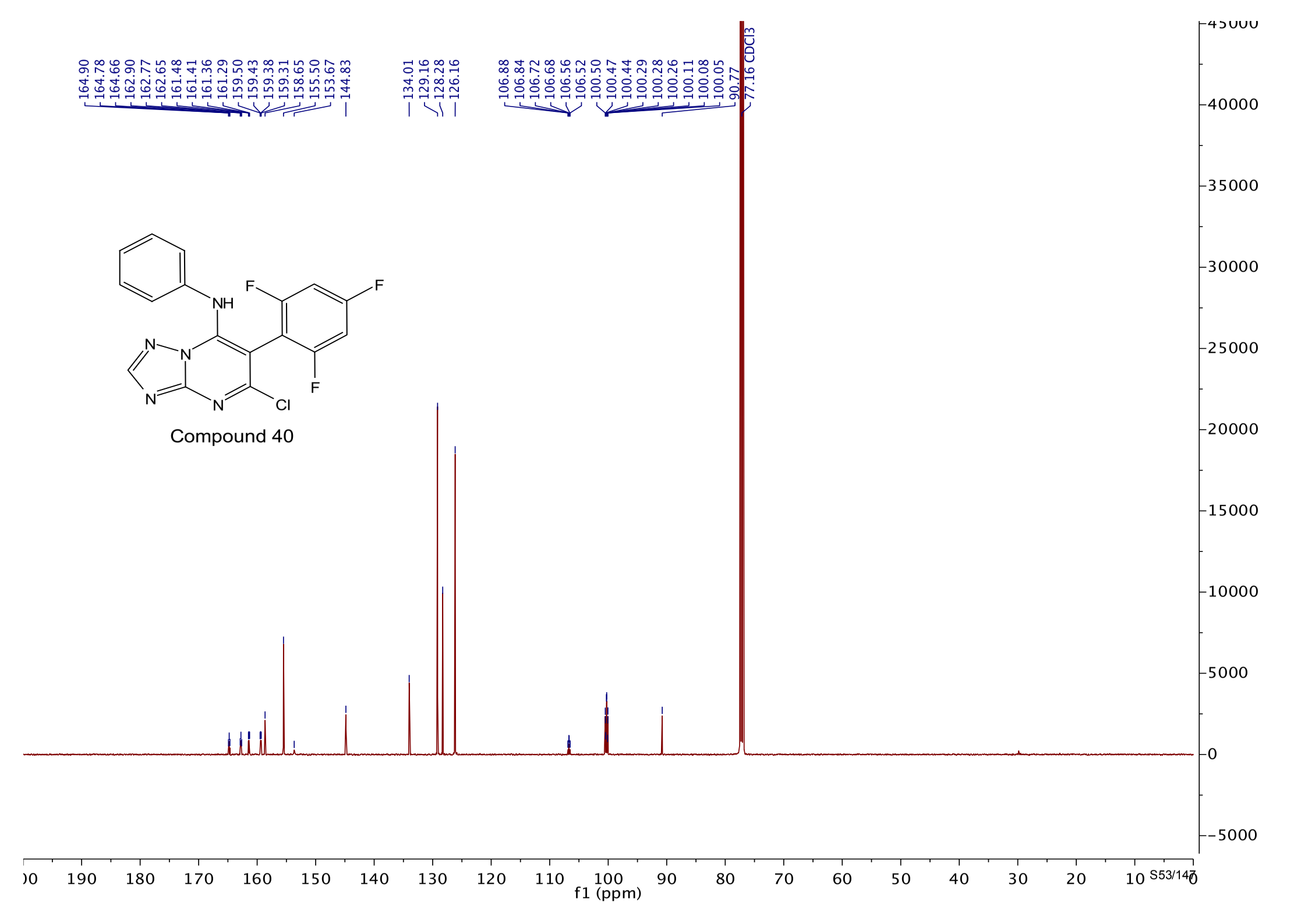
164.90
164.78
164.66
162.90
162.77
162.65
161.48
161.41
161.36
161.29
159.50
159.43
159.38
159.31
158.65
155.50
153.67
144.83
134.01
129.16
128.28
126.16
106.88
106.84
106.72
106.68
106.56
106.52
100.50
100.47
100.44
100.29
100.28
100.26
100.11
100.08
100.05
90.77
77.16 CDCl3
NH
F
F
F
N
N
N
N
Cl
Compound 40
45000
40000
35000
30000
25000
20000
15000
10000
5000
0
-5000
f1 (ppm)
S53/147

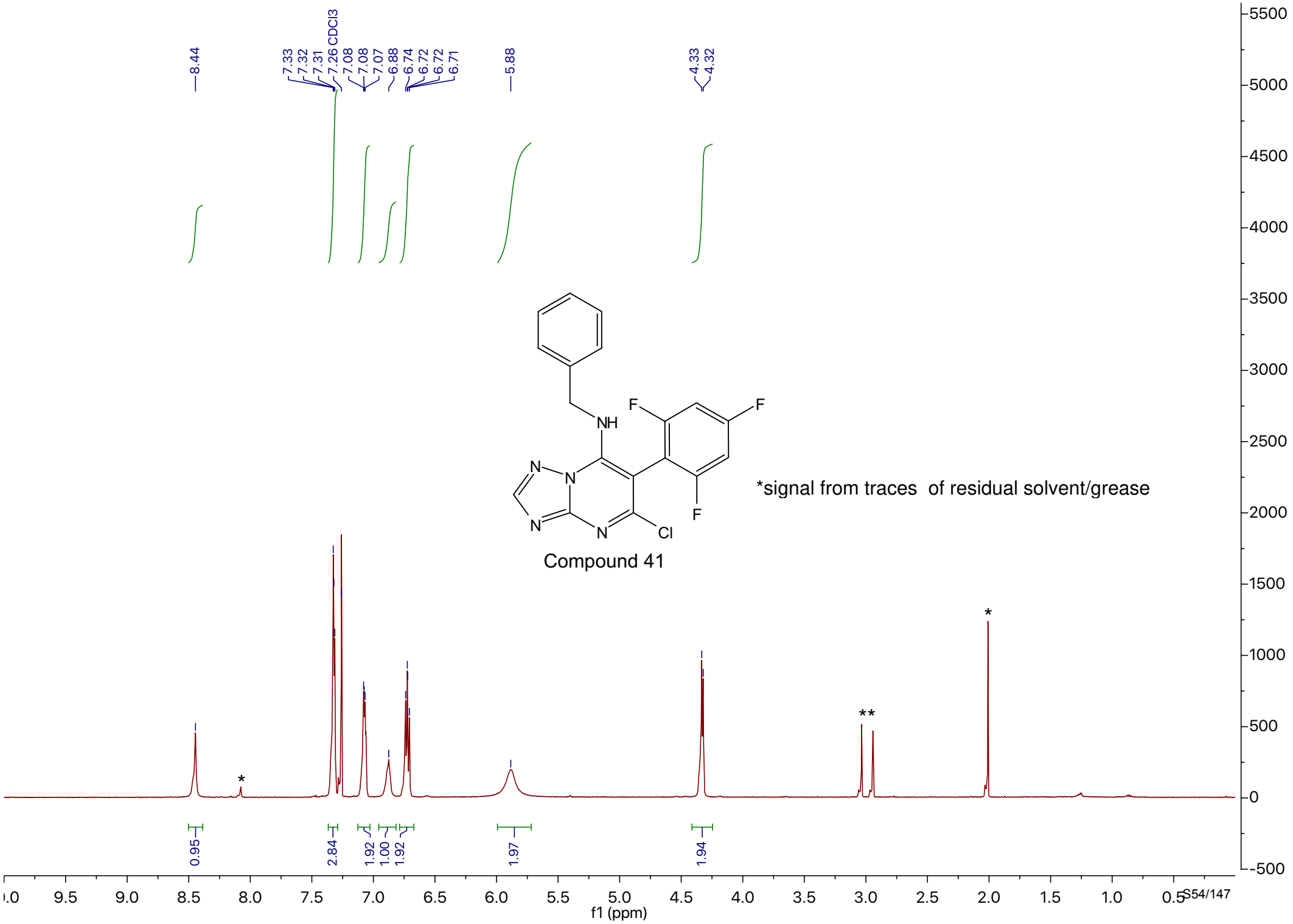
8.44
7.33
7.32
7.31
7.26 CDCl3
7.08
7.08
7.07
6.88
6.74
6.72
6.72
6.71
5.88
4.33
4.32
NH
F
F
F
N
N
N
N
Cl
*signal from traces of residual solvent/grease
Compound 41
*
*
**
*
0.95
2.84
1.92
1.00
1.92
1.97
1.94
f1 (ppm)
S54/147

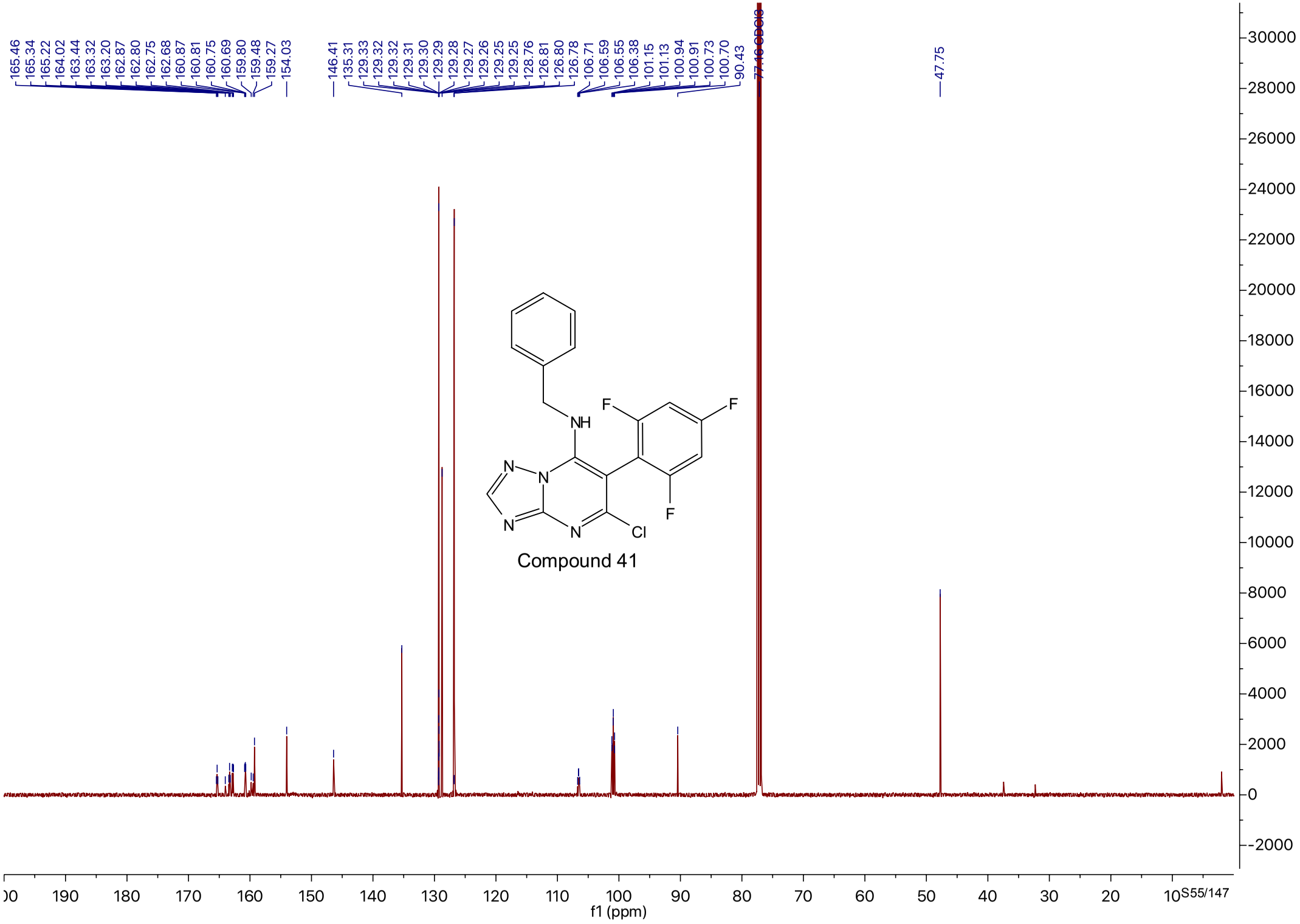
165.46
165.34
165.22
164.02
163.44
163.32
163.20
162.87
162.80
162.75
162.68
160.87
160.81
160.75
160.69
159.80
159.48
159.27
154.03
146.41
135.31
129.33
129.32
129.32
129.31
129.30
129.29
129.28
129.27
129.26
129.25
129.25
128.76
126.81
126.80
126.78
106.71
106.59
106.55
106.38
101.15
101.13
100.94
100.91
100.73
100.70
90.43
77.16 CDCl3
47.75
NH
F
F
F
N
N
N
N
Cl
Compound 41
30000
28000
26000
24000
22000
20000
18000
16000
14000
12000
10000
8000
6000
4000
2000
0
-2000
190
180
170
160
150
140
130
120
110
100
90
80
70
60
50
40
30
20
10
f1 (ppm)

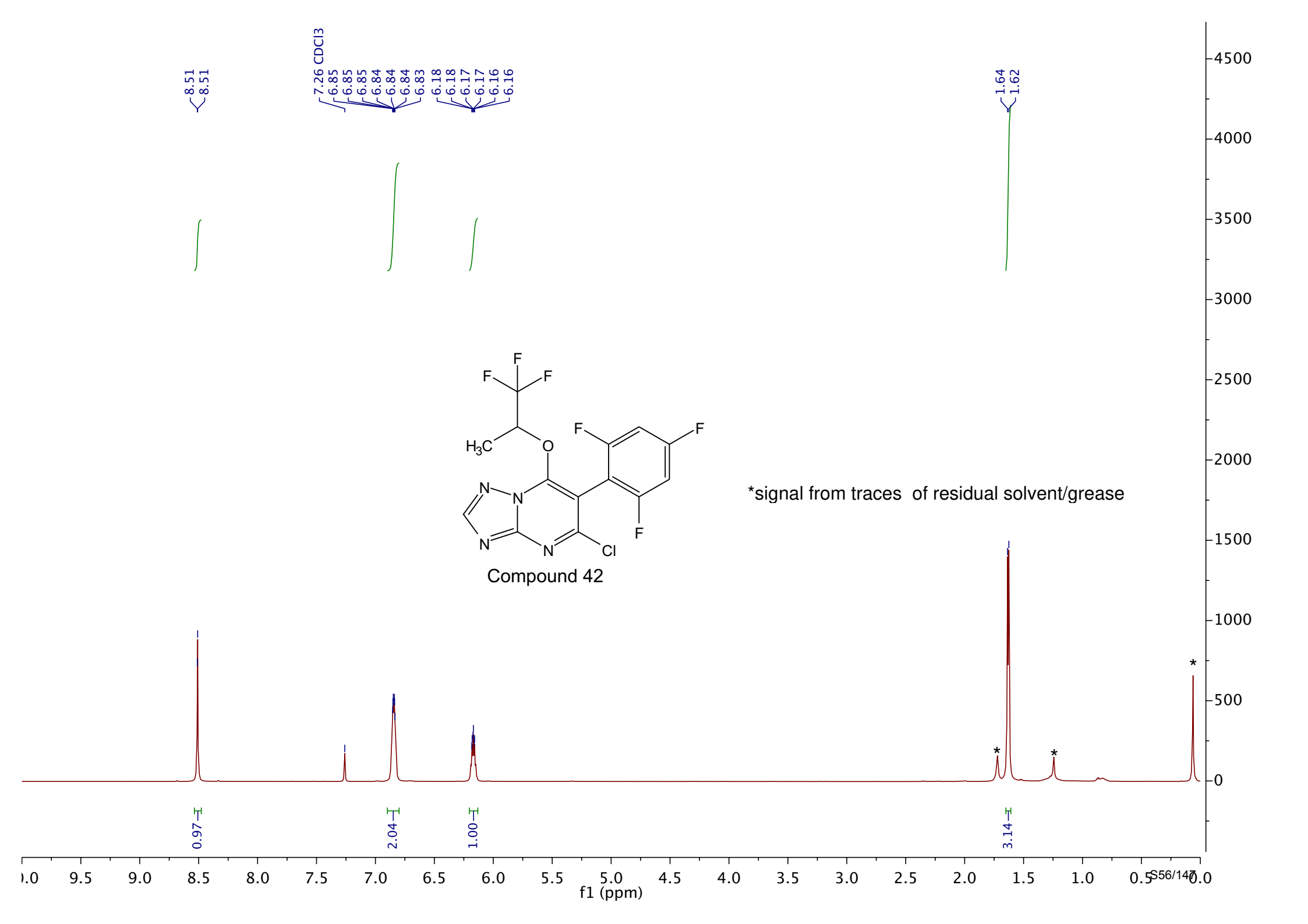
8.51
8.51
7.26 CDCl3
6.85
6.85
6.85
6.84
6.84
6.84
6.83
6.18
6.18
6.17
6.17
6.16
6.16
1.64
1.62
F
F
F
H3C
O
F
F
N
N
N
N
Cl
F
*signal from traces of residual solvent/grease
Compound 42
0.97
2.04
1.00
3.14
*
*
*
4500
4000
3500
3000
2500
2000
1500
1000
500
0
9.5
9.0
8.5
8.0
7.5
7.0
6.5
6.0
5.5
5.0
4.5
4.0
3.5
3.0
2.5
2.0
1.5
1.0
0.5
0.0
f1 (ppm)

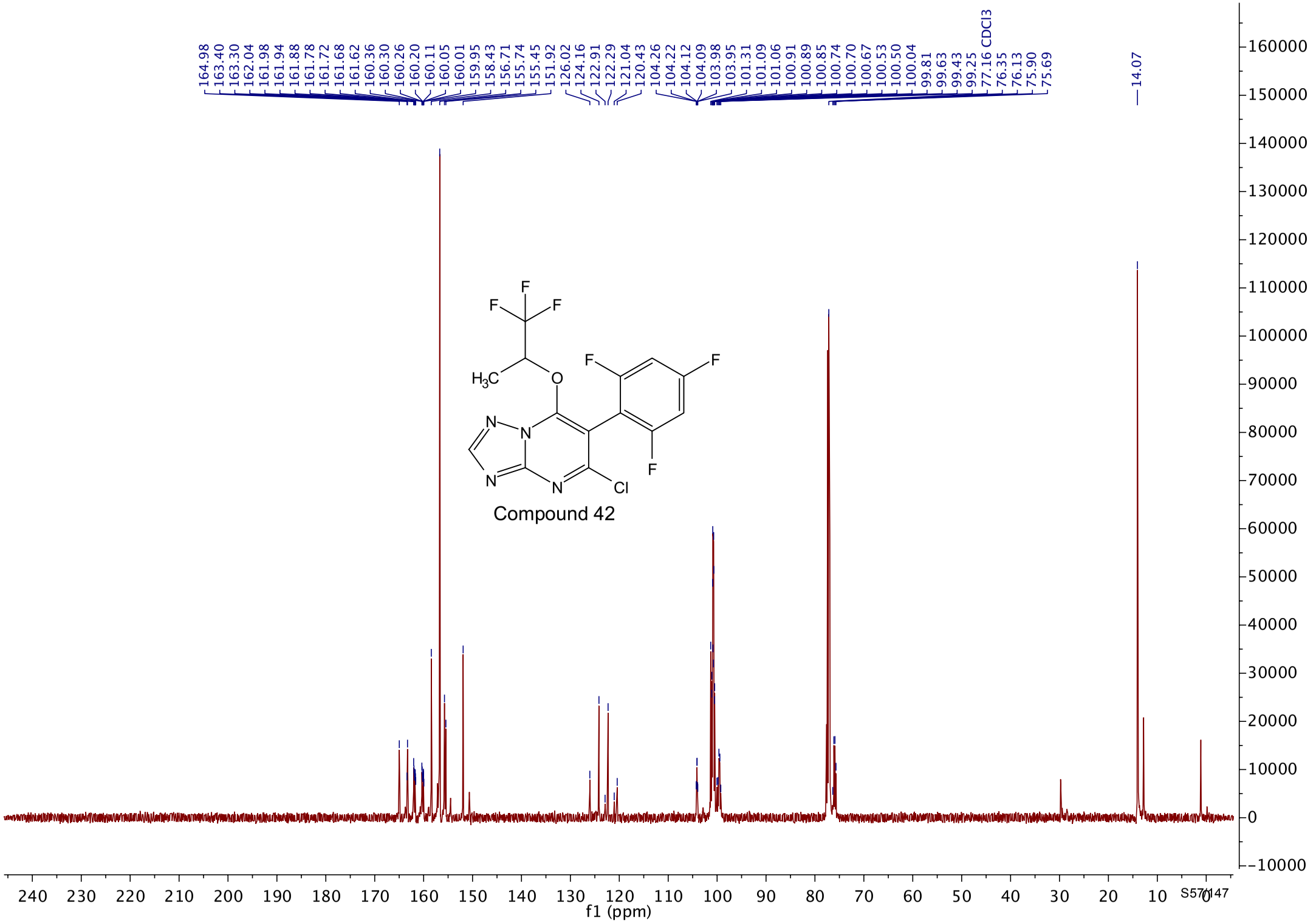
164.98
163.40
163.30
162.04
161.98
161.94
161.88
161.78
161.72
161.68
161.62
160.36
160.30
160.26
160.20
160.11
160.05
160.01
159.95
158.43
156.71
155.74
155.45
151.92
126.02
124.16
122.91
122.29
121.04
120.43
104.26
104.22
104.12
104.09
103.98
103.95
101.31
101.09
101.06
100.91
100.89
100.85
100.74
100.70
100.67
100.53
100.50
100.04
99.81
99.63
99.43
99.25
77.16 CDCl3
76.35
76.13
75.90
75.69
14.07
F
F
F
H3C
O
F
F
N
N
N
N
Cl
Compound 42
160000
150000
140000
130000
120000
110000
100000
90000
80000
70000
60000
50000
40000
30000
20000
10000
0
-10000
240
230
220
210
200
190
180
170
160
150
140
130
120
110
100
90
80
70
60
50
40
30
20
10
0
f1 (ppm)
S57/147

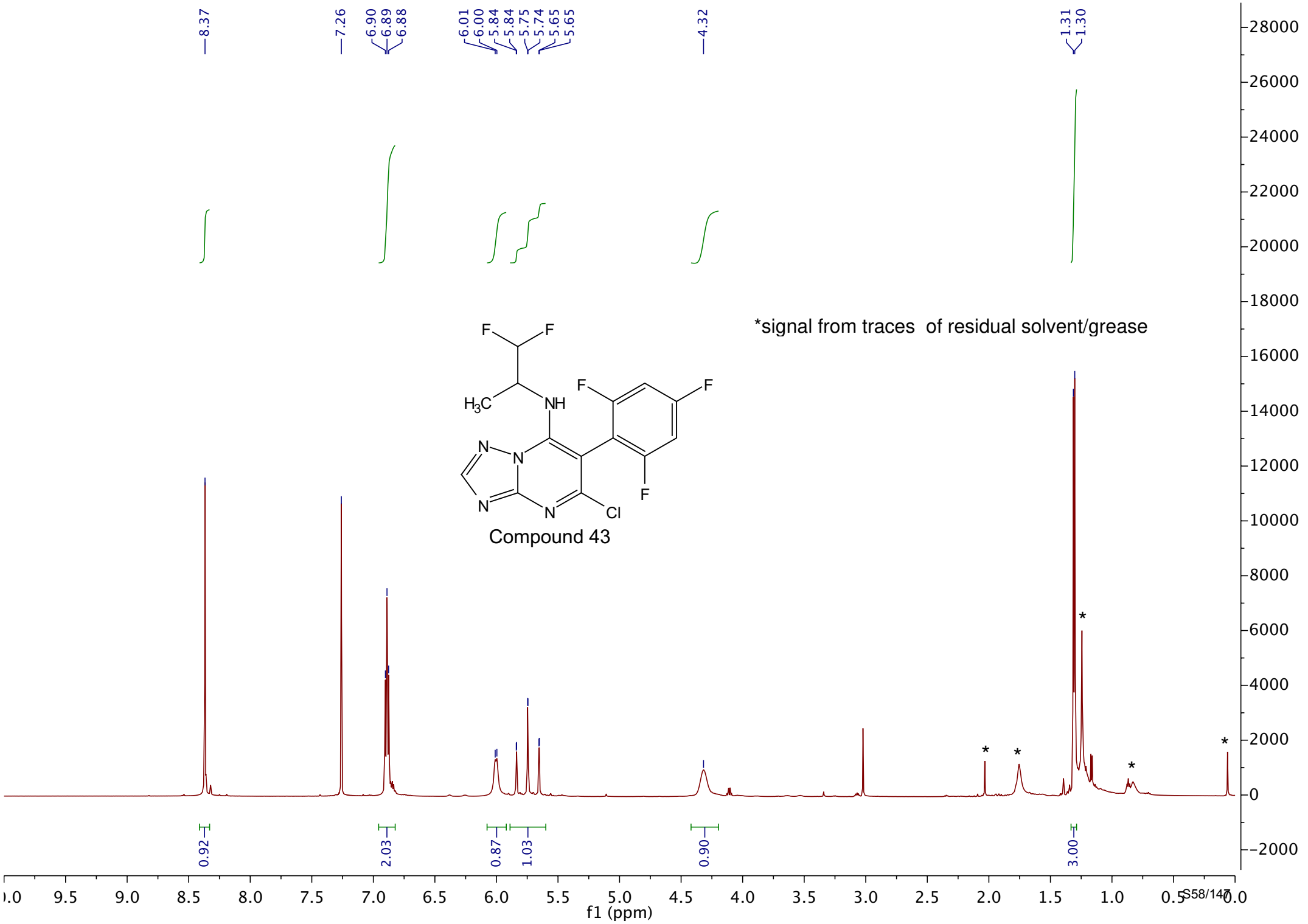
8.37
7.26
6.90
6.89
6.88
6.01
6.00
5.84
5.84
5.75
5.74
5.65
5.65
4.32
1.31
1.30
F
F
H3C
NH
F
F
N
N
N
N
Cl
F
Compound 43
*signal from traces of residual solvent/grease
0.92
2.03
0.87
1.03
0.90
3.00
f1 (ppm)

165.40
165.30
165.20
163.71
163.61
162.39
162.35
162.33
162.29
162.29
162.25
162.23
162.20
160.71
160.66
160.63
160.61
160.58
157.94
155.46
154.22
146.36
116.22
114.59
112.96
106.06
106.02
105.92
105.89
105.78
105.75
101.83
101.80
101.65
101.63
101.61
101.48
101.46
101.44
101.29
101.26
90.88
77.37 CDCl3
77.16 CDCl3
76.95 CDCl3
51.24
51.09
50.93
46.07
42.31
38.75
29.82
14.64
14.61
14.59
Compound 43
f1 (ppm)
S59/1470

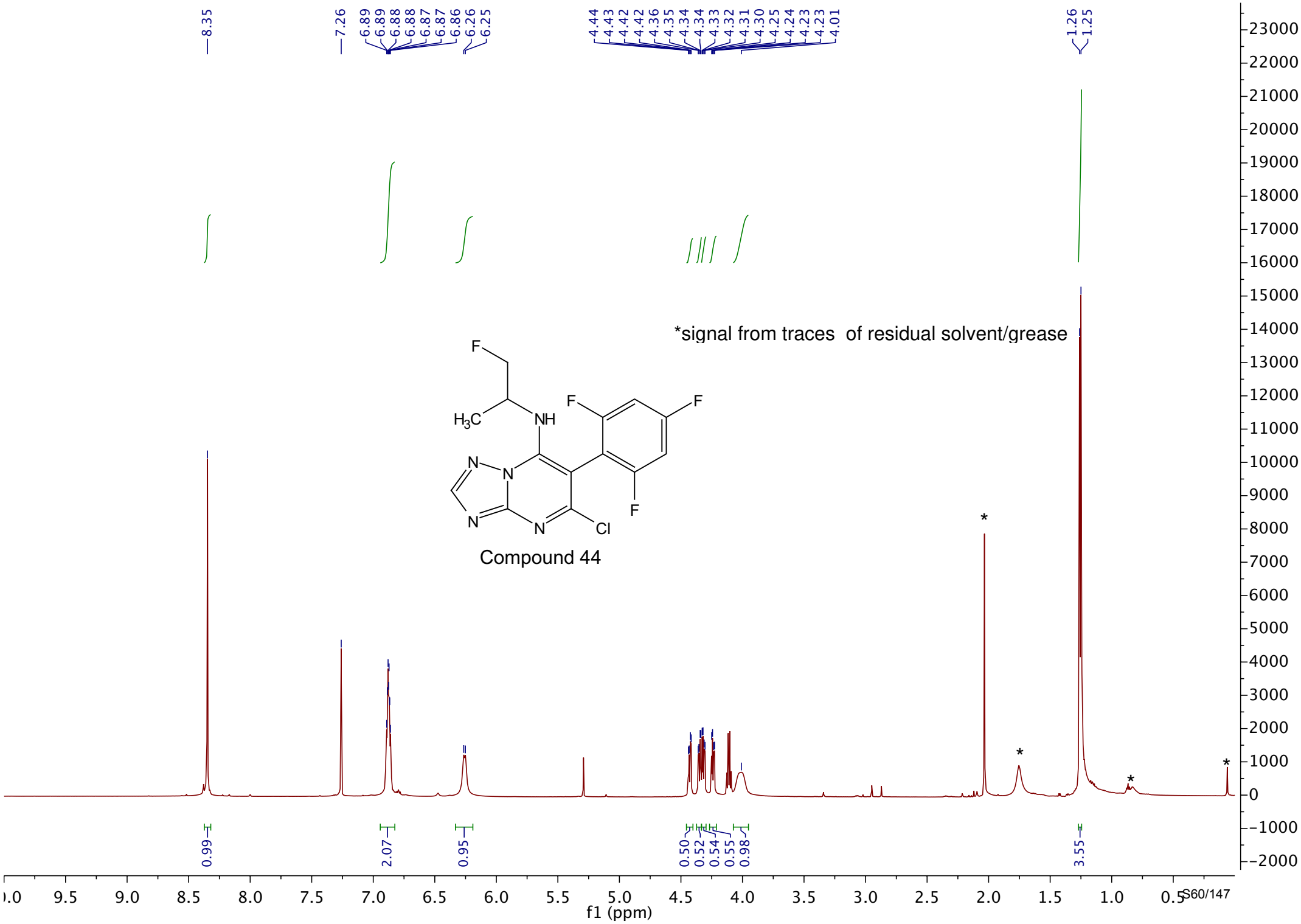
8.35
7.26
6.89
6.89
6.88
6.88
6.87
6.87
6.86
6.26
6.25
4.44
4.43
4.42
4.42
4.36
4.35
4.34
4.34
4.33
4.32
4.31
4.30
4.25
4.24
4.23
4.01
1.26
1.25
*signal from traces of residual solvent/grease
F
H3C
NH
F
F
F
N
N
N
N
Cl
Compound 44
0.99
2.07
0.95
0.50
0.52
0.54
0.55
0.98
3.55
f1 (ppm)
S60/147

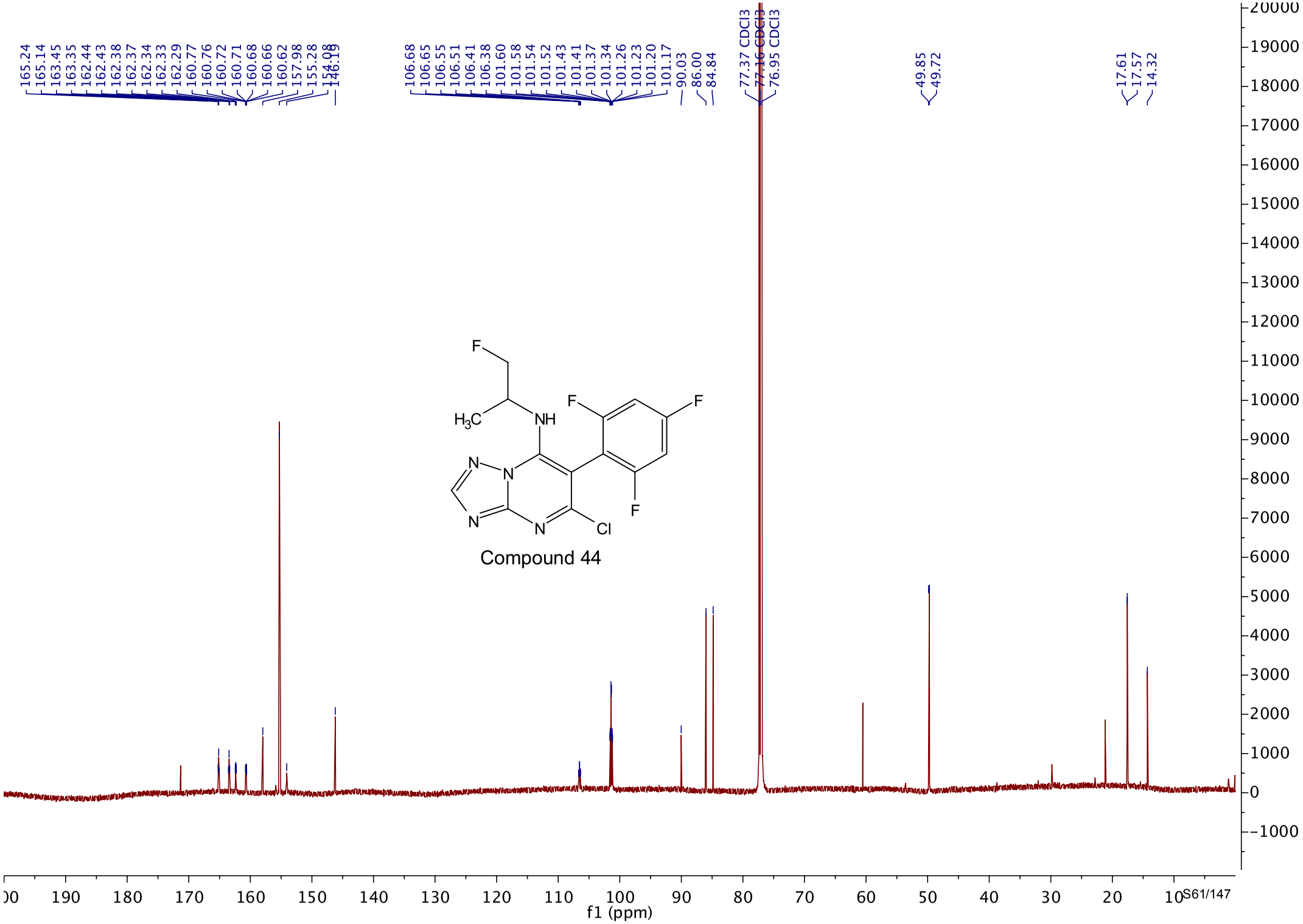
165.24
165.14
163.45
163.35
162.44
162.43
162.38
162.37
162.34
162.33
162.29
160.77
160.76
160.72
160.71
160.68
160.66
160.62
157.98
155.28
154.98
146.19
106.68
106.65
106.55
106.51
106.41
106.38
101.60
101.58
101.54
101.52
101.43
101.41
101.37
101.34
101.26
101.23
101.20
101.17
90.03
86.00
84.84
77.37 CDCl3
77.16 CDCl3
76.95 CDCl3
49.85
49.72
17.61
17.57
14.32
F
H3C
NH
F
F
N
N
N
N
Cl
F
Compound 44
f1 (ppm)
S61/147

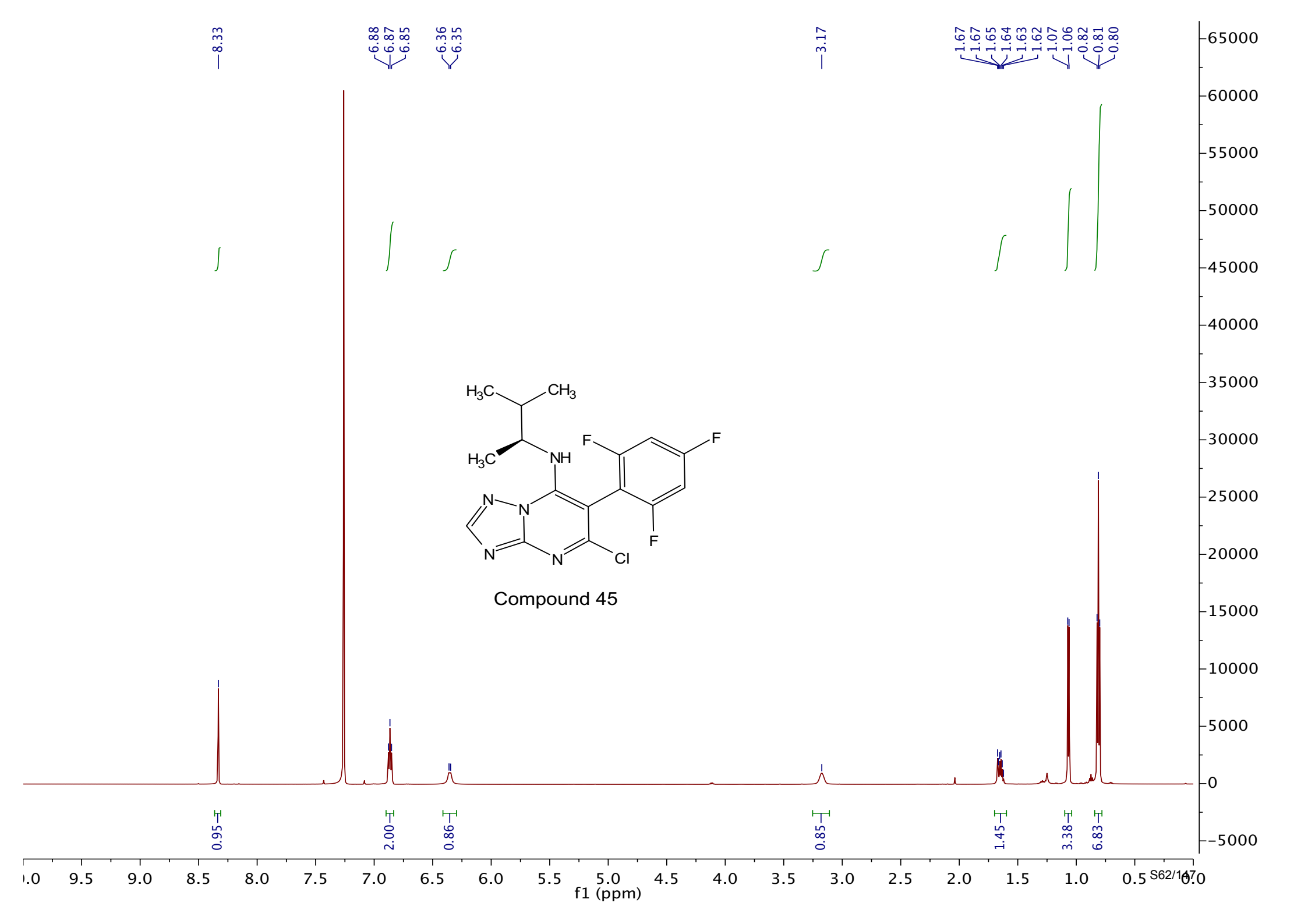
8.33
6.88
6.87
6.85
6.36
6.35
3.17
1.67
1.67
1.65
1.64
1.63
1.62
1.07
1.06
0.82
0.81
0.80
H3C
CH3
H3C
NH
F
F
F
N
N
N
N
Cl
Compound 45
0.95
2.00
0.86
0.85
1.45
3.38
6.83
f1 (ppm)
S62/147

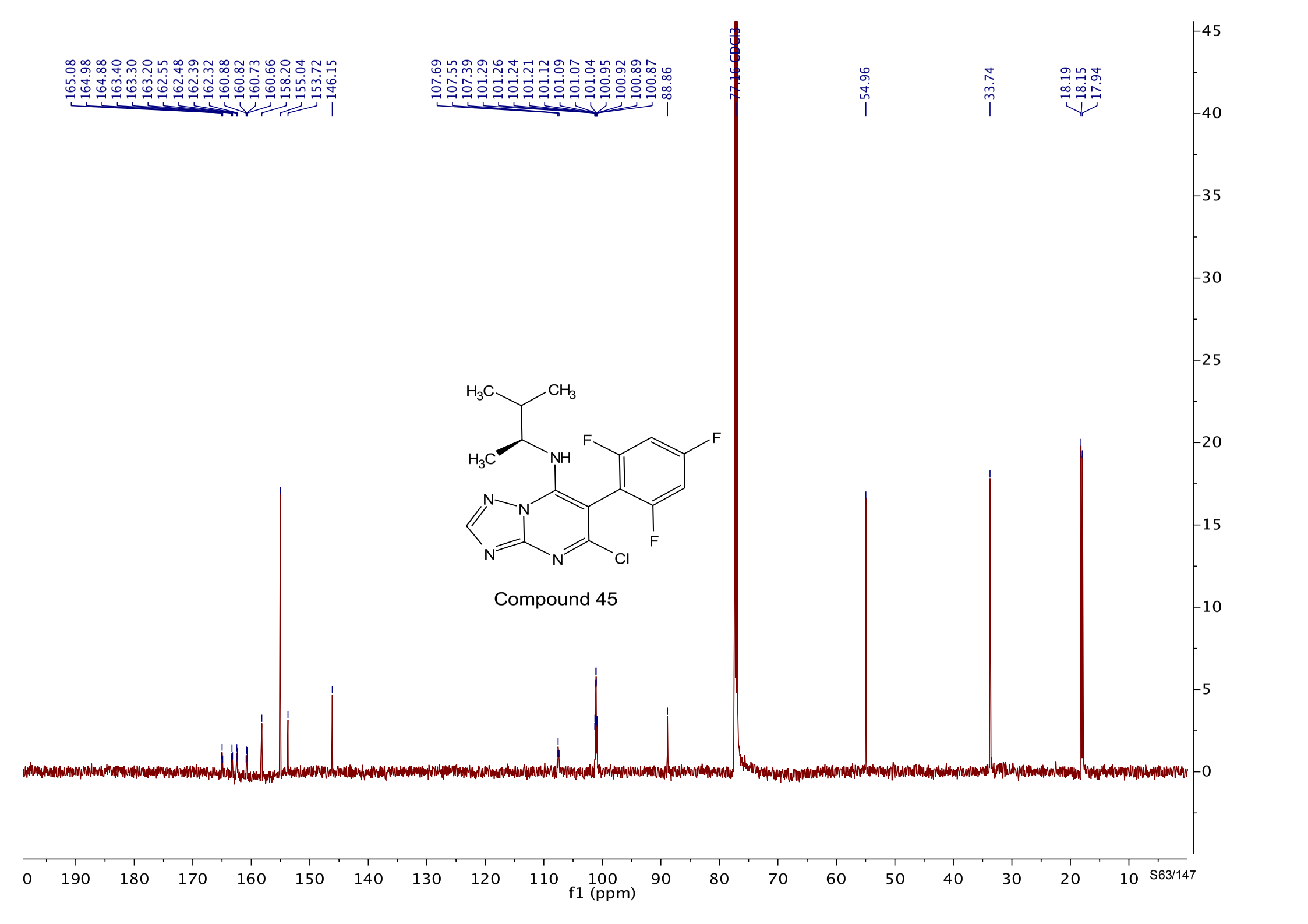
165.08
164.98
164.88
163.40
163.30
163.20
162.55
162.48
162.39
162.32
160.88
160.82
160.73
160.66
158.20
155.04
153.72
146.15
107.69
107.55
107.39
101.29
101.26
101.24
101.21
101.12
101.09
101.07
101.04
100.95
100.92
100.89
100.87
88.86
77.16 CDCl3
54.96
33.74
18.19
18.15
17.94
H3C
CH3
H3C
NH
F
F
F
N
N
N
N
Cl
Compound 45
45
40
35
30
25
20
15
10
5
0
0
190
180
170
160
150
140
130
120
110
100
90
80
70
60
50
40
30
20
10
f1 (ppm)
S63/147

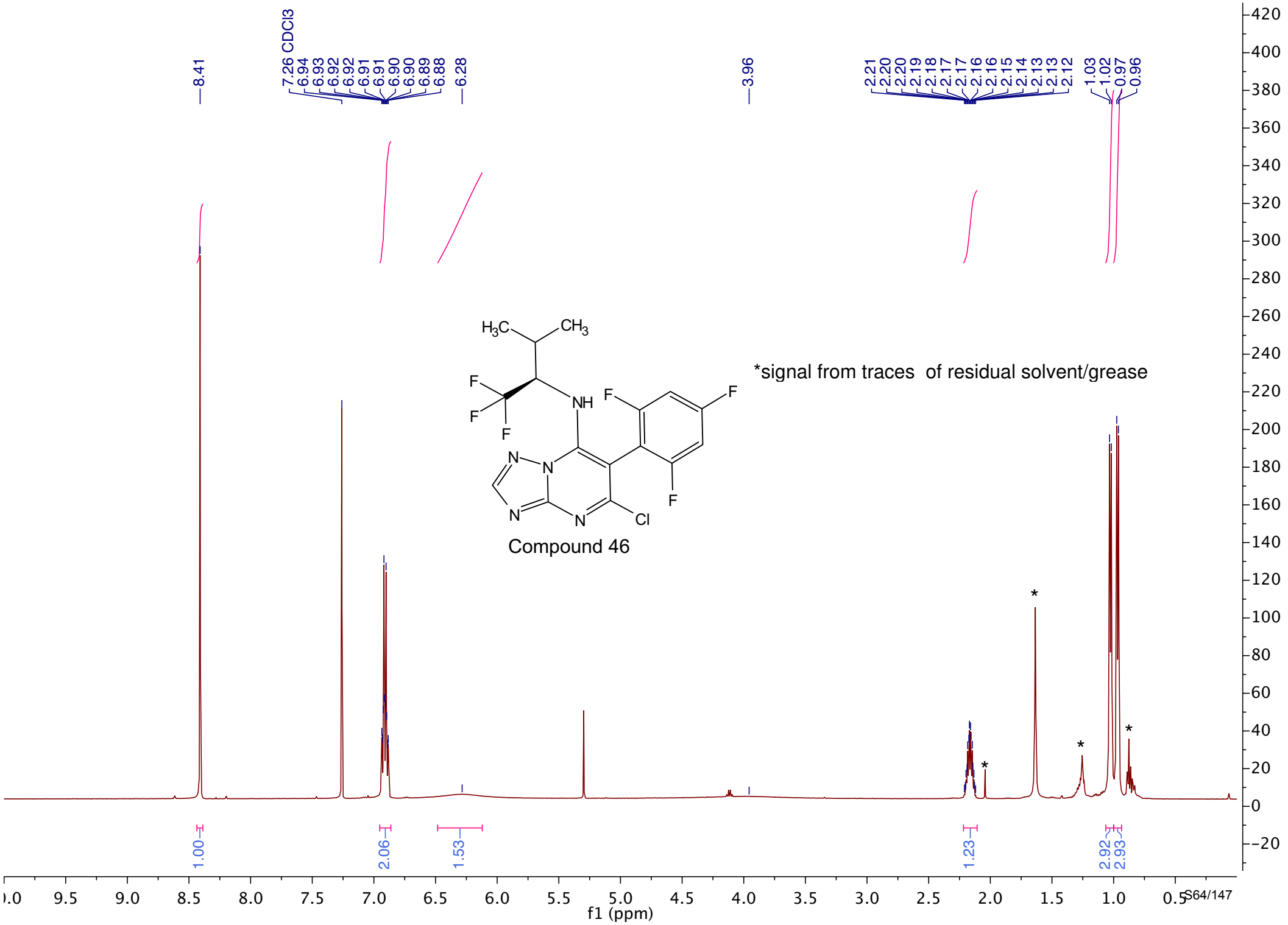
8.41
7.26 CDCl3
6.94
6.93
6.92
6.92
6.91
6.91
6.90
6.90
6.89
6.88
6.28
3.96
2.21
2.20
2.20
2.19
2.18
2.17
2.17
2.16
2.16
2.15
2.14
2.13
2.13
2.12
1.03
1.02
0.97
0.96
H3C
CH3
F
F
F
NH
F
F
F
N
N
N
N
Cl
Compound 46
*signal from traces of residual solvent/grease
1.00
2.06
1.53
1.23
2.92
2.93
f1 (ppm)

165.77
165.65
165.53
163.74
163.62
163.50
162.62
162.55
162.50
162.17
160.60
160.53
160.48
160.42
160.36
160.29
160.24
160.17
155.50
146.50
127.85
125.60
123.34
121.09
102.02
101.99
101.82
101.78
101.61
101.58
101.51
101.50
101.31
101.29
101.11
101.09
90.94
59.27
59.04
58.80
58.57
28.27
19.74
16.67
Compound 46
f1 (ppm)
S65/147

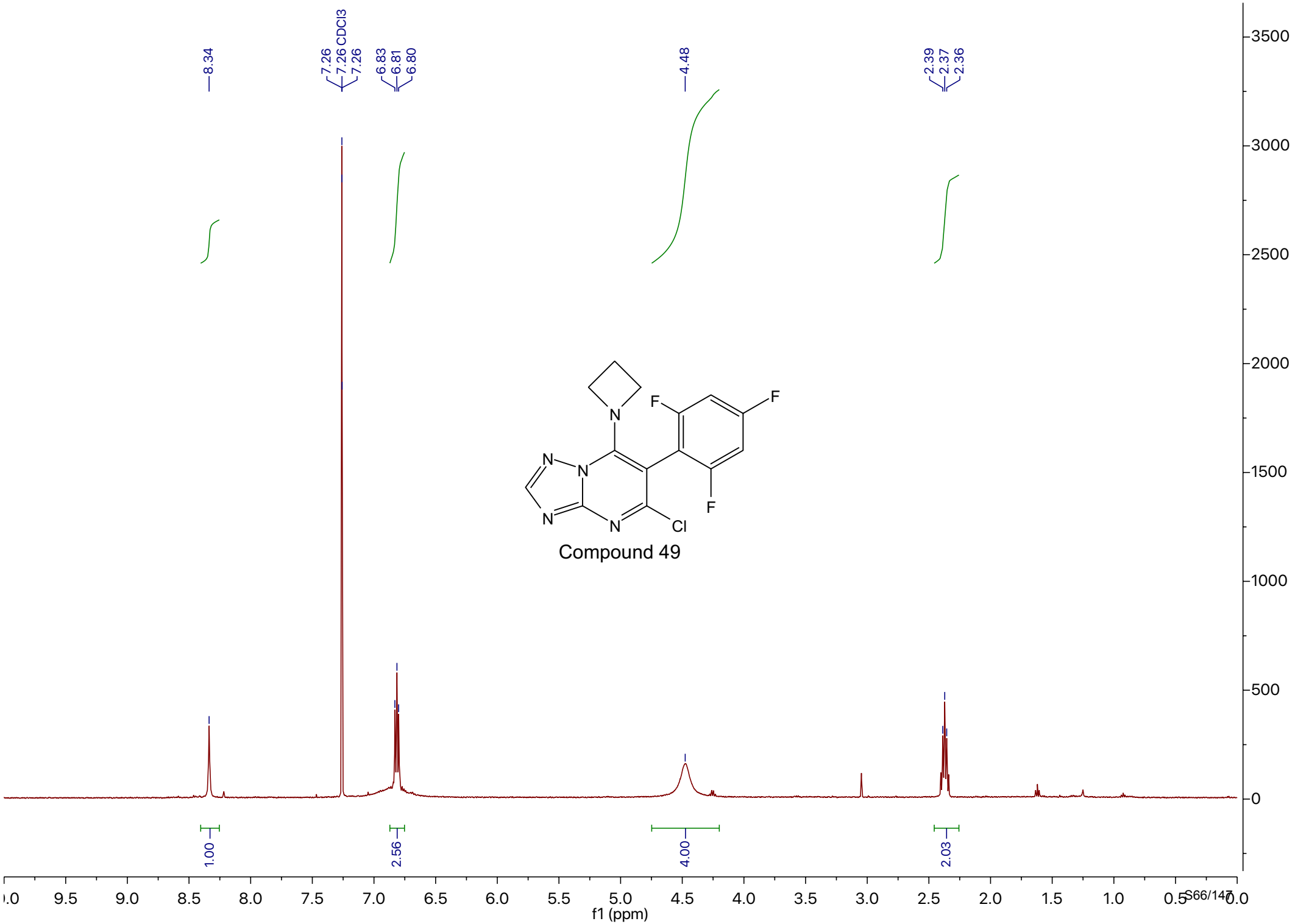
8.34
7.26
7.26 CDCl3
7.26
6.83
6.81
6.80
4.48
2.39
2.37
2.36
F
F
F
N
N
N
N
N
Cl
1.00
2.56
4.00
2.03
f1 (ppm)

Compound 49

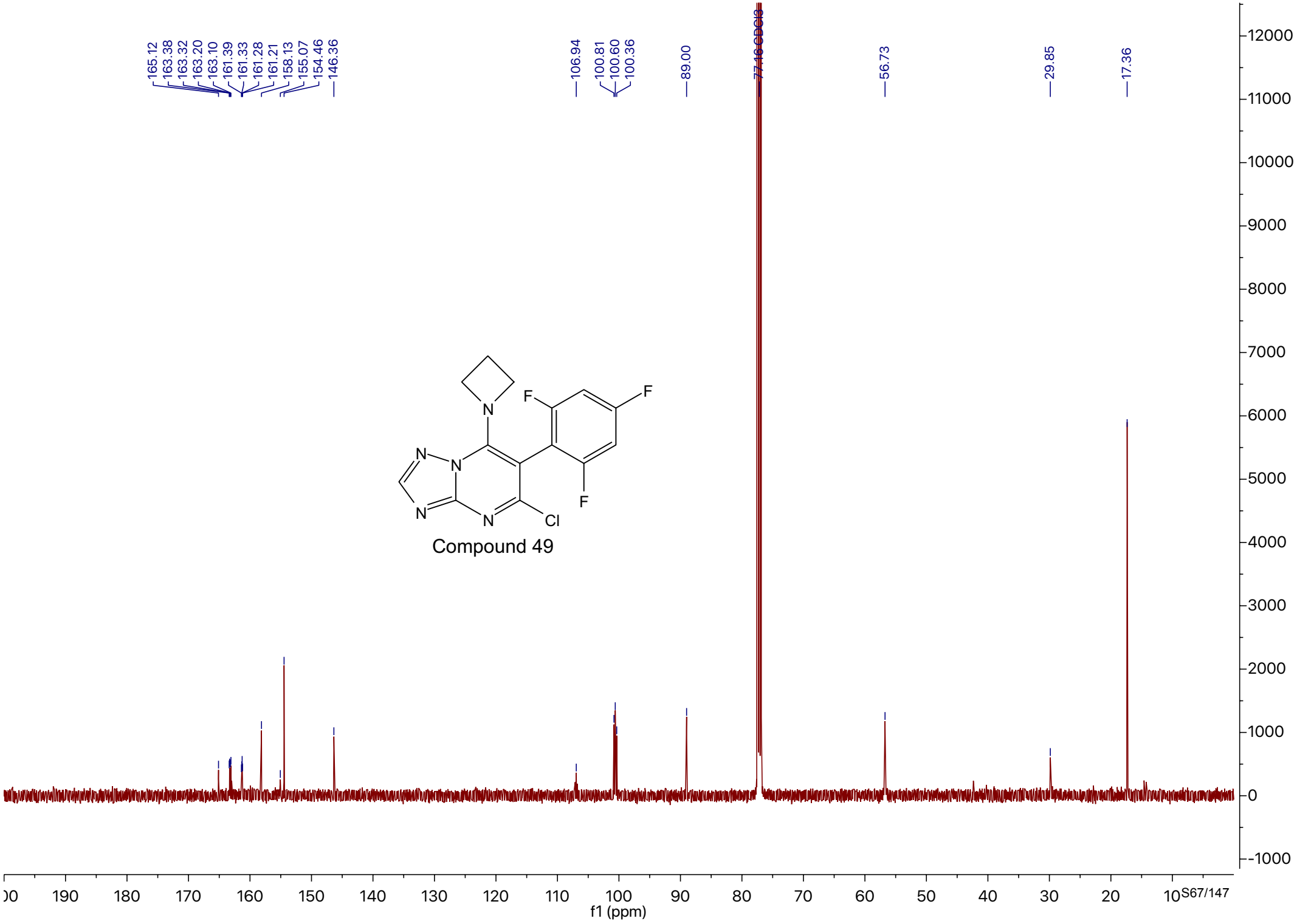
165.12
163.38
163.32
163.20
163.10
161.39
161.33
161.28
161.21
158.13
155.07
154.46
146.36
106.94
100.81
100.60
100.36
89.00
77.16 CDCl3
56.73
29.85
17.36
F
F
F
N
N
N
N
N
Cl
Compound 49
12000
11000
10000
9000
8000
7000
6000
5000
4000
3000
2000
1000
0
-1000
190
180
170
160
150
140
130
120
110
100
90
80
70
60
50
40
30
20
10
f1 (ppm)

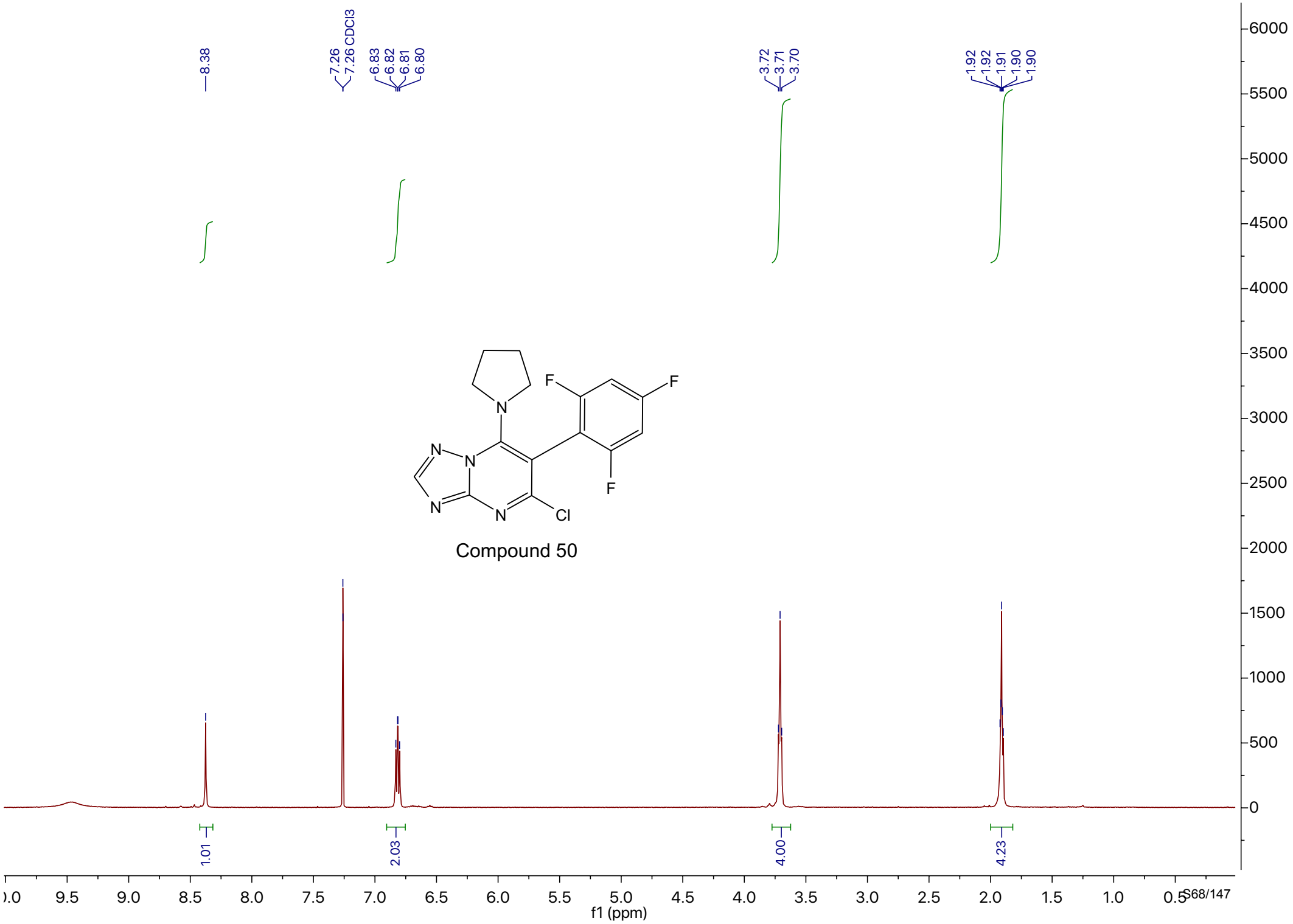
8.38
7.26
7.26 CDCl3
6.83
6.82
6.81
6.80
3.72
3.71
3.70
1.92
1.92
1.91
1.90
1.90
F
F
F
N
N
N
N
N
Cl
1.01
2.03
4.00
4.23
f1 (ppm)

Compound 50

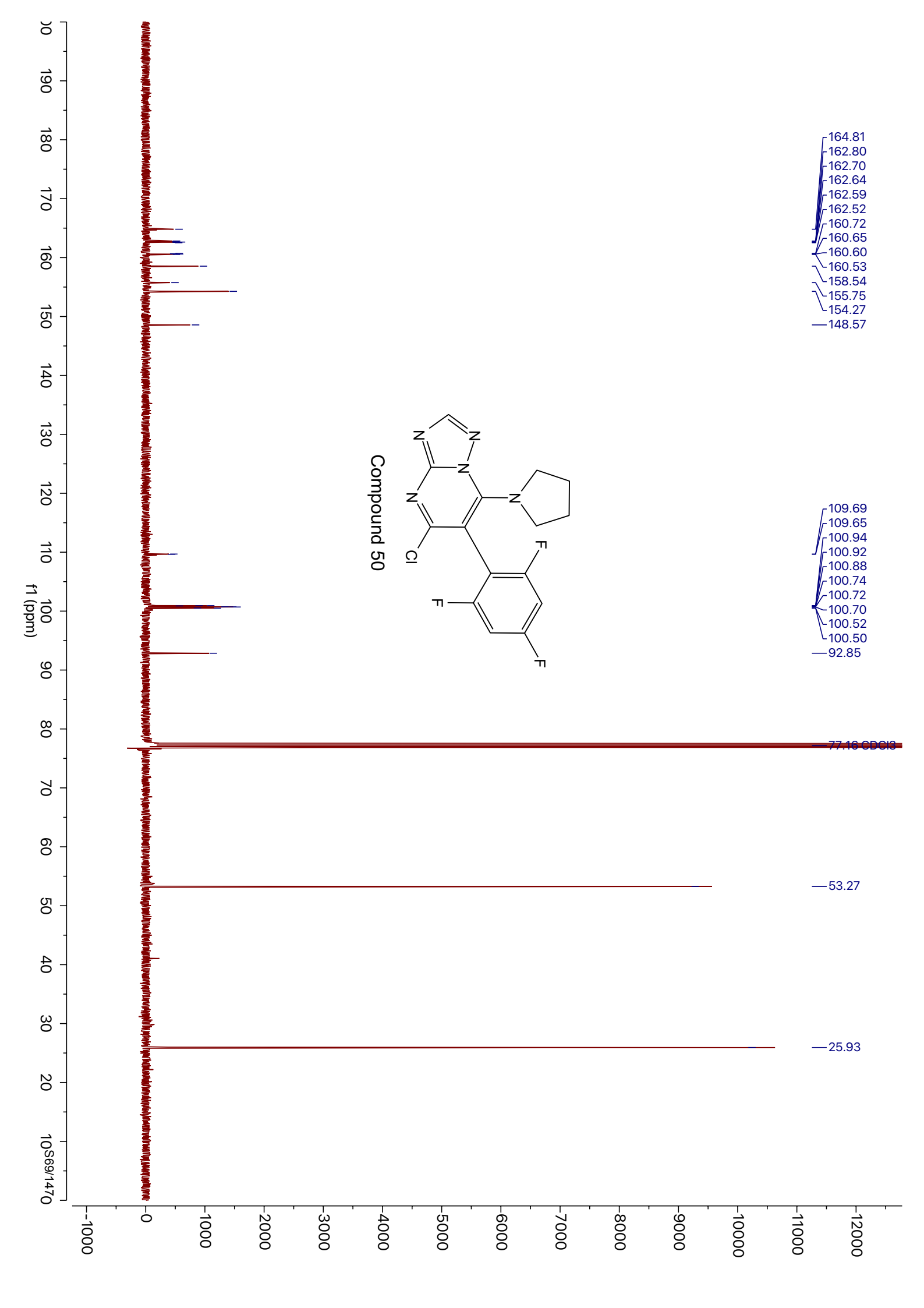
164.81
162.80
162.70
162.64
162.59
162.52
160.72
160.65
160.60
160.53
158.54
155.75
154.27
148.57
109.69
109.65
100.94
100.92
100.88
100.74
100.72
100.70
100.52
100.50
92.85
77.16 CDCl3
53.27
25.93
Compound 50
N
N
N
N
Cl
F
F
F
f1 (ppm)
S69/1470

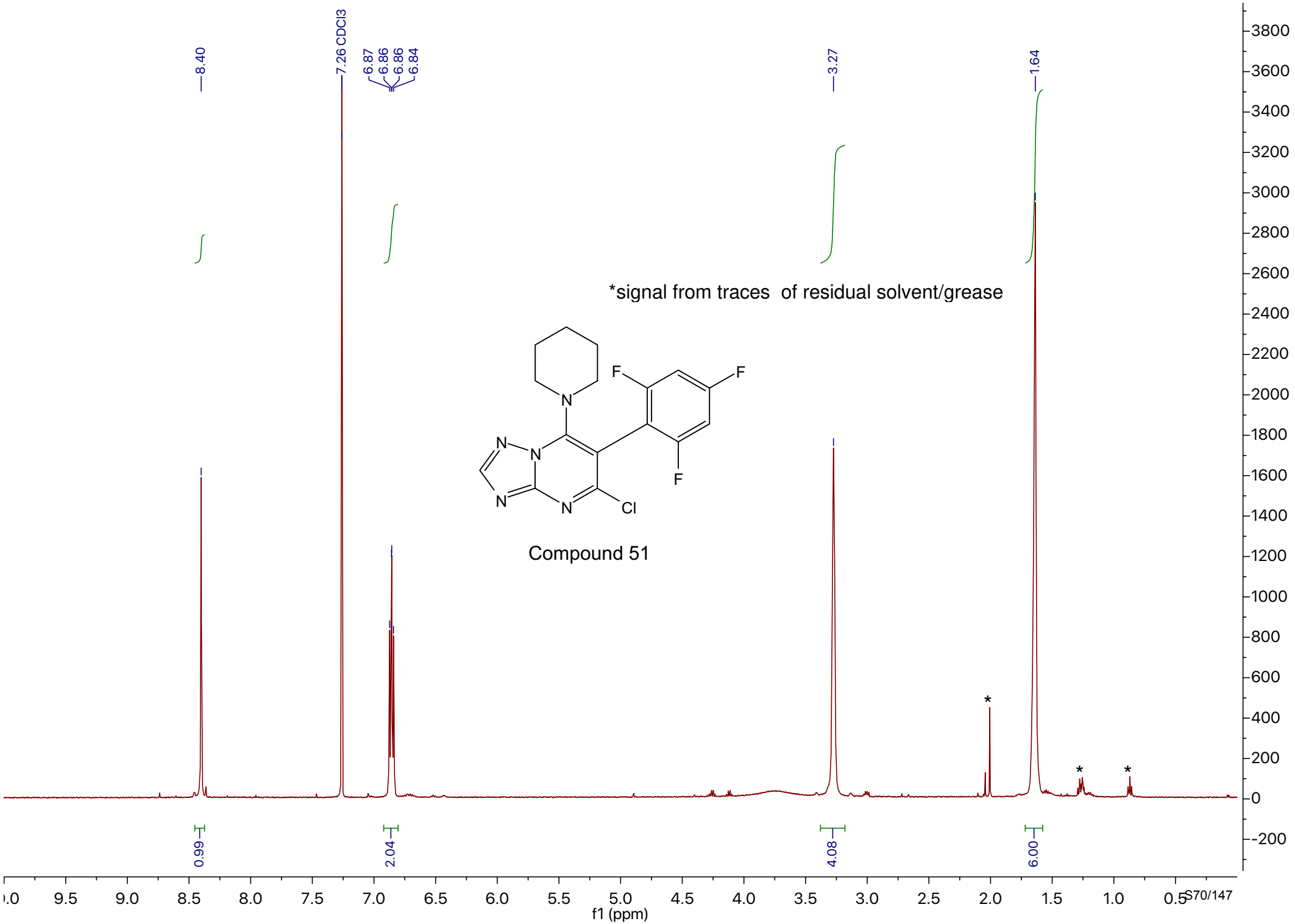
8.40
7.26 CDCl3
6.87
6.86
6.86
6.84
3.27
1.64
*signal from traces of residual solvent/grease
F
F
F
N
N
N
N
N
Cl
Compound 51
0.99
2.04
4.08
6.00
f1 (ppm)
S70/147

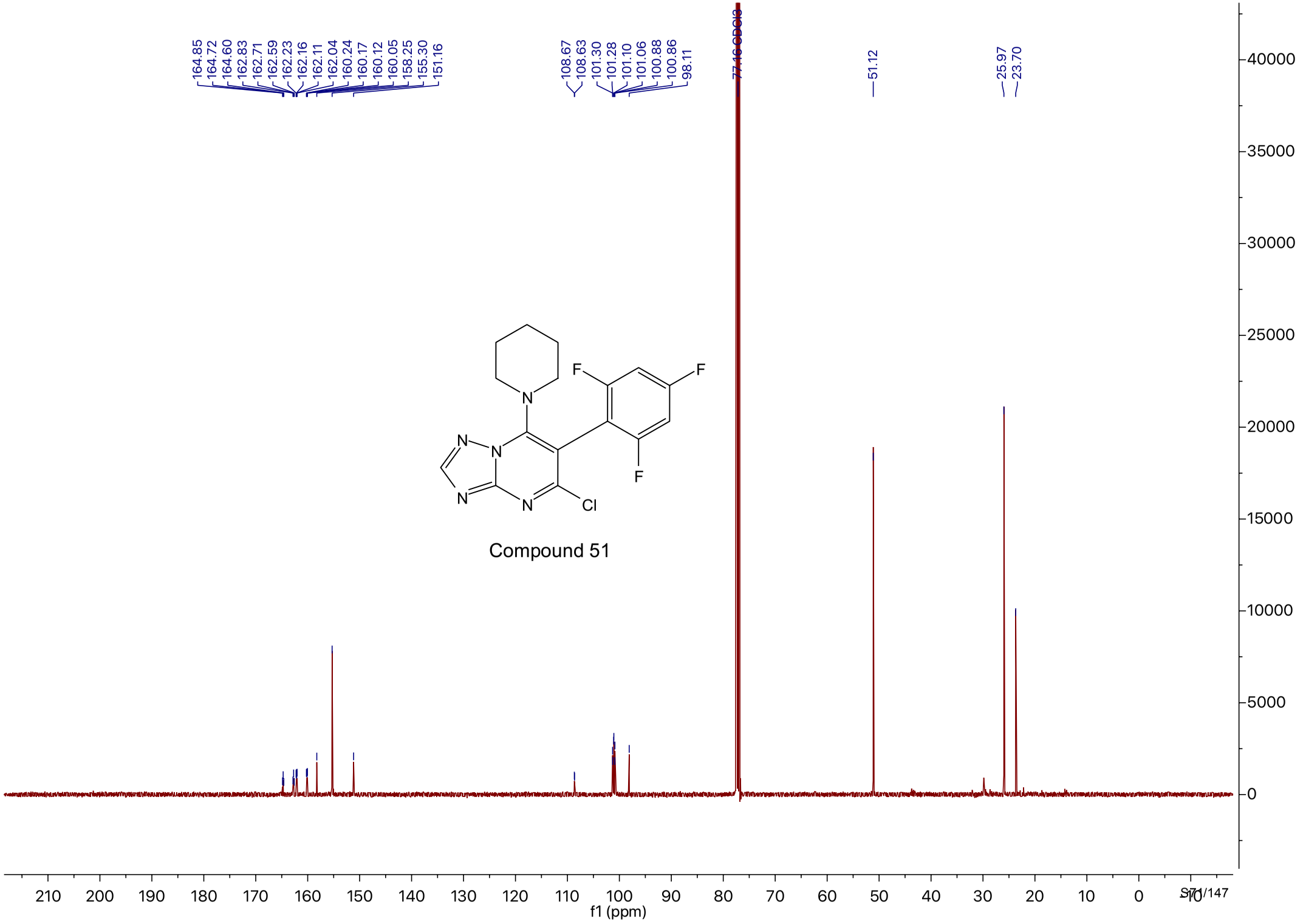
164.85
164.72
164.60
162.83
162.71
162.59
162.23
162.16
162.11
162.04
160.24
160.17
160.12
160.05
158.25
155.30
151.16
108.67
108.63
101.30
101.28
101.10
101.06
100.88
100.86
98.11
77.16 CDCl3
51.12
25.97
23.70
F
F
F
N
N
N
N
N
Cl
Compound 51
40000
35000
30000
25000
20000
15000
10000
5000
0
210
200
190
180
170
160
150
140
130
120
110
100
90
80
70
60
50
40
30
20
10
0
f1 (ppm)

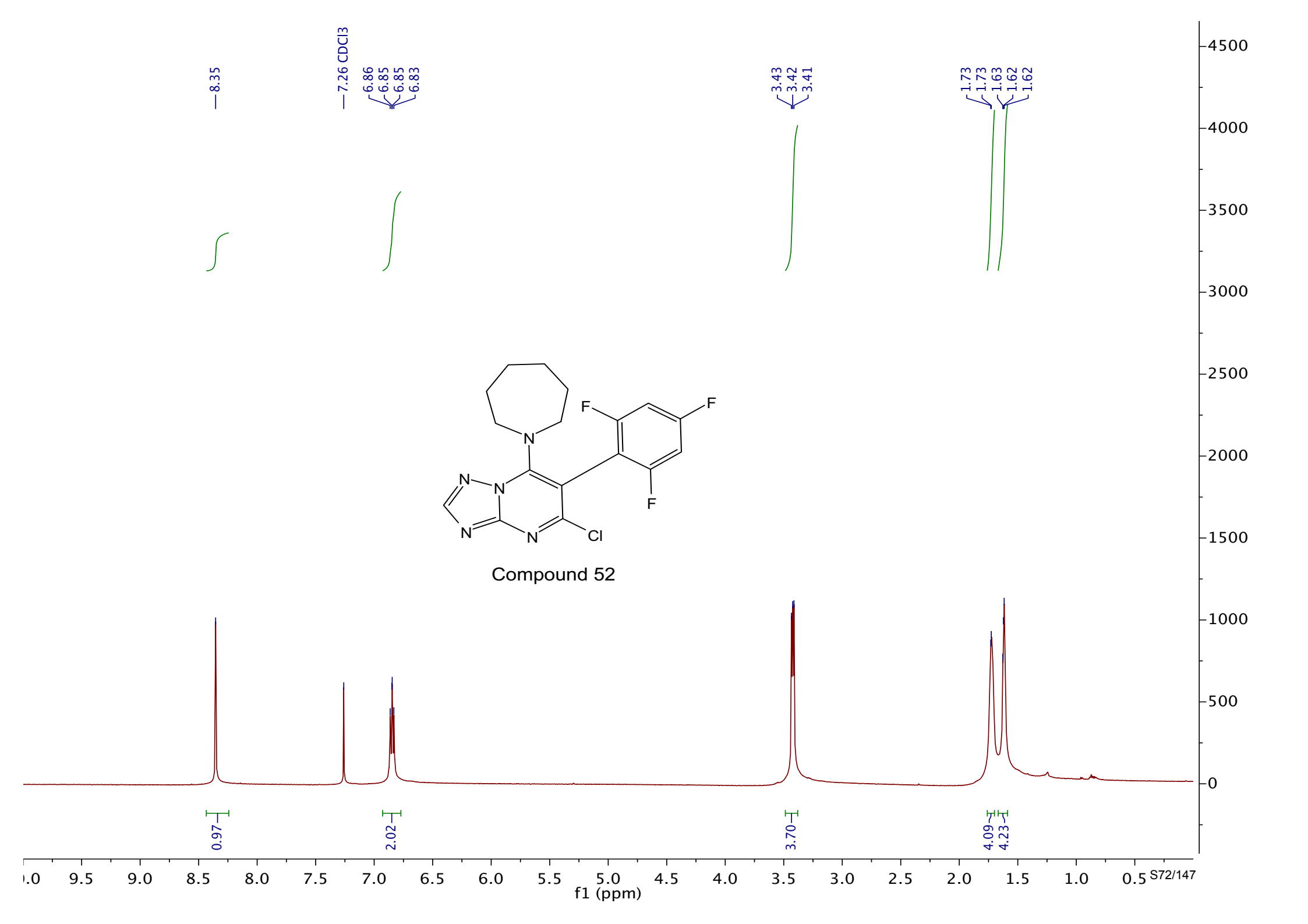
8.35
7.26 CDCl3
6.86
6.85
6.85
6.83
3.43
3.42
3.41
1.73
1.73
1.63
1.62
1.62
F
F
F
N
N
N
N
N
Cl
Compound 52
0.97
2.02
3.70
4.09
4.23
f1 (ppm)
S72/147

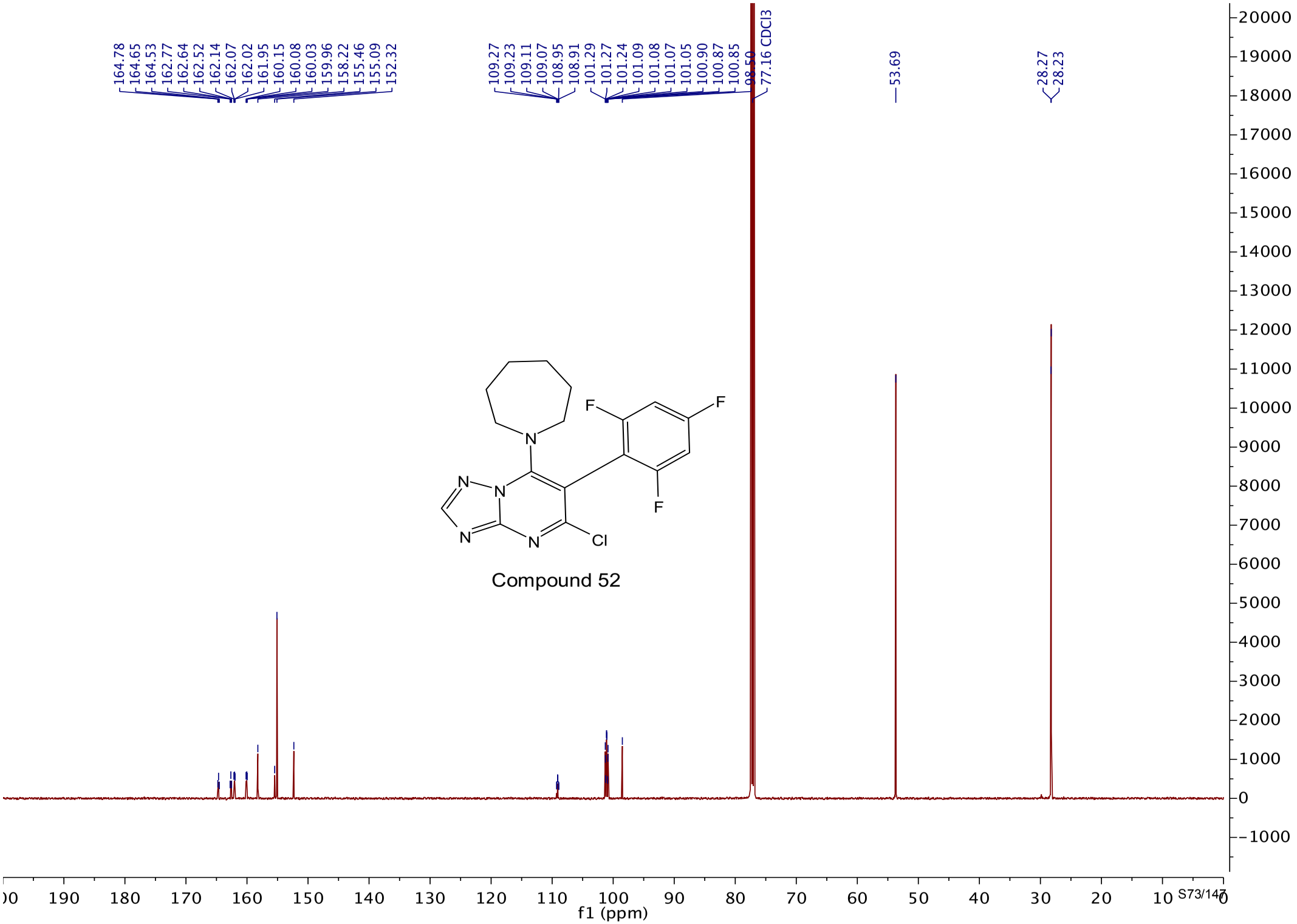
164.78
164.65
164.53
162.77
162.64
162.52
162.14
162.07
162.02
161.95
160.15
160.08
160.03
159.96
158.22
155.46
155.09
152.32
109.27
109.23
109.11
109.07
108.95
108.91
101.29
101.27
101.24
101.09
101.08
101.07
101.05
100.90
100.87
100.85
98.50
77.16 CDCl3
53.69
28.27
28.23
F
F
F
N
N
N
N
N
Cl
Compound 52
f1 (ppm)
S73/147

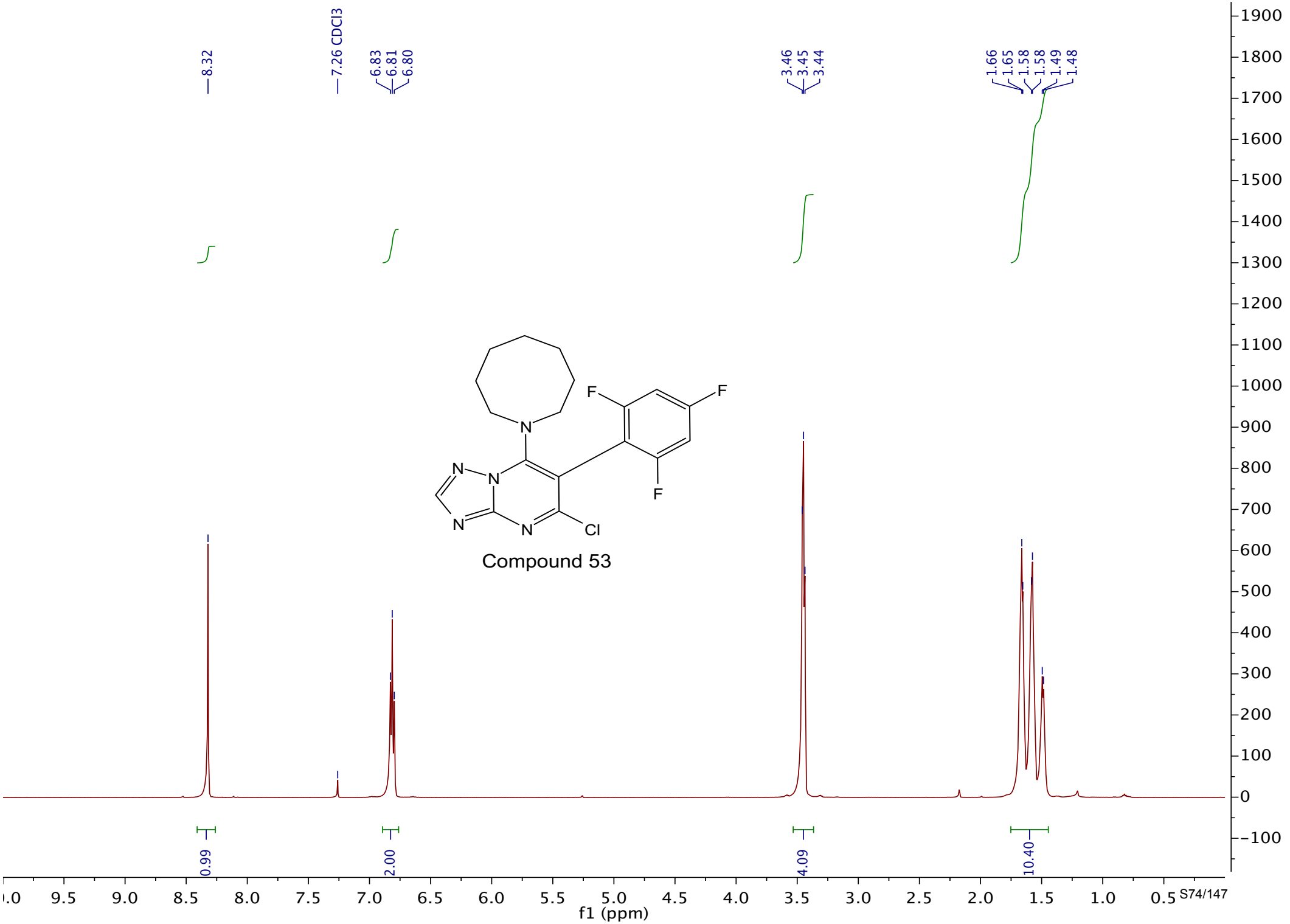
8.32
7.26 CDCl3
6.83
6.81
6.80
3.46
3.45
3.44
1.66
1.65
1.58
1.58
1.49
1.48
F
F
F
N
N
N
N
N
Cl
Compound 53
0.99
2.00
4.09
10.40
f1 (ppm)
S74/147

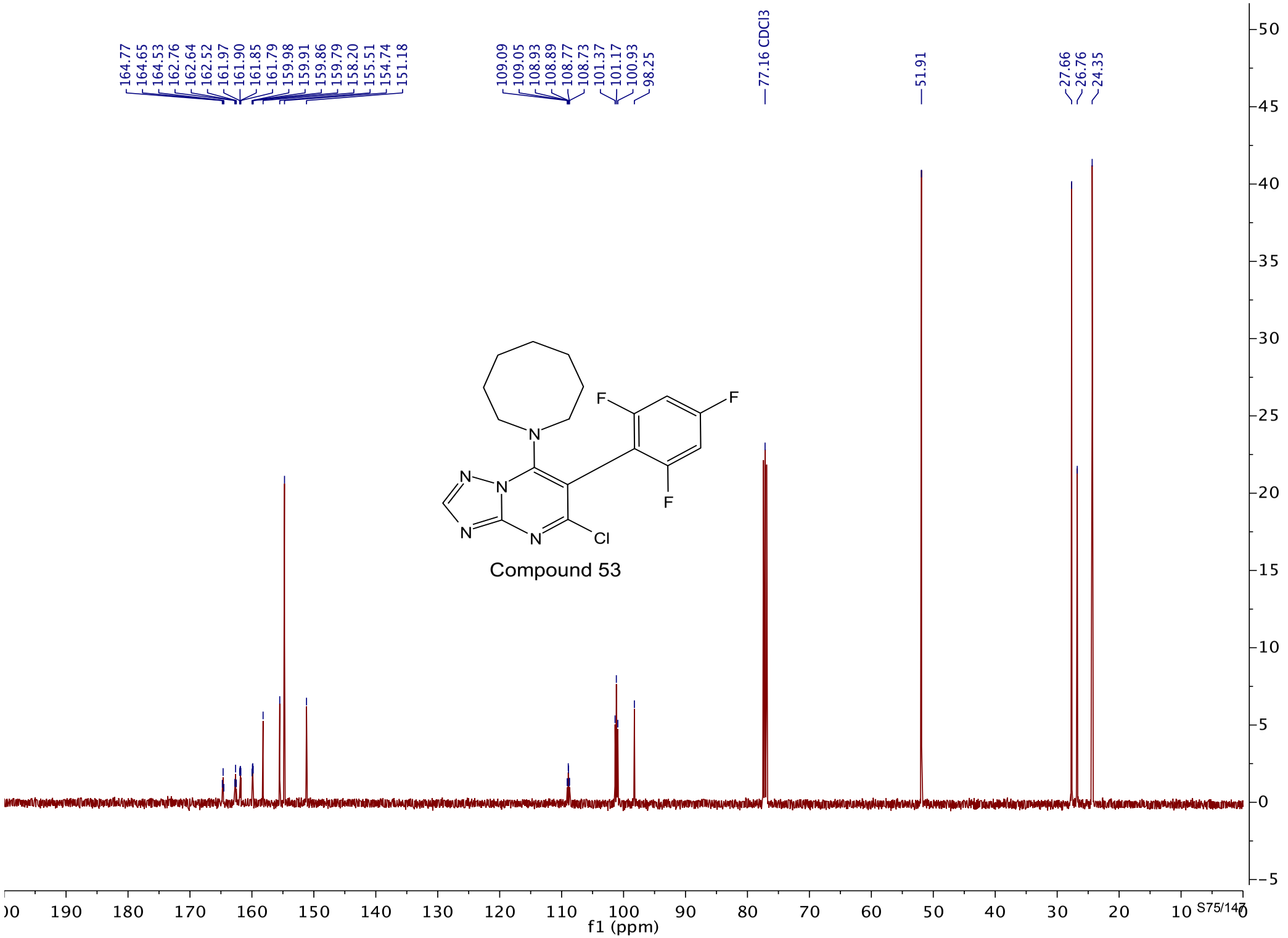
164.77
164.65
164.53
162.76
162.64
162.52
161.97
161.90
161.85
161.79
159.98
159.91
159.86
159.79
158.20
155.51
154.74
151.18
109.09
109.05
108.93
108.89
108.77
108.73
101.37
101.17
100.93
98.25
77.16 CDCl3
51.91
27.66
26.76
24.35
F
F
F
N
N
N
N
N
Cl
Compound 53
f1 (ppm)
S75/147

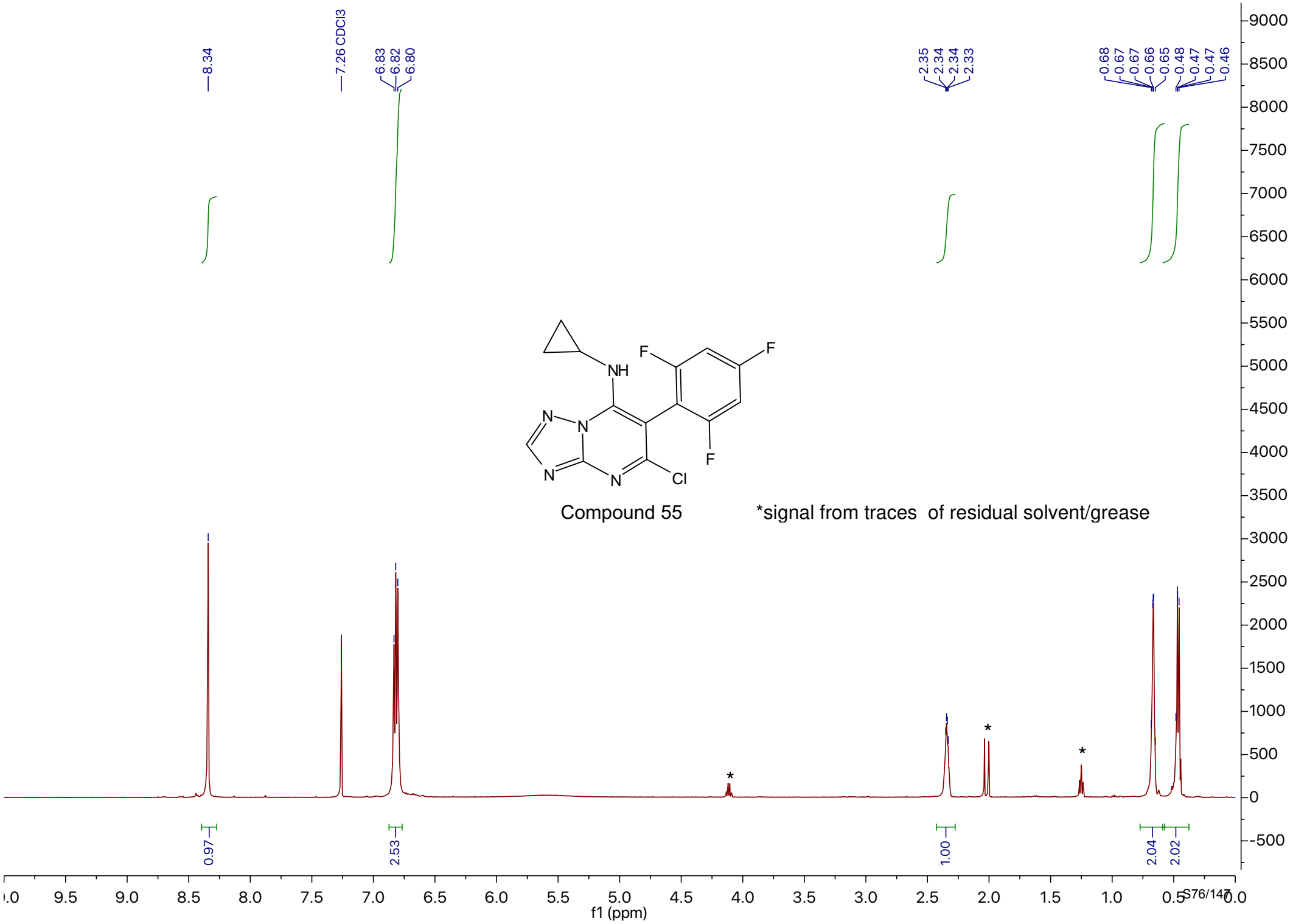

Compound 55

*signal from traces of residual solvent/grease

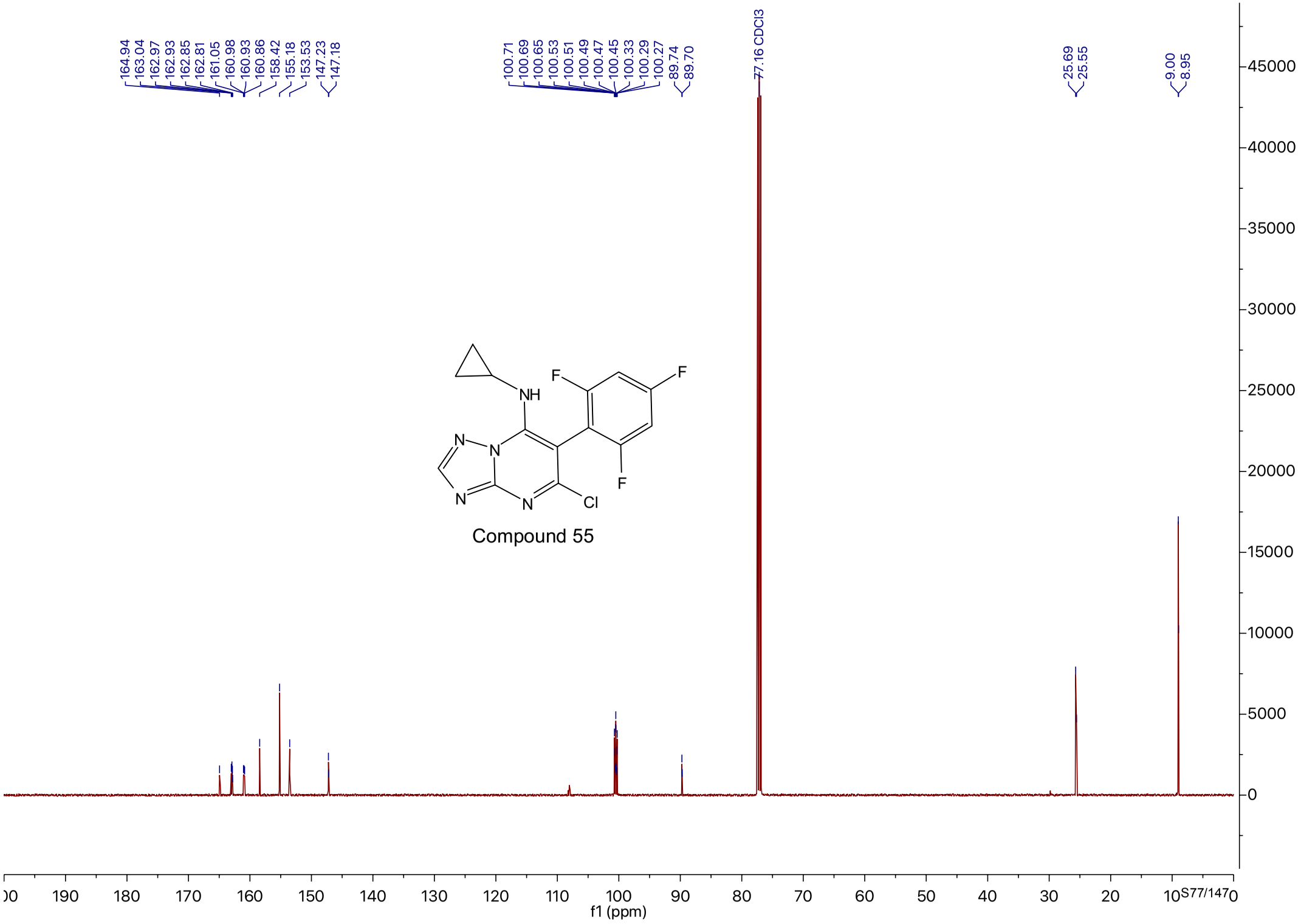
164.94
163.04
162.97
162.93
162.85
162.81
161.05
160.98
160.93
160.86
158.42
155.18
153.53
147.23
147.18
100.71
100.69
100.65
100.53
100.51
100.49
100.47
100.45
100.33
100.29
100.27
89.74
89.70
77.16 CDCl3
25.69
25.55
9.00
8.95
NH
F
F
F
N
N
N
N
Cl
Compound 55
45000
40000
35000
30000
25000
20000
15000
10000
5000
0
f1 (ppm)
S77/147

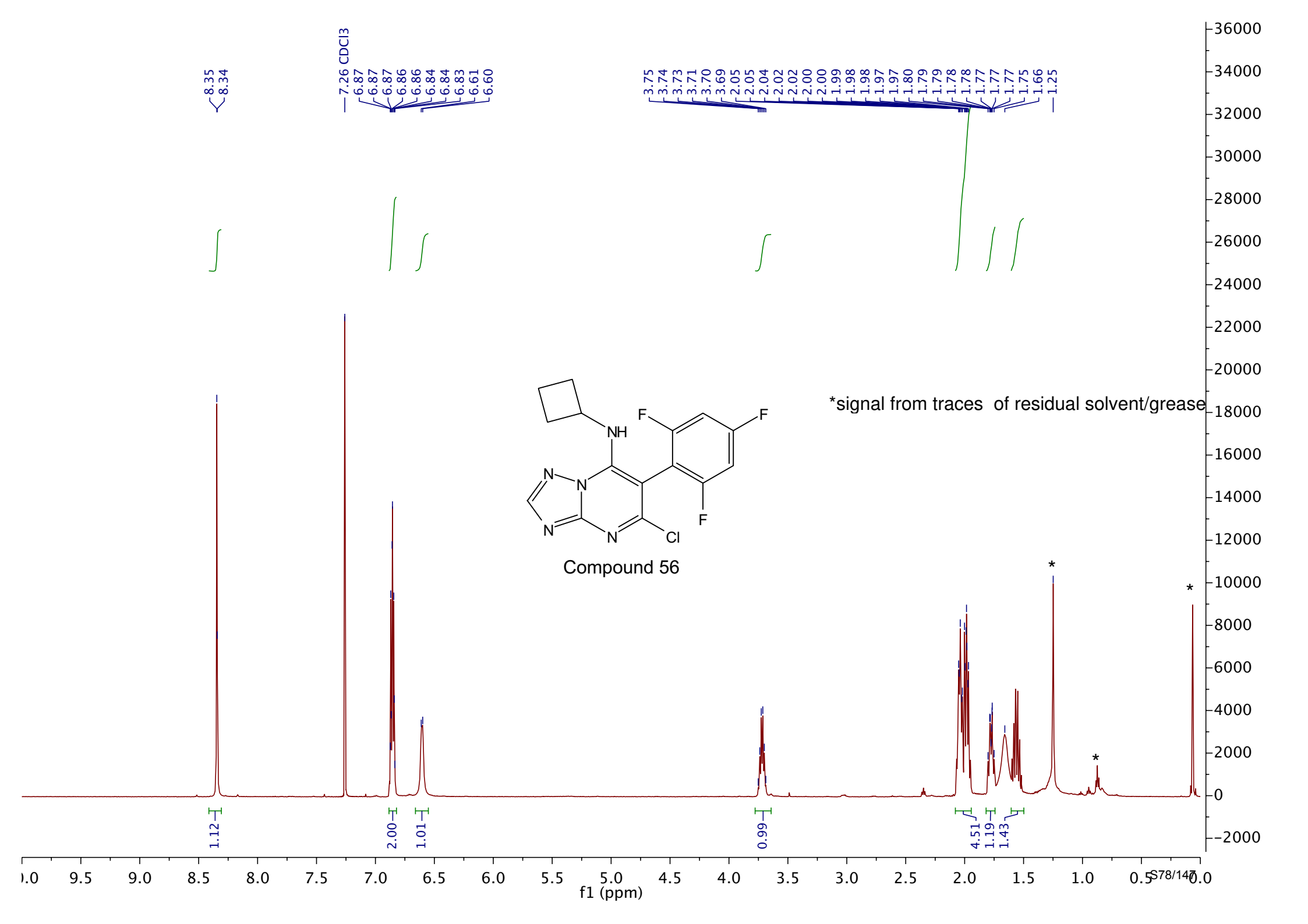
8.35
8.34
7.26 CDCl3
6.87
6.87
6.87
6.86
6.86
6.84
6.84
6.83
6.61
6.60
3.75
3.74
3.73
3.71
3.70
3.69
2.05
2.05
2.04
2.02
2.02
2.00
2.00
1.99
1.98
1.98
1.97
1.97
1.80
1.79
1.79
1.78
1.78
1.77
1.77
1.77
1.75
1.66
1.25
NH
F
F
F
N
N
N
N
Cl
Compound 56
*signal from traces of residual solvent/grease
1.12
2.00
1.01
0.99
4.51
1.19
1.43
f1 (ppm)

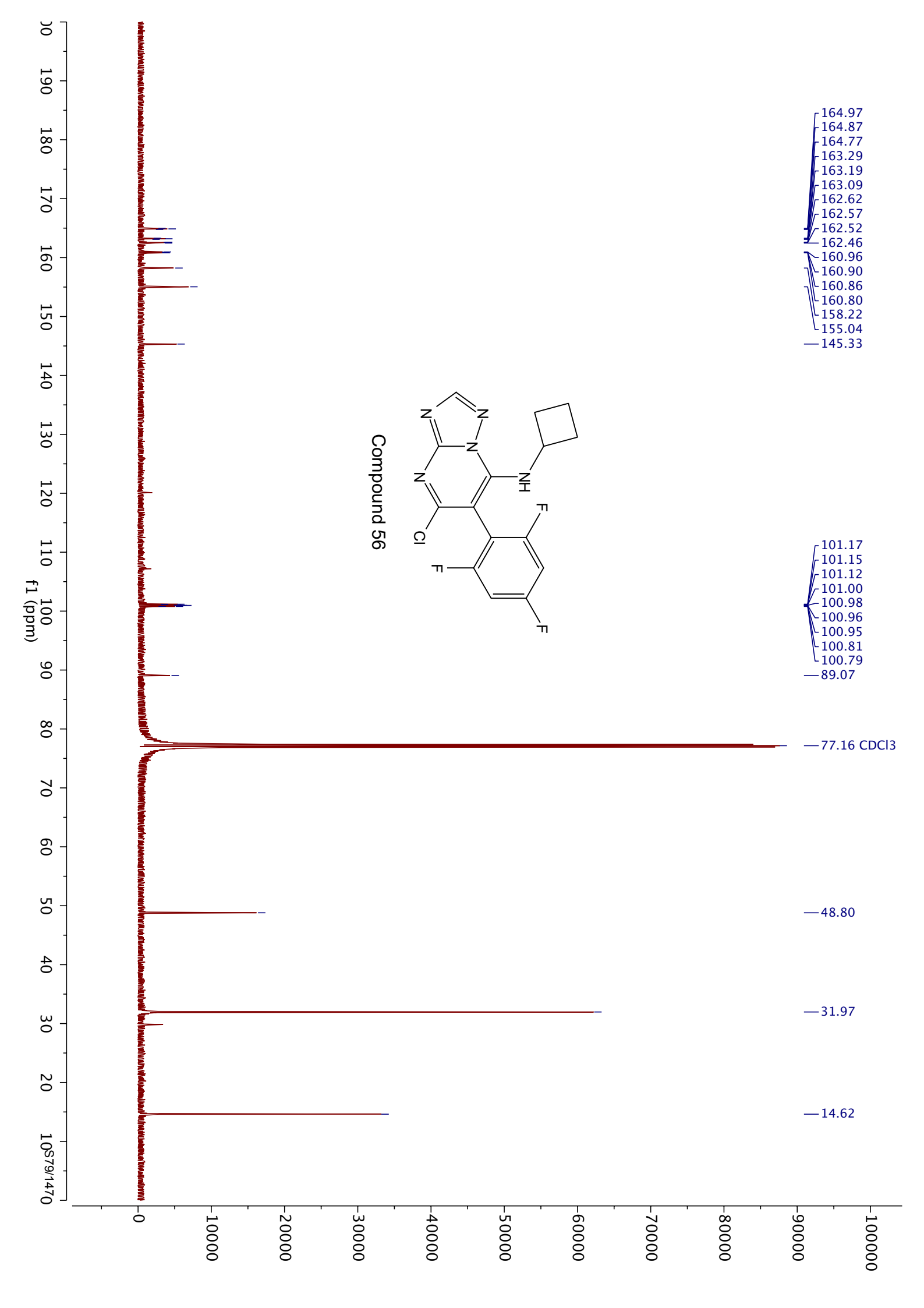
Compound 56
f1 (ppm)
164.97
164.87
164.77
163.29
163.19
163.09
162.62
162.57
162.52
162.46
160.96
160.90
160.86
160.80
158.22
155.04
145.33
101.17
101.15
101.12
101.00
100.98
100.96
100.95
100.81
100.79
89.07
77.16 CDCl3
48.80
31.97
14.62
N
N
N
N
NH
Cl
F
F
F

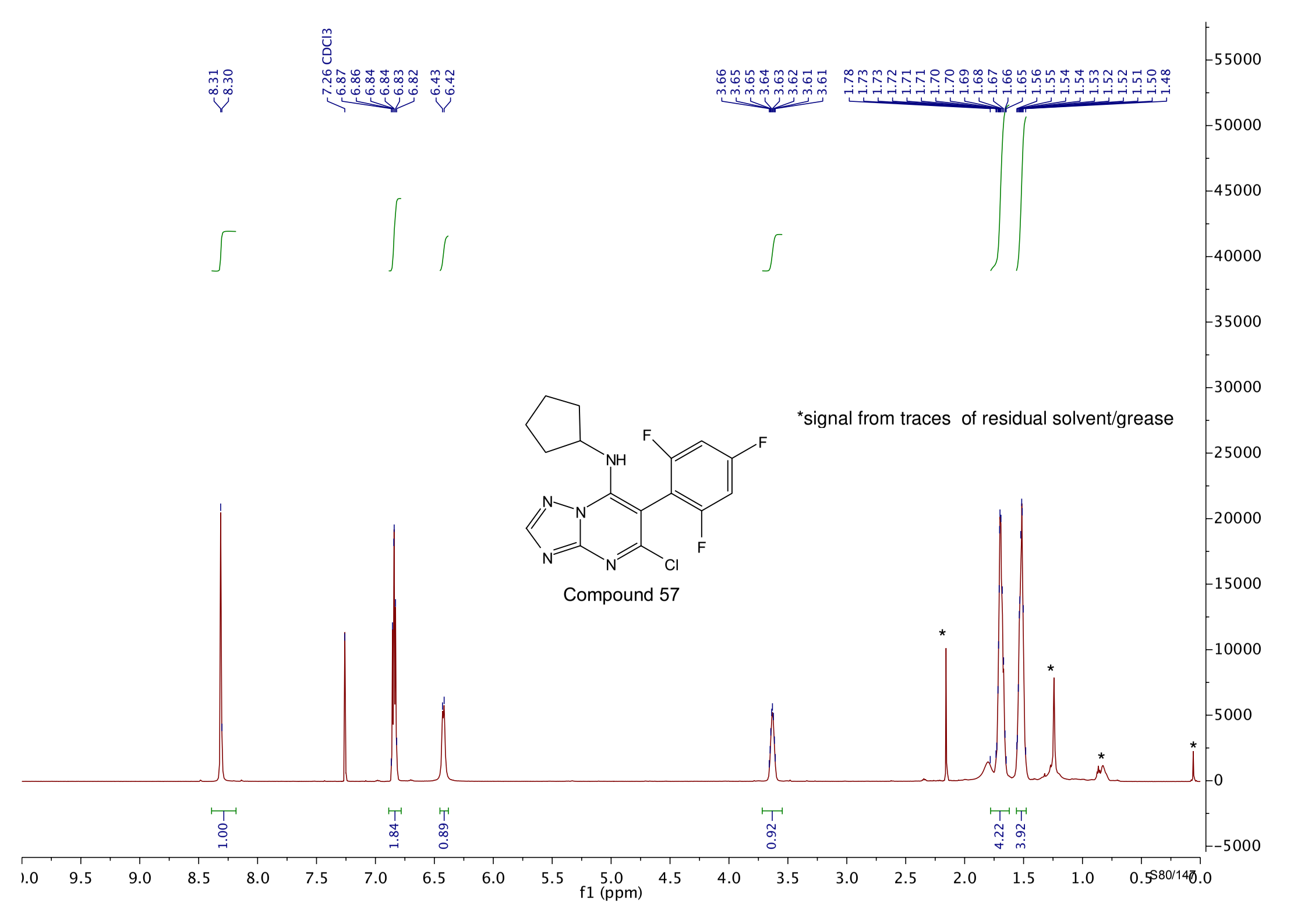
8.31
8.30
7.26 CDCl3
6.87
6.86
6.84
6.84
6.83
6.82
6.43
6.42
3.66
3.65
3.65
3.64
3.63
3.62
3.61
3.61
1.78
1.73
1.73
1.72
1.71
1.71
1.70
1.70
1.69
1.68
1.67
1.66
1.65
1.56
1.55
1.54
1.54
1.53
1.52
1.52
1.51
1.50
1.48
NH
F
F
F
N
N
N
N
Cl
Compound 57
*signal from traces of residual solvent/grease
1.00
1.84
0.89
0.92
4.22
3.92
f1 (ppm)
S80/147

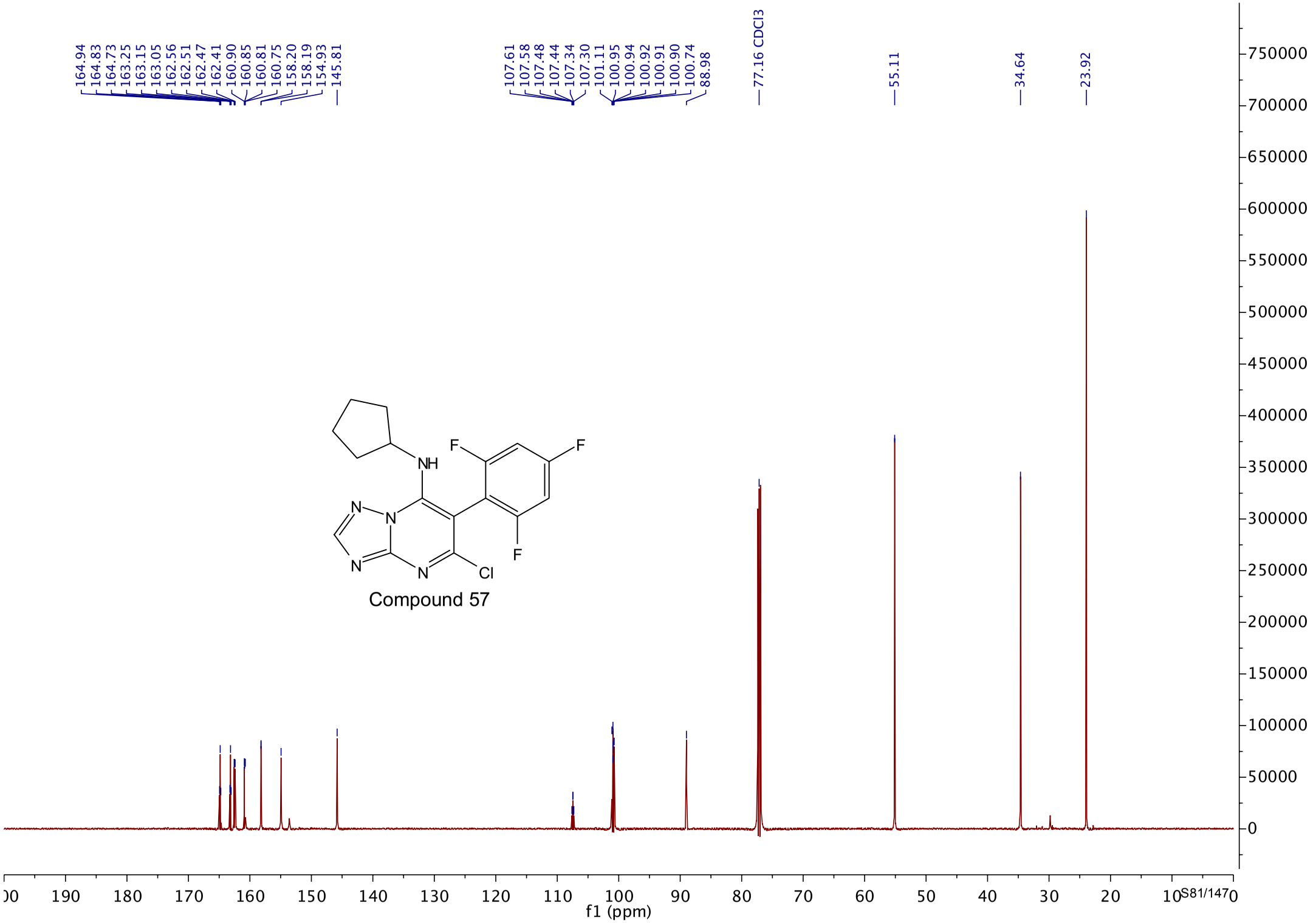
164.94
164.83
164.73
163.25
163.15
163.05
162.56
162.51
162.47
162.41
160.90
160.85
160.81
160.75
158.20
158.19
154.93
145.81
107.61
107.58
107.48
107.44
107.34
107.30
101.11
100.95
100.94
100.92
100.91
100.90
100.74
88.98
77.16 CDCl3
55.11
34.64
23.92
NH
F
F
F
N
N
N
N
Cl
Compound 57
750000
700000
650000
600000
550000
500000
450000
400000
350000
300000
250000
200000
150000
100000
50000
0
190
180
170
160
150
140
130
120
110
100
90
80
70
60
50
40
30
20
10
f1 (ppm)
S81/147

Compound 58
f1 (ppm)
1.00
1.90
1.05
1.18
1.97
2.31
1.07
2.16
1.16
2.01
8.33
7.26 CDCl3
6.90
6.89
6.89
6.89
6.88
6.87
6.87
6.86
6.85
6.85
6.84
6.38
6.36
3.09
3.07
3.05
3.03
1.82
1.82
1.80
1.79
1.72
1.71
1.71
1.70
1.69
1.68
1.67
1.55
1.54
1.53
1.52
1.51
1.51
1.28
1.27
1.26
1.26
1.25
1.24
1.23
1.23
1.22
1.21
1.20
1.17
1.16
1.15
1.14
1.14
1.13
1.12
1.12
1.11
1.11
1.10
1.09
1.09
1.08
0.99
0.98
0.97
0.96
0.95
0.95
0.94
0.93
0.92
0.91
0.90
0.90
N
N
N
N
NH
Cl
F
F
F

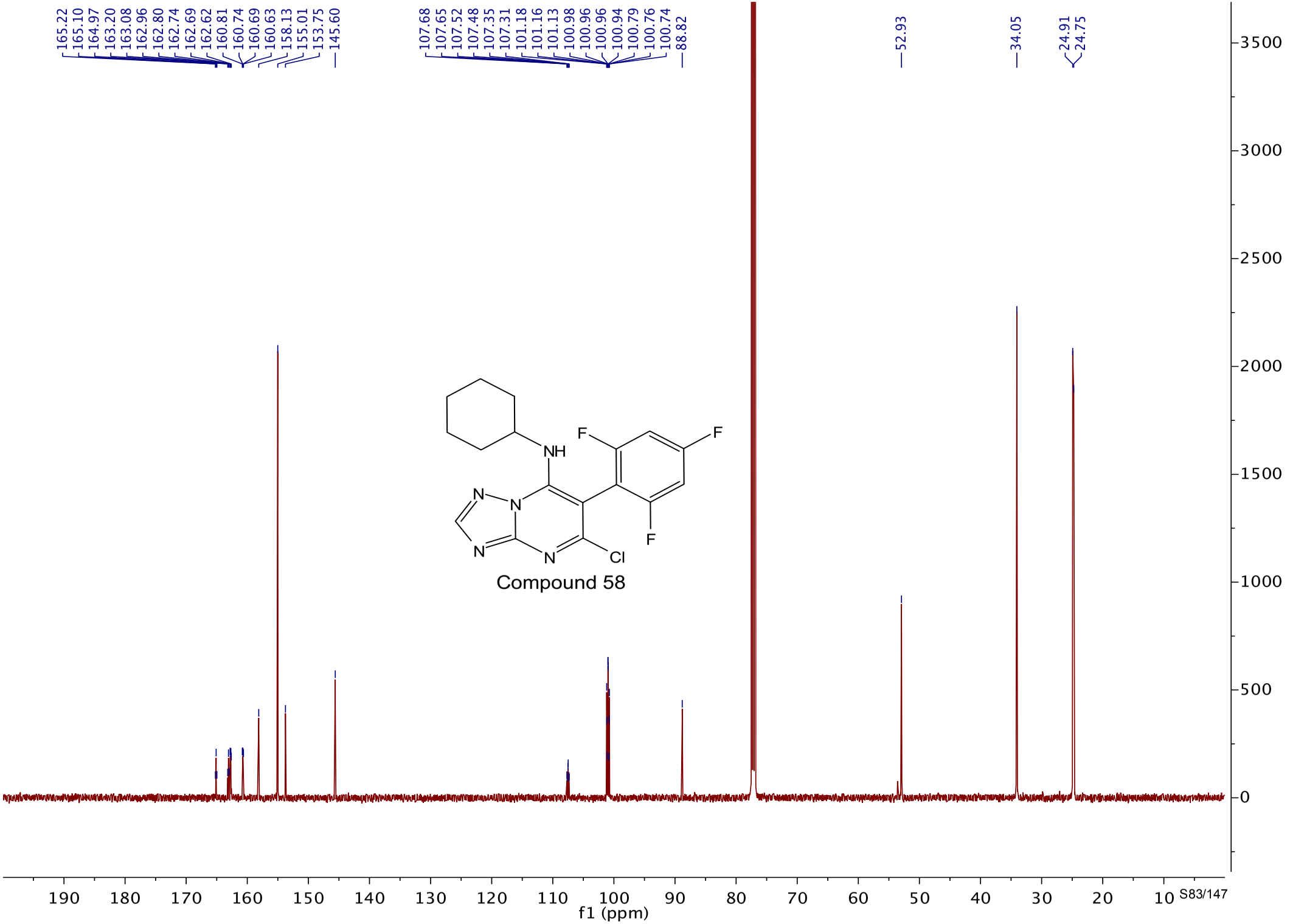
165.22
165.10
164.97
163.20
163.08
162.96
162.80
162.74
162.69
162.62
160.81
160.74
160.69
160.63
158.13
155.01
153.75
145.60
107.68
107.65
107.52
107.48
107.35
107.31
101.18
101.16
101.13
100.98
100.96
100.96
100.94
100.79
100.76
100.74
88.82
52.93
34.05
24.91
24.75
NH
F
F
F
N
N
N
N
Cl
Compound 58
3500
3000
2500
2000
1500
1000
500
0
190
180
170
160
150
140
130
120
110
100
90
80
70
60
50
40
30
20
10
f1 (ppm)

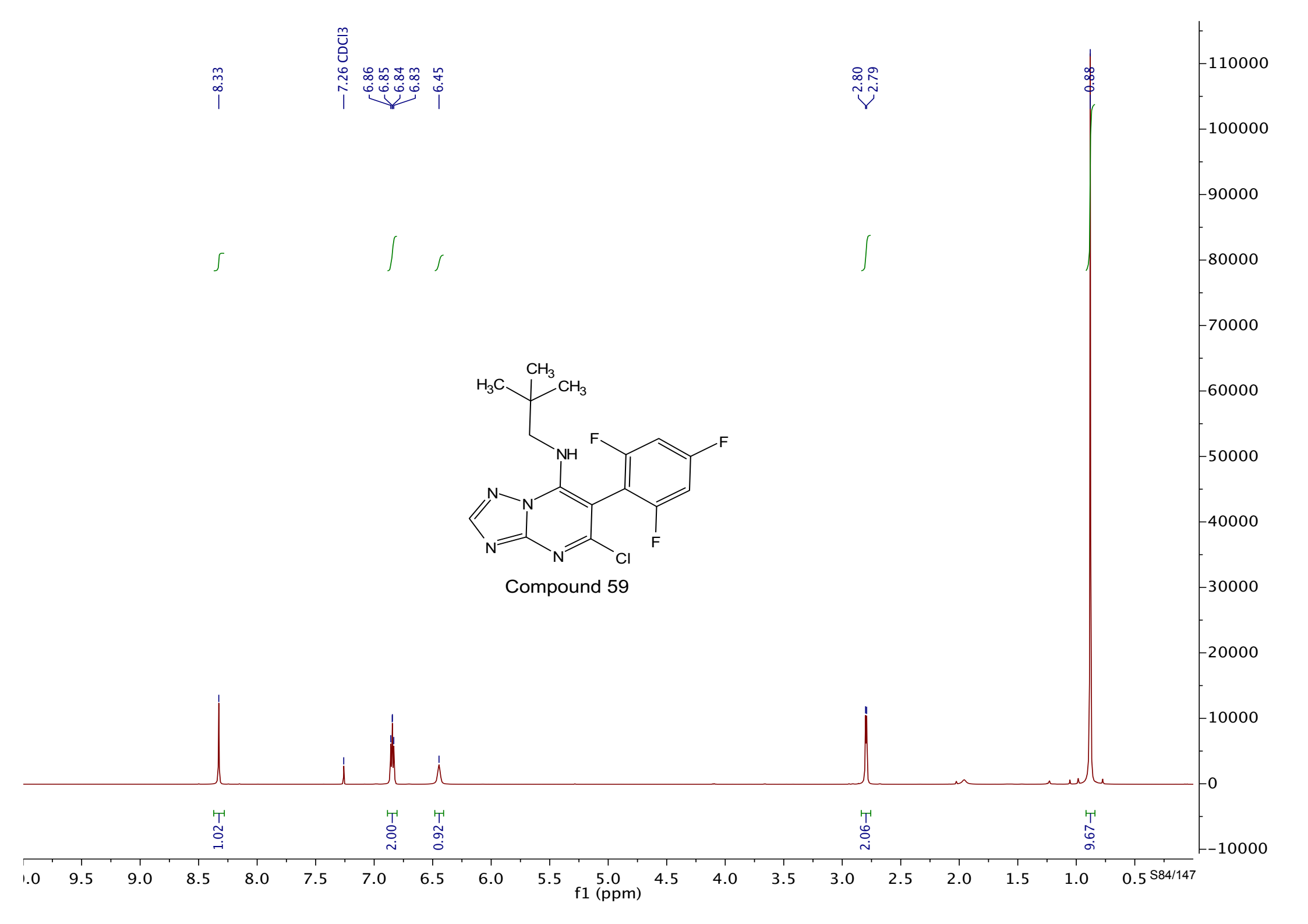
8.33
7.26 CDCl3
6.86
6.85
6.84
6.83
6.45
2.80
2.79
0.88
1.02
2.00
0.92
2.06
9.67
f1 (ppm)
S84/147

Compound 59

Compound 59
N
N
N
N
NH
Cl
F
F
F
H3C
CH3
CH3
165.01
164.91
164.81
163.23
163.13
162.52
162.46
162.42
162.36
160.86
160.80
160.76
160.70
158.08
155.03
153.65
146.68
107.53
107.49
107.39
107.36
107.25
107.22
101.09
101.05
100.92
100.90
100.89
100.76
100.72
88.91
77.16 CDCl3
54.56
31.81
26.86
f1 (ppm)
S85/147

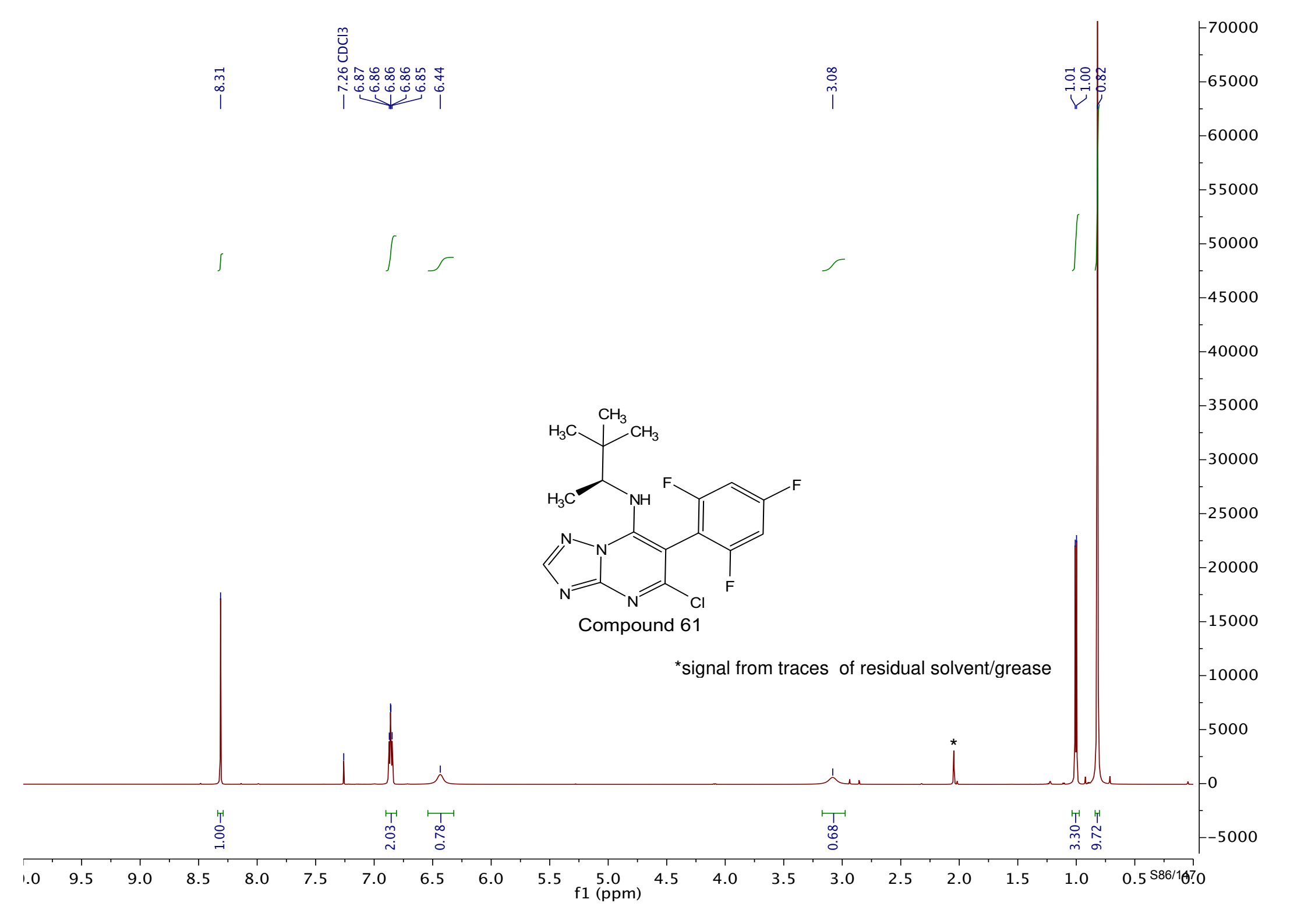
8.31
7.26 CDCl3
6.87
6.86
6.86
6.86
6.85
6.44
3.08
1.01
1.00
0.82
CH3
H3C
CH3
H3C
NH
F
F
F
N
N
N
N
Cl
Compound 61
*signal from traces of residual solvent/grease
*
1.00
2.03
0.78
0.68
3.30
9.72
f1 (ppm)
S86/147

164.91
163.33
163.23
163.13
162.43
162.37
162.33
162.28
162.18
162.13
162.03
160.77
160.71
160.67
160.61
160.46
158.13
154.94
153.61
146.25
107.69
107.66
107.55
107.52
107.42
107.39
101.30
101.28
101.16
101.13
101.11
100.99
100.96
100.93
100.82
100.80
88.60
77.16 CDCl3
58.07
34.72
25.78
16.58
Compound 61
f1 (ppm)
S87/147

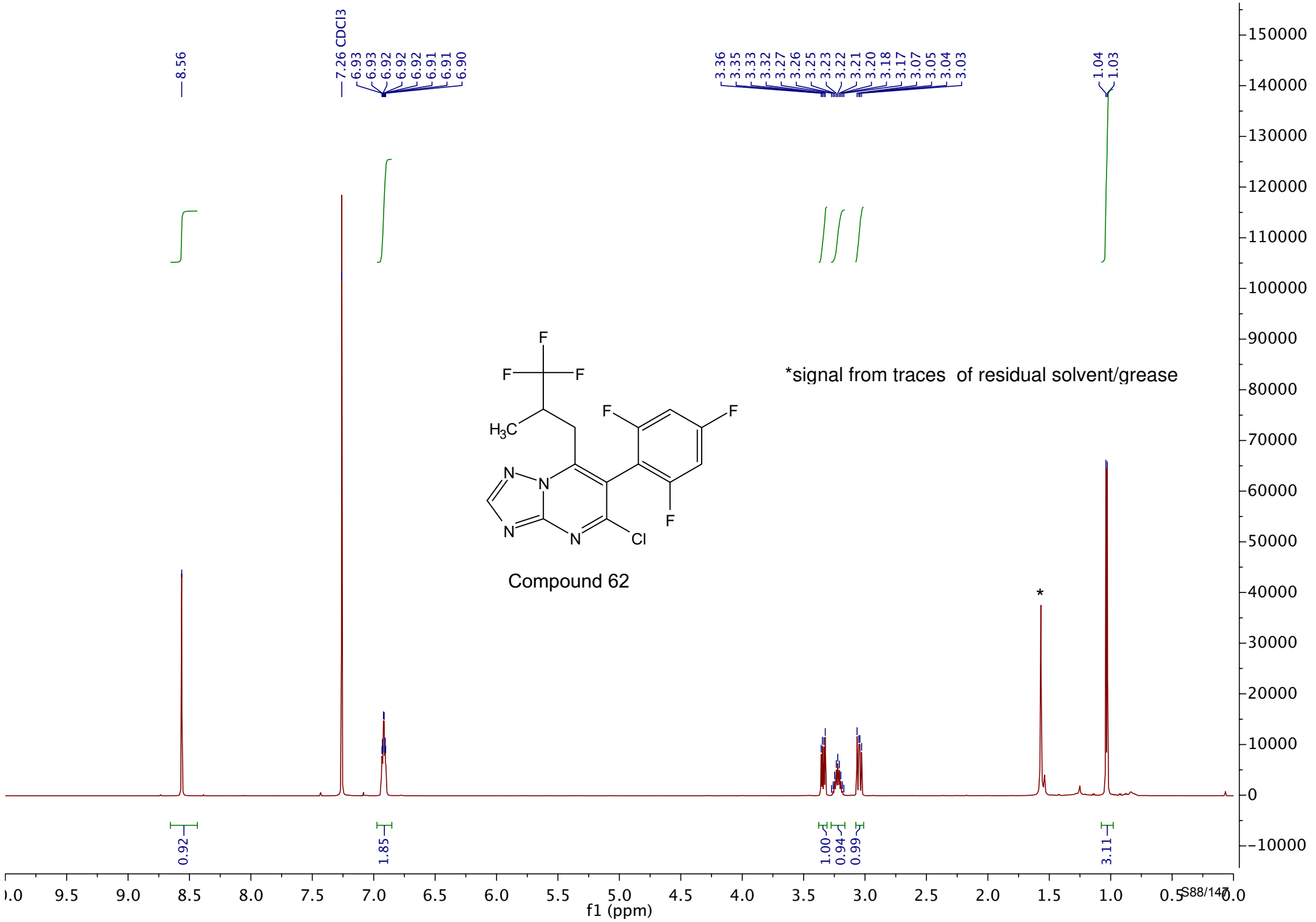
8.56
7.26 CDCl3
6.93
6.93
6.92
6.92
6.92
6.91
6.91
6.90
3.36
3.35
3.33
3.32
3.27
3.26
3.25
3.23
3.22
3.21
3.20
3.18
3.17
3.07
3.05
3.04
3.03
1.04
1.03
F
F
F
H3C
F
F
N
N
N
N
Cl
*signal from traces of residual solvent/grease
Compound 62
*
0.92
1.85
1.00
0.94
0.99
3.11
f1 (ppm)

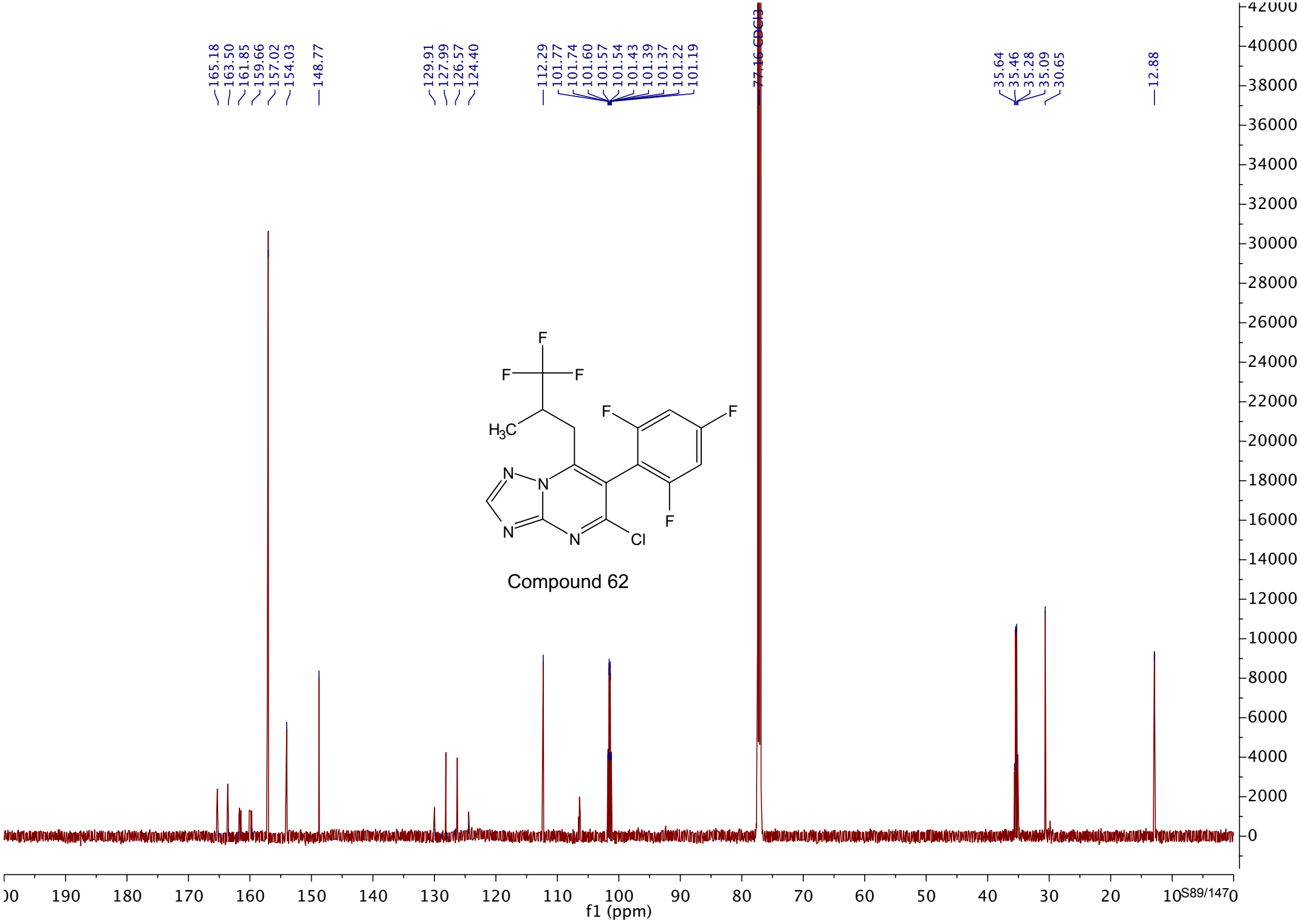
165.18
163.50
161.85
159.66
157.02
154.03
148.77
129.91
127.99
126.57
124.40
112.29
101.77
101.74
101.60
101.57
101.54
101.43
101.39
101.37
101.22
101.19
77.16 CDCl3
35.64
35.46
35.28
35.09
30.65
12.88
F
F
F
H3C
F
F
N
N
N
N
Cl
Compound 62
f1 (ppm)
S89/147

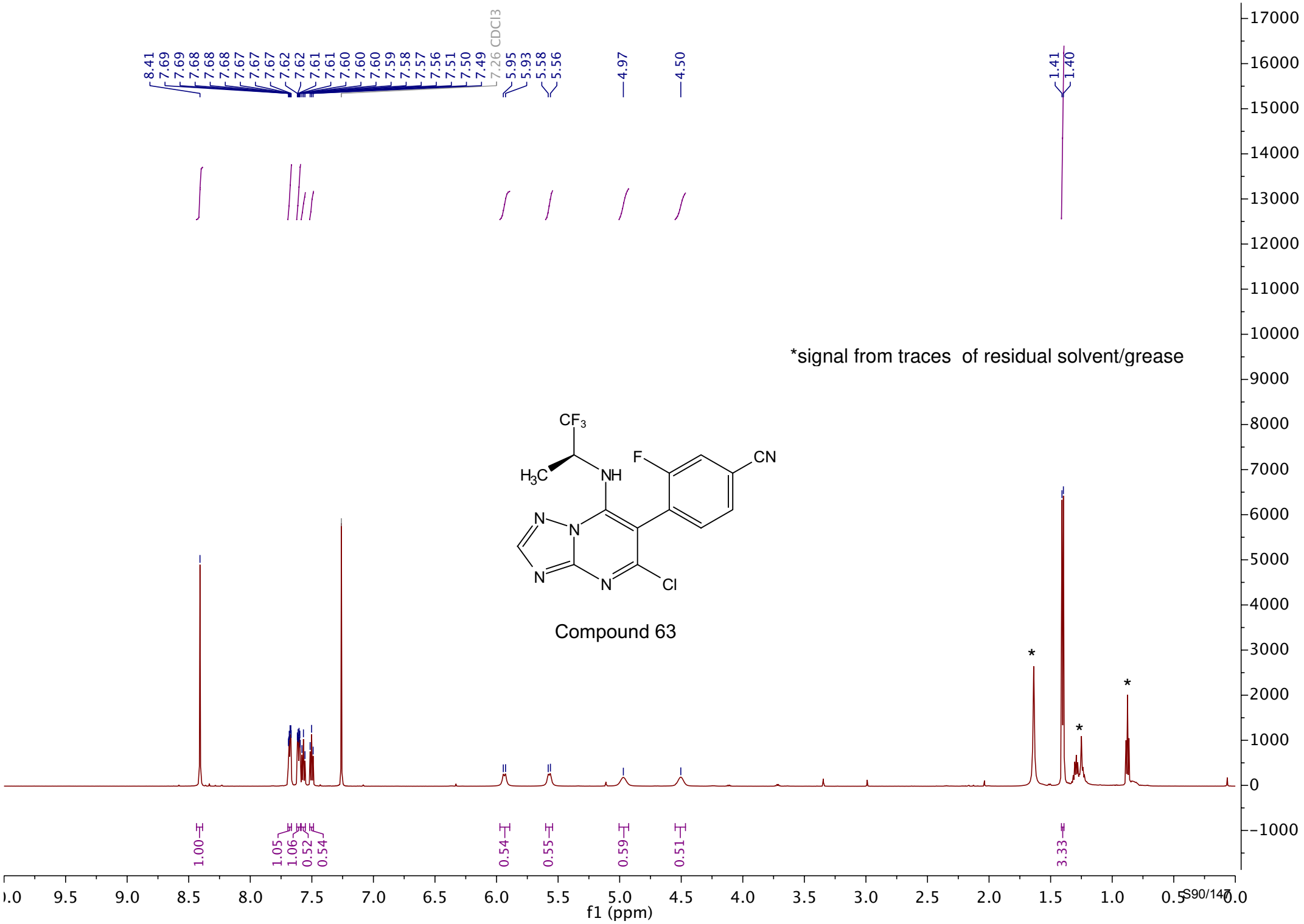
8.41
7.69
7.69
7.68
7.68
7.68
7.67
7.67
7.67
7.62
7.62
7.61
7.61
7.60
7.60
7.60
7.59
7.58
7.57
7.56
7.51
7.50
7.49
7.26 CDCl3
5.95
5.93
5.58
5.56
4.97
4.50
1.41
1.40
*signal from traces of residual solvent/grease
CF3
H3C
NH
F
CN
N
N
N
N
Cl
Compound 63
1.00
1.05
1.06
0.52
0.54
0.54
0.55
0.59
0.51
3.33
f1 (ppm)
S90/147

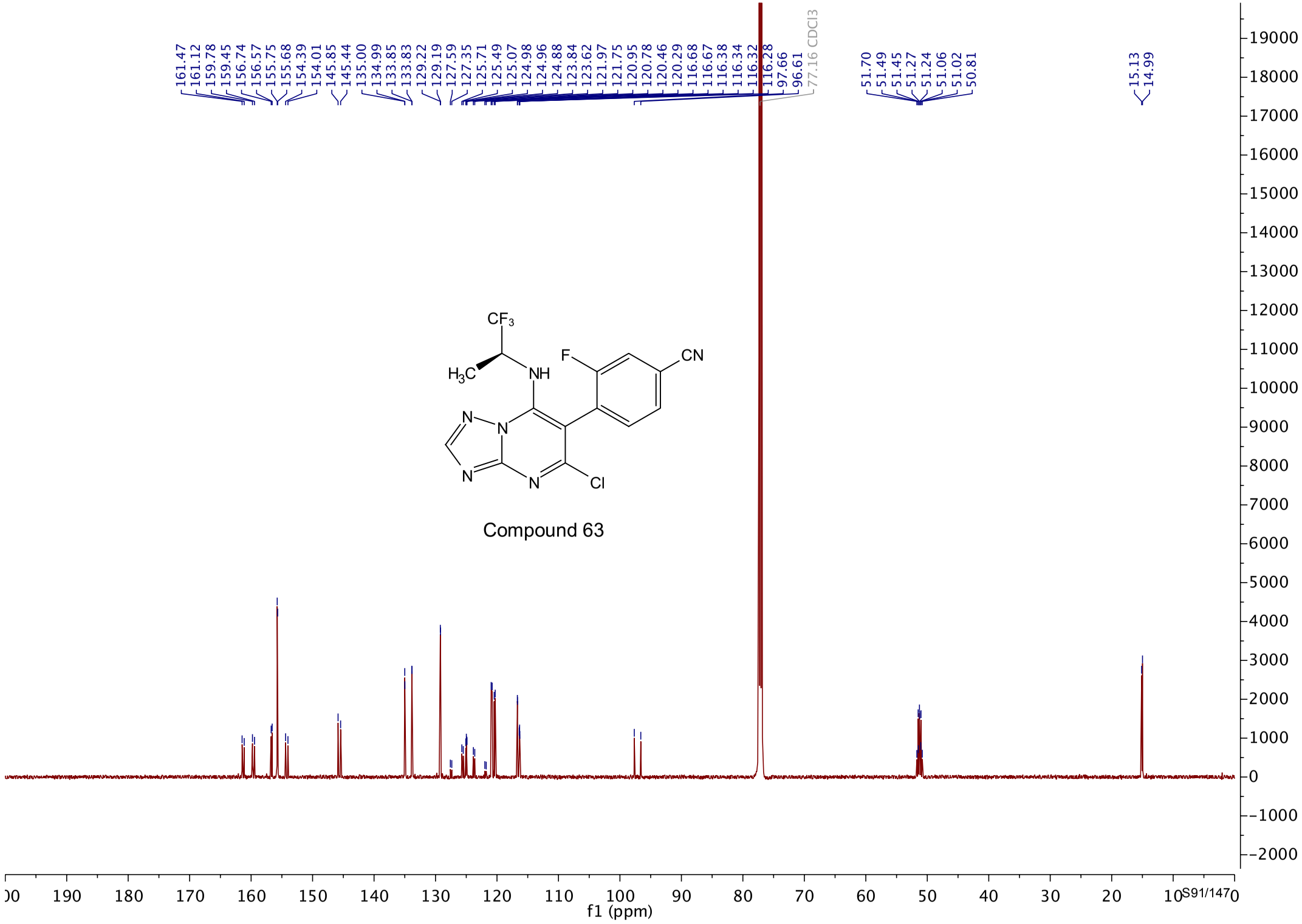
161.47
161.12
159.78
159.45
156.74
156.57
155.75
155.68
154.39
154.01
145.85
145.44
135.00
134.99
133.85
133.83
129.22
129.19
127.59
127.35
125.71
125.49
125.07
124.98
124.96
124.88
123.84
123.62
121.97
121.75
120.95
120.78
120.46
120.29
116.68
116.67
116.38
116.34
116.32
116.28
97.66
96.61
77.16 CDCl3
51.70
51.49
51.45
51.27
51.24
51.06
51.02
50.81
15.13
14.99
CF3
H3C
NH
F
CN
N
N
N
N
Cl
Compound 63
19000
18000
17000
16000
15000
14000
13000
12000
11000
10000
9000
8000
7000
6000
5000
4000
3000
2000
1000
0
-1000
-2000
190
180
170
160
150
140
130
120
110
100
90
80
70
60
50
40
30
20
10
f1 (ppm)

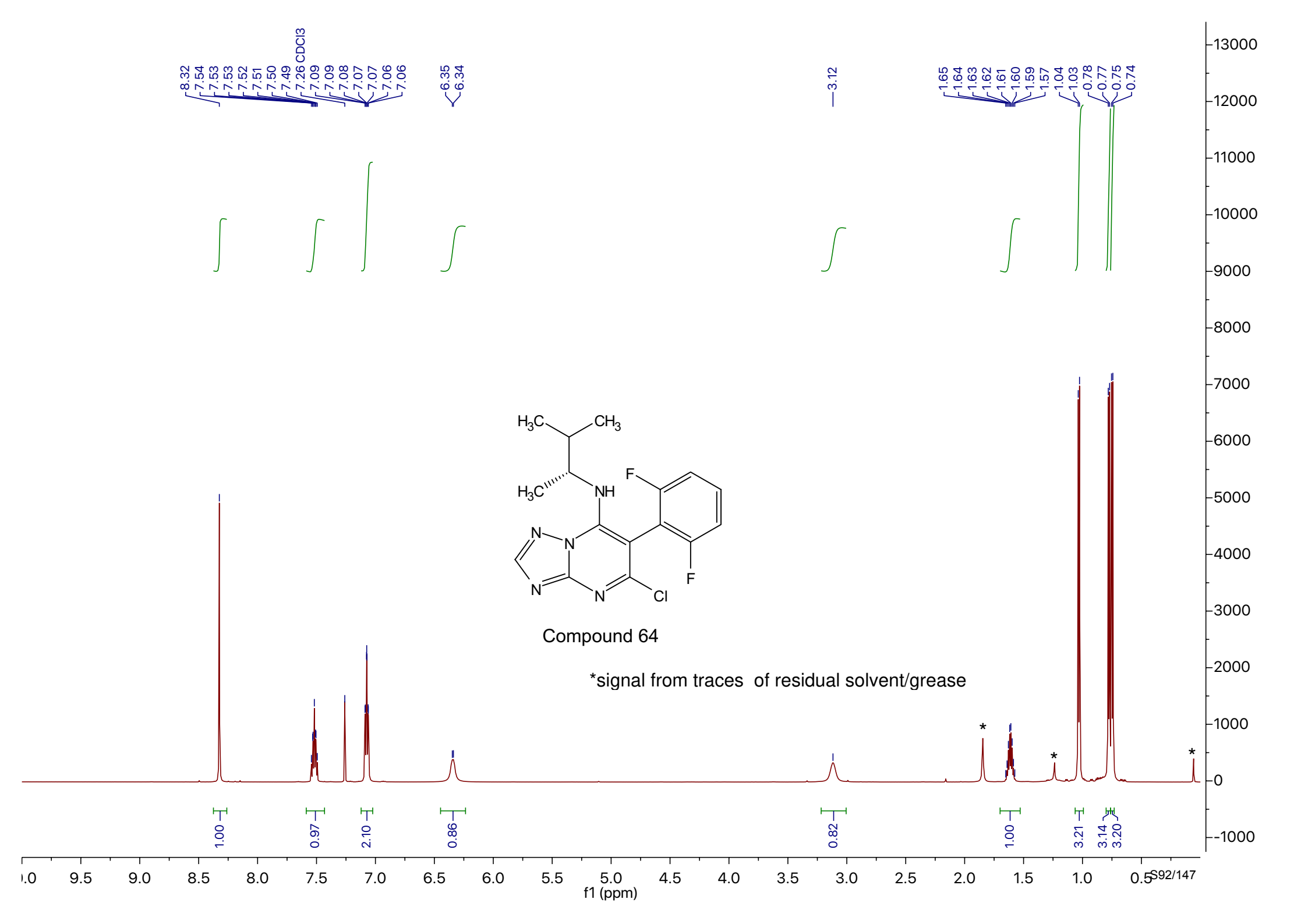
8.32
7.54
7.53
7.53
7.52
7.51
7.50
7.49
7.26 CDCl3
7.09
7.09
7.08
7.07
7.07
7.06
7.06
6.35
6.34
3.12
1.65
1.64
1.63
1.62
1.61
1.60
1.59
1.57
1.04
1.03
0.78
0.77
0.75
0.74
H3C
CH3
H3C
NH
F
F
N
N
N
N
Cl
Compound 64
*signal from traces of residual solvent/grease
1.00
0.97
2.10
0.86
0.82
1.00
3.21
3.14
3.20
f1 (ppm)
S92/147

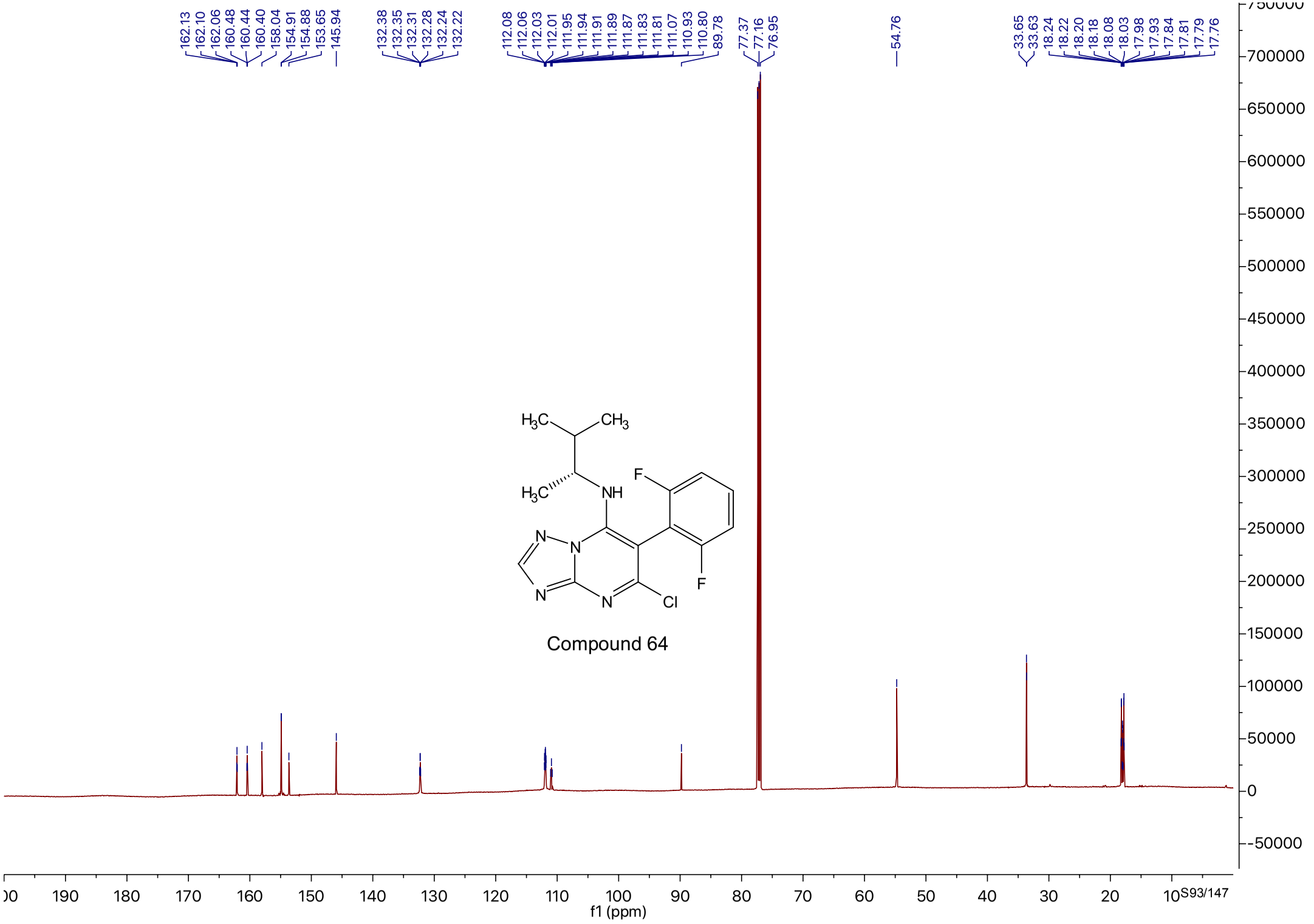
162.13
162.10
162.06
160.48
160.44
160.40
158.04
154.91
154.88
153.65
145.94
132.38
132.35
132.31
132.28
132.24
132.22
112.08
112.06
112.03
112.01
111.95
111.94
111.91
111.89
111.87
111.83
111.81
111.07
110.93
110.80
89.78
77.37
77.16
76.95
54.76
33.65
33.63
18.24
18.22
18.20
18.18
18.08
18.03
17.98
17.93
17.84
17.81
17.79
17.76
H3C
CH3
H3C
NH
F
F
N
N
N
N
Cl
Compound 64
700000
650000
600000
550000
500000
450000
400000
350000
300000
250000
200000
150000
100000
50000
0
-50000
190
180
170
160
150
140
130
120
110
100
90
80
70
60
50
40
30
20
10
f1 (ppm)

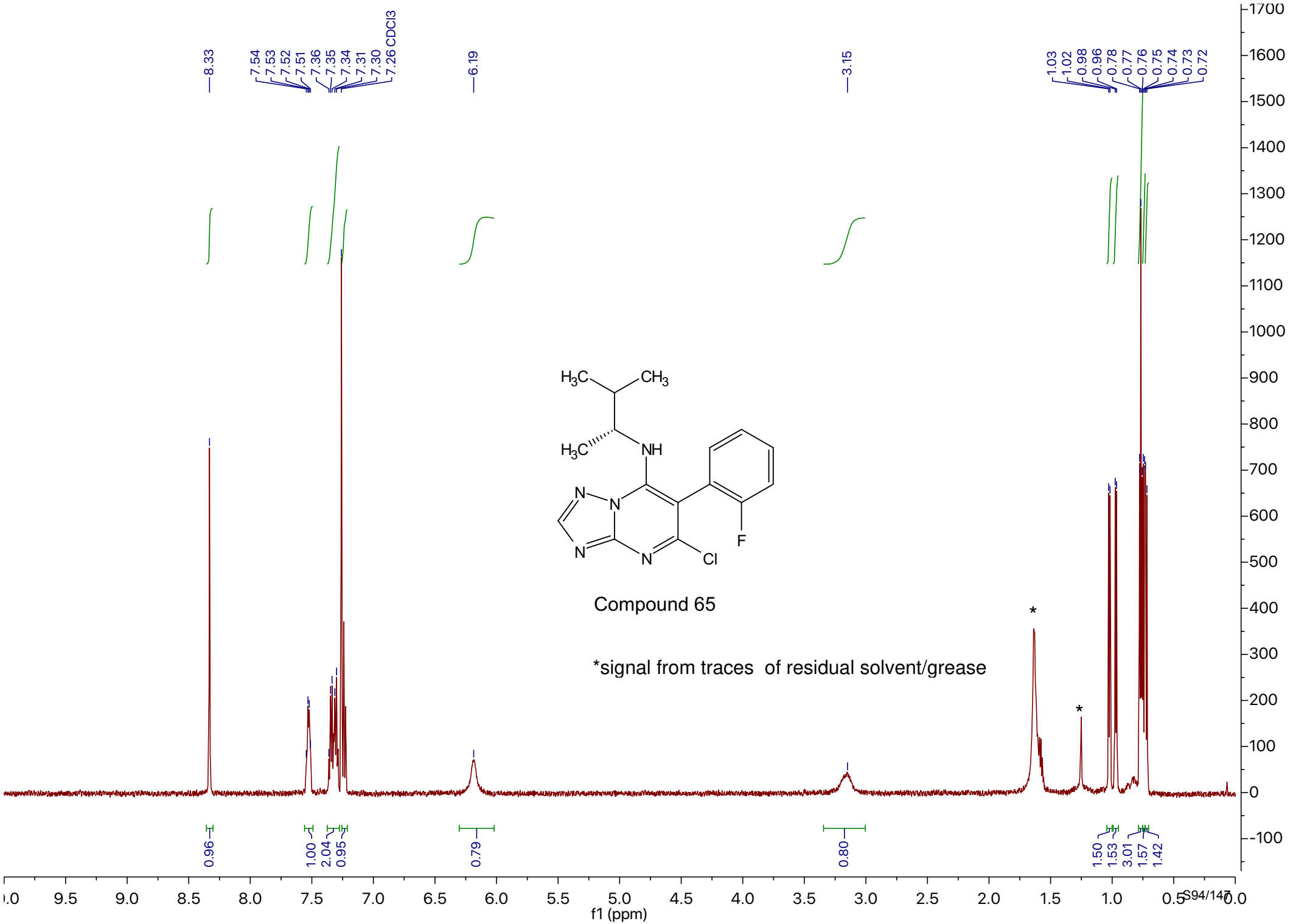
8.33
7.54
7.53
7.52
7.51
7.36
7.35
7.34
7.31
7.30
7.26 CDCl3
6.19
3.15
1.03
1.02
0.98
0.96
0.78
0.77
0.76
0.75
0.74
0.73
0.72
H3C
CH3
H3C
NH
N
N
N
N
Cl
F
Compound 65
*signal from traces of residual solvent/grease
*
*
0.96
1.00
2.04
0.95
0.79
0.80
1.50
1.53
3.01
1.57
1.42
f1 (ppm)
S94/147

Compound 65
161.69
161.63
160.04
159.98
158.31
158.23
153.92
152.71
146.03
133.62
133.61
132.99
132.12
132.06
132.01
124.97
124.94
124.91
124.89
121.05
120.94
120.88
120.77
116.49
116.48
116.34
116.33
97.15
97.00
77.16 CDCl3
54.76
54.60
33.78
33.48
18.29
17.99
17.82
17.74
17.63
f1 (ppm)
S95/1470

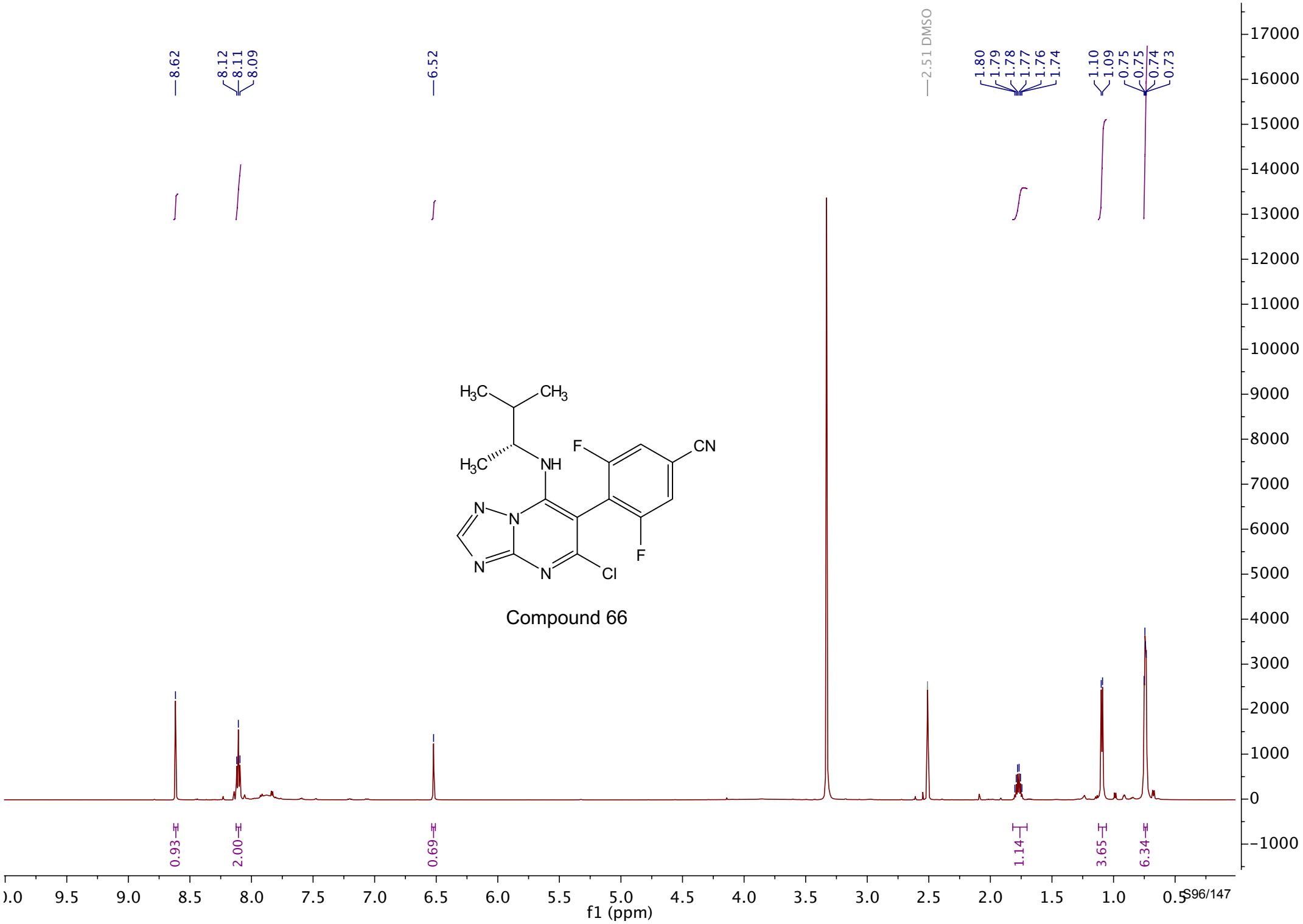
8.62
8.12
8.11
8.09
6.52
2.51 DMSO
1.80
1.79
1.78
1.77
1.76
1.74
1.10
1.09
0.75
0.75
0.74
0.73
0.93
2.00
0.69
1.14
3.65
6.34
f1 (ppm)
S96/147

Compound 66

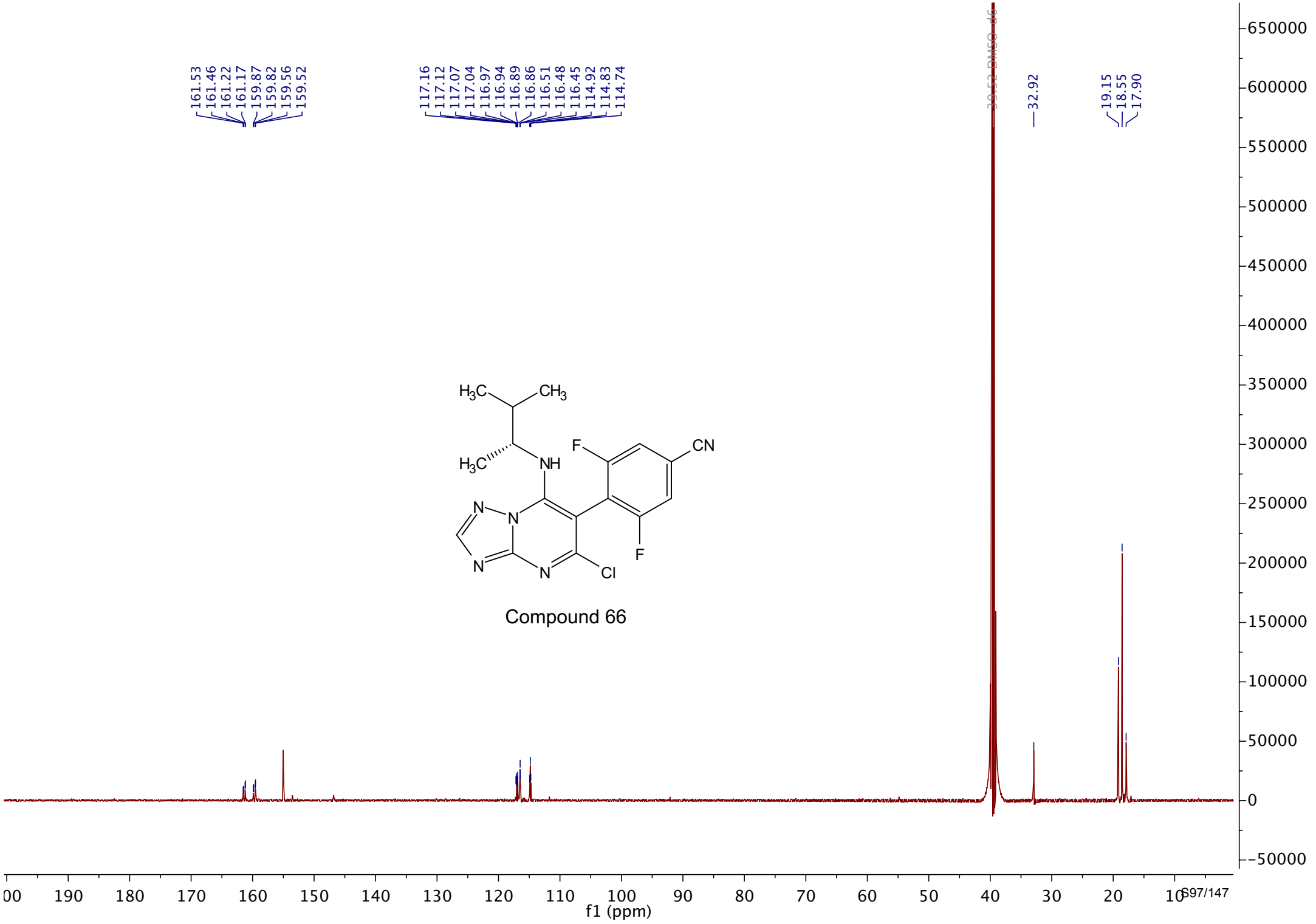
161.53
161.46
161.22
161.17
159.87
159.82
159.56
159.52
117.16
117.12
117.07
117.04
116.97
116.94
116.89
116.86
116.51
116.48
116.45
114.92
114.83
114.74
39.52 DMSO-d6
32.92
19.15
18.55
17.90
650000
600000
550000
500000
450000
400000
350000
300000
250000
200000
150000
100000
50000
0
−50000
f1 (ppm)
S97/147

Compound 66

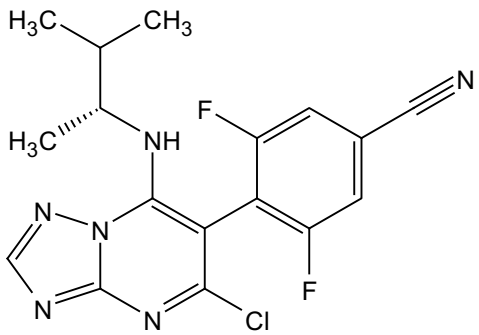
H3C
CH3
H3C
NH
N
N
N
N
F
F
N
Cl

Compound 66

-103.92
-103.94
-104.41
-104.43
3600
3400
3200
3000
2800
2600
2400
2200
2000
1800
1600
1400
1200
1000
800
600
400
200
0
-200
-400
-600
100
90
80
70
60
50
40
30
20
10
0
-10
-20
-30
-40
-50
-60
-70
-80
-90
-100
-110
-120
-130
-140
-150
f1 (ppm)

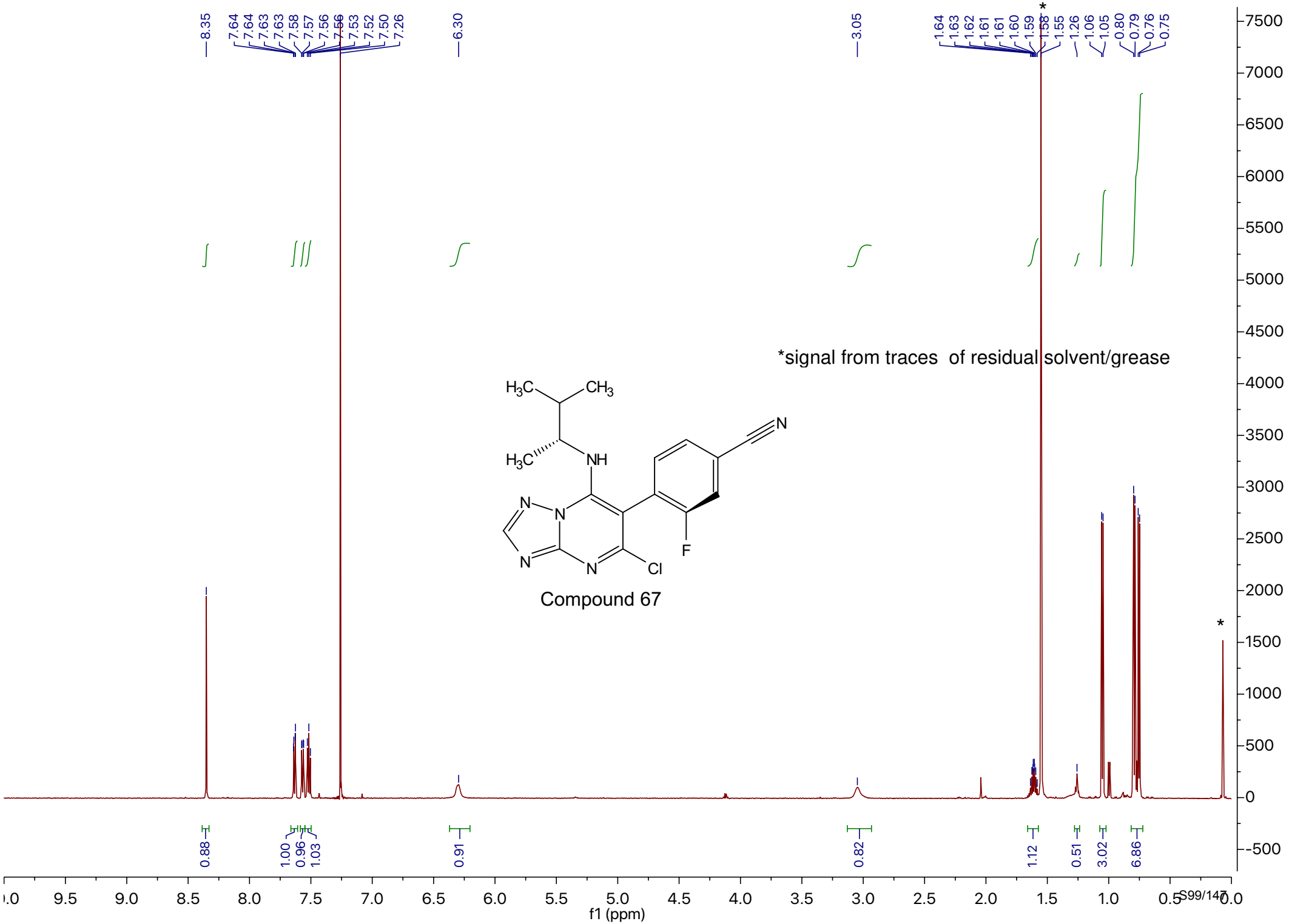
8.35
7.64
7.64
7.63
7.63
7.58
7.57
7.56
7.56
7.53
7.52
7.50
7.26
6.30
3.05
1.64
1.63
1.62
1.61
1.61
1.60
1.59
1.58
1.55
1.26
1.06
1.05
0.80
0.79
0.76
0.75
*
*signal from traces of residual solvent/grease
H3C
CH3
H3C
NH
N
N
N
N
Cl
F
N
Compound 67
0.88
1.00
0.96
1.03
0.91
0.82
1.12
0.51
3.02
6.86
f1 (ppm)
S99/147

161.41
159.74
156.91
155.20
153.57
145.68
135.09
134.42
134.40
128.58
128.55
127.09
126.99
120.22
120.05
117.01
117.00
115.49
115.43
94.38
77.38
77.17
77.16 CDCl3
76.96
54.86
33.81
18.20
17.91
17.82
Compound 67
f1 (ppm)

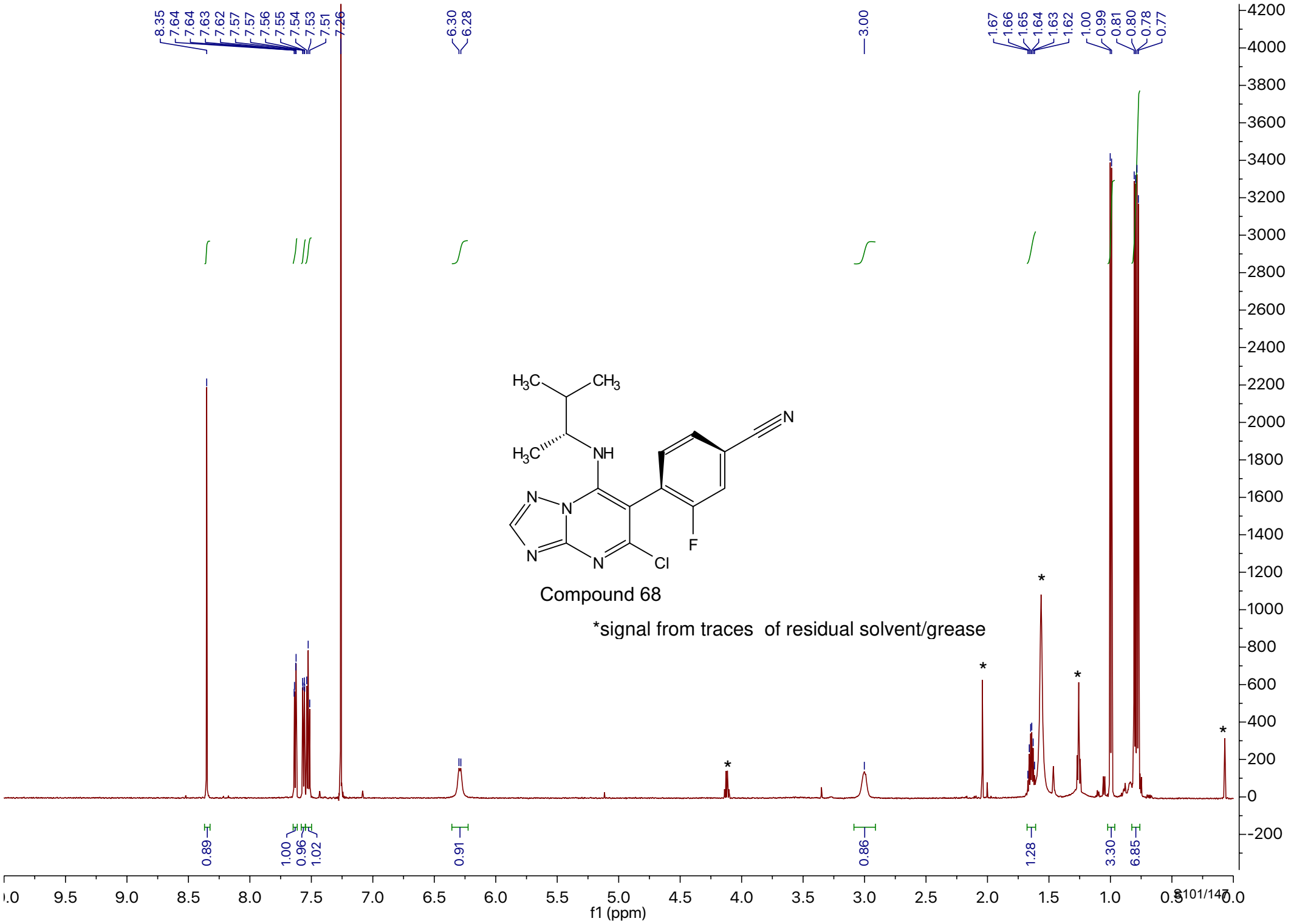
8.35
7.64
7.64
7.63
7.62
7.57
7.57
7.56
7.55
7.54
7.53
7.51
7.26
6.30
6.28
3.00
1.67
1.66
1.65
1.64
1.63
1.62
1.00
0.99
0.81
0.80
0.78
0.77
0.89
1.00
0.96
1.02
0.91
0.86
1.28
3.30
6.85
f1 (ppm)
Compound 68
*signal from traces of residual solvent/grease

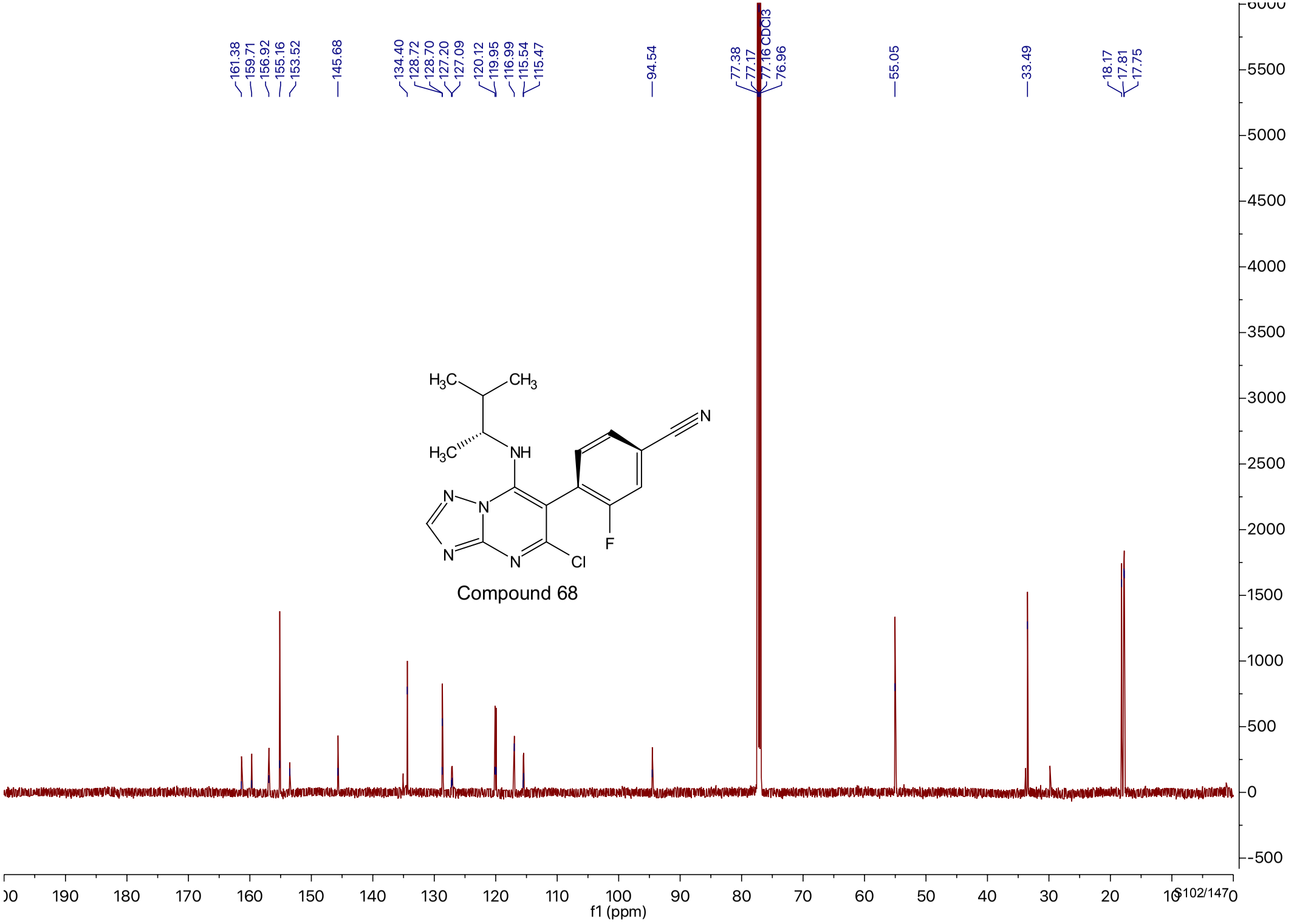
161.38
159.71
156.92
155.16
153.52
145.68
134.40
128.72
128.70
127.20
127.09
120.12
119.95
116.99
115.54
115.47
94.54
77.38
77.17
77.16 CDCl3
76.96
55.05
33.49
18.17
17.81
17.75
H3C
CH3
H3C
NH
N
N
N
N
Cl
F
N
Compound 68
f1 (ppm)
S102/147

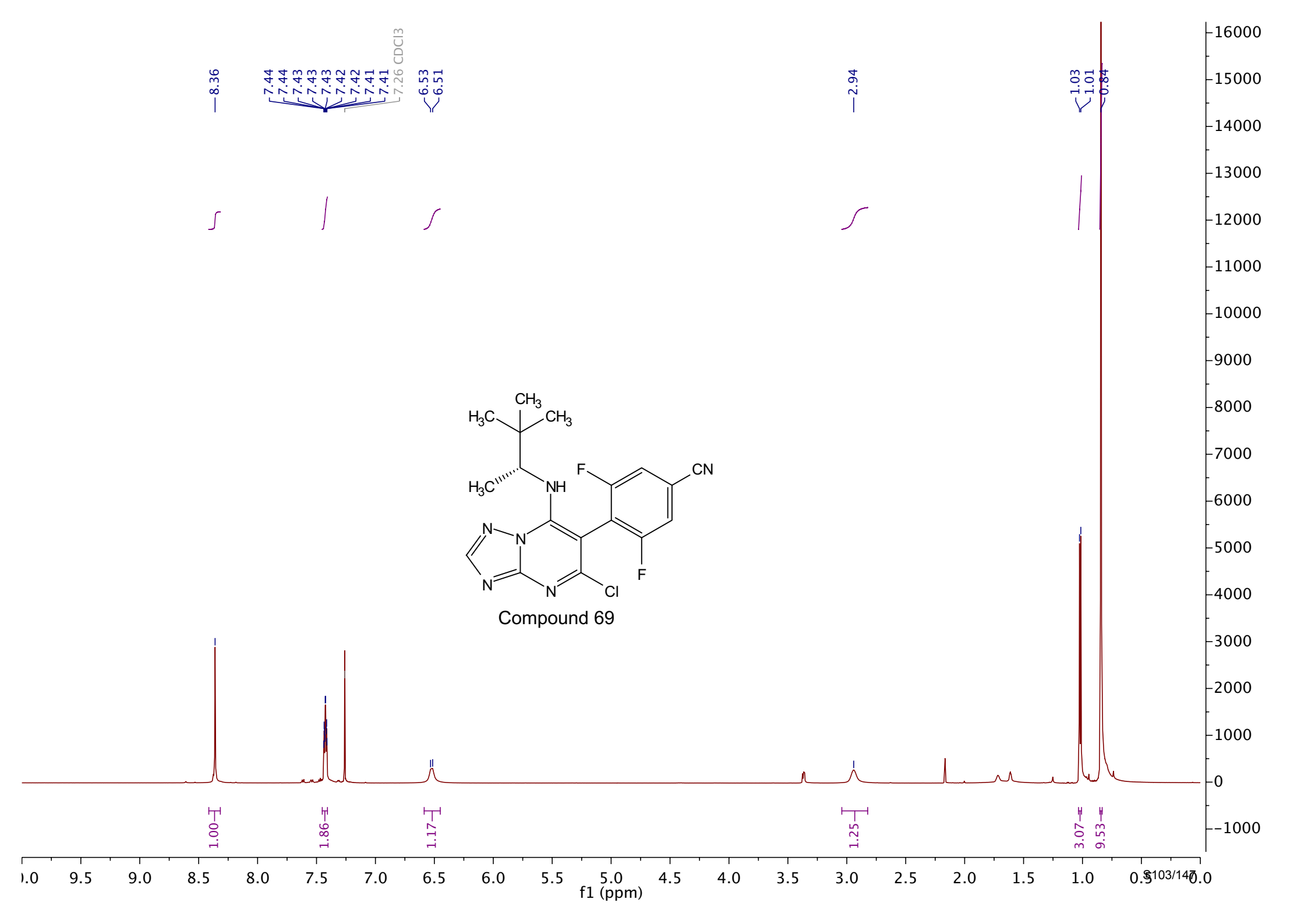
8.36
7.44
7.44
7.43
7.43
7.43
7.42
7.42
7.41
7.41
7.26 CDCl3
6.53
6.51
2.94
1.03
1.01
0.84
1.00
1.86
1.17
1.25
3.07
9.53
f1 (ppm)

CH3
H3C
CH3
H3C
NH
F
CN
N
N
N
N
Cl
F

Compound 69

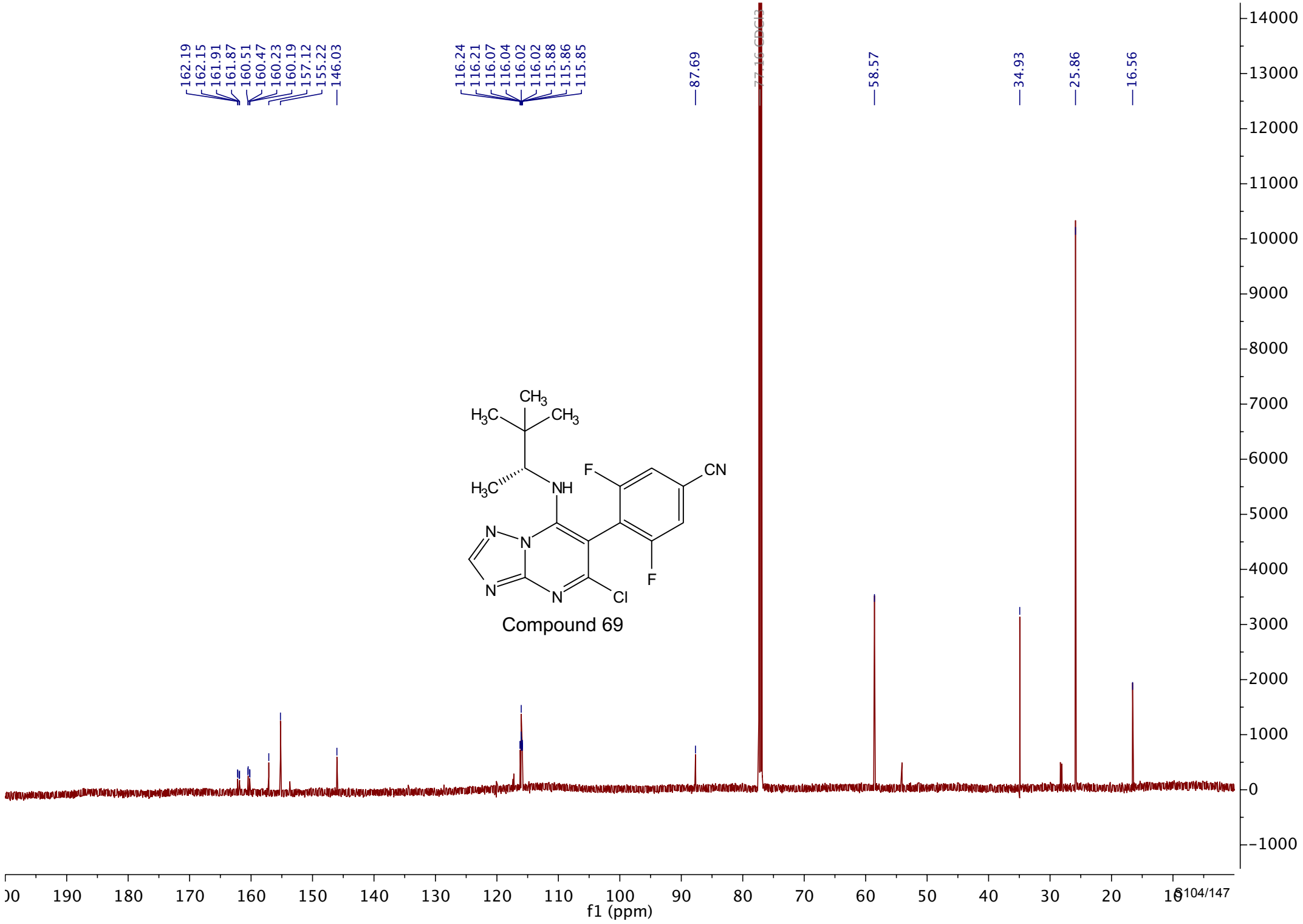
162.19
162.15
161.91
161.87
160.51
160.47
160.23
160.19
157.12
155.22
146.03
116.24
116.21
116.07
116.04
116.02
116.02
115.88
115.86
115.85
87.69
77.16 CDCl3
58.57
34.93
25.86
16.56
CH3
H3C
CH3
H3C
NH
F
CN
N
N
N
N
Cl
F
Compound 69
14000
13000
12000
11000
10000
9000
8000
7000
6000
5000
4000
3000
2000
1000
0
-1000
190
180
170
160
150
140
130
120
110
100
90
80
70
60
50
40
30
20
f1 (ppm)

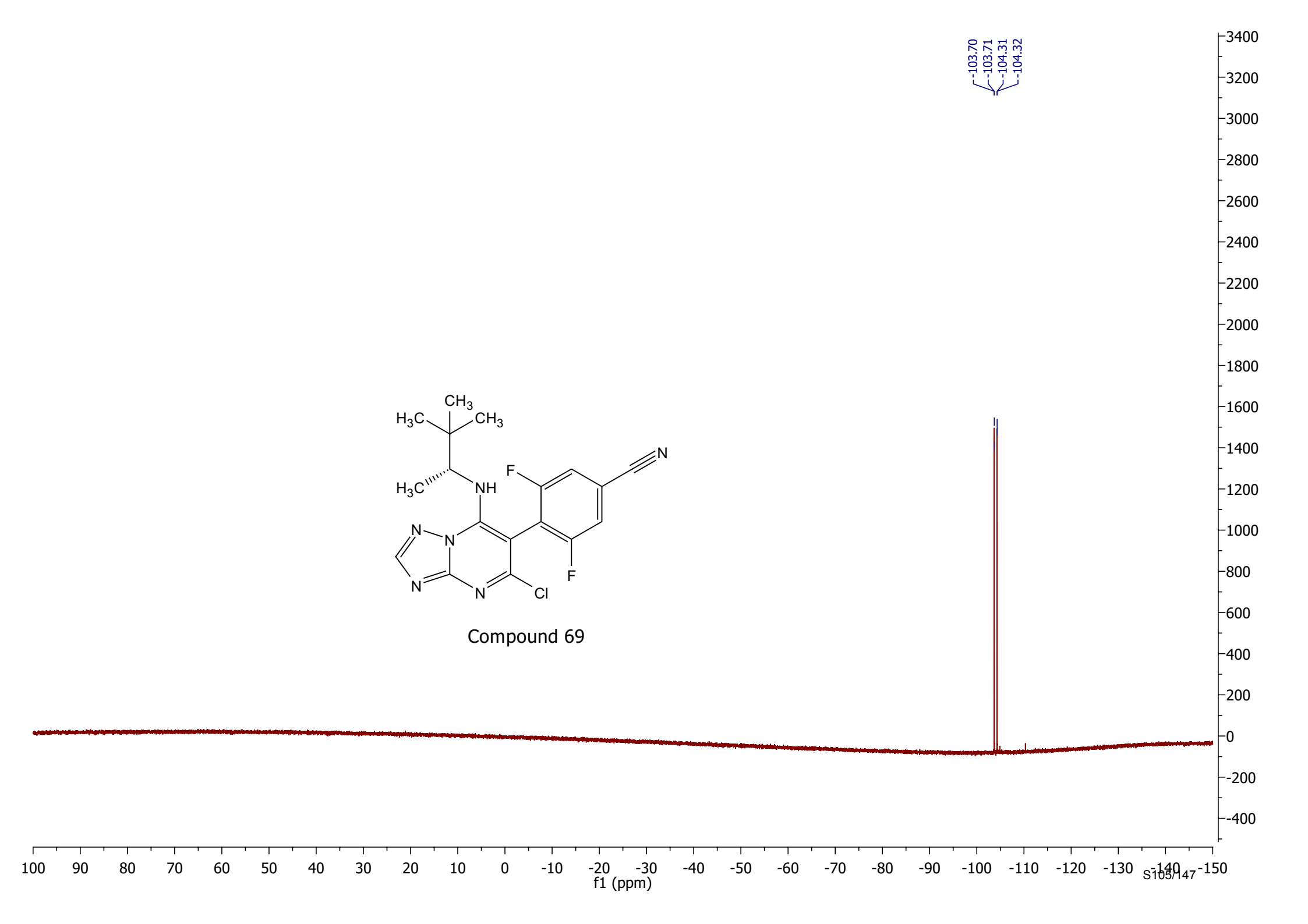
-103.70
-103.71
-104.31
-104.32
CH3
H3C
CH3
H3C
NH
F
N
N
N
N
N
Cl
F
Compound 69
f1 (ppm)
S105/147

Compound 70
f1 (ppm)
1.00
0.98
0.93
0.92
0.99
1.03
1.34
1.67
5.37
4.24
8.38
8.38
7.65
7.65
7.64
7.64
7.64
7.64
7.63
7.63
7.58
7.58
7.57
7.57
7.57
7.56
7.56
7.56
7.54
7.53
7.53
7.52
7.52
7.50
7.26 CDCl3
6.37
2.97
2.95
2.91
2.88
1.02
1.00
0.95
0.93
0.82
0.81
S106/147

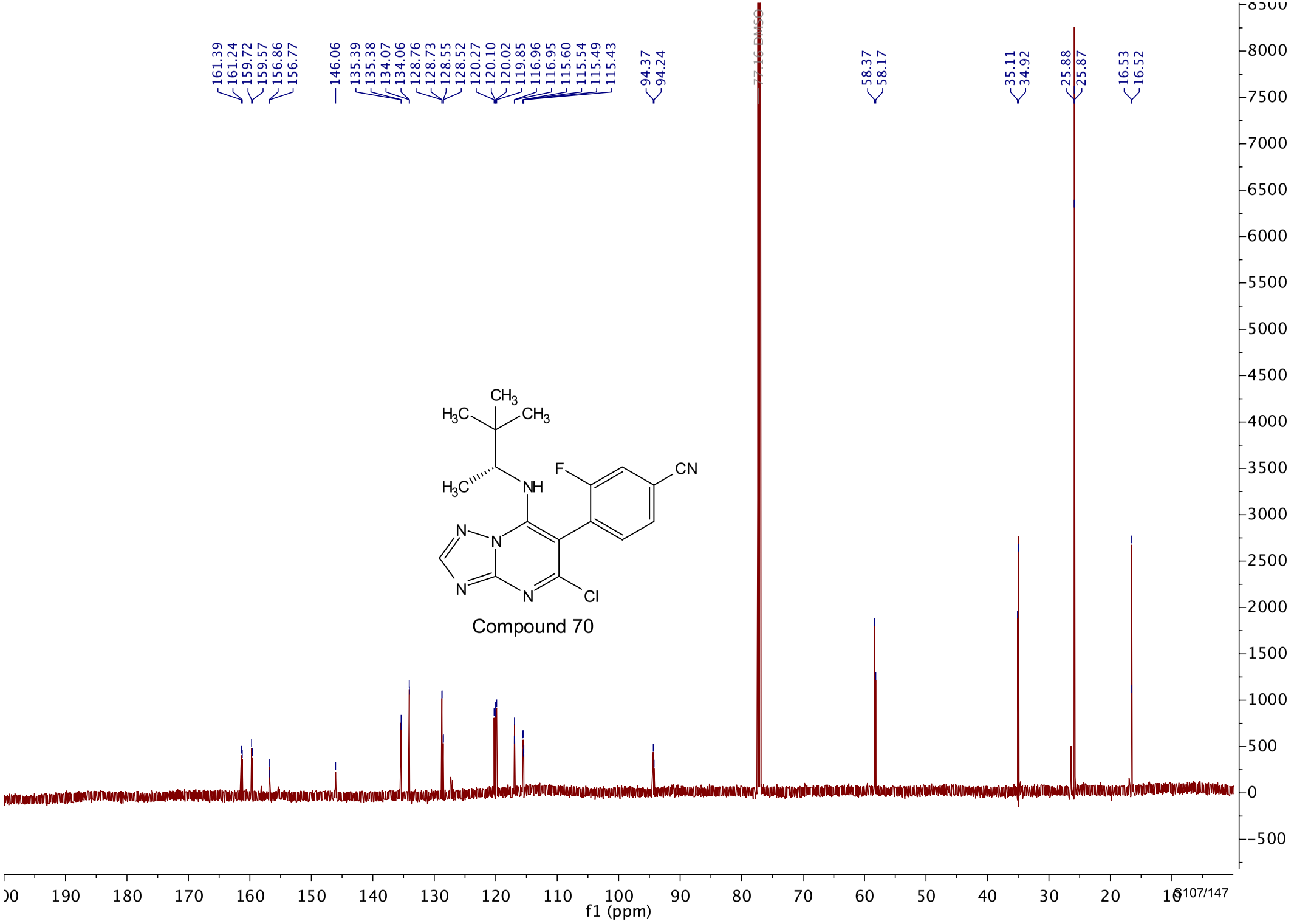
161.39
161.24
159.72
159.57
156.86
156.77
146.06
135.39
135.38
134.07
134.06
128.76
128.73
128.55
128.52
120.27
120.10
120.02
119.85
116.96
116.95
115.60
115.54
115.49
115.43
94.37
94.24
77.16 DMSO
58.37
58.17
35.11
34.92
25.88
25.87
16.53
16.52
CH3
H3C
CH3
H3C
NH
F
CN
N
N
N
N
Cl
Compound 70
f1 (ppm)
107/147

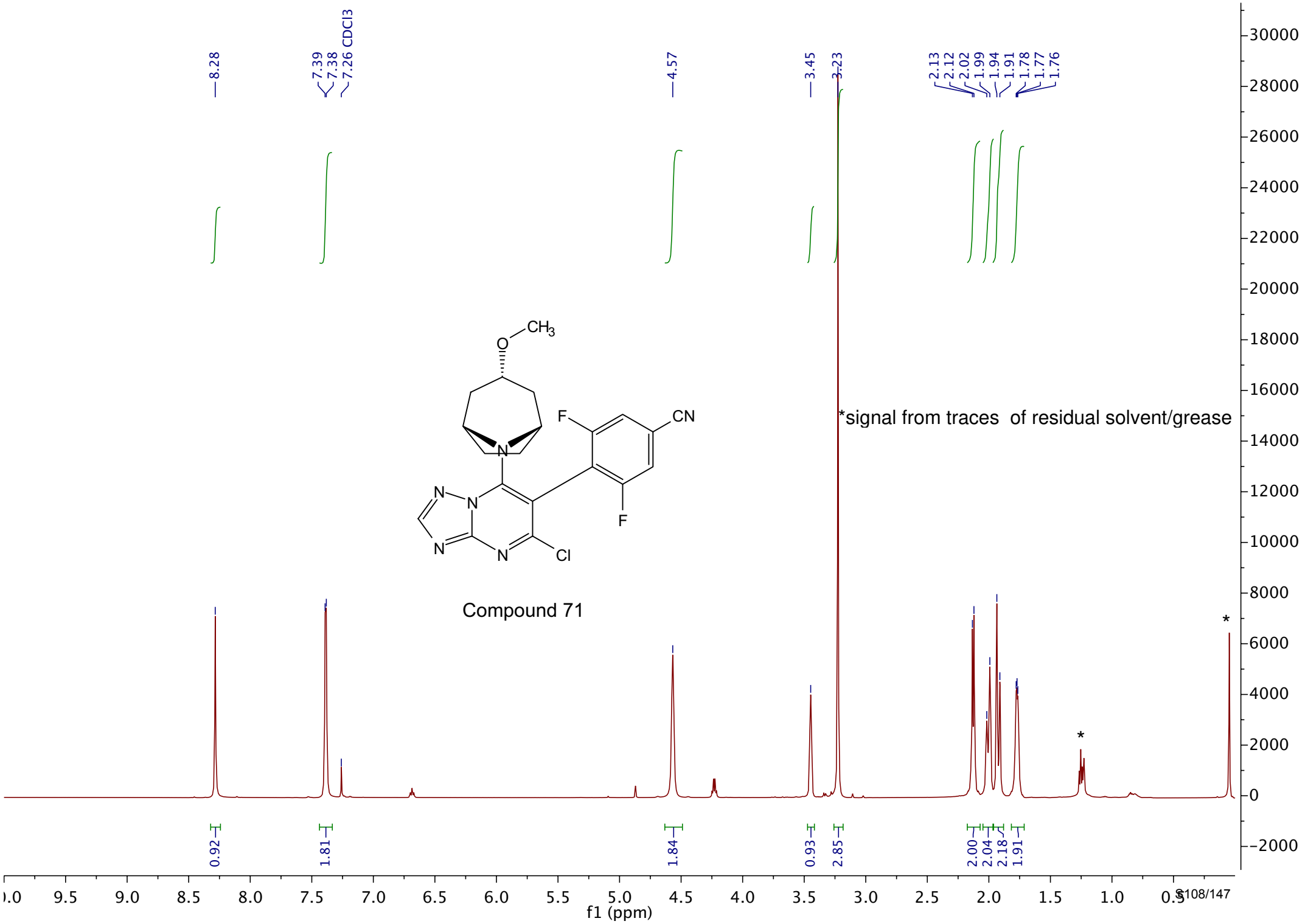
8.28
7.39
7.38
7.26 CDCl3
4.57
3.45
3.23
2.13
2.12
2.02
1.99
1.94
1.91
1.78
1.77
1.76
O
CH3
N
F
CN
F
N
N
N
N
Cl
Compound 71
*signal from traces of residual solvent/grease
0.92
1.81
1.84
0.93
2.85
2.00
2.04
2.18
1.91
f1 (ppm)
S108/147

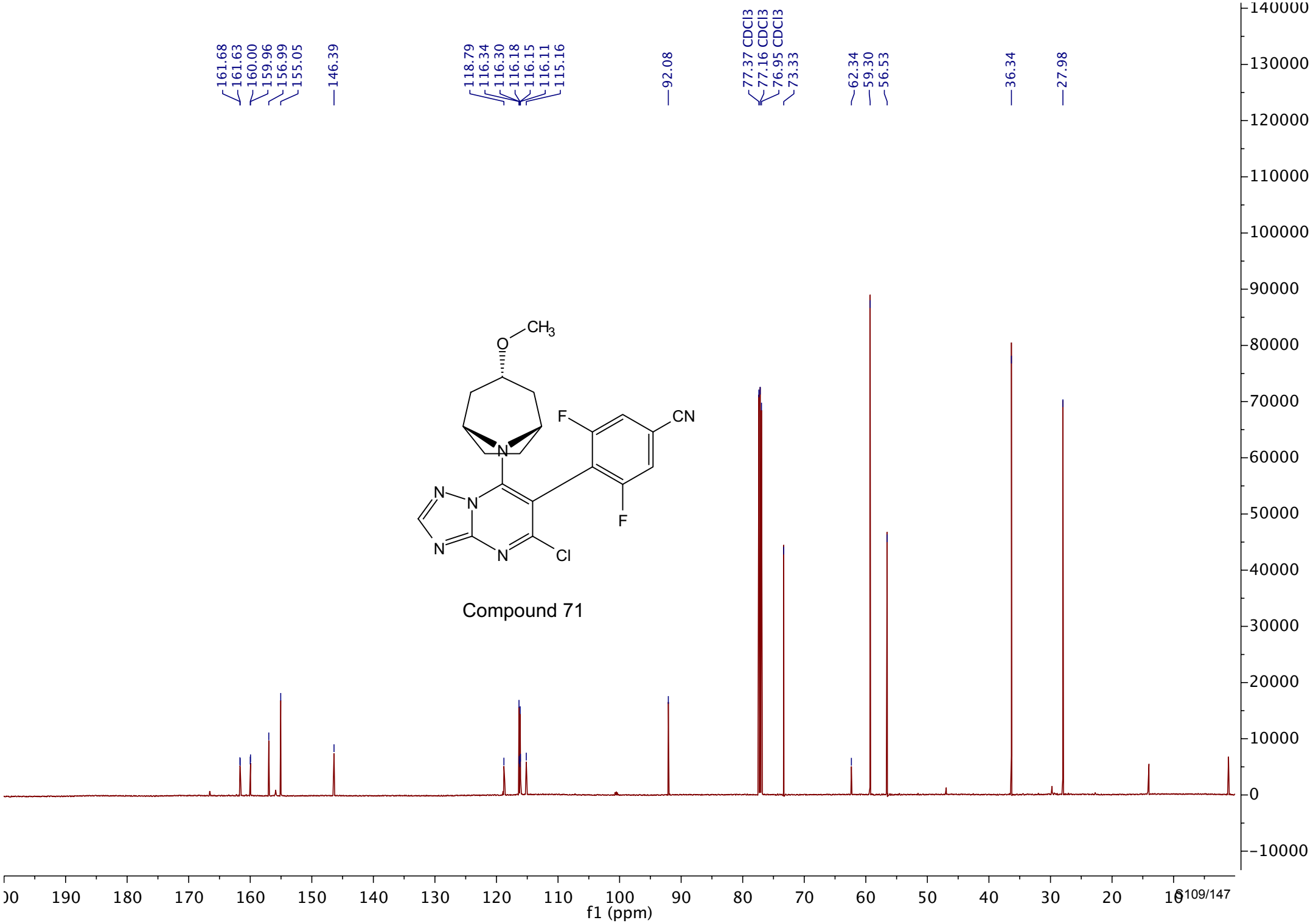
161.68
161.63
160.00
159.96
156.99
155.05
146.39
118.79
116.34
116.30
116.18
116.15
116.11
115.16
92.08
77.37 CDCl3
77.16 CDCl3
76.95 CDCl3
73.33
62.34
59.30
56.53
36.34
27.98
O
CH3
N
F
CN
F
N
N
N
N
Cl
Compound 71
f1 (ppm)
S109/147

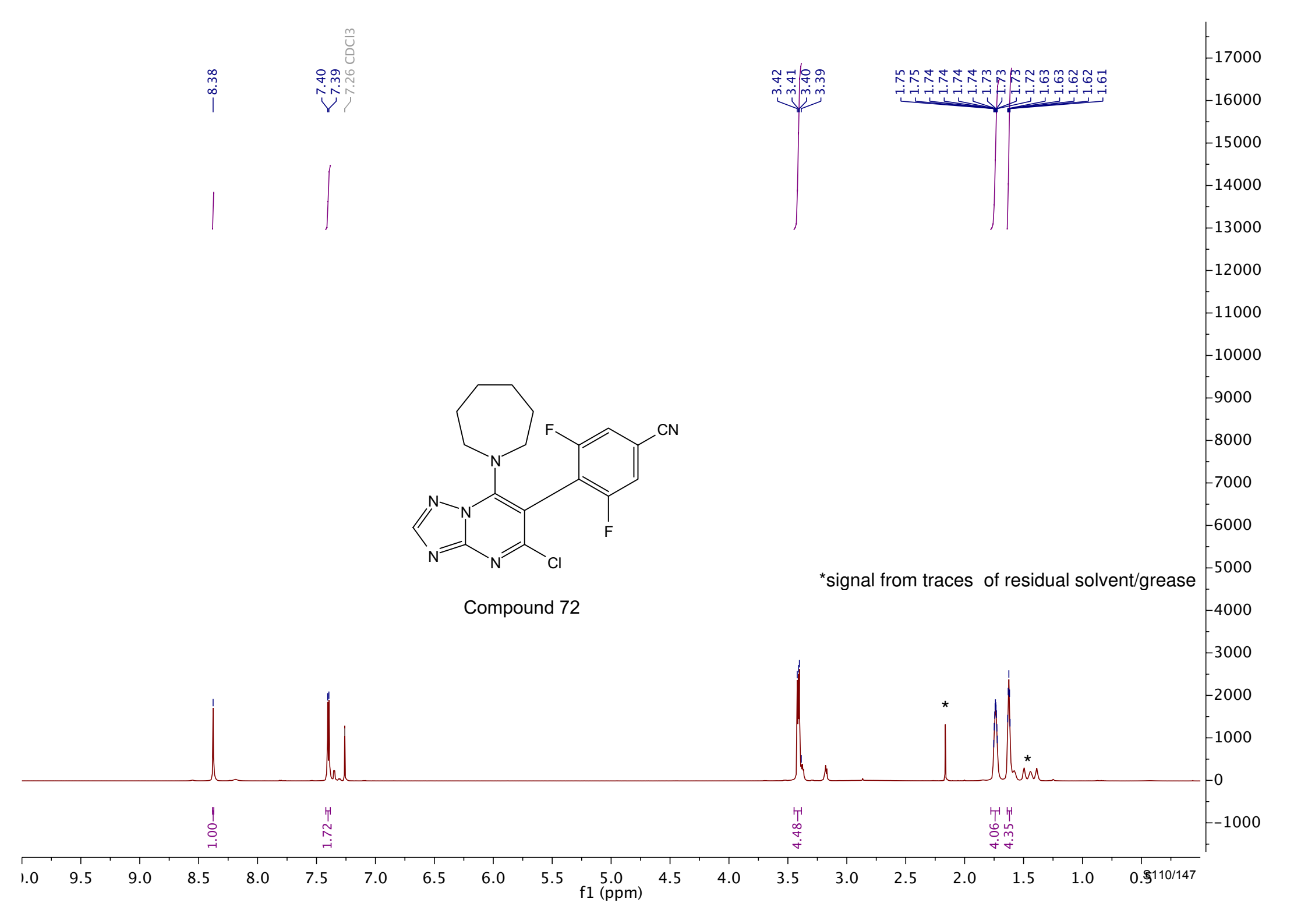
8.38
7.40
7.39
7.26 CDCl3
3.42
3.41
3.40
3.39
1.75
1.75
1.74
1.74
1.74
1.74
1.73
1.73
1.73
1.72
1.63
1.63
1.62
1.62
1.61
F
CN
N
N
N
N
N
F
Cl
Compound 72
*signal from traces of residual solvent/grease
1.00
1.72
4.48
4.06
4.35
f1 (ppm)

Compound 72
161.60
161.56
159.92
159.88
157.14
155.26
152.10
118.74
118.61
118.48
116.21
116.20
116.18
116.06
116.02
115.20
115.12
115.04
97.32
77.16 CDCl3
53.99
51.22
29.47
28.27
28.17
27.28
27.07
f1 (ppm)
11/11/1470

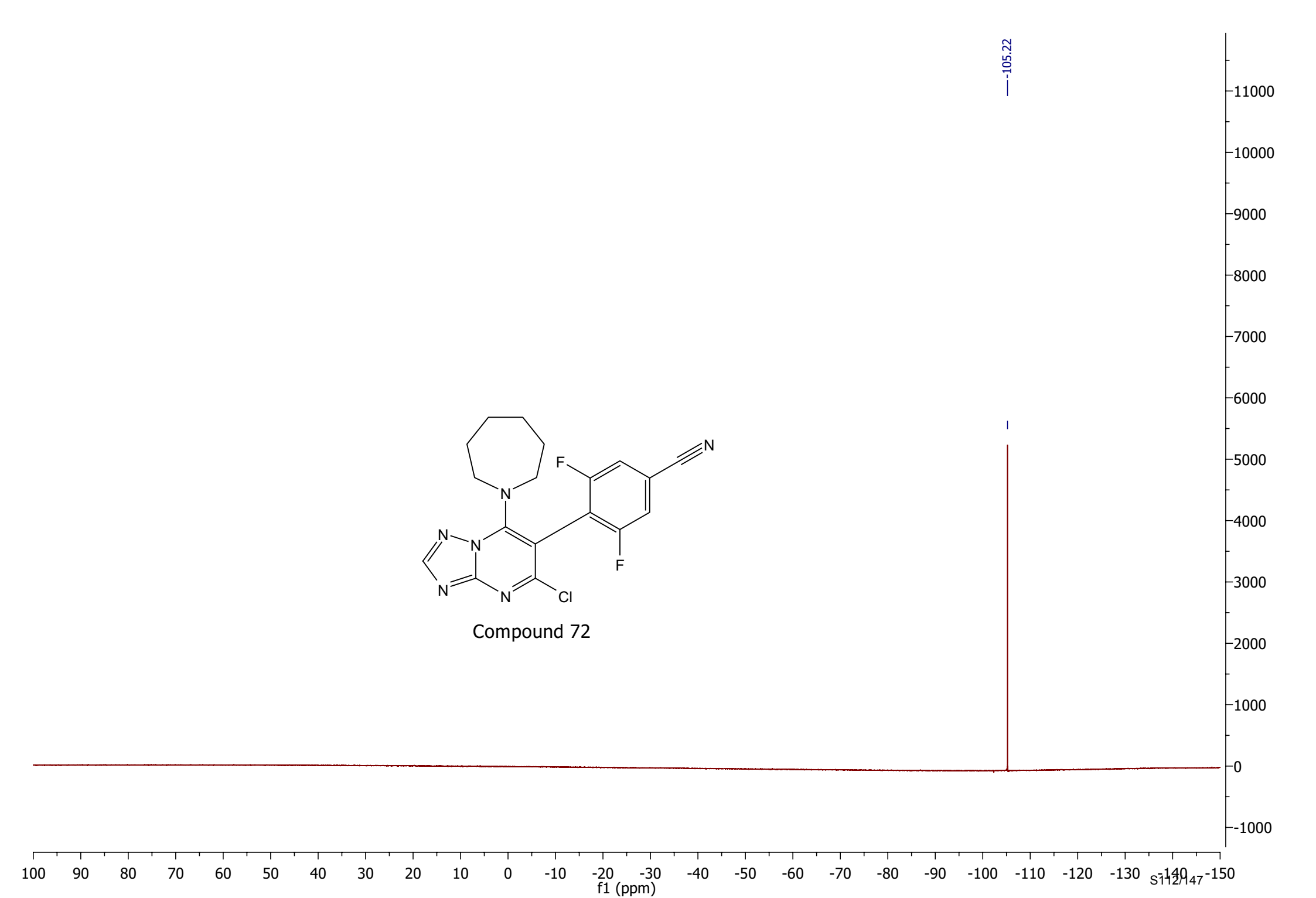
-105.22
11000
10000
9000
8000
7000
6000
5000
4000
3000
2000
1000
0
-1000
100 90 80 70 60 50 40 30 20 10 0 -10 -20 -30 -40 -50 -60 -70 -80 -90 -100 -110 -120 -130 -140 -150
f1 (ppm)
F
N
N
N
N
N
Cl
F
N

Compound 72

Compound 73
N
N
N
N
N
Cl
F
CN
f1 (ppm)
1.00
0.95
0.92
0.97
4.15
4.12
4.03
8.34
7.62
7.61
7.60
7.60
7.54
7.53
7.52
7.52
7.49
7.48
7.47
7.26 CDCl3
3.37
3.36
3.35
1.72
1.72
1.71
1.70
1.70
1.69
1.61
1.61
1.60
1.60
1.59

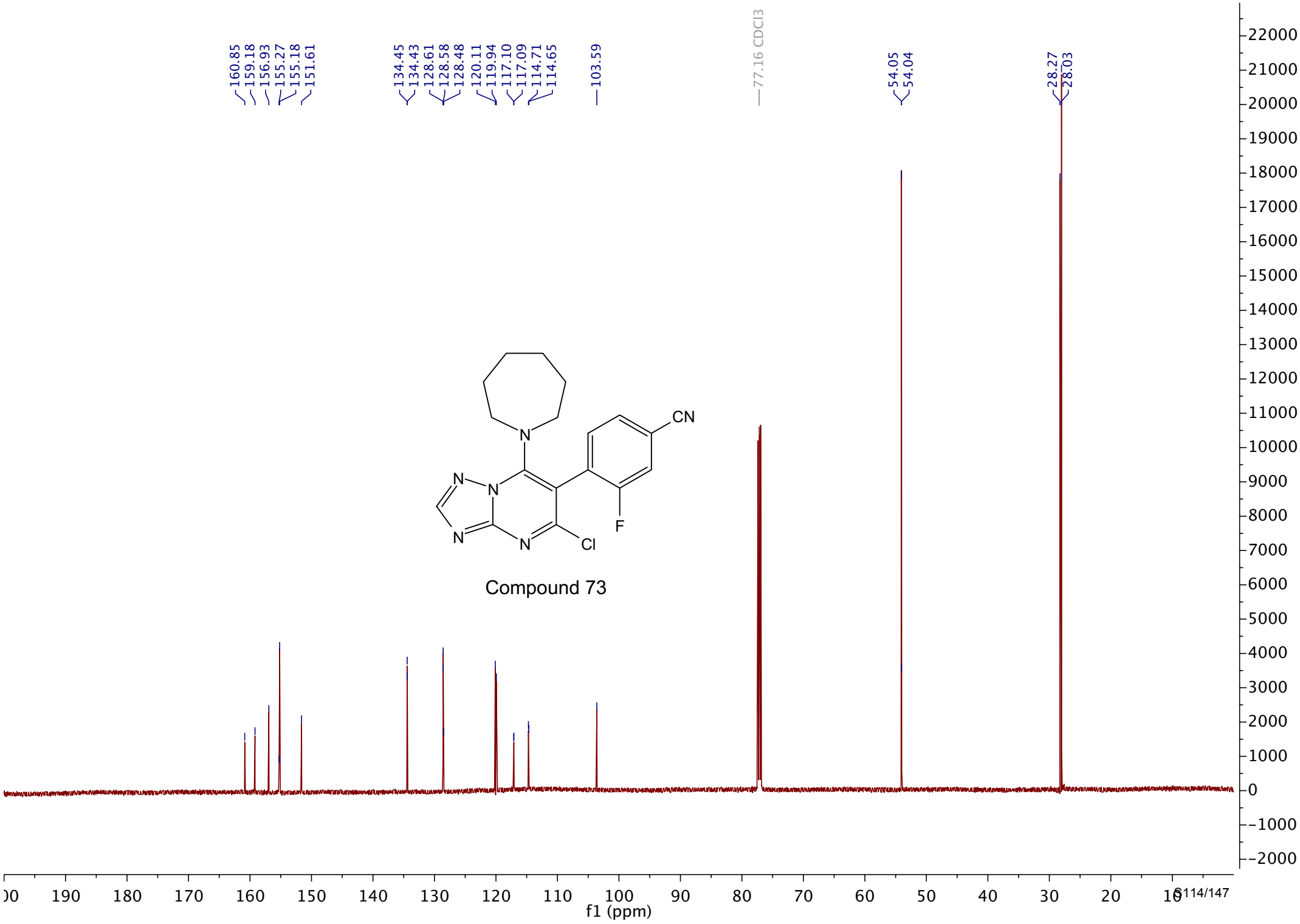
160.85
159.18
156.93
155.27
155.18
151.61
134.45
134.43
128.61
128.58
128.48
120.11
119.94
117.10
117.09
114.71
114.65
103.59
77.16 CDCl3
54.05
54.04
28.27
28.03
CN
F
Cl
N
N
N
N
N
Compound 73
f1 (ppm)
S114/147

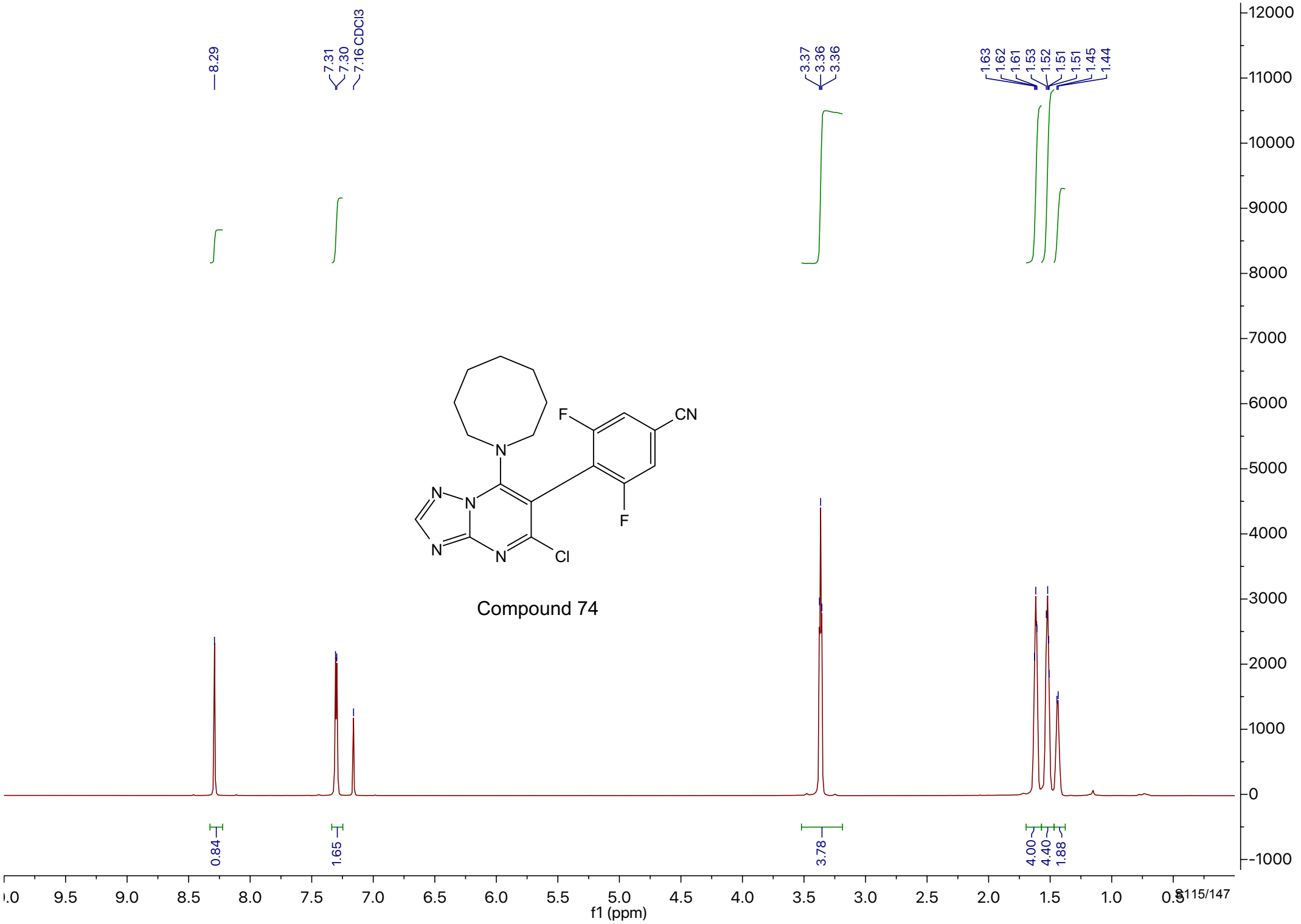
8.29
7.31
7.30
7.16 CDCl3
3.37
3.36
3.36
1.63
1.62
1.61
1.53
1.52
1.51
1.51
1.45
1.44
F
CN
N
N
N
N
N
F
Cl
Compound 74
0.84
1.65
3.78
4.00
4.40
1.88
f1 (ppm)
S115/147

TAL-314-2.1.fid

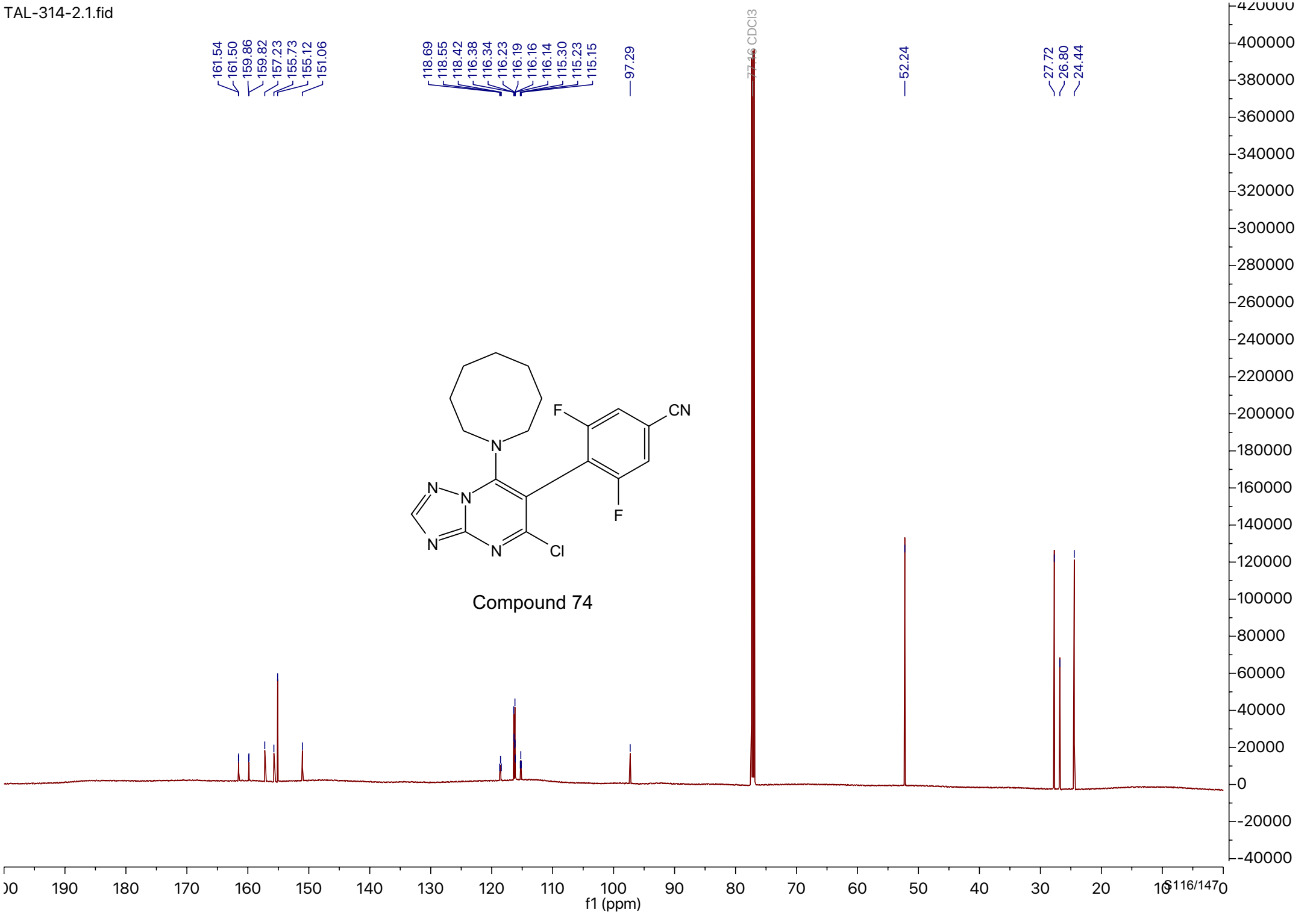

Compound 74

TAL-345-2.1.fid

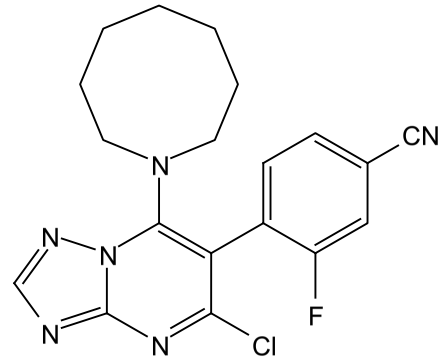

Compound 75

f1 (ppm)

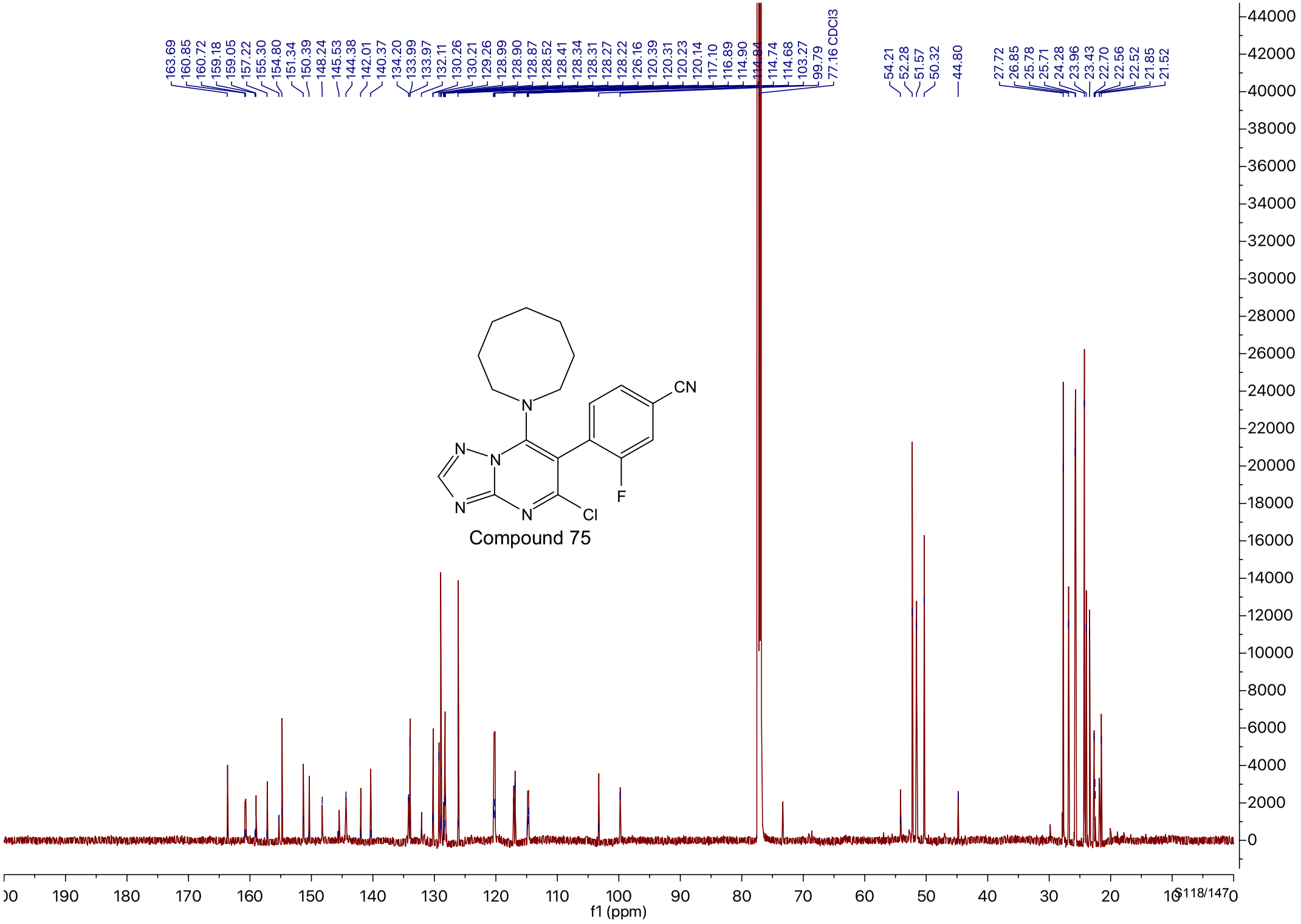
163.69
160.85
160.72
159.18
159.05
157.22
155.30
154.80
151.34
150.39
148.24
145.53
144.38
142.01
140.37
134.20
133.99
133.97
132.11
130.26
130.21
129.26
128.99
128.90
128.87
128.52
128.41
128.34
128.31
128.27
128.22
126.16
120.39
120.31
120.23
120.14
117.10
116.89
114.90
114.84
114.74
114.68
103.27
99.79
77.16 CDCl3
54.21
52.28
51.57
50.32
44.80
27.72
26.85
25.78
25.71
24.28
23.96
23.43
22.70
22.56
22.52
21.85
21.52
CN
F
Cl
N
Compound 75
f1 (ppm)
S118/147

Graph

Sample Name	69
Application Name	UV Only (Administrator)
Method Name	Analytical UV Only
Configuration Name	UV Only Config
Version	17
Data Instrument Name	Detector
Data Channel Name	159 Channel 1
Notes	
Injection Number	2

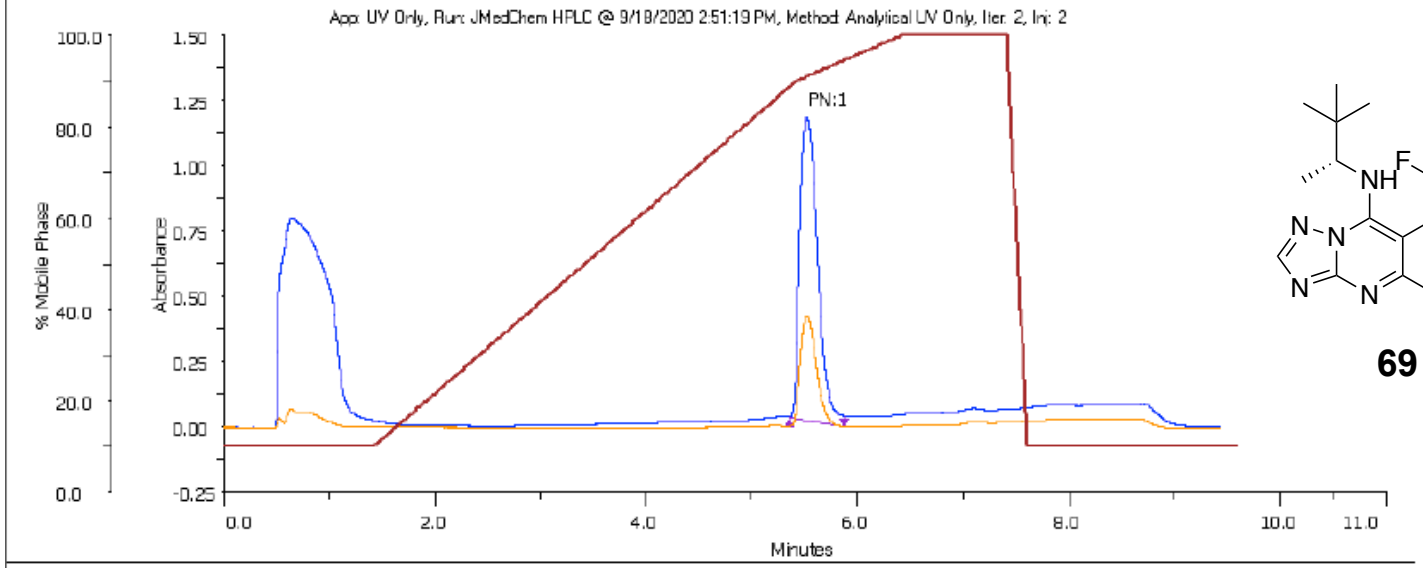

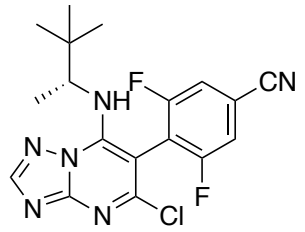

69

Sample Table

Sample Name	Retention Time (min)	Area (mAUmin x100)	Area %	Height (AU)					
69	5.529	23132.6158	100	1.166					

Graph

Sample Name	66
Application Name	UV Only (Administrator)
Method Name	Analytical UV Only
Configuration Name	UV Only Config
Version	17
Data Instrument Name	Detector
Data Channel Name	159 Channel 1
Notes	
Injection Number	3

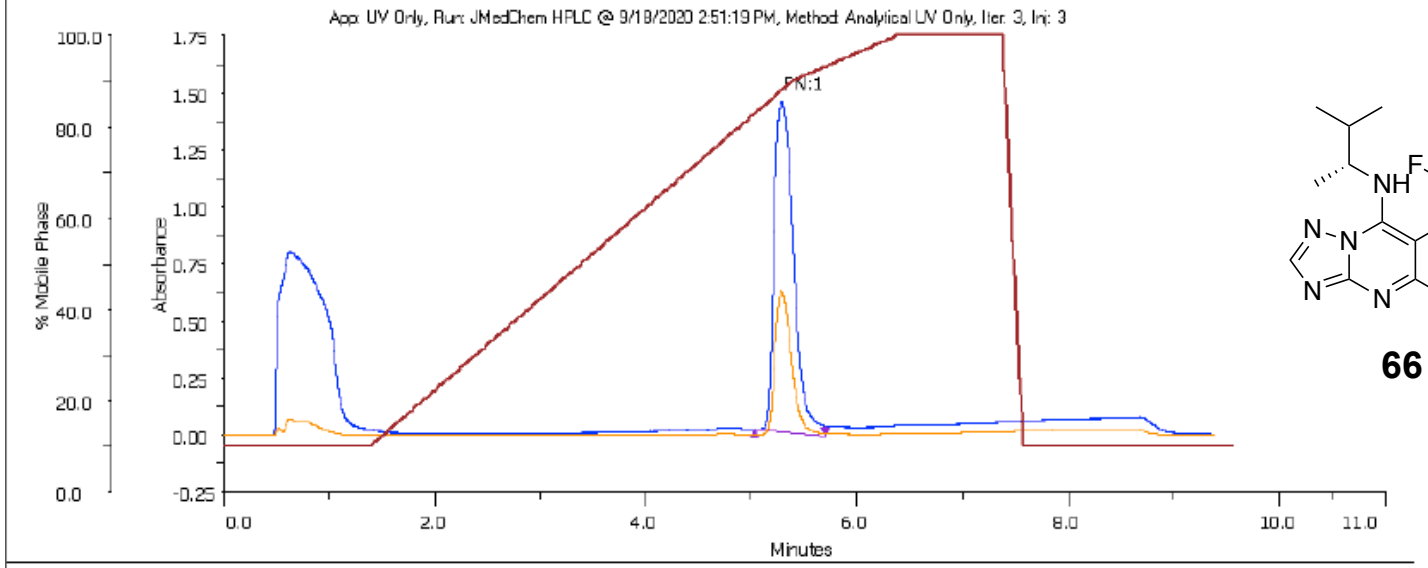

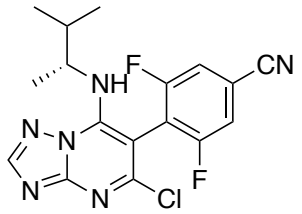

66

Sample Table

Sample Name	Retention Time (min)	Area (mAUmin x100)	Area %	Height (AU)					
66	5.299	31371.6585	100	1.45					

Graph

Sample Name	72
Application Name	UV Only (Administrator)
Method Name	Analytical UV Only
Configuration Name	UV Only Config
Version	17
Data Instrument Name	Detector
Data Channel Name	159 Channel 1
Notes	
Injection Number	4

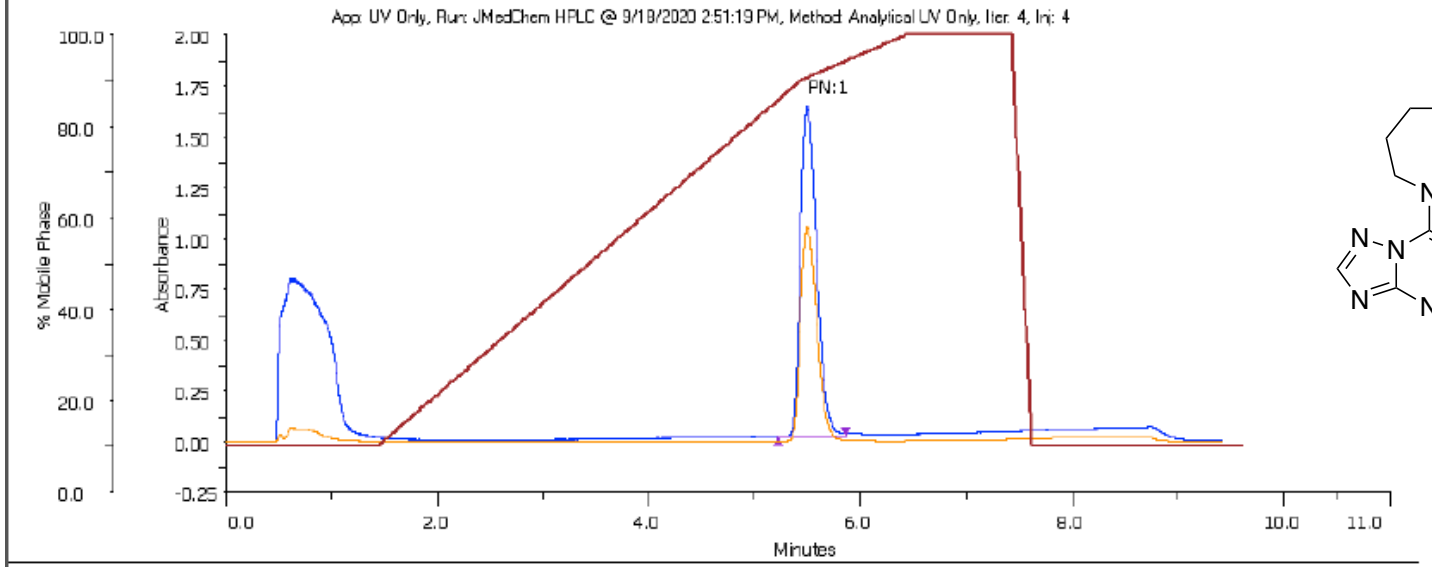

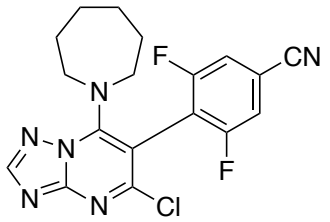

72

Sample Table

Sample Name	Retention Time (min)	Area (mAUmin x100)	Area %	Height (AU)					
72	5.504	28724.2049	100	1.627					

Graph

Sample Name	51
Application Name	UV Only (Administrator)
Method Name	Analytical UV Only
Configuration Name	UV Only Config
Version	17
Data Instrument Name	Detector
Data Channel Name	159 Channel 1
Notes	
Injection Number	5

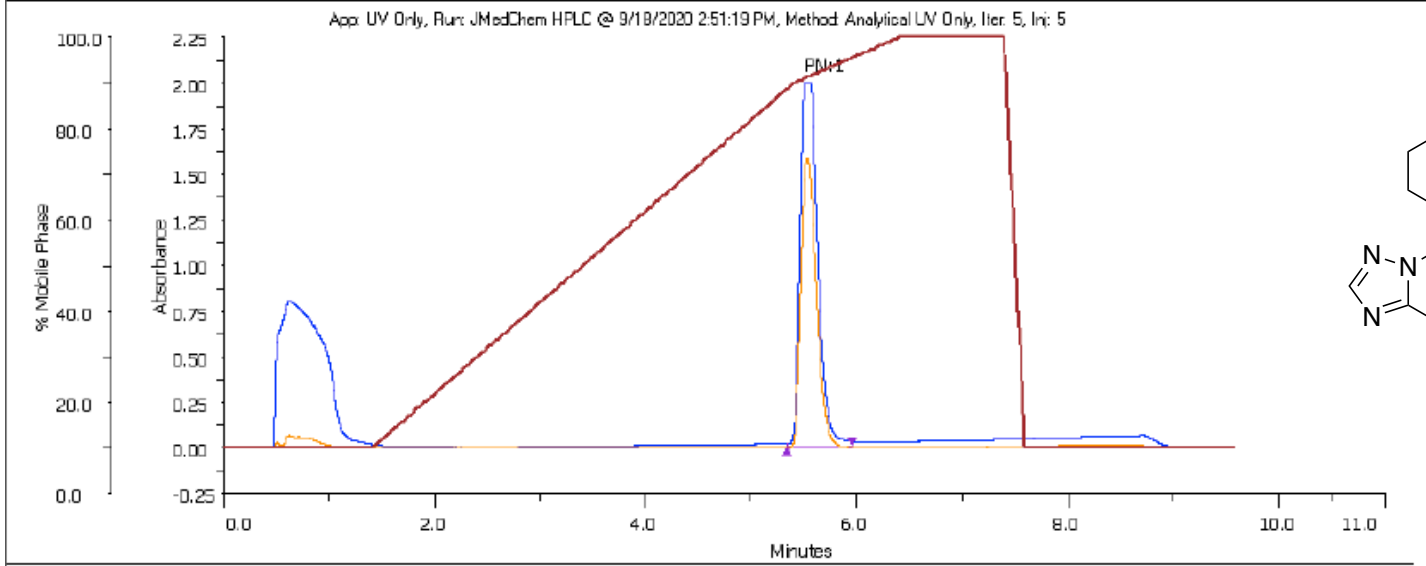

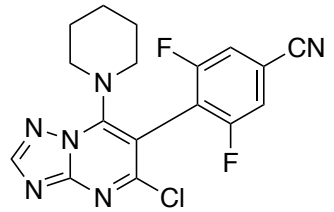

51

Sample Table

Sample Name	Retention Time (min)	Area (mAUmin x100)	Area %	Height (AU)					
51	5.517	38736.4657	100	1.987					

Graph

Sample Name	64
Application Name	UV Only (Administrator)
Method Name	Analytical UV Only
Configuration Name	UV Only Config
Version	17
Data Instrument Name	Detector
Data Channel Name	159 Channel 1
Notes	
Injection Number	6

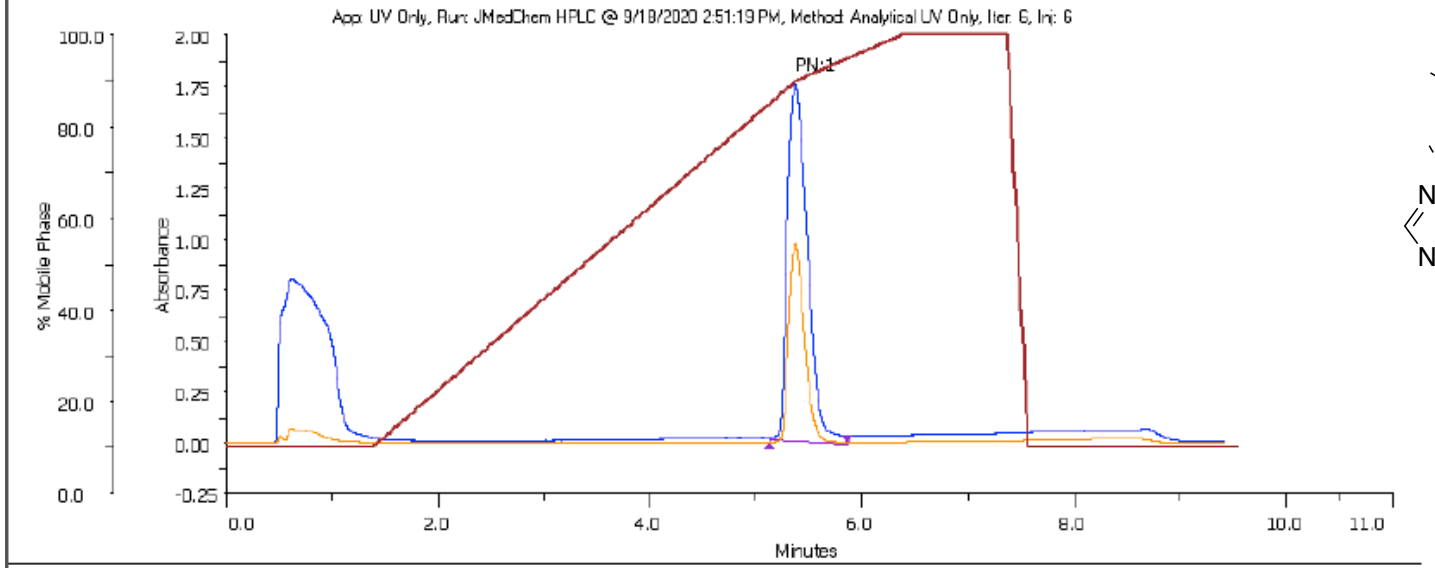

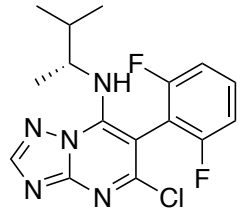

64

Sample Table

Sample Name	Retention Time (min)	Area (mAUmin x100)	Area %	Height (AU)					
64	5.373	39104.2447	100	1.761					

Graph

Sample Name	74
Application Name	UV Only (Administrator)
Method Name	Analytical UV Only
Configuration Name	UV Only Config
Version	17
Data Instrument Name	Detector
Data Channel Name	159 Channel 1
Notes	
Injection Number	7

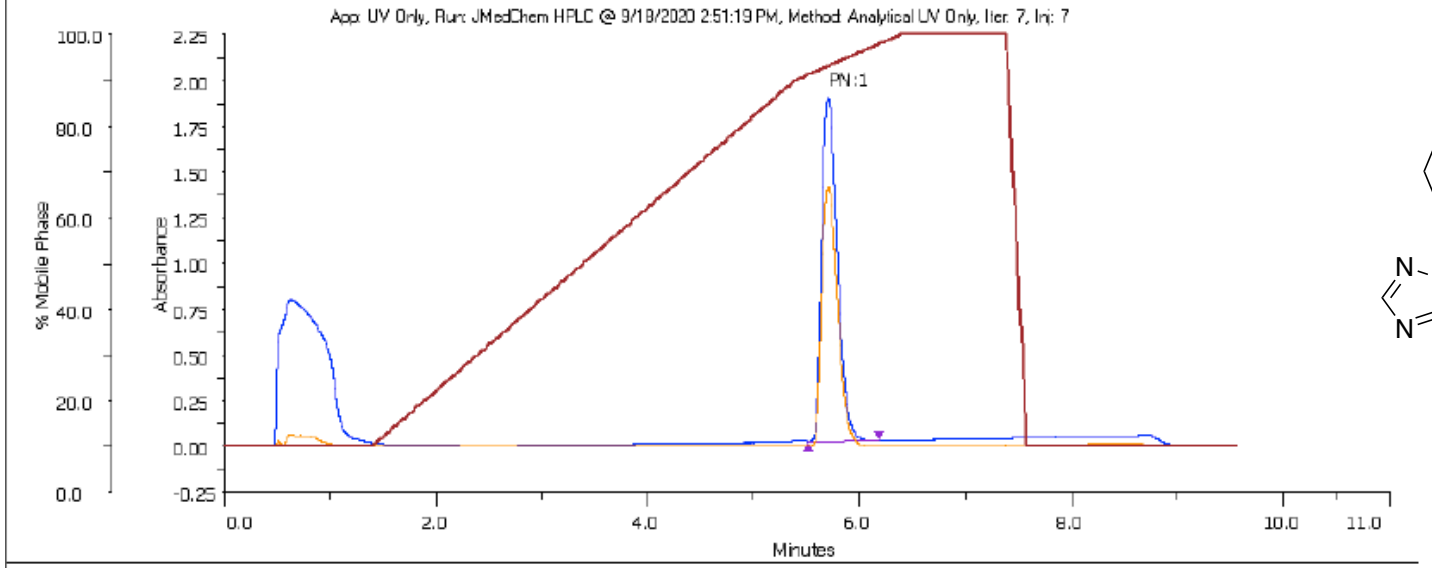

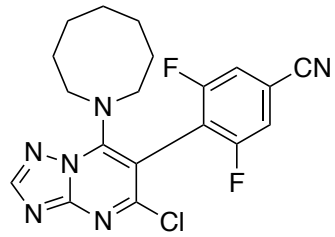

74

Sample Table

Sample Name	Retention Time (min)	Area (mAUmin x100)	Area %	Height (AU)					
74	5.712	32280.4836	100	1.874					

Graph

Sample Name	30
Application Name	UV Only (Administrator)
Method Name	Analytical UV Only
Configuration Name	UV Only Config
Version	17
Data Instrument Name	Detector
Data Channel Name	159 Channel 1
Notes	
Injection Number	8

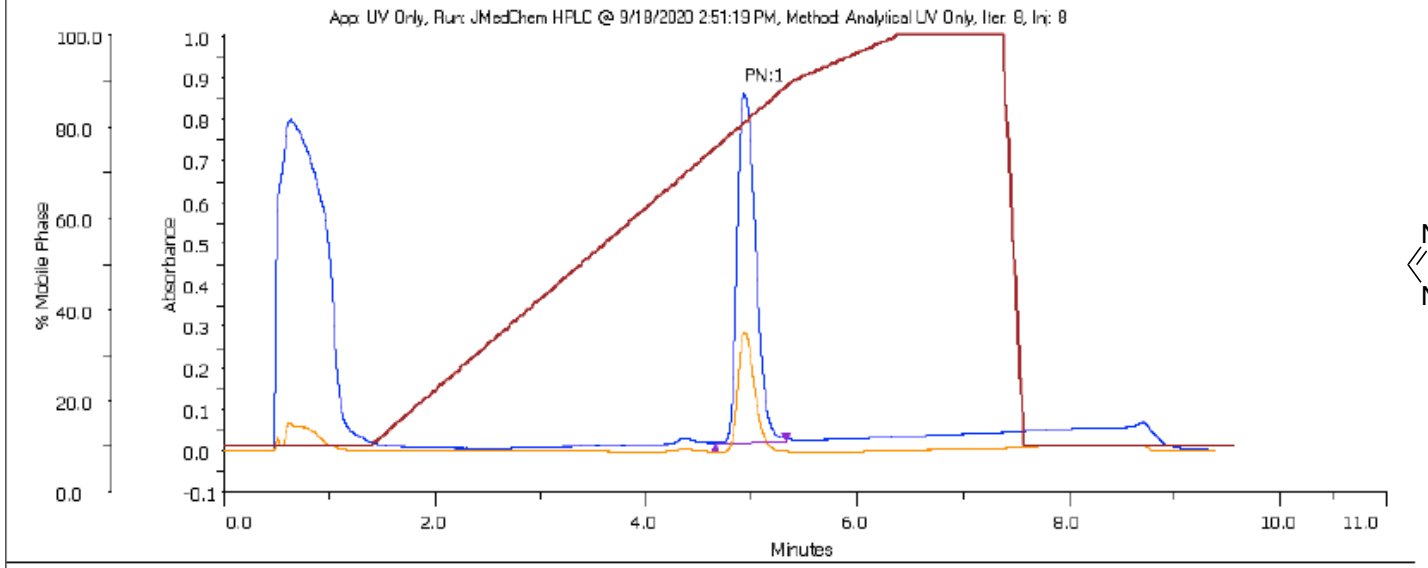

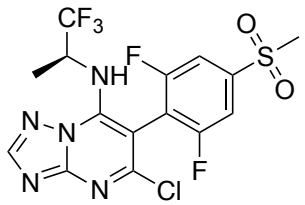

30

Sample Table

Sample Name	Retention Time (min)	Area (mAUmin x100)	Area %	Height (AU)					
30	4.933	17037.6122	100	0.84					

Graph

Sample Name	71
Application Name	UV Only (Administrator)
Method Name	Analytical UV Only
Configuration Name	UV Only Config
Version	17
Data Instrument Name	Detector
Data Channel Name	159 Channel 1
Notes	
Injection Number	9

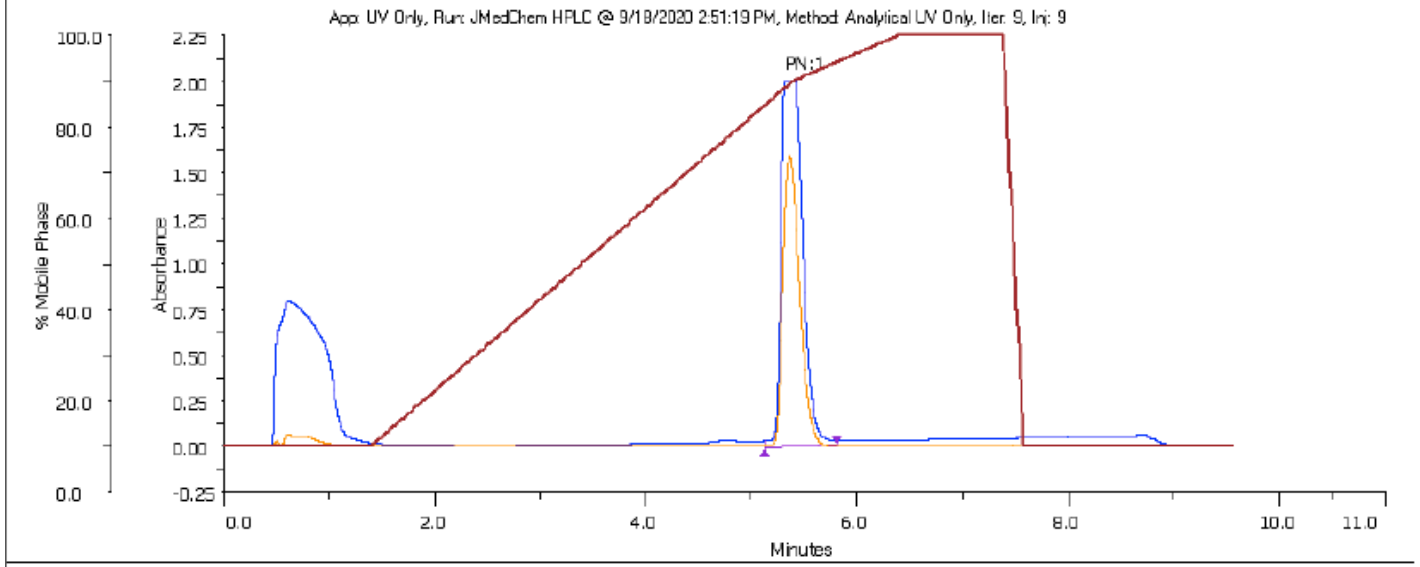

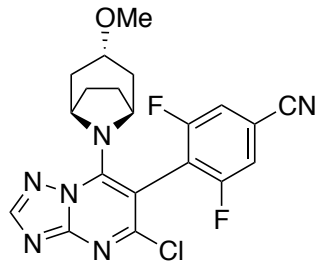

71

Sample Table

Sample Name	Retention Time (min)	Area (mAUmin x100)	Area %	Height (AU)					
71	5.326	47603.6358	100	2.001					

Graph

Sample Name	29
Application Name	UV Only (Administrator)
Method Name	Analytical UV Only
Configuration Name	UV Only Config
Version	17
Data Instrument Name	Detector
Data Channel Name	159 Channel 1
Notes	
Injection Number	10

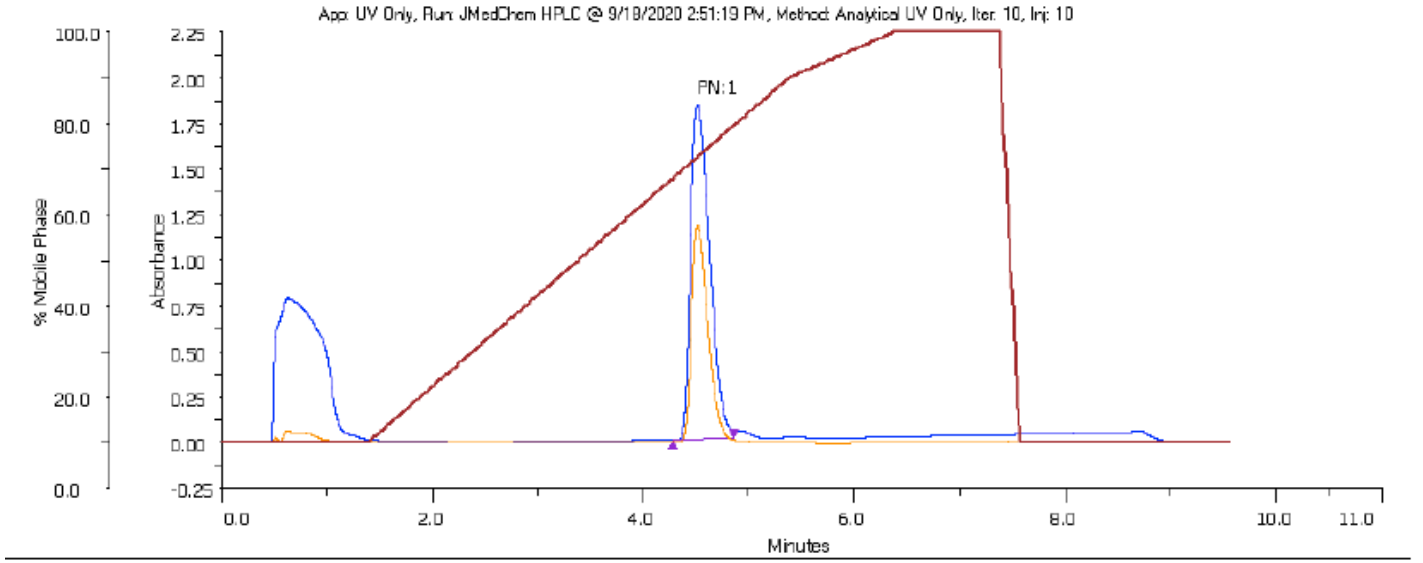

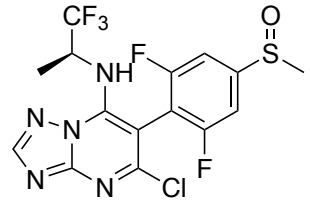

29

Sample Table

Sample Name	Retention Time (min)	Area (mAUmin x100)	Area %	Height (AU)
29	4.519	38639.9498	100	1.834

Graph

Sample Name	67
Application Name	UV Only (Administrator)
Method Name	Analytical UV Only
Configuration Name	UV Only Config
Version	17
Data Instrument Name	Detector
Data Channel Name	159 Channel 1
Notes	
Injection Number	15

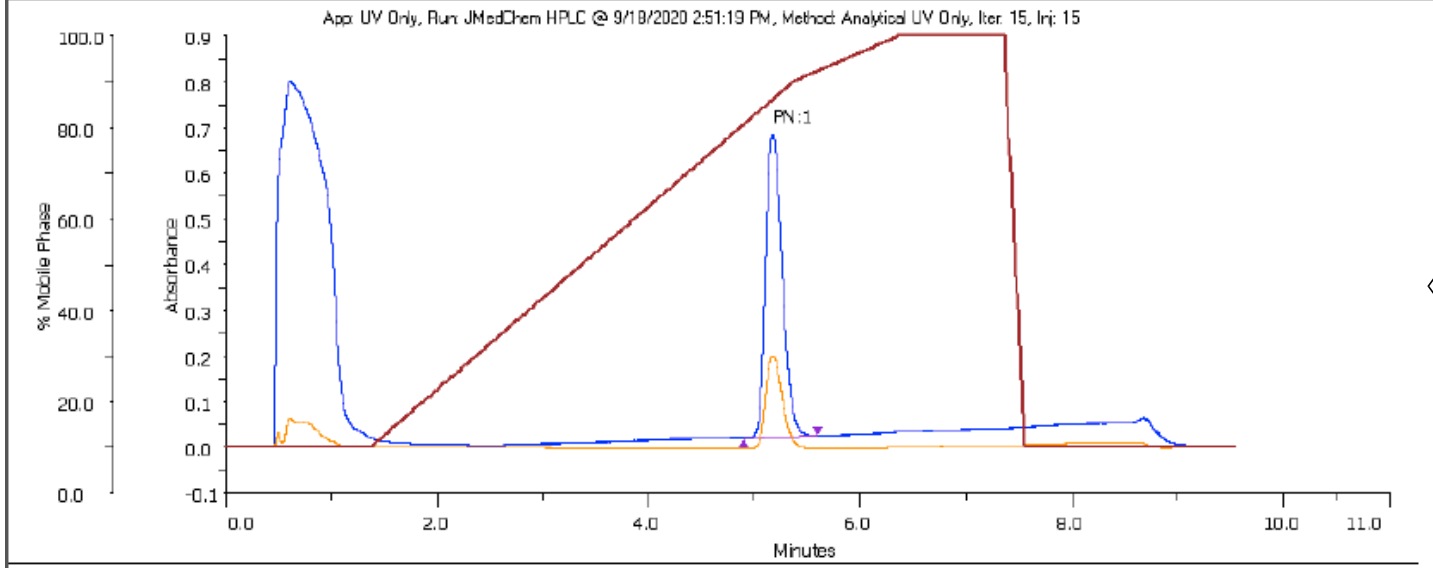

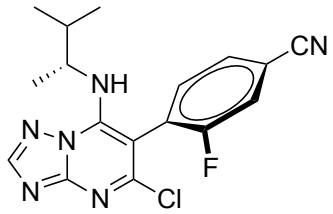

67

Sample Table

Sample Name	Retention Time (min)	Area (mAUmin x100)	Area %	Height (AU)					
67	5.176	12156.9832	100	0.662					

Crystal Structure Report

For The Ballatore Lab @ UCSD

Maximilian Bernbeck
UCSD Crystallography Lab
5128 Urey Hall
9500 Gilman Dr
La Jolla, CA 92093-0358
Tel: (858) 822-3871
Fax: (858) 822-3872
mbernbec@ucsd.edu

Experimental Summary

The single crystal X-ray diffraction studies were carried out on a Bruker APEX II Ultra CCD diffractometer equipped with Mo K_α radiation (λ = 0.71073). Crystals of the subject compound were recrystallized from evaporating dichloromethane. A 0.346 x 0.209 x 0.068 mm colorless plate crystal was mounted on a Cryoloop with Paratone oil.

Data were collected in a nitrogen gas stream at 100(2) K using ϕ and ϖ scans. Crystal-to-detector distance was 40 mm using exposure time 4 seconds with a scan width of 0.8°. Data collection was 100.0 complete to 25.242° in θ. A total of 30086 reflections were collected. 3902 reflections were found to be symmetry independent, with a R_{int} of 0.0438. Indexing and unit cell refinement indicated a **Primitive Monoclinic** lattice. The space group was found to be $\boldsymbol{P2_1}$**.** The data were integrated using the Bruker SAINT Software program and scaled using the SADABS software program. Solution by direct methods (SHELXT) produced a complete phasing model consistent with the proposed structure.

All nonhydrogen atoms were refined anisotropically by full-matrix least-squares (SHELXL-2014). All carbon bonded hydrogen atoms were placed using a riding model. Their positions were constrained relative to their parent atom using the appropriate HFIX command in SHELXL-2014.

Notes: Excellent data and refinement

Compound 68 (CCDC : 1995770)

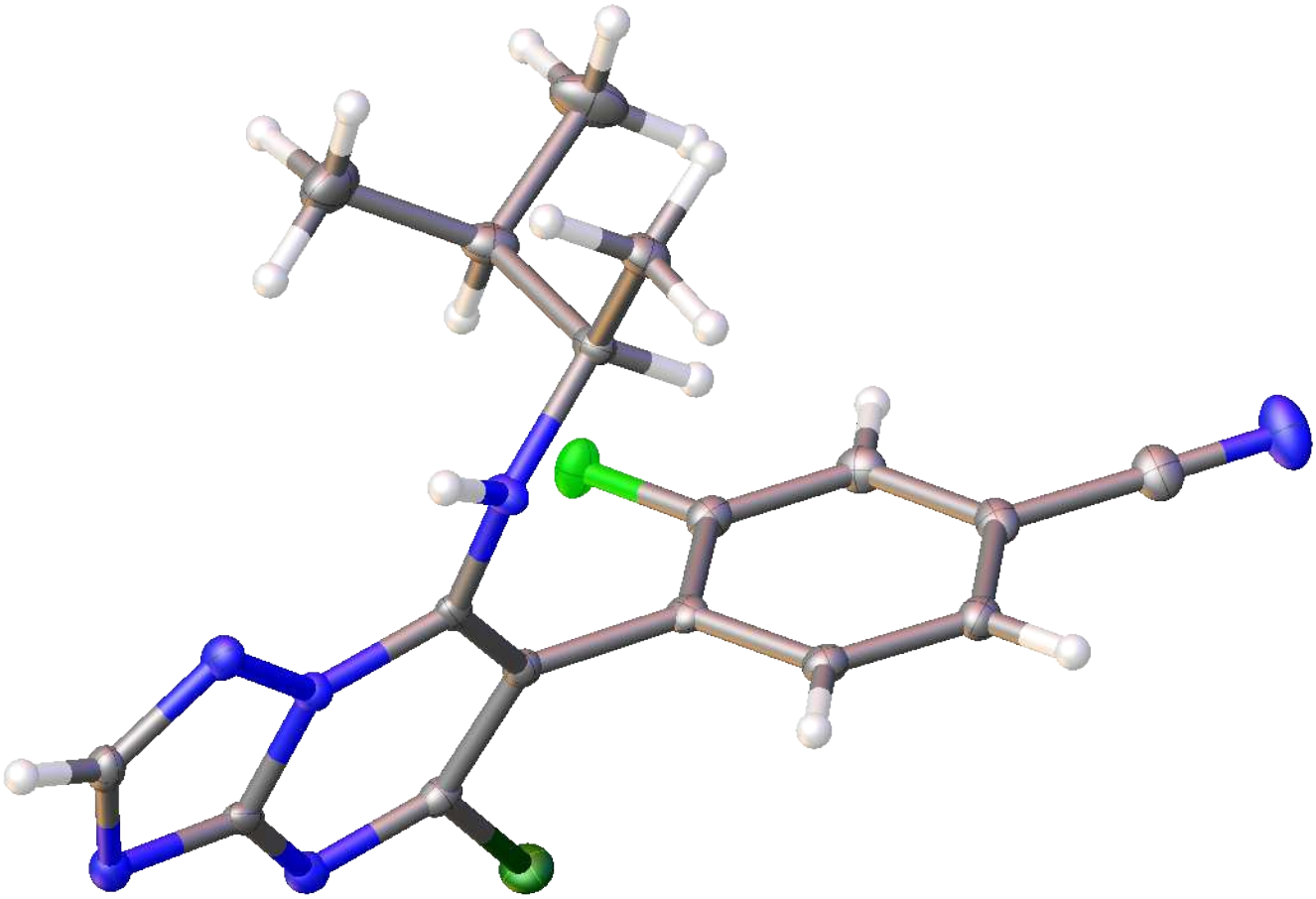

Table S-2. Crystal data and structure refinement for Ballatore_TAL_374_2.

Identification code	ballatore_tal_374_2_0m	
Empirical formula	C17 H16 Cl F N6	
Formula weight	358.81	
Temperature	100.15 K	
Wavelength	0.71073 Å	
Crystal system	Monoclinic	
Space group	P 1 21 1	
Unit cell dimensions	a = 10.0763(6) Å	α= 90°.
	b = 6.6106(4) Å	β= 105.610(2)°.
	c = 13.2029(9) Å	γ = 90°.
Volume	847.01(9) $Å^3$	
Z	2	
Density (calculated)	1.407 Mg/m^3	
Absorption coefficient	0.249 mm^{-1}	
F(000)	372	
Crystal size	0.346 x 0.209 x 0.068 mm^3	
Theta range for data collection	1.601 to 27.517°.	
Index ranges	-13<=h<=13, -8<=k<=8, -17<=l<=17	
Reflections collected	30086	
Independent reflections	3902 [R(int) = 0.0438]	
Completeness to theta = 25.242°	100.0 %	
Absorption correction	Semi-empirical from equivalents	
Max. and min. transmission	0.7456 and 0.5946	
Refinement method	Full-matrix least-squares on F^2	
Data / restraints / parameters	3902 / 2 / 232	
Goodness-of-fit on F^2	1.067	
Final R indices [I>2sigma(I)]	R1 = 0.0254, wR2 = 0.0607	
R indices (all data)	R1 = 0.0275, wR2 = 0.0620	
Absolute structure parameter	0.000(19)	
Extinction coefficient	n/a	
Largest diff. peak and hole	0.280 and -0.188 $e.Å^{-3}$	

Table S-3. Atomic coordinates (x 10^4) and equivalent isotropic displacement parameters ($Å^2$x 10^3) for Ballatore_TAL_374_2. U(eq) is defined as one third of the trace of the orthogonalized U^{ij} tensor.

	x	y	z	U(eq)
Cl(1)	6697(1)	4428(1)	5611(1)	18(1)
F(1)	5512(1)	7291(2)	3510(1)	19(1)
N(1)	852(2)	2407(3)	1238(1)	26(1)
N(2)	9255(2)	4468(3)	5609(1)	14(1)
N(3)	11621(2)	4436(3)	5522(1)	15(1)
N(4)	11164(1)	4330(3)	3726(1)	14(1)
N(5)	9971(1)	4325(3)	4031(1)	11(1)
N(6)	8576(2)	4128(3)	2334(1)	12(1)
C(1)	1969(2)	2736(3)	1692(2)	18(1)
C(2)	3391(2)	3139(3)	2239(2)	15(1)
C(3)	3770(2)	5080(3)	2625(2)	16(1)
C(4)	5137(2)	5415(3)	3138(1)	14(1)
C(5)	6144(2)	3921(3)	3287(1)	12(1)
C(6)	5728(2)	1988(3)	2896(1)	14(1)
C(7)	4367(2)	1599(3)	2374(1)	15(1)
C(8)	7603(2)	4295(3)	3868(1)	12(1)
C(9)	8008(2)	4416(3)	4976(1)	13(1)
C(10)	8662(2)	4255(3)	3364(1)	11(1)
C(11)	10257(2)	4404(3)	5111(1)	13(1)
C(12)	12094(2)	4387(4)	4655(1)	15(1)
C(13)	7465(2)	4991(3)	1478(1)	13(1)
C(14)	7392(2)	7304(3)	1609(2)	18(1)
C(15)	8702(3)	8395(3)	1566(2)	28(1)
C(16)	6128(3)	8165(4)	808(2)	30(1)
C(17)	7708(2)	4322(4)	438(1)	17(1)

Table S-4. Bond lengths [Å] and angles [°] for Ballatore_TAL_374_2.

Cl(1)-C(9)	1.7443(16)	C(10)-N(6)-C(13)	125.51(16)
F(1)-C(4)	1.350(2)	N(1)-C(1)-C(2)	178.4(2)
N(1)-C(1)	1.144(3)	C(3)-C(2)-C(1)	119.29(19)
N(2)-C(9)	1.309(2)	C(7)-C(2)-C(1)	119.98(18)
N(2)-C(11)	1.345(2)	C(7)-C(2)-C(3)	120.73(18)
N(3)-C(11)	1.335(2)	C(4)-C(3)-C(2)	117.77(18)
N(3)-C(12)	1.354(2)	F(1)-C(4)-C(3)	118.09(17)
N(4)-N(5)	1.3662(19)	F(1)-C(4)-C(5)	118.59(17)
N(4)-C(12)	1.328(2)	C(3)-C(4)-C(5)	123.33(18)
N(5)-C(10)	1.376(2)	C(4)-C(5)-C(6)	117.44(17)
N(5)-C(11)	1.378(2)	C(4)-C(5)-C(8)	122.55(17)
N(6)-C(10)	1.342(2)	C(6)-C(5)-C(8)	119.98(17)
N(6)-C(13)	1.475(2)	C(7)-C(6)-C(5)	120.83(18)
C(1)-C(2)	1.445(3)	C(6)-C(7)-C(2)	119.90(18)
C(2)-C(3)	1.395(3)	C(9)-C(8)-C(5)	120.98(14)
C(2)-C(7)	1.393(3)	C(10)-C(8)-C(5)	121.78(15)
C(3)-C(4)	1.379(3)	C(10)-C(8)-C(9)	116.63(15)
C(4)-C(5)	1.392(3)	N(2)-C(9)-Cl(1)	114.51(12)
C(5)-C(6)	1.399(3)	N(2)-C(9)-C(8)	128.50(15)
C(5)-C(8)	1.484(2)	C(8)-C(9)-Cl(1)	116.96(13)
C(6)-C(7)	1.383(3)	N(5)-C(10)-C(8)	114.68(14)
C(8)-C(9)	1.412(2)	N(6)-C(10)-N(5)	116.10(14)
C(8)-C(10)	1.401(2)	N(6)-C(10)-C(8)	129.21(16)
C(13)-C(14)	1.542(3)	N(2)-C(11)-N(5)	122.09(15)
C(13)-C(17)	1.524(2)	N(3)-C(11)-N(2)	128.83(15)
C(14)-C(15)	1.518(3)	N(3)-C(11)-N(5)	109.07(14)
C(14)-C(16)	1.530(3)	N(4)-C(12)-N(3)	117.39(15)
		N(6)-C(13)-C(14)	110.28(16)
C(9)-N(2)-C(11)	113.96(13)	N(6)-C(13)-C(17)	107.78(15)
C(11)-N(3)-C(12)	102.35(13)	C(17)-C(13)-C(14)	114.38(17)
C(12)-N(4)-N(5)	100.71(13)	C(15)-C(14)-C(13)	113.51(18)
N(4)-N(5)-C(10)	125.41(13)	C(15)-C(14)-C(16)	111.58(19)
N(4)-N(5)-C(11)	110.47(13)	C(16)-C(14)-C(13)	110.30(18)
C(10)-N(5)-C(11)	124.12(14)		

Table S-5. Anisotropic displacement parameters ($Å^2 x\ 10^3$) for Ballatore_TAL_374_2. The anisotropic displacement factor exponent takes the form: $-2\pi^2[\ h^2\ a^{*2}U^{11} + ...\ + 2\ h\ k\ a^*\ b^*\ U^{12}\ ]$

	U^{11}	U^{22}	U^{33}	U^{23}	U^{13}	U^{12}
Cl(1)	19(1)	24(1)	15(1)	0(1)	11(1)	0(1)
F(1)	16(1)	13(1)	29(1)	-4(1)	7(1)	0(1)
N(1)	15(1)	38(1)	25(1)	-11(1)	5(1)	0(1)
N(2)	18(1)	13(1)	12(1)	-1(1)	4(1)	-1(1)
N(3)	14(1)	14(1)	16(1)	0(1)	2(1)	0(1)
N(4)	11(1)	14(1)	17(1)	1(1)	5(1)	1(1)
N(5)	11(1)	12(1)	12(1)	0(1)	4(1)	1(1)
N(6)	11(1)	17(1)	10(1)	1(1)	4(1)	2(1)
C(1)	17(1)	23(1)	17(1)	-4(1)	8(1)	1(1)
C(2)	13(1)	21(1)	12(1)	-1(1)	6(1)	-1(1)
C(3)	13(1)	18(1)	18(1)	1(1)	7(1)	3(1)
C(4)	16(1)	13(1)	14(1)	-1(1)	7(1)	0(1)
C(5)	13(1)	15(1)	11(1)	2(1)	6(1)	-1(1)
C(6)	16(1)	13(1)	13(1)	1(1)	6(1)	1(1)
C(7)	17(1)	15(1)	13(1)	-1(1)	5(1)	-2(1)
C(8)	13(1)	10(1)	12(1)	0(1)	4(1)	0(1)
C(9)	16(1)	11(1)	14(1)	0(1)	8(1)	-1(1)
C(10)	12(1)	8(1)	12(1)	0(1)	2(1)	1(1)
C(11)	16(1)	10(1)	11(1)	2(1)	1(1)	0(1)
C(12)	11(1)	13(1)	18(1)	0(1)	3(1)	0(1)
C(13)	12(1)	16(1)	12(1)	2(1)	3(1)	1(1)
C(14)	24(1)	18(1)	13(1)	2(1)	6(1)	6(1)
C(15)	38(1)	18(1)	27(1)	1(1)	9(1)	-6(1)
C(16)	35(1)	30(1)	22(1)	4(1)	5(1)	17(1)
C(17)	19(1)	18(1)	12(1)	0(1)	3(1)	3(1)

Table S-6. Hydrogen coordinates (x 10^4) and isotropic displacement parameters ($Å^2$x 10^3) for Ballatore_TAL_374_2.

	x	y	z	U(eq)
H(6)	9382(19)	4050(40)	2228(16)	15
H(3)	3109	6135	2537	19
H(6A)	6388	930	2990	16
H(7)	4098	283	2107	18
H(12)	13053	4393	4709	17
H(13)	6571	4399	1527	16
H(14)	7261	7555	2323	22
H(15A)	9492	7790	2078	41
H(15B)	8631	9828	1735	41
H(15C)	8828	8272	858	41
H(16A)	6246	8027	99	45
H(16B)	6023	9598	961	45
H(16C)	5304	7421	853	45
H(17A)	8584	4877	376	25
H(17B)	6955	4817	-145	25
H(17C)	7739	2842	414	25

Compound 111 (CCDC: 2003391)

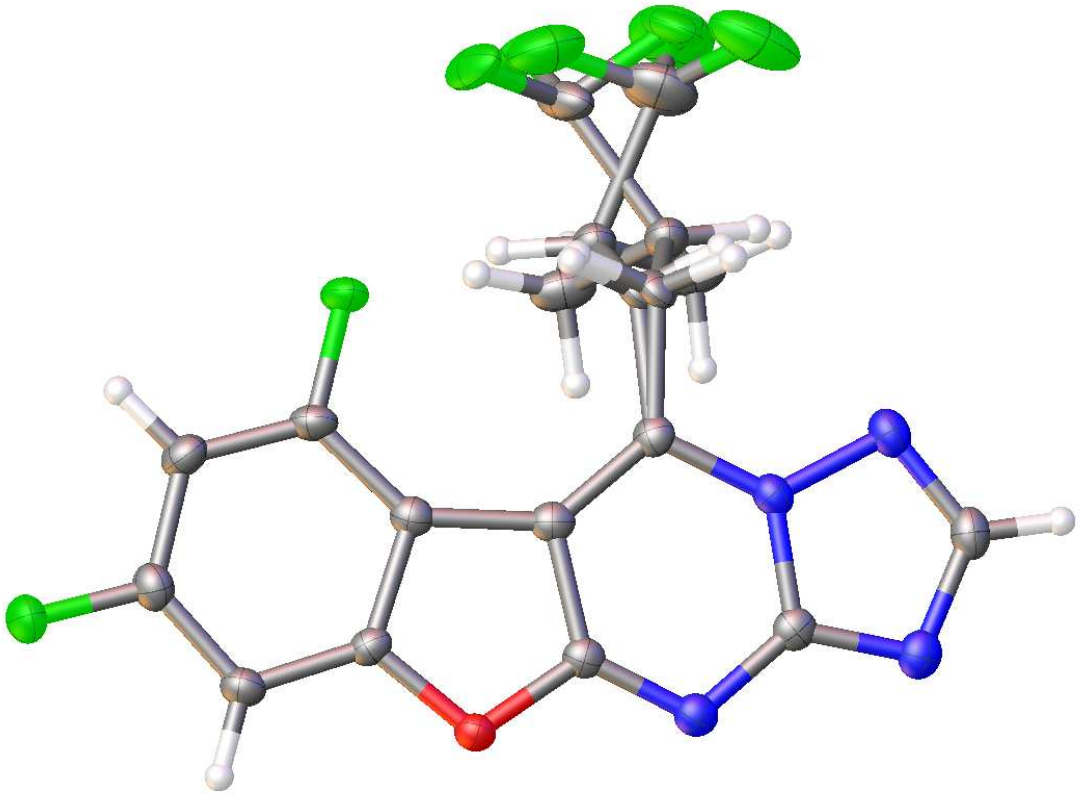

Table S-7. Crystal data and structure refinement for Ballatore_BRL_I_205.

Identification code	ballatore_brl_i_205_redo_0m_a	
Empirical formula	C15 H9 F5 N4 O	
Formula weight	356.26	
Temperature	100.0 K	
Wavelength	1.54178 Å	
Crystal system	Triclinic	
Space group	P-1	
Unit cell dimensions	a = 9.71530(10) Å	α= 94.8510(10)°.
	b = 10.56760(10) Å	β= 92.2480(10)°.
	c = 14.1191(2) Å	γ = 98.7440(10)°.
Volume	1425.59(3) $Å^3$	
Z	4	
Density (calculated)	1.660 Mg/m^3	
Absorption coefficient	1.358 mm^{-1}	
F(000)	720	
Crystal size	0.22 x 0.18 x 0.08 mm^3	
Theta range for data collection	3.146 to 66.663°.	
Index ranges	-11<=h<=11, -12<=k<=12, -16<=l<=16	
Reflections collected	40759	
Independent reflections	4785 [R(int) = 0.0301]	
Completeness to theta = 66.663°	94.9 %	
Absorption correction	Semi-empirical from equivalents	
Max. and min. transmission	0.5201 and 0.4391	
Refinement method	Full-matrix least-squares on F^2	
Data / restraints / parameters	4785 / 54 / 541	
Goodness-of-fit on F^2	1.136	
Final R indices [I>2sigma(I)]	R1 = 0.0458, wR2 = 0.1157	
R indices (all data)	R1 = 0.0479, wR2 = 0.1169	
Extinction coefficient	n/a	
Largest diff. peak and hole	0.554 and -0.309 $e.Å^{-3}$	

Table S-8. Atomic coordinates (x 10^4) and equivalent isotropic displacement parameters ($Å^2$x 10^3) for Ballatore_BRL_I_205. U(eq) is defined as one third of the trace of the orthogonalized U^{ij} tensor.

	x	y	z	U(eq)
F(1A)	-4692(1)	7745(1)	2031(1)	30(1)
F(2A)	-417(1)	6403(1)	1393(1)	27(1)
O(1A)	-1541(2)	7147(1)	4558(1)	19(1)
N(1A)	2472(2)	5921(2)	5918(1)	23(1)
N(2A)	351(2)	6604(2)	5362(1)	20(1)
N(3A)	2089(2)	5926(2)	4356(1)	19(1)
N(4A)	3341(2)	5483(2)	4462(2)	23(1)
C(1A)	3490(2)	5510(2)	5397(2)	24(1)
C(2A)	1587(2)	6176(2)	5251(2)	19(1)
C(3A)	-272(2)	6739(2)	4558(2)	18(1)
C(4A)	-1975(2)	7152(2)	3611(2)	18(1)
C(5A)	-3243(2)	7473(2)	3331(2)	21(1)
C(6A)	-3482(2)	7413(2)	2360(2)	23(1)
C(7A)	-2563(2)	7055(2)	1698(2)	24(1)
C(8A)	-1323(2)	6746(2)	2031(2)	21(1)
C(9A)	-975(2)	6779(2)	3000(2)	19(1)
C(10A)	156(2)	6500(2)	3612(2)	19(1)
C(11A)	1423(2)	6088(2)	3512(2)	19(1)
F(3A)	1637(5)	5153(4)	545(3)	43(1)
F(4A)	3352(6)	4316(5)	1114(4)	41(1)
F(5A)	1453(4)	3108(3)	646(2)	45(1)
C(12A)	2240(20)	5877(9)	2644(11)	19(2)
C(13A)	2108(6)	4429(5)	2357(4)	23(1)
C(14A)	636(6)	3728(5)	2225(4)	33(1)
C(15A)	1938(8)	4231(6)	1113(5)	32(1)
F(3B)	2266(6)	4818(6)	737(3)	61(1)
F(4B)	2850(4)	3043(4)	1147(3)	64(1)
F(5B)	4193(5)	4820(4)	1545(4)	68(1)
C(12B)	2010(20)	5748(8)	2569(10)	19(2)
C(13B)	1423(5)	4404(5)	2089(4)	23(1)
C(14B)	1753(6)	3326(4)	2660(4)	33(1)

C(15B)	2868(11)	4281(7)	1432(7)	48(2)
F(1C)	12809(1)	-954(1)	2253(1)	31(1)
F(2C)	8755(2)	158(2)	866(1)	33(1)
O(1B)	9263(2)	313(1)	4181(1)	20(1)
N(1B)	4954(2)	1600(2)	4798(1)	23(1)
N(2B)	7197(2)	920(2)	4637(1)	20(1)
N(3B)	5672(2)	1252(2)	3343(1)	19(1)
N(4B)	4399(2)	1644(2)	3211(1)	24(1)
C(1C)	4048(2)	1830(2)	4106(2)	25(1)
C(2C)	5988(2)	1242(2)	4309(2)	19(1)
C(3C)	7998(2)	651(2)	3957(2)	18(1)
C(4C)	9867(2)	72(2)	3328(2)	19(1)
C(5C)	11161(2)	-314(2)	3276(2)	21(1)
C(6C)	11577(2)	-534(2)	2361(2)	24(1)
C(7C)	10802(3)	-377(2)	1551(2)	26(1)
C(8C)	9524(2)	12(2)	1659(2)	23(1)
C(9C)	9004(2)	245(2)	2552(2)	19(1)
C(10C)	7754(2)	635(2)	2952(2)	18(1)
C(11C)	6509(2)	939(2)	2628(2)	18(1)
F(3D)	6369(2)	1651(3)	-287(2)	46(1)
F(4D)	4247(3)	1488(2)	108(2)	48(1)
F(5D)	5411(2)	3354(2)	-26(1)	45(1)
C(12D)	5958(7)	954(9)	1629(2)	19(1)
C(13D)	5995(3)	2309(3)	1313(2)	26(1)
C(14D)	7430(4)	3131(3)	1465(2)	39(1)
C(15D)	5523(5)	2210(4)	286(3)	33(1)
F(3C)	6509(18)	926(19)	-329(11)	46(4)
F(4C)	4890(30)	2060(30)	88(18)	54(5)
F(5C)	6850(20)	3040(16)	-297(11)	66(4)
C(12C)	6170(70)	860(80)	1583(11)	19(1)
C(13C)	6720(30)	2190(18)	1174(13)	26(1)
C(14C)	6440(30)	3435(18)	1689(17)	39(1)
C(15C)	6230(40)	2010(30)	150(16)	33(1)

Table S-9. Bond lengths [Å] and angles [°] for Ballatore_BRL_I_205.

F(1A)-C(6A)	1.353(3)	C(13A)-C(15A)	1.748(7)
F(2A)-C(8A)	1.350(2)	C(14A)-H(14G)	0.9800
O(1A)-C(3A)	1.367(3)	C(14A)-H(14I)	0.9800
O(1A)-C(4A)	1.386(3)	C(14A)-H(14H)	0.9800
N(1A)-C(1A)	1.356(3)	F(3B)-C(15B)	1.334(12)
N(1A)-C(2A)	1.322(3)	F(4B)-C(15B)	1.333(8)
N(2A)-C(2A)	1.356(3)	F(5B)-C(15B)	1.324(11)
N(2A)-C(3A)	1.294(3)	C(12B)-H(12C)	0.9900
N(3A)-N(4A)	1.375(3)	C(12B)-H(12D)	0.9900
N(3A)-C(2A)	1.392(3)	C(12B)-C(13B)	1.536(7)
N(3A)-C(11A)	1.369(3)	C(13B)-H(13B)	1.0000
N(4A)-C(1A)	1.320(3)	C(13B)-C(14B)	1.515(7)
C(1A)-H(1A)	0.9500	C(13B)-C(15B)	1.728(8)
C(3A)-C(10A)	1.428(3)	C(14B)-H(14D)	0.9800
C(4A)-C(5A)	1.378(3)	C(14B)-H(14E)	0.9800
C(4A)-C(9A)	1.403(3)	C(14B)-H(14F)	0.9800
C(5A)-H(5A)	0.9500	F(1C)-C(6C)	1.348(3)
C(5A)-C(6A)	1.376(4)	F(2C)-C(8C)	1.354(3)
C(6A)-C(7A)	1.386(3)	O(1B)-C(3C)	1.364(3)
C(7A)-H(7A)	0.9500	O(1B)-C(4C)	1.382(3)
C(7A)-C(8A)	1.372(3)	N(1B)-C(1C)	1.352(3)
C(8A)-C(9A)	1.392(3)	N(1B)-C(2C)	1.325(3)
C(9A)-C(10A)	1.452(3)	N(2B)-C(2C)	1.348(3)
C(10A)-C(11A)	1.375(3)	N(2B)-C(3C)	1.299(3)
C(11A)-C(12A)	1.502(7)	N(3B)-N(4B)	1.374(3)
C(11A)-C(12B)	1.504(6)	N(3B)-C(2C)	1.387(3)
F(3A)-C(15A)	1.371(8)	N(3B)-C(11C)	1.372(3)
F(4A)-C(15A)	1.363(9)	N(4B)-C(1C)	1.328(3)
F(5A)-C(15A)	1.318(7)	C(1C)-H(1C)	0.9500
C(12A)-H(12F)	0.9900	C(3C)-C(10C)	1.427(3)
C(12A)-H(12E)	0.9900	C(4C)-C(5C)	1.383(3)
C(12A)-C(13A)	1.535(8)	C(4C)-C(9C)	1.394(3)
C(13A)-H(13A)	1.0000	C(5C)-H(5C)	0.9500
C(13A)-C(14A)	1.505(8)	C(5C)-C(6C)	1.380(3)

C(6C)-C(7C)	1.380(4)	C(11A)-N(3A)-N(4A)	126.20(19)
C(7C)-H(7C)	0.9500	C(11A)-N(3A)-C(2A)	124.84(19)
C(7C)-C(8C)	1.376(3)	C(1A)-N(4A)-N(3A)	101.24(18)
C(8C)-C(9C)	1.393(3)	N(1A)-C(1A)-H(1A)	121.2
C(9C)-C(10C)	1.459(3)	N(4A)-C(1A)-N(1A)	117.7(2)
C(10C)-C(11C)	1.370(3)	N(4A)-C(1A)-H(1A)	121.2
C(11C)-C(12D)	1.490(4)	N(1A)-C(2A)-N(2A)	128.2(2)
C(11C)-C(12C)	1.491(10)	N(1A)-C(2A)-N(3A)	109.93(19)
F(3D)-C(15D)	1.340(4)	N(2A)-C(2A)-N(3A)	121.8(2)
F(4D)-C(15D)	1.356(5)	O(1A)-C(3A)-C(10A)	111.39(19)
F(5D)-C(15D)	1.340(4)	N(2A)-C(3A)-O(1A)	119.16(19)
C(12D)-H(12A)	0.9900	N(2A)-C(3A)-C(10A)	129.4(2)
C(12D)-H(12B)	0.9900	O(1A)-C(4A)-C(9A)	111.37(19)
C(12D)-C(13D)	1.531(9)	C(5A)-C(4A)-O(1A)	122.94(19)
C(13D)-H(13D)	1.0000	C(5A)-C(4A)-C(9A)	125.7(2)
C(13D)-C(14D)	1.523(4)	C(4A)-C(5A)-H(5A)	123.0
C(13D)-C(15D)	1.494(5)	C(6A)-C(5A)-C(4A)	114.1(2)
C(14D)-H(14A)	0.9800	C(6A)-C(5A)-H(5A)	123.0
C(14D)-H(14B)	0.9800	F(1A)-C(6A)-C(5A)	117.6(2)
C(14D)-H(14C)	0.9800	F(1A)-C(6A)-C(7A)	117.8(2)
F(3C)-C(15C)	1.35(3)	C(5A)-C(6A)-C(7A)	124.6(2)
F(4C)-C(15C)	1.31(4)	C(6A)-C(7A)-H(7A)	121.0
F(5C)-C(15C)	1.37(3)	C(8A)-C(7A)-C(6A)	117.9(2)
C(12C)-H(12G)	0.9900	C(8A)-C(7A)-H(7A)	121.0
C(12C)-H(12H)	0.9900	F(2A)-C(8A)-C(7A)	118.4(2)
C(12C)-C(13C)	1.59(9)	F(2A)-C(8A)-C(9A)	119.5(2)
C(13C)-H(13C)	1.0000	C(7A)-C(8A)-C(9A)	122.1(2)
C(13C)-C(14C)	1.517(11)	C(4A)-C(9A)-C(10A)	105.91(19)
C(13C)-C(15C)	1.492(11)	C(8A)-C(9A)-C(4A)	115.6(2)
C(14C)-H(14J)	0.9800	C(8A)-C(9A)-C(10A)	138.5(2)
C(14C)-H(14K)	0.9800	C(3A)-C(10A)-C(9A)	104.91(19)
C(14C)-H(14L)	0.9800	C(11A)-C(10A)-C(3A)	117.3(2)
C(3A)-O(1A)-C(4A)	106.40(16)	C(11A)-C(10A)-C(9A)	137.8(2)
C(2A)-N(1A)-C(1A)	102.18(19)	N(3A)-C(11A)-C(10A)	114.0(2)
C(3A)-N(2A)-C(2A)	112.59(19)	N(3A)-C(11A)-C(12A)	115.0(11)
N(4A)-N(3A)-C(2A)	108.96(19)	N(3A)-C(11A)-C(12B)	121.8(9)

C(10A)-C(11A)-C(12A)	130.8(11)	C(14B)-C(13B)-C(15B)	90.3(4)
C(10A)-C(11A)-C(12B)	124.1(9)	C(15B)-C(13B)-H(13B)	117.8
C(11A)-C(12A)-H(12F)	109.8	C(13B)-C(14B)-H(14D)	109.5
C(11A)-C(12A)-H(12E)	109.8	C(13B)-C(14B)-H(14E)	109.5
C(11A)-C(12A)-C(13A)	109.3(6)	C(13B)-C(14B)-H(14F)	109.5
H(12F)-C(12A)-H(12E)	108.3	H(14D)-C(14B)-H(14E)	109.5
C(13A)-C(12A)-H(12F)	109.8	H(14D)-C(14B)-H(14F)	109.5
C(13A)-C(12A)-H(12E)	109.8	H(14E)-C(14B)-H(14F)	109.5
C(12A)-C(13A)-H(13A)	116.5	F(3B)-C(15B)-C(13B)	88.8(6)
C(12A)-C(13A)-C(15A)	106.6(8)	F(4B)-C(15B)-F(3B)	108.0(8)
C(14A)-C(13A)-C(12A)	114.7(9)	F(4B)-C(15B)-C(13B)	108.0(6)
C(14A)-C(13A)-H(13A)	116.5	F(5B)-C(15B)-F(3B)	108.3(7)
C(14A)-C(13A)-C(15A)	80.3(4)	F(5B)-C(15B)-F(4B)	107.0(7)
C(15A)-C(13A)-H(13A)	116.5	F(5B)-C(15B)-C(13B)	133.5(6)
C(13A)-C(14A)-H(14G)	109.5	C(3C)-O(1B)-C(4C)	106.34(17)
C(13A)-C(14A)-H(14I)	109.5	C(2C)-N(1B)-C(1C)	102.62(19)
C(13A)-C(14A)-H(14H)	109.5	C(3C)-N(2B)-C(2C)	112.48(19)
H(14G)-C(14A)-H(14I)	109.5	N(4B)-N(3B)-C(2C)	109.63(18)
H(14G)-C(14A)-H(14H)	109.5	C(11C)-N(3B)-N(4B)	125.0(2)
H(14I)-C(14A)-H(14H)	109.5	C(11C)-N(3B)-C(2C)	125.37(19)
F(3A)-C(15A)-C(13A)	124.9(5)	C(1C)-N(4B)-N(3B)	100.83(19)
F(4A)-C(15A)-F(3A)	104.4(6)	N(1B)-C(1C)-H(1C)	121.3
F(4A)-C(15A)-C(13A)	87.7(5)	N(4B)-C(1C)-N(1B)	117.5(2)
F(5A)-C(15A)-F(3A)	106.7(6)	N(4B)-C(1C)-H(1C)	121.3
F(5A)-C(15A)-F(4A)	104.9(5)	N(1B)-C(2C)-N(2B)	128.7(2)
F(5A)-C(15A)-C(13A)	121.8(5)	N(1B)-C(2C)-N(3B)	109.5(2)
C(11A)-C(12B)-H(12C)	108.4	N(2B)-C(2C)-N(3B)	121.81(19)
C(11A)-C(12B)-H(12D)	108.4	O(1B)-C(3C)-C(10C)	111.55(18)
C(11A)-C(12B)-C(13B)	115.3(5)	N(2B)-C(3C)-O(1B)	119.1(2)
H(12C)-C(12B)-H(12D)	107.5	N(2B)-C(3C)-C(10C)	129.3(2)
C(13B)-C(12B)-H(12C)	108.4	O(1B)-C(4C)-C(5C)	122.7(2)
C(13B)-C(12B)-H(12D)	108.4	O(1B)-C(4C)-C(9C)	111.73(19)
C(12B)-C(13B)-H(13B)	117.8	C(5C)-C(4C)-C(9C)	125.5(2)
C(12B)-C(13B)-C(15B)	94.5(6)	C(4C)-C(5C)-H(5C)	122.8
C(14B)-C(13B)-C(12B)	113.3(9)	C(6C)-C(5C)-C(4C)	114.4(2)
C(14B)-C(13B)-H(13B)	117.8	C(6C)-C(5C)-H(5C)	122.8

F(1C)-C(6C)-C(5C)	117.7(2)	C(13D)-C(14D)-H(14C)	109.5
F(1C)-C(6C)-C(7C)	118.0(2)	H(14A)-C(14D)-H(14B)	109.5
C(7C)-C(6C)-C(5C)	124.3(2)	H(14A)-C(14D)-H(14C)	109.5
C(6C)-C(7C)-H(7C)	121.0	H(14B)-C(14D)-H(14C)	109.5
C(8C)-C(7C)-C(6C)	118.1(2)	F(3D)-C(15D)-F(4D)	105.3(3)
C(8C)-C(7C)-H(7C)	121.0	F(3D)-C(15D)-C(13D)	113.0(4)
F(2C)-C(8C)-C(7C)	118.3(2)	F(4D)-C(15D)-C(13D)	112.3(3)
F(2C)-C(8C)-C(9C)	119.7(2)	F(5D)-C(15D)-F(3D)	107.5(3)
C(7C)-C(8C)-C(9C)	122.0(2)	F(5D)-C(15D)-F(4D)	105.5(4)
C(4C)-C(9C)-C(10C)	105.87(19)	F(5D)-C(15D)-C(13D)	112.8(3)
C(8C)-C(9C)-C(4C)	115.7(2)	C(11C)-C(12C)-H(12G)	109.5
C(8C)-C(9C)-C(10C)	138.4(2)	C(11C)-C(12C)-H(12H)	109.5
C(3C)-C(10C)-C(9C)	104.51(19)	C(11C)-C(12C)-C(13C)	111(5)
C(11C)-C(10C)-C(3C)	117.6(2)	H(12G)-C(12C)-H(12H)	108.1
C(11C)-C(10C)-C(9C)	137.9(2)	C(13C)-C(12C)-H(12G)	109.5
N(3B)-C(11C)-C(12D)	117.4(3)	C(13C)-C(12C)-H(12H)	109.5
N(3B)-C(11C)-C(12C)	127(2)	C(12C)-C(13C)-H(13C)	106.0
C(10C)-C(11C)-N(3B)	113.4(2)	C(14C)-C(13C)-C(12C)	119(2)
C(10C)-C(11C)-C(12D)	129.2(3)	C(14C)-C(13C)-H(13C)	106.0
C(10C)-C(11C)-C(12C)	120(2)	C(15C)-C(13C)-C(12C)	105(2)
C(11C)-C(12D)-H(12A)	108.8	C(15C)-C(13C)-H(13C)	106.0
C(11C)-C(12D)-H(12B)	108.8	C(15C)-C(13C)-C(14C)	114(2)
C(11C)-C(12D)-C(13D)	113.6(5)	C(13C)-C(14C)-H(14J)	109.5
H(12A)-C(12D)-H(12B)	107.7	C(13C)-C(14C)-H(14K)	109.5
C(13D)-C(12D)-H(12A)	108.8	C(13C)-C(14C)-H(14L)	109.5
C(13D)-C(12D)-H(12B)	108.8	H(14J)-C(14C)-H(14K)	109.5
C(12D)-C(13D)-H(13D)	108.2	H(14J)-C(14C)-H(14L)	109.5
C(14D)-C(13D)-C(12D)	113.2(3)	H(14K)-C(14C)-H(14L)	109.5
C(14D)-C(13D)-H(13D)	108.2	F(3C)-C(15C)-F(5C)	108(3)
C(15D)-C(13D)-C(12D)	109.1(3)	F(3C)-C(15C)-C(13C)	114(2)
C(15D)-C(13D)-H(13D)	108.2	F(4C)-C(15C)-F(3C)	111(2)
C(15D)-C(13D)-C(14D)	109.7(3)	F(4C)-C(15C)-F(5C)	106(3)
C(13D)-C(14D)-H(14A)	109.5	F(4C)-C(15C)-C(13C)	109(3)
C(13D)-C(14D)-H(14B)	109.5	F(5C)-C(15C)-C(13C)	109(2)

Symmetry transformations used to generate equivalent atoms:

Table S-10. Anisotropic displacement parameters ($Å^2$x 10^3) for Ballatore_BRL_I_205. The anisotropic displacement factor exponent takes the form: $-2\pi^2[h^2 a^{*2}U^{11} + ... + 2 h k a^* b^* U^{12}]$

	U^{11}	U^{22}	U^{33}	U^{23}	U^{13}	U^{12}
F(1A)	26(1)	42(1)	26(1)	3(1)	-1(1)	16(1)
F(2A)	30(1)	37(1)	18(1)	0(1)	6(1)	16(1)
O(1A)	20(1)	21(1)	18(1)	0(1)	2(1)	6(1)
N(1A)	24(1)	20(1)	24(1)	1(1)	-2(1)	2(1)
N(2A)	21(1)	18(1)	22(1)	0(1)	1(1)	2(1)
N(3A)	18(1)	18(1)	23(1)	2(1)	2(1)	4(1)
N(4A)	20(1)	21(1)	29(1)	3(1)	1(1)	5(1)
C(1A)	21(1)	21(1)	29(2)	4(1)	-4(1)	3(1)
C(2A)	22(1)	14(1)	20(1)	0(1)	0(1)	1(1)
C(3A)	20(1)	14(1)	20(1)	0(1)	2(1)	2(1)
C(4A)	23(1)	16(1)	16(1)	1(1)	2(1)	3(1)
C(5A)	22(1)	20(1)	21(1)	1(1)	4(1)	5(1)
C(6A)	22(1)	22(1)	27(1)	3(1)	-1(1)	6(1)
C(7A)	31(1)	24(1)	17(1)	2(1)	1(1)	7(1)
C(8A)	26(1)	20(1)	19(1)	1(1)	7(1)	6(1)
C(9A)	20(1)	15(1)	21(1)	2(1)	3(1)	3(1)
C(10A)	21(1)	16(1)	20(1)	1(1)	3(1)	2(1)
C(11A)	21(1)	17(1)	19(1)	4(1)	1(1)	3(1)
F(3A)	65(3)	58(2)	18(2)	12(2)	6(2)	43(2)
F(4A)	37(3)	56(3)	38(3)	12(2)	23(2)	28(2)
F(5A)	81(3)	41(2)	17(2)	-14(1)	0(2)	27(2)
C(12A)	12(5)	21(2)	22(2)	4(1)	4(3)	2(2)
C(13A)	25(3)	26(2)	20(3)	-2(2)	0(2)	8(2)
C(14A)	46(2)	26(2)	25(2)	-3(1)	11(2)	2(2)
C(15A)	39(4)	36(4)	28(4)	11(3)	15(3)	22(3)
F(3B)	75(4)	82(4)	29(3)	-3(2)	14(3)	22(3)
F(4B)	72(3)	56(2)	64(3)	-22(2)	16(2)	24(2)
F(5B)	52(3)	64(3)	88(3)	-14(2)	34(2)	16(2)
C(12B)	12(5)	21(2)	22(2)	4(1)	4(3)	2(2)
C(13B)	25(3)	26(2)	20(3)	-2(2)	0(2)	8(2)
C(14B)	46(2)	26(2)	25(2)	-3(1)	11(2)	2(2)
C(15B)	52(6)	40(4)	54(6)	-7(3)	19(5)	16(4)

F(1C)	22(1)	33(1)	40(1)	0(1)	5(1)	11(1)
F(2C)	33(1)	53(1)	16(1)	1(1)	2(1)	18(1)
O(1B)	22(1)	22(1)	16(1)	2(1)	-1(1)	4(1)
N(1B)	23(1)	21(1)	23(1)	-2(1)	6(1)	1(1)
N(2B)	23(1)	19(1)	16(1)	2(1)	3(1)	0(1)
N(3B)	18(1)	20(1)	19(1)	-1(1)	1(1)	2(1)
N(4B)	19(1)	27(1)	25(1)	-2(1)	2(1)	6(1)
C(1C)	20(1)	25(1)	28(1)	-5(1)	7(1)	2(1)
C(2C)	24(1)	17(1)	16(1)	0(1)	4(1)	-1(1)
C(3C)	20(1)	14(1)	18(1)	1(1)	-1(1)	1(1)
C(4C)	23(1)	16(1)	18(1)	1(1)	3(1)	1(1)
C(5C)	21(1)	20(1)	24(1)	3(1)	-3(1)	3(1)
C(6C)	18(1)	21(1)	34(2)	1(1)	4(1)	5(1)
C(7C)	27(1)	28(1)	24(1)	-1(1)	8(1)	5(1)
C(8C)	24(1)	27(1)	17(1)	2(1)	0(1)	6(1)
C(9C)	19(1)	17(1)	18(1)	1(1)	1(1)	2(1)
C(10C)	22(1)	16(1)	16(1)	1(1)	3(1)	1(1)
C(11C)	21(1)	16(1)	18(1)	1(1)	3(1)	1(1)
F(3D)	66(1)	59(2)	19(1)	-2(1)	3(1)	34(1)
F(4D)	50(1)	58(1)	36(1)	6(1)	-17(1)	11(1)
F(5D)	66(1)	47(1)	28(1)	12(1)	3(1)	27(1)
C(12D)	19(3)	23(2)	17(1)	-3(1)	0(1)	7(2)
C(13D)	37(2)	28(1)	17(1)	4(1)	1(1)	12(1)
C(14D)	57(2)	27(2)	31(2)	6(1)	1(2)	-1(1)
C(15D)	42(2)	35(2)	26(2)	3(1)	-2(2)	19(2)
F(3C)	63(9)	45(5)	32(7)	-7(5)	4(6)	17(6)
F(4C)	47(5)	71(13)	48(10)	0(10)	-13(5)	25(7)
F(5C)	107(10)	55(6)	28(7)	15(6)	-9(8)	-12(7)
C(12C)	19(3)	23(2)	17(1)	-3(1)	0(1)	7(2)
C(13C)	37(2)	28(1)	17(1)	4(1)	1(1)	12(1)
C(14C)	57(2)	27(2)	31(2)	6(1)	1(2)	-1(1)
C(15C)	42(2)	35(2)	26(2)	3(1)	-2(2)	19(2)

Table S-11. Hydrogen coordinates (x 10^4) and isotropic displacement parameters ($Å^2$x 10^3) for Ballatore_BRL_I_205.

	x	y	z	U(eq)
H(1A)	4283	5252	5694	28
H(5A)	-3894	7714	3770	25
H(7A)	-2786	7024	1035	28
H(12F)	3228	6251	2782	22
H(12E)	1868	6309	2115	22
H(13A)	2807	3968	2665	28
H(14G)	202	3732	2840	49
H(14I)	643	2838	1967	49
H(14H)	103	4157	1781	49
H(12C)	3030	5814	2663	22
H(12D)	1819	6393	2131	22
H(13B)	492	4288	1737	28
H(14D)	2765	3408	2779	49
H(14E)	1404	2497	2303	49
H(14F)	1304	3378	3269	49
H(1C)	3192	2113	4254	30
H(5C)	11717	-420	3823	26
H(7C)	11142	-532	937	31
H(12A)	4984	504	1566	23
H(12B)	6514	471	1197	23
H(13D)	5323	2745	1690	32
H(14A)	7405	3960	1207	58
H(14B)	8117	2688	1139	58
H(14C)	7690	3275	2148	58
H(12G)	5148	649	1457	23
H(12H)	6606	169	1256	23
H(13C)	7762	2254	1179	32
H(14J)	6881	4164	1366	58
H(14K)	6824	3509	2347	58
H(14L)	5432	3437	1688	58